

FOSSIL ANGIOSPERM WOODS FROM THE JOSE CREEK MEMBER  
OF THE MCRAE FORMATION

by

Joan M. Parrott, M.A.

A dissertation submitted to the Graduate Council of  
Texas State University in partial fulfillment  
of the requirements for the degree of  
Doctor of Philosophy  
with a Major in Aquatic Resources and Integrative Biology  
May 2019

Committee Members:

Garland Upchurch Jr., Co-Chair

Paula Williamson, Co-Chair

Chris Nice

Cindy Looy

Lisa Boucher

**COPYRIGHT**

by

Joan M. Parrott

2019

## **FAIR USE AND AUTHOR'S PERMISSION STATEMENT**

### **Fair Use**

This work is protected by the Copyright Laws of the United States (Public Law 94-553, Section 107). Consistent with fair use as defined in the Copyright Laws, brief quotations from this material are allowed with proper acknowledgement. Use of this material for financial gain without the author's express written permission is not allowed.

### **Duplication Permission**

As the copyright holder of this work I, Joan M. Parrott, refuse permission to copy in excess of the "Fair Use" exemption without my written permission.

## **DEDICATION**

I dedicate this, in particular, to my husband David, for his unwavering encouragement, timely suggestions, technical assistance, help with materials acquisition and his participation as the best field hand ever. This work is also dedicated to the members of my family, Samuel, Matthew and Elissa, whose own educational journeys have provided much inspiration.

## **ACKNOWLEDGEMENTS**

The author thanks Garland Upchurch, Jr. for extending the opportunity to work on fossil woods from the McRae Formation and for placing all aspects of this work in a broader context; the members of the committee, Paula Williamson, Chris Nice, Lisa Boucher and Cindy Looy; Jon Richie, Dori Contreras and Ann Marie Prue for their camaraderie and assistance collecting materials on field trips; Emilio Estrada-Ruiz for igniting interest in wood identification in the Upchurch lab and his instruction in field identification of fossil woods, slide preparation and wood anatomy; Greg Mack for joining our lab on field expeditions and his contribution of geologic information and age determination for the McRae Formation; Elisabeth Wheeler for invaluable assistance with anatomical descriptions, manuscript comments, background information and guidance; Patrick Herendeen for information and discussion; and the Texas State University Department of Biology for encouragement and financial support. A special thank you is extended to David Lemke for his support in the field and for providing assistance with photography and acquisition of materials. Use of the Texas State University Department of Geology Hillquist saws and related materials was greatly appreciated. This work was supported, in part, by the National Science Foundation Grant DEB 1655985 to G. R. Upchurch and a Texas State University Doctoral Research Support Fellowship Award.

## TABLE OF CONTENTS

	<b>Page</b>
ACKNOWLEDGEMENTS .....	v
LIST OF TABLES .....	xi
LIST OF FIGURES .....	xiii
ABSTRACT .....	xviii
 CHAPTER	
I. FOREST OF GIANTS: AN <i>IN SITU</i> ANGIOSPERM FOREST OF LATE CRETACEOUS (CAMPANIAN) SOUTH-CENTRAL NEW MEXICO, USA .....	
	1
ABSTRACT .....	1
INTRODUCTION.....	3
GEOLOGIC SETTING.....	4
MATERIALS AND METHODS.....	5
Slide preparation .....	6
DESCRIPTIONS.....	8
McRae Group IA sp. 1, Lauraceae .....	8
Comparison to extant woods.....	10
Comparison to fossil woods.....	12
Comparison to fossil woods identified through a search of the InsideWood database .....	12
Comparison to <i>Laurinoxyon (Ulminium)</i> species .....	14
Comparison to fossil genera and / or type species attributed to Lauraceae .....	15
Remarks.....	16
Biogeography .....	20
Other fossil evidence .....	21
McRae Group IIIB sp. 4, Cannabaceae? Moraceae?	
Urticaceae? .....	24
Comparison to extant woods.....	26
Comparison to fossil woods.....	28

Comparison to fossil genera attributed to [Cannabaceae [Moraceae + Urticaceae]].....	28
Comparison to similar fossil woods found through search of the InsideWood database and the subsequent literature review.....	30
Other fossil evidence.....	31
McRae Group IIIB sp. 6, Kirkiaceae .....	33
Comparison to extant woods.....	35
Comparison to fossil woods .....	38
Comparison to fossil woods identified through a search of the InsideWood database.....	38
Comparison to fossil woods and generic diagnoses associated with Burseraceae .....	39
Comparison to <i>Paraphyllanthoxylon</i> species .....	41
Descriptions of <i>Paraphyllanthoxylon</i> without attribution to a specific family .....	43
Biogeography .....	45
Rethinking attribution of <i>Paraphyllanthoxylon</i> -like woods.....	48
The competing hypothesis – if it’s anything, it’s Laurales.....	50
Other fossil evidence.....	55
Attribution.....	56
McRae Group IIIB sp. 5, cf. Sapotaceae .....	57
Comparison to extant woods.....	59
Comparison to fossil woods.....	62
Comparison to fossil woods identified through a search of the InsideWood database.....	62
Comparison to fossil genera attributed to Juglandaceae.....	63
Comparison to fossil genera attributed to Sapotaceae.....	64
Biogeography .....	66
Other fossil evidence.....	67
DISCUSSION.....	69
Climatic evidence .....	70
Angiosperm stature.....	71

Biogeography.....	72
Lauraceae.....	73
Kirkiaceae.....	73
Sapotaceae.....	74
FUTURE STUDY .....	75
Logjam locality associated with the Forest of Giants .....	75
CONCLUSIONS.....	76
REFERENCES .....	103

II. SIGNIFICANCE AND SYSTEMATIC ASSIGNMENT OF LATE CRETACEOUS  
*PLATANUS*-LIKE FOSSIL WOODS FROM THE MCRAE FORMATION (LATE  
CAMPANIAN) OF SOUTH-CENTRAL NEW MEXICO, USA.....129

ABSTRACT.....	129
INTRODUCTION.....	130
GEOLOGIC SETTING.....	132
MATERIALS AND METHODS.....	133
DESCRIPTIONS.....	136
McRae Group IIC sp. 1 .....	137
McRae Group IIC sp. 2 .....	142
McRae Group IIC sp. 3 .....	145
McRae Group IIC sp. 4 .....	148
DISCUSSION.....	151
InsideWood database search code .....	151
Comparison to extant woods.....	151
Comparison to fossil woods.....	155
<i>Plataninium</i> or <i>Platanoxylon</i> ? .....	157
<i>Platanoxylon</i> Andreánszky.....	160
Generic diagnosis.....	160
Rationale for a new genus of Cretaceous and some early Cenozoic <i>Platanus</i> -like woods .....	161
Estimation of <i>Platanus</i> divergence time.....	165
Other fossil evidence.....	166
CONCLUSIONS.....	169
REFERENCES .....	190

III. THE ANGIOSPERM WOOD FLORA OF THE UPPER CRETACEOUS  
(CAMPANIAN) MCRAE FORMATION, SOUTH-CENTRAL NEW MEXICO:  
DIVERSITY AND SIGNIFICANCE.....199

ABSTRACT.....	199
INTRODUCTION.....	200
GEOLOGIC SETTING.....	202
MATERIALS AND METHODS.....	204
ORGANIZATION OF MCRAE FORMATION ANGIOSPERM	
WOODS.....	207
SYSTEMATIC DESCRIPTIONS.....	210
McRae Group I: Idioblasts (probable oil cells) present.....	210
Group IA: Axial parenchyma scanty paratracheal	
a. Vessel-ray pitting with reduced borders, round to oval to horizontally elongate (Richter Type II).....	211
b. Vessel-ray pitting of two types -) reduced border oval to elongate, horizontal, diagonal or curved (Richter Type II), 2) large, simple.....	213
Group IB: Axial parenchyma aliform to confluent.....	218
McRae Group II: Exclusively Scalariform Perforation	
Plates.....	221
Group IIA: Rays <10 cells wide.....	221
a. Axial parenchyma common.....	221
i. Vessel-ray parenchyma pits of two types.....	221
ii. Vessel-ray parenchyma pits of one type, small.....	224
b. Axial parenchyma not common, vessel diameter <100 µm, fiber pits “discontinuous”.....	230
Group IIB: Rays >10 cells wide, uniseriate rays common (rays of two sizes).....	234
McRae Group III: Exclusively simple perforation plates.....236	
Group IIIA: Vessels exclusively solitary.....	237
a. Axial parenchyma rare, vasicentric tracheids, rays 1-2 seriate.....	237
i. Vessels diameter >100 µm, septate fibers.....	237
ii. Vessels diameter <100 µm, non-septate fibers.....	244

b. Axial parenchyma common .....	246
i. Rays >10 cells wide .....	246
ii. Rays <10 cells wide.....	247
Group IIIB: Vessels both solitary and in radial multiples .....	252
a. Axial parenchyma rare to scanty paratracheal .....	252
b. Axial parenchyma common.....	256
McRae Group IV: Simple & scalariform perforation plates (absent oil cells) .....	257
DISCUSSION.....	259
Climatic evidence .....	262
Search for family affinity.....	263
Future study .....	267
REFERENCES .....	333

## LIST OF TABLES

<b>Table</b>	<b>Page</b>
1.1 Comparison of <i>Laurinoxylon</i> sp. 1 McRae Group IA sp. 1, TXSTATE 1250, to fossil woods identified through a search of InsideWood database .....	77
1.2 Comparison of <i>Laurinoxylon</i> sp. 1, McRae Group IA sp. 1, TXSTATE 1250 to fossil genera and type species of Lauraceae.....	79
1.3a. Comparison of McRae Group IIIB sp. 4, TXSTATE 1287 to Urticales (Rosales) fossil genera and woods.....	82
1.3b. Comparison of McRae Group IIIB sp. 4, TXSTATE 1287 to Urticales (Rosales) fossil genera and woods.....	83
1.4. Forest of Giants log and stump diameters, and estimated maximum height.....	85
1.5. Comparison of McRae Group IIIB sp. 6, TXSTATE 1232-1246 to <i>Kirkia</i> species .....	86
1.6. Comparison of McRae Group IIIB sp. 6, TXSTATE 1232-1246 to similar species of <i>Paraphyllanthoxylon</i> .....	87
1.7. McRae Formation Forest of Giants woods.....	89
2.1. Comparison of McRae Group IIB, <i>Platanus</i> -like woods and <i>Platanus</i> .....	170
2.2. Comparison of McRae Group IIB, <i>Platanus</i> -like woods and similar fossil species .....	172
2.3. Transitions in anatomical features through time.....	175
3.1. Groups IA, IB, IC – McRae Formation woods with oil cells.....	269
3.2. Groups IIA, IIB – McRae Formation woods with exclusively scalariform perforation plates.....	271

3.3. Group IIA – Comparison of McRae Formation <i>Agujoxylon</i> and <i>Metcalfexylon</i> specimens to type species and previously reported occurrences from North America.....	273
3.4. Group IIA – Comparison of the McRae Formation Group IIA specimens “lumped” into Group IIA sp. 3 .....	275
3.5. Group IIIA – McRae Formation woods with simple perforation plates, vessels exclusively solitary .....	277
3.6. Group IIIA – Comparison of specimens representing <i>Fulleroxylon</i> sp. nov. and <i>Fulleroxylon armendarisense</i> .....	280
3.7. Group IIIB – McRae Formation woods with simple perforation plates, vessels solitary and in radial multiples .....	282
3.8. Group IV – McRae Formation wood with both simple and scalariform perforation plates (oil cells absent) .....	285

## LIST OF FIGURES

Figure	Page
1.1. Map showing the location and geology of the McRae Formation, south-central New Mexico (Estrada-Ruiz et al. 2018) .....	91
1.2. McRae wood holoxylotype Group IA sp. 1 (TXSTATE 1250) Lauraceae .....	92
1.3. McRae wood holoxylotype Group IA sp. 1 (TXSTATE 1250) Lauraceae .....	93
1.4. McRae wood holoxylotype Group IA sp. 1 (TXSTATE 1250) Lauraceae .....	94
1.5. McRae wood holoxylotype Group IIIB sp. 4 (TXSTATE 1287) cf. Cannabaceae? Moraceae? Urticaceae? .....	95
1.6. McRae wood holoxylotype Group IIIB sp. 4 (TXSTATE 1287) cf. Cannabaceae? Moraceae? Urticaceae? .....	96
1.7. McRae wood holoxylotype Group IIIB sp. 4 (TXSTATE 1287) cf. Cannabaceae? Moraceae? Urticaceae? .....	97
1.8. <i>Paraphyllanthoxylon</i> cf. <i>cenomaniana</i> Takahshi and Suzuki (holoxylotype) (TXSTATE 1232) cf. [Kirkiaceae [Burseraceae + Anacardiaceae]] .....	98
1.9. <i>Paraphyllanthoxylon</i> cf. <i>cenomaniana</i> Takahshi and Suzuki (holoxylotype) (TXSTATE 1232) cf. [Kirkiaceae [Burseraceae + Anacardiaceae]] .....	99
1.10. <i>Forest of Giants in situ</i> stumps .....	100
1.11. McRae wood holoxylotype Group IIIB sp. 5 (TXSTATE 1288) cf. Sapotaceae .....	101
1.12. McRae wood holoxylotype Group IIIB sp. 5 (TXSTATE 1288) cf. Sapotaceae .....	102
2.1. Map showing the location and geology of the McRae Formation, south-central New Mexico (Estrada-Ruiz et al. 2018) .....	177

2.2. Holoxylotype of McRae wood Group IIB sp. 2 (TXSTATE 1212) Platanaceae .....	178
2.3. McRae wood Group IIC sp. 1 (TXSTATE 1212, 1267-1270) Platanaceae .....	179
2.4. McRae wood Group IIC sp. 1 (TXSTATE 1212, 1267-1270) Platanaceae .....	180
2.5. McRae wood Group IIC sp. 1 (TXSTATE 1212, 1267-1270) Platanaceae .....	181
2.6. McRae wood Group IIC sp. 2 (TXSTATE 1203, 1271-1272) Platanaceae .....	182
2.7. McRae wood Group IIC sp. 2 (TXSTATE 1203, 1271-1272) Platanaceae .....	183
2.8. McRae wood Group IIC sp. 3 (TXSTATE 1273) Platanaceae.....	184
2.9. McRae wood Group IIC sp. 3 (TXSTATE 1273) Platanaceae.....	185
2.10. McRae wood Group IIC sp. 3 (TXSTATE 1273) Platanaceae .....	186
2.11. McRae wood Group IIC sp. 4 (TXSTATE 1274) Platanaceae .....	187
2.12. McRae wood Group IIC sp. 4 (TXSTATE 1274) Platanaceae .....	188
2.13. Unexplained fine bars silhouetted against vessels.....	189
3.1. Maps showing the location and geology of the McRae Formation, south-central New Mexico (Estrada-Ruiz et al. 2018) .....	286
3.2. McRae wood holoxylotype Group IA sp. 2 (TXSTATE 1251) Lauraceae .....	287
3.3. McRae wood holoxylotype Group IA sp. 2 (TXSTATE 1251) Lauraceae .....	288
3.4. McRae wood holoxylotype Group IA sp. 3 (TXSTATE 1252) Lauraceae .....	289
3.5. McRae wood holoxylotype Group IA sp. 3 (TXSTATE 1252) Lauraceae .....	290
3.6. McRae wood paraxylotype Group IA sp. 3 (TXSTATE 1253) Lauraceae .....	291
3.7. McRae wood holoxylotype Group IA sp. 4 (TXSTATE 1254) Lauraceae .....	292

3.8. McRae wood holoxylotype Group IA sp. 4 (TXSTATE 1254) Lauraceae .....	293
3.9. McRae wood holoxylotype Group IB sp. 1 (TXSTATE 1255) Lauraceae .....	294
3.10. McRae wood holoxylotype Group IB sp. 1 (TXSTATE 1255) Lauraceae.....	295
3.11. McRae wood paraxylotype Group IB sp. 1 (TXSTATE 1256) Lauraceae .....	296
3.12. <i>Agujoxylon olacaceoides</i> Wheeler and Lehman (TXSTATE 1257) cf. Olacaceae .....	297
3.13. <i>Agujoxylon olacaceoides</i> Wheeler and Lehman (TXSTATE 1257) cf. Olacaceae .....	298
3.14. McRae wood holoxylotype Group IIA sp. 1 (TXSTATE 1259).....	299
3.15. McRae wood holoxylotype Group IIA sp. 1 (TXSTATE 1259).....	300
3.16. McRae wood holoxylotype Group IIA sp. 2 (TXSTATE 1260).....	301
3.17. McRae wood holoxylotype Group IIA sp. 2 (TXSTATE 1260).....	302
3.18. <i>Metcalfeoxylon kirtlandense</i> Wheeler, McClammer and LaPasha (TXSTATE 1261) .....	303
3.19. <i>Metcalfeoxylon kirtlandense</i> Wheeler, McClammer and LaPasha (TXSTATE 1261) .....	304
3.20. McRae wood holoxylotype Group IIA sp. 3 (TXSTATE 1262).....	305
3.21. McRae wood paraxylotype Group IIA sp. 3 (TXSTATE 1262) .....	306
3.22. McRae wood paraxylotype Group IIA sp. 3 (TXSTATE 1263) .....	307
3.23. McRae wood paraxylotype Group IIA sp. 3 (TXSTATE 1264) .....	308
3.24. McRae wood paraxylotype Group IIA sp. 3 (TXSTATE 1264) .....	309
3.25. <i>icacinoxylon</i> sp. 1 (holoxylotype) (TXSTATE 1265) cf. Icacinaceae .....	310

3.26. <i> Icacinoxylon </i> sp. 1 (holoxylotype) (TXSTATE 1265) cf. Icacinaceae .....	311
3.27. <i> Fulleroxylon </i> sp 1 (holoxylotype) (TXSTATE 1275) cf. Connaraceae .....	312
3.28. <i> Fulleroxylon </i> sp 1 (holoxylotype) (TXSTATE 1275) cf. Connaraceae .....	313
3.29. <i> Fulleroxylon </i> sp 1 (holoxylotype) (TXSTATE 1275) cf. Connaraceae .....	314
3.30. McRae wood holoxylotype Group IIIA sp. 1 (TXSTATE 1278) .....	315
3.31. McRae wood holoxylotype Group IIIA sp. 1 (TXSTATE 1278) .....	316
3.32. McRae wood holoxylotype Group IIIA sp. 2 (TXSTATE 1279) .....	317
3.33. McRae wood holoxylotype Group IIIA sp. 2 (TXSTATE 1279) .....	318
3.34. McRae wood holoxylotype Group IIIA sp. 3 (TXSTATE 1280) .....	319
3.35. McRae wood holoxylotype Group IIIA sp. 3 (TXSTATE 1280) .....	320
3.36. McRae wood holoxylotype Group IIIA sp. 4 (TXSTATE 1281) .....	321
3.37. McRae wood holoxylotype Group IIIA sp. 4 (TXSTATE 1281) .....	322
3.38. McRae wood holoxylotype Group IIIA sp. 4 (TXSTATE 1281) .....	323
3.39. McRae wood holoxylotype Group IIIB sp. 1 (TXSTATE 1283) .....	324
3.40. McRae wood holoxylotype Group IIIB sp. 1 (TXSTATE 1283) .....	325
3.41. McRae wood holoxylotype Group IIIB sp. 2 (TXSTATE 1284) .....	326
3.42. McRae wood holoxylotype Group IIIB sp. 2 (TXSTATE 1284) .....	327
3.43. McRae wood paraxylotype Group IIIB sp. 2 (TXSTATE 1285) .....	328
3.44. McRae wood holoxylotype Group IIIB sp. 3 (TXSTATE 1286) .....	329
3.45. McRae wood holoxylotype Group IIIB sp. 3 (TXSTATE 1286) .....	330

3.46. McRae wood holoxylotype Group IV sp. 1 (TXSTATE 1289) .....	331
3.47. McRae wood holoxylotype Group IV sp. 1 (TXSTATE 1289) .....	332

## ABSTRACT

The Jose Creek Member of the McRae Formation, south-central New Mexico, preserves a diverse mixed angiosperm and conifer flora of Late Campanian (76.5–72.5 Ma) age. The Jose Creek Member is of special interest because it provides an abundance of fossil evidence in the form of leaves, reproductive structures, and silicified woods found *in situ* and as float. The wood flora, as currently understood, is one of the three most diverse Cretaceous wood floras in the world, and the only one where the majority of wood types represent mature wood. The focus of the present study is non-monocot angiosperms. To date, approximately thirty-five species have been discovered, representing both members of the magnoliid clade and eudicots. Many of the McRae xyloids are common elements in other Cretaceous wood assemblages. Most magnoliids represent Lauraceae (~seven wood types), a dominant element in modern Asian tropical and subtropical vegetation. Assignment of these woods to the family Lauraceae is supported by the presence of idioblasts containing dark contents presumed to represent oil cells characteristic of modern Lauraceae. The McRae lauraceous woods represent multiple genera and include xyloids differentiated by axial parenchyma distributions ranging from scarce to confluent. The remaining xyloids represent eudicots. Two genera (*Agujoxylon* and *Metcalfeoxylon*) with exclusively scalariform perforation plates co-occur in assemblages in the southwest of North America. Four xyloids have a combination

of exceptionally wide (>10 cells wide) and nearly homogeneous rays, wood anatomical features that characterize extant *Platanus*. The exclusively solitary vessels and scalariform perforation plates are considered ancestral to extant *Platanus* and suggest the woods represent a stem lineage of modern Platanaceae. The *Platanus*-like woods fall outside the generic limits for *Platanoxylon*, warranting a new genus. While extant Platanaceae is represented by a single genus with few species, an extensive record of fossil leaves and reproductive structures documents a major radiation and diversification of the family Platanaceae during the mid- to Late Cretaceous and supports recognition of a new fossil genus for early *Platanus*-like woods. The Forest of Giants is an assemblage of exceptionally large angiosperm *in situ* stumps and logs that represent a riparian forest preserved in a sequence of fluvial sandstones. Four wood xylotypes have been recognized. The site is dominated by one species of *Paraphyllanthoxylon*-like wood with anatomical features that, in a wood where oil cells are not present, suggest affinity with the extant clade [Kirkiaceae [Burseraceae + Anacardiaceae]] within Sapindales. The presence of ray cells interpreted as gum cells in at least some specimens supports Kirkiaceae as the probable modern affinity for some, if not all the *Paraphyllanthoxyon*-like woods. One McRae *Paraphyllanthoxylon*-like stump is the largest Cretaceous angiosperm stump yet recorded worldwide (2 m in stem diameter). Three individual stumps represent probable Lauraceae, Sapotaceae and

Urticales (Rosales). The Forest of Giants xyloypes have features that are common in tropical woods, including the absence of well-defined growth rings and presence of large vessels vulnerable to freeze-induced embolisms. Woods from the Forest of Giants add to a growing body of evidence from *in situ* assemblages for large angiosperms as the dominant tree form in some localities during the Late Cretaceous, especially in regions of warmer climate such as the southern Western Interior of North America. Affinities of most woods with simple perforation plates are, as yet, unidentified. The McRae Formation flora will provide unique insight into the stature and diversification of angiosperms at a critical period in their radiation.

*Keywords:* McRae Formation, Jose Creek Member, South-central New Mexico, Late Campanian, Late Cretaceous, fossil angiosperm wood, *Laurinoxylon*, Lauraceae, *Platanoxylon*, *Plataninium*, *Platanus*, Platanaceae, *Paraphyllanthoxylon*, Kirkiaceae, Urticales, Sapotaceae.

I. FOREST OF GIANTS: AN *IN SITU* ANGIOSPERM FOREST OF LATE CRETACEOUS  
(CAMPANIAN) SOUTH-CENTRAL NEW MEXICO, USA

ABSTRACT

A fossil forest of well-preserved, *in situ* angiosperms provides important data on Late Cretaceous angiosperm stature, diversity and ecology. The assemblage, from the Jose Creek Member of the McRae Formation, south-central New Mexico, USA, is of late Campanian age ( $75.0 \pm 1.1$  Ma to  $73.2 \pm 0.7$  Ma, zircon U–Pb dating). The assemblage consists of at least 15 *in situ* angiosperm stumps and 5 angiosperm logs that represent riparian forest preserved in a sequence of fluvial sandstones. Four angiosperm fossil woods (xylotypes) have been discovered. The first is assigned as a new species to the fossil genus *Laurinoxylon*. This xylotype has exclusively simple perforation plates and scanty paratracheal axial parenchyma, which are consistent with the extant Lauraceae *Ocotea* complex. To recognize the possible phylogenetic position of the fossil, a new subgenus is warranted within *Laurinoxylon*. The second xylotype has possible affinities within the “Urticales” families of Cannabaceae, Moraceae and Urticaceae (Rosales). This xylotype is characterized by common uniseriate rays, multiseriate rays with several marginal rows of square and upright cells and predominantly paratracheal, vasicentric, lozenge-aliform or unilateral axial parenchyma. The dominant Paraphyllanthoxylon-like xylotype closely resembles Kirkiaceae. Its features include vessels that are solitary and in radial multiples of 2–3, simple perforation plates, alternate intervessel pits, scanty paratracheal axial parenchyma, rays 2 – 3 (up to 5) seriate, and septate fibers. These wood anatomical features suggest affinity with extant Kirkiaceae in the clade [Kirkiaceae

[Burseraceae + Anacardiaceae]] within Sapindales. Affinities with Laurales have been proposed for species with similar features (absent gum cells) placed within *Paraphyllanthoxylon*. The fourth xylotype is unique among McRae types in having diffuse-porous to semi-ring porous wood and axial parenchyma forming regular lines 1–3 cells wide. These features, in addition to a tendency for diagonal vessel arrangement, vessel-ray parenchyma pitting with distinct borders or with reduced borders, common uniseriate rays, and multiseriate rays with marginal rows of square or upright cells, suggest affinity to extant Sapotaceae. This is the earliest record for a fossil wood attributed to Sapotaceae and it will be assigned to a new genus.

While reports of large angiosperm woods, especially *in situ* assemblages, are limited, the fossil record supports Cretaceous angiosperms varied from herbaceous to large tree forms. This Forest of Giants contains the world's largest known Cretaceous angiosperm tree, with a 2.0 m stem diameter at the top of the buttress roots. Stem diameters for the Forest of Giants stumps and logs range from 0.4 m – 2.0 m (average = 1.0 m). Using different tree equations, tree height estimates range between 12 – 29 m and 20 – 64 m. The McRae xylotypes have features that are common in tropical woods, including the absence of well-defined growth rings and presence of large vessels vulnerable to freeze-induced embolisms. The Forest of Giants adds to a growing body of evidence from *in situ* assemblages for large angiosperm trees as dominants in some localities during the Late Cretaceous, especially in regions of warmer climate such as the southern Western Interior of North America.

*Keywords* – Angiosperm, fossil wood, Late Cretaceous, *Paraphyllanthoxylon*, *Laurinoxylon*, Sapotaceae, Kirkiaceae

## INTRODUCTION

The Forest of Giants locality comprises the largest reported Campanian assemblage of colossal *in situ* stumps and logs that represent the remains of a riparian forest exposed in the sandstones of the Jose Creek Member of the McRae Formation in south-central New Mexico, USA. Cretaceous floras, in all environments, are of continued interest, as the cataloging of species in various habitats informs understanding of the progress of diversification and radiation of angiosperms at a crucial point in their emergence and eventual rise to dominance. A well-constrained age for the member,  $75.0 \pm 1.1$  Ma to  $73.2 \pm 0.7$  Ma based on U-Pb dates (Mack et al. 2015, Amato et al. 2017) enhances the value of the findings.

The exceptional size of the Forest of Giants specimens (up to 2.0 m stem diameter measured above the buttress roots) is noteworthy. Because the spatial and temporal relationship of the individual stumps cannot be determined due to stratigraphic uniformity at the site, it cannot be determined over what time interval these large stature trees dominated the area. Represented by single stumps scattered among the dominant xylotype are three specimens tentatively identified as *Laurinoxylon* sp. (Lauraceae), Sapotaceae and Urticales (Rosales). Absence of small diameter axes at the site suggests that understory species were not preserved. No specimens of conifer were found, providing additional insight into the species association.

The Forest of Giants adds to a growing body of evidence that large canopy-

forming angiosperm trees not only existed (Crane 1987, Wolfe and Upchurch 1987, Wing and Boucher 1998), but dominated in stature in some southern latitude habitats by latest Cretaceous. This extends our understanding of the role of angiosperms in the vegetation of the southern Western Interior of North America during the Late Cretaceous (Late Campanian), possibly reflective of the early importance of large angiosperms in warmer climates relative to floras at higher latitudes (Wing et al. 1993, Wing and Boucher 1998, Wing et al. 2012). This supports a latitudinally graded pattern in the angiosperm rise to dominance.

This paper describes four angiosperm fossil woods that encompass the diversity of the Forest of Giants assemblage. It continues the investigation of fossils from the Jose Creek Member of the McRae Formation which to date include approximately 35 non-monocot angiosperm fossil wood species, several monocot angiosperm wood species, about 6 conifer wood species and over 100 species of leaves and reproductive structures. (Upchurch and Mack 1998, Estrada-Ruiz et al. 2012a, 2012b, 2018).

## GEOLOGIC SETTING

The Forest of Giants is a collection of exceptionally large stumps preserved *in situ* in a series of fluvial overbank sandstones and logs preserved in cross-bedded fluvial sandstones. The locality occurs low in the Jose Creek Member of the McRae Formation in south-central New Mexico. These Upper Cretaceous sediments are exposed in the northwestern part of the Love Ranch Basin (Seager et al. 1986, 1997, Amato et al. 2017) in the southern San Andres Mountains near Truth or Consequences, New Mexico (Mack et al. 1998). During the Late Cretaceous, this site

was about 200 km inland from the Western Interior Seaway (Roberts and Kirschbaum 1995) at approximately 39° paleolatitude (Upchurch et al. 2015).

The original Lozinsky et al. (1984) estimate of the minimum age of the McRae Formation based on “index fossils” and the occurrence of *Tyrannosaurs rex* in the upper Hall Lake Member (Gillette et al. 1986) strongly supported a Lancian age (late Maastrichtian) for the Hall Lake Member. Upchurch and Mack (1998) proposed a middle to lower Maastrichtian (possibly late Campanian) age for the underlying Jose Creek Member, based on late Maastrichtian vertebrates from the Hall Lake Member and numerous species of conifer macrofossils shared with the Vermejo Formation. A late Campanian age is now indicated for the Jose Creek Member, based on U-Pb dating of zircons from volcanic ashes and a dacite clast from the Jose Creek Member. These give an age for the Jose Creek Member of  $75.0 \pm 1.1$  Ma to  $>73.2 \pm 0.7$  Ma (Amato et al. 2017).

## MATERIALS AND METHODS

The fossil woods described herein were collected from the Jose Creek Member of the Upper Cretaceous McRae Formation in south-central New Mexico. Samples were obtained from a large assemblage of *in situ* stumps and logs (Forest of Giants) found scattered atop and along hillsides of a remote area of the Armendaris Ranch. The size of the stumps and logs indicates that the environment was sufficiently stable, at least intermittently, to allow growth of large trees, while evidence that sandstone encases the woods indicates deposition in one or more high-energy events. Lack of obvious stratification and the dip of the beds made it impossible to determine whether the stumps came from the same bed. Few stumps

remained intact. Most showed evidence of heart rot and had deteriorated to mounds of cobble-sized pieces that were determined to be stumps or logs by noting the convergence of rays clearly visible on rock surfaces. A decision was made to collect samples only from identifiable stumps and logs since it was not possible to differentiate between unrelated float and debris traceable to a stump or log. This was because the float showed no differences in mineralogy or anatomy that were visible in the field with a 20X hand lens. No conifer woods or fossil leaves were found. Minimum stem diameter was estimated by locating the approximate center of the trunk, measuring along the longest ray to determine the radius and then multiplying by two. These measurements surely underestimate the original diameter because the outermost portion of stumps were not preserved. The length of logs and height of intact stumps was recorded. If buttress roots were present, their diameter was measured. Samples for wood anatomy were collected from the periphery of each trunk and near the center of each trunk where it was possible to obtain material. GPS coordinates and photographs were taken for each stump and log. Metal tags with the locality number and assigned stump or log number were placed near each entity for easy relocation and to identify it for future studies.

### **Slide preparation**

Slides were prepared by cutting blocks exposing transverse (TS), tangential (TLS) and radial (RLS) faces from mature wood (periphery) samples, and the blocks affixed to glass slides using Norland Optical Adhesive 72. Exposing the adhesive to UV light (standard blacklight bulb) for 16 hours was sufficient to hold blocks in place for sectioning and grinding to the desired thickness. Coverslips were affixed

with the same Norland Optical Adhesive 72 to avoid optical problems that might result from using different adhesive and mounting mediums. Slides were labeled with the year and site location, 2012-48, the Stump or Log number, and numbered according to the angle of cut (i.e., X-1, X-2; T-1; R-1).

Slides were observed, measurements and photographs taken using a Nikon Eclipse 50i microscope and a Nikon DS-Fi1 camera head and Nikon DS-L2 camera control unit. Observations were made and recorded following the recommendations of the International Association of Wood Anatomists Committee (1989). Possible affinities were selected by searching the InsideWood online database (InsideWood 2004–onward; Wheeler 2011), and compared to details in Metcalfe and Chalk (1950) and relevant literature cited with the InsideWood descriptions.

Woods are identified by the abbreviation TXSTATE and a sequential specimen number. Taxonomic names follow APG IV (Stevens 2001 onwards, Chase et al. 2016) and Cantino et al. (2007). Slides and remnant pieces of woods are housed in the Texas State University Paleobotanical Collections, San Marcos, Texas. Locality data are archived in the Texas State University Paleobotanical Collections. The exact locality information is not provided here because the material was collected on private land, and looting of fossil wood localities is common in the American West.

## DESCRIPTIONS

### **McRae Group IA sp. 1, Lauraceae**

*Clade* – Magnoliid

*Order* – Laurales

*Family* – Lauraceae

*Genus* – *Laurinoxylon* Felix

*Subgenus* – proposed

*Subgeneric diagnosis* – Wood diffuse porous. Vessels solitary and in short radial multiples, mean tangential diameters small to medium (50-200  $\mu\text{m}$ ); exclusively simple perforation plates; intervessel pits alternate; vessel-ray parenchyma pits oval to horizontally or diagonally elongate. Axial parenchyma scanty paratracheal to vasicentric. Rays 2–6-seriate, rarely uniseriate and rarely >1 mm in height, heterocellular, all procumbent or with usually one row of marginal square to upright cells; idioblasts associated with rays.

*Species* – McRae Group IA sp. 1

*Specific diagnosis* – Wood diffuse porous. Vessels solitary and in short radial multiples, mean tangential diameters medium (100-200  $\mu\text{m}$ ); exclusively simple perforation plates; intervessel pits alternate, small to medium 6-10  $\mu\text{m}$ ; vessel-ray parenchyma pits oval to horizontally or diagonally elongate. Fibers septate and non-septate. Axial parenchyma scanty paratracheal. Rays 2–6-seriate, rarely uniseriate and rarely >1 mm in height, heterocellular, all procumbent or with usually one row of marginal square to upright cells; idioblasts (“oil cells”) large, common in ray margins and occasionally within the ray body.

*Holoxylotype* – TXSTATE 1250 (Fig. 1.2–1.4).

*Stratigraphic horizon* – McRae Formation, Jose Creek Member

*Age* – Late Campanian

*Material* – *In situ* stump with stem diameter of 0.6 m (Fig. 1.2)

*Locality* – Texas State University Paleobotanical Locality 2012-48

*Description* – *Growth rings* absent. *Wood* diffuse porous (Fig. 1.3A). *Vessels* solitary (25%) and in radial multiples of 2–3 (5) (mostly 2), average 12 (SD 2, range 9–16) mm<sup>2</sup>, solitary vessels oval in outline, average tangential diameter 127 (SD 23, range 57–160) μm; vessel element length average 359 (SD 117, range 193–694) μm (Fig. 1.3B); perforation plates exclusively simple; intervessel pits alternate, rounded in outline, small to medium, 6–10 μm in diameter (Fig. 1.3D). *Vessel-ray pits* not well preserved, oval to horizontally elongate (Richter Type II) (Richter 1981) (Fig. 1.3E–F); *vessel-axial parenchyma pits* similar to vessel-ray pits. *Tyloses* common, thin-walled (Fig. 1.3C). *Fibers* angular in cross section, thin-walled to thick-walled (Fig. 1.3G), pits not observed, septate (Fig. 1.4A) and nonseptate. *Axial parenchyma* scanty paratracheal (Fig. 1.4B), more than eight cells per parenchyma strand. *Rays* 2–6 (mostly 4–5) seriate (Fig. 1.4C), multiseriate rays homocellular composed of procumbent cells or heterocellular with 1 marginal row of upright or square cells (Fig. 1.4D), procumbent cells of variable size, often larger at the margins; ray height average 20 (SD 10, range 6–48) cells or average 557 (SD 283, range 209–1411) μm, rarely > 1mm μm high; average 9 (SD 1, range 7–11)/mm; uniseriate rays not

observed. *Oil cells* common, large, at the ray margin (Fig. 1.4D–E) or occasionally at side of ray (Fig.4F).

*Description in IAWA Hardwood List codes (IAWA Committee 1989) –*

2 5 13 22 23 25 26 32 42 47 53 56 65 66 78 94 98 102v 104 106 115 124

### **Comparison to extant woods**

The combination of anatomical features diffuse porous wood (5p), vessels solitary and in short radial multiples (9a 10a), simple perforation plates (13r 14a), alternate intervessel pitting (22r), pits not minute (24a), libriform fibers (60a 62a), septate and non-septate fibers (65p 66p), axial parenchyma scanty paratracheal (78p 80a 83a 85a 86a 89a), rays not exclusively uniseriate (96a), multiseriate rays mostly (4-5) cells wide (98p 99a), and heterocellular (105a 106p 108a), rays composed of procumbent cells with mostly 1 row square and upright cells, storied structure absent (118a 119a 120a), and idioblasts (“oil cells”) associated with ray parenchyma (124p) occurs in the family Lauraceae (Metcalf and Chalk, 1950; Stern 1954, Richter 1981; InsideWood-2004 onwards).

A search of the InsideWood database (InsideWood 2004-onwards, Wheeler 2011) using the above codes retrieved four genera of Lauraceae (*Aspidostemon*, *Caryodaphnopsis*, *Litsea*, and *Nectandra*). Conducting the search allowing 1 “mismatch” identified a single genus in each of seven families (Asteraceae, Burseraceae, Capparaceae, Kirkiaceae, Lamiaceae, Pittosporaceae and Solanaceae), all with a “mismatch” feature indicating the absence of oil cells, which excluded them from consideration. The search also retrieved six additional genera of Lauraceae (*Endlicheria*, *Laurus*, *Lindera*, *Neolistea* and *Ocotea*), all with the

“mismatch” feature of rays < 4-seriate, and *Persea* with a “mismatch” feature of axial parenchyma vasicentric, rather than scanty paratracheal.

The McRae Group IA sp. 1 is distinguished from *Caryodaphnopsis* by having rays generally <1mm tall while those of *Caryodaphnopsis* frequently exceed 2 mm in height, a distinguishing feature for the genus (van der Werff and Richter 1985); according to Detienne (Woods of Madagascar. CIRAD Unpublished), *Aspidostemon* species differ in having a tendency to storied rays; most species of *Endlicheria*, *Larus*, *Lindera* differ by having both simple and scalariform perforation plates (Richter in Metcalfe 1987, InsideWood 2004-onwards), as do many species of *Litsea* and *Neolisteia* (InsideWood 2004-onwards). This McRae wood shares some features with species of *Nectandra*. While many *Nectandra* species have both simple and scalariform perforation plates, a subset resemble the McRae Group IA sp. 1 by having only simple perforation plates and only scanty paratracheal axial parenchyma, though most *Nectandra* species have vasicentric or aliform to confluent axial parenchyma. The McRae wood is most consistent with species of *Ocotea* in which most species have simple perforation plates, many with only scanty paratracheal axial parenchyma, and some with oil cells associated with rays only. Vessel-ray pitting in *Ocotea* is similar to the McRae fossil in some species (e.g., *Ocotea leucoxydon*, *O. usambarensis*); however, pits are often larger and rounded, as opposed to the elongated pits in the fossil. Intervessel pit size in extant species is generally larger, but overlaps with the fossil. The fossil has wider rays; rays of *Ocotea* rarely reach 4-seriate (InsideWood 2004-onward), while the fossil’s rays are mostly 4–5-seriate.

## **Comparison to fossil woods**

Initially, the comparisons to other fossil woods were not focused on woods attributed to Lauraceae. It started with a search of the InsideWood fossil wood database to determine if similar woods had been attributed to families other than Lauraceae. When Lauraceae again emerged as the most probable affinity, a comparison was made to the most similar fossil Lauraceae species in *Laurinoxylon* and *Ulminium* (a name rejected in favor of the conserved name *Laurinoxylon* by Doweld 2017) from the InsideWood database and the literature. Finally, the wood was compared to the generic diagnoses and type species descriptions of fossil genera within the family Lauraceae to ascertain if the fossil fell within an existing generic diagnosis.

**Comparison to fossil woods identified through a search of the InsideWood database.** A search of the InsideWood database using a feature code array similar to that used in the extant wood search (i.e., 5p 9a 10a 13p 14a 22p 36a 60a 62a 65p 78p 80a 83a 85a 86a 89a 96a 98p 99a 105a 106p 108a 118a 119a 120a 124p) with 0 mismatches identified species attributed to Lauraceae plus one species of Adoxaceae. Expanding the search to 1 “mismatch” returned many more species attributed to Lauraceae, as well as woods in eight additional families (e.g., Akaniaceae, Anacardiaceae, Burseraceae, Euphorbiaceae, Fagaceae, Malvaceae, Phyllanthaceae and Verbenaceae), and woods where affinity has not been established. While these woods shared basic anatomical features, all woods attributed to families other than Lauraceae captured by the search had a “mismatch” feature indicating the absence (or questionable presence) of oil cells, excluding

them as probable matches for this McRae wood (InsideWood-2004 onwards). For example, the search returned *Paraphyllanthoxylon vancouverense* Jud et al. (2017) as a potential match (Table 1.1). The *P. vancouverense* vessel, axial parenchyma and ray characteristics resemble the McRae Group IA sp. 1. However, the distribution and size of enlarged ray cells observed in *P. vancouverense* did not match those of this McRae fossil and the presence of enlarged cells could not be confirmed in radial view of *P. vancouverense*. Thus, *P. vancouverense* was excluded.

Of those woods not definitively attributed to Lauraceae, a Page (1980) Group XIA wood, (sample CASG 60443) is similar to the McRae Group IA sp. 1. Differences include a high percentage of solitary vessels in the Page sample, smaller diameter vessels, longer vessel elements, the presence of uniseriate rays (though infrequent), and rays with more upright margin rows. Perhaps most significantly, Page does not assert that oil cells are present, rather cells are described as enlarged and possibly crystalliferous. The InsideWood database indicates large cells are variably associated with rays, but does not confirm they are oil cells. However, neither account of CASG 60443 describes cells comparable to the oil cells observed in the McRae Group IA sp. 1.

The Denver Basin sample, DB.D1 Xylo type 4b (Lauraceae), is described as having enlarged ray marginal cells that appear similar to the McRae Group IA sp. 1, but the cells were not conclusively oil cells. Rays are narrower (2-4 cells wide) and shorter (average 324  $\mu\text{m}$ ), and vessel density is more than double that of the McRae Group IA sp. 1, making the wood an unlikely match (Wheeler and Michalski 2003).

**Comparison to *Laurinoxylon (Ulminium)* species.** Woods of *Laurinoxylon* species similar to McRae Group IA sp. 1 were retrieved from the InsideWood fossil database, both through the use of the feature code search and by scanning all fossil woods attributed to Lauraceae (Table 1.1). No exact match was found. *Laurinoxylon neagui* Iamandei and Iamandei (1977) and *L. ehrendorferi* Berger (1953) differ in having wider vessels and vasicentric axial. *Laurinoxylon ehrendorferi* has narrower rays and oil cells in axial parenchyma. As the name implies, *L. microtracheale* Süss (1958) is differentiated by having relatively small vessel diameters, as well as higher vessel density, minute intervessel pits, and small, bordered vessel-ray pits. *Laurinoxylon. aff. czechense* (Prakash, Březinová and Bůžek) Mantzouka, Karakitsios, Sakala and Wheeler (2016), *L. namsangensis* Lakhanpal, Prakash and Awasthi (1978), *L. perseamimatus* Petrescu (comparison based on InsideWood–2004 onward), and *L. stichkai* Boonchai and Manchester (2012) differ in having narrower rays (up to 3 cells wide). *Laurinoxylon. aff. czechense* (Prakash, Březinová and Bůžek) Mantzouka, Karakitsios, Sakala and Wheeler, and *L. stichkai* Boonchai and Manchester report vessels in clusters, though rarely. *Laurinoxylon stichkai* differs by having oil cells in axial parenchyma.

The fossil wood most closely resembles *Ulminium porosum* Wheeler, Scott and Barghoorn (1977) (treated as *Laurinoxylon porosum* by Dupéron - Laudoueneix and Dupéron 2005, Gregory et al. 2009), from the early middle Eocene Gallatin Fossil Forest and Amethyst Mountain of Yellowstone National Park, Wyoming. Both woods have diffuse porosity, vessels solitary or in radial multiples mostly 2-3, with a slight tendency for diagonal arrangement (observable, though not pronounced in

the McRae Group IA sp. 1). Axial parenchyma distribution is comparable. Uniseriate rays are rare or absent in both woods. Multiseriate ray width, height and cellular composition, and the position and size of oil cells (at the ray margin) are similar. *Ulminium porosum* differs from this McRae wood in having indistinct growth boundaries, somewhat smaller vessel diameters and higher vessel density. Septate fibers are not reported for *U. porosum*. Vessel-ray pits are larger, rounder and appear to have more reduced borders than the McRae fossil, but comparison of vessel-ray pit borders was hindered by the quality of preservation in the McRae wood, which is unfortunate, because vessel-ray pitting is an important feature for differentiating lauraceous species (Richter 1981, Richter in Metcalfe 1987, Gottwald 1992, 1997). Richter also considered the presence/absence of septate fibers to be of value in differentiating taxa (Richter in Metcalfe, 1987); the McRae fossil has septate fibers. Finally, Wheeler et al. 1977 noted the unusually high vessel density of *U. porosum*, a feature not shared by the McRae wood. Therefore, while the McRae Group IA sp. 1 is similar to *U. porosum*, it is not conspecific.

#### **Comparison to fossil genera and / or type species attributed to**

**Lauraceae.** A number of lauraceous fossil wood genera have been proposed. Comparison of the McRae fossil wood to the generic diagnoses and type species descriptions (Table 1.2) did not yield an exact match. *Paraperseoxylon scalariforme* (Scott and Wheeler) Wheeler and Manchester 2002, *Ocoteoxylon tigurinum* Schuster 1906, *Cinnamomoxylon areiosum* Gottwald 1997, and *Sassafrasoxylon lipnicense* Brezinova and Süß 1988 all have some scalariform perforation plates. *Caryodaphnopsylon richteri* Gottwald 1992 has very wide and very tall rays.

*Beilschmiedioxylon africanum* Dupéron -Laudoueneix and Dupéron 2005 and *Cryptocaryoxylon gippslandicum* Leisman 1986 have banded axial parenchyma, and *Machilusoxyton hindusthanensis* Bande 1971 (as emended by Ingle 1974) has vasicentric (1–2 cell sheath) axial parenchyma rather than scanty paratracheal. *Mezilaurinoxylon eiporosum* Wheeler and Manchester (2002) differs by having Richter Type “c” (large and window-like) vessel-ray parenchyma pitting, unlike the elongate pitting observed in the McRae fossil, and oil cells that are not common and only slightly enlarged in radial view. *Olmosoxyton upchurchii* Estrada-Ruiz, Martinez-Cabrera and Cevallos-Ferriz 2010 has a high percentage of solitary vessels, Richter type “b” and “c” vessel-ray parenchyma pitting, rays that are taller, more homogeneous and “grouped,” and oil cells that are neither large nor located primarily at the ray margin.

The generic diagnosis for *Laurinoxylon* as emended by Dupéron et al. (2008) encompasses the McRae fossil, though the McRae wood is distinctly different than the type specimen. *Laurinoxylon diluviale* (Unger) Felix (1883) emend. Dupéron et al. (2008) differs from the study wood by having distinct growth boundaries, vessels diffuse to semi-porous, solitary and in radial multiples of 2-7, simple and scalariform perforation plates, non-septate fibers (septate fibers not reported), and axial parenchyma in vasicentric sheaths 1-2 cells wide.

### **Remarks**

The anatomical features of the McRae Group IA sp. 1 are most similar to the genus *Ocotea* and, to a lesser degree, a subset of species in *Nectandra*. While the phylogenetic relationships within Lauraceae are not completely resolved, a

relationship between *Ocotea* and *Nectandra* has long been recognized. The Stern (1954) summary of early taxonomic treatments for Lauraceae illustrates the difficulty experienced by numerous botanists as they delimited genera and attempted to establish phylogenetic relationships within the family. While the use of different morphological characters resulted in different groupings of genera (Stern 1954, Kostermans 1957, Richter 1981, 1996) *Ocotea* and *Nectandra* were consistently closely associated in the various treatments. Kosterman's 1957 classification recognized the association between *Ocotea* and *Nectandra* based on floral characters. The van der Werff and Richter (1996) phylogenetic classification integrated inflorescence structure and wood and bark anatomy, including axial parenchyma distribution, fibers as septate or non-septate and vessel morphology, features readily observable in fossil woods. Within the framework of van der Werff and Richter, the McRae fossil's anatomical features fall within the tribe Perseeae Nees (which included *Ocotea* and *Nectandra*), a grouping of mostly neotropical genera united in their wood anatomy by the absence of marginal parenchyma and the presence of septate fibers. Chanderbali et al. (2001) further explored the phylogeny of Lauraceae with evidence from chloroplast and nuclear genomes, defining a Perseeae Laureae clade that included an *Ocotea* complex that, again, included *Ocotea* and *Nectandra*. The 2005 molecular study by Rohwer and Rudolph confirmed the association of these genera in the Cinnamomeae within their core Lauraceae.

The use of wood anatomy as the basis of phylogeny has long been recognized as problematic. Early workers observed that species of Lauraceae are not easily

distinguished on the basis of wood anatomy (Stern 1954). Stern offered a hypothesis for the difficulty, noting that the apparent variability found within subfamilial taxa might be caused by the choice of taxonomic characters used to circumscribe groups, a sentiment echoed by Richter (1981, in Metcalfe 1987). Richter (in Metcalfe 1987) later observed that wood anatomy of Lauraceae is not as uniform as had been suggested (Metcalfe and Chalk 1950). While there is overlap within and between groups of genera, some smaller genera can be distinguished on the basis of wood anatomy alone. He found some anatomical features (e.g., axial parenchyma distribution, intervessel and vessel-ray parenchyma pitting, and perforation plate composition) to be significant for delimiting taxonomic groups, with others (e.g., oil cell distribution and size and vessel arrangement) informative only at the species level. The *Ocotea* complex as defined by Chanderbali et al. (2001) and the Cinnamomeae (a subset of Core Lauraceae) recognized by Rowher and Rudolph (2005) are united by two of the anatomical features Richter thought significant for Lauraceae. They have exclusively simple perforation plates and scanty paratracheal or vasicentric axial parenchyma.

Fossil woods that are similar to woods of the *Ocotea* complex and the Cinnamomeae fall within the diagnosis of the fossil genus *Laurinoxylon*, as does the McRae fossil. The genus was not proposed within a phylogenetic context to imply relationship between fossil woods and a particular extant genus or clade. Rather, the original diagnosis (Unger 1842, 1847) reflected anatomical features of a single wood. Over time, recognition of anatomical oversights in descriptions of the *Laurinoxylon* type material led to changes in the diagnosis that have broadened the

scope of the genus to encompass woods with anatomical features found in multiple extant genera assigned to the Chanderbali et al. (2001) Perseeae Laureae clade and the Rohwer and Rudolph (2005) core Lauraceae.

The majority of lauraceous fossil woods have been placed in either *Laurinoxylon* Felix or the synonymous genus *Ulminium* Unger. The history of the source material for the type specimen upon which both generic names were based has been recounted in detail (Dupéron et al. 2008). While both genera were based on the same type specimen, the original diagnoses for the genera differed. Unger (1842, 1847) described and illustrated the type, *Ulminium diluviale*, as having both simple and scalariform perforation plates, but he did not report the presence of idioblasts, although he clearly includes them in the illustration. Felix (1883) proposed changing the name to *Laurinoxylon* when he observed idioblasts and he stated that he could not confirm the presence of scalariform perforation plates. Dupéron et al. (2008) re-examined the type specimen and emended the *Laurinoxylon* diagnosis to confirm the presence of both simple and scalariform perforation plates. In the interim, woods with both character states (exclusively simple vs. both simple and scalariform perforation plates) have been called *Laurinoxylon* or *Ulminium*. A proposal by Doweld (2017) to conserve the name *Laurinoxylon* over *Ulminium*, if adopted, would clarify the nomenclatural issue.

The McRae fossil is assigned to the form genus *Laurinoxylon*. However, the wood shares anatomical features with extant genera whose relationship has been recognized in multiple phylogenetic analyses and are currently recognized as part of a clade within the core Lauraceae (or Perseeae Laureae). To place this wood in a

phylogenetic context, I am proposing a subgenus within *Laurinoxylon* for lauraceous fossil woods with exclusively simple perforation plates and axial parenchyma limited to scanty paratracheal to vasicentric.

Bailey's 1924 prediction is relevant:

“Accumulations of ... form-genera will be attacked by future ‘splitters’ and ‘lumpers’, and, as more reliable information concerning the vascular tissues of the Dicotyledons as a whole becomes available, will be assigned to more specific genetic relationships.”

### **Biogeography**

If affinities suggested for this fossil are correct, there are biogeographic implications. The McRae Formation is dated at 76.5-72.5 Ma (Amato et al. 2017). Chanderbali et al. (2001) estimated the probable radiation of the terminal Perseeae-Laureae clade from North Africa to Laurasia at  $44 \pm 7$  Ma (Early Tertiary). The Rohwer and Rudolph (2005) study accepted that date as the best available estimate, in absence of new fossil evidence. The age of this McRae wood suggests that Perseeae-Laureae were in North America prior to that estimated date. The McRae fossil cannot be assigned unambiguously to one extant genus, but the similarity to members of a terminal lauraceous clade may at least help establish the age of a stem lineage (Renner 2005). The uncertainty of the fossil placement at the stem node vs. a crown node would be problematic if it were used as a calibration fossil, given that an incorrect position could contribute to error in the age estimate, either to younger age bias or age overestimation, respectively (Bell and Donoghue 2005). The uncertainty is less an issue if the fossil is used merely to test the latest age estimate.

The fossil represents either the stem of the Perseeae-Laureae clade or the crown, so if the molecular age estimate postulates neither as being present in North America by 76.5-72.5 Ma, the molecular age estimate is in question. Recognition of incongruence between the fossil evidence and the most current molecular date is a necessary geologic test in the ongoing development of molecular dating methods (Wilf and Escapa 2015, 2016).

This fossil evidence, in combination with a growing number of examples of Lauraceae in North America during the Cretaceous and early Cenozoic, may ultimately influence the parameters used to estimate the Eocene radiation of this group. It is hoped that affinity of the remaining McRae lauraceous fossil woods can be assigned with greater confidence, and that descriptions of multiple woods may spur interest, where reports of isolated fossils are sometimes dismissed. For example, an Antarctica Late Cretaceous wood attributed to *Sassafras* (*Sassafrasoxylon gottwaldii*) (Poole et al. 2000), possible evidence of early establishment of the Perseeae-Laureae in Gondwana, was discounted on the grounds that it was more likely an example of convergence (Rohwer and Rudolph 2005). Such conclusions might warrant reevaluation as isolated fossils fit into a larger pattern.

### **Other fossil evidence**

The number of reports for Cretaceous Lauraceae from North American (wood, leaves and floral and reproductive structures) is growing. Page (1967) described two woods from the Upper Cretaceous Panoche formation in California as species of *Ulminium* Unger (Lauraceae), and Estrada-Ruiz et al. (2010) attributed

*Olmosoxylon* from the Olmos formation (Campanian-Maastrichtian) to Lauraceae. Estrada-Ruiz et al. (2018) described *Laurinoxylon rennerae* from the Jose Creek Member, McRae Formation (Late Campanian).

From the Jose Creek Member, McRae Formation, Upchurch and Mack (1998) informally reported the presence of pinnate lauraceous leaves with looped and curved secondary veins and a thickened marginal vein, features characteristic of Lauraceae. Elsewhere in North America, Upchurch et al. (1994) report three leaves attributed to Laurales *Dicotylophyllum ovato-decurrens*, *Landonia* cf. *L. calophylla* and aff. *Pabiania* sp. from the Lower Cretaceous (upper Albian) Potomac Group, VA. Upchurch and Dilcher (1990) described the Lauralen leaf species *Pabiania variloba* and three lauraceous leaf species in a new genus *Pandemophyllum* as *P. kvacekii*, *P. attenuatum*, and *P. sp.*, from the (now) latest Albian Rose Creek locality of the Dakota Formation of Nebraska. Lauralean cuticle from the site comprised six species in three genera (60% of lower-leaf cuticle), confirming the importance of Lauraceae in the assemblage. In Europe, the leaf genus *Eucalyptolaurus* is recognized as an early (latest Albian to Cenomanian) member of Lauraceae (Coiffard et al. 2009).

Lauraceae are often identified using epidermal characters from leaves or dispersed cuticle (Dilcher 1974, Upchurch 1995, Christophel et al. 1996, Nishida and van der Werff 2007, 2011). The taxonomic significance of cuticular characters is still being debated (Graham 2012), but the technique has been extensively studied and found to be useful in delimiting extant Lauraceae, particularly at the generic level (Dilcher 1974, Christophel et al. 1996, Nishida and van der Werff 2007, 2011). In North America, Lauraceae was found to be the most diverse group of Magnoliidae in

dispersed cuticle assemblages from the late Maastrichtian Sugarite Coal of the Raton Formation, NM, where Lauraceae and their close relatives comprised 23% of total cuticle fragments (Upchurch 1995). Lauraceae and their close relatives were also found as a significant component of an unnamed Maastrichtian coal from Starkville North (Upchurch 1995).

Outside of North America, one species of Lauraceae was identified from cuticle from the Cretaceous/Tertiary boundary on Seymour Island, Antarctica (Upchurch and Askin 1989) and Pole (2007) found Lauraceae to be a common element in dispersed cuticle assemblages in New Zealand from the Late Cretaceous onward.

Floral evidence includes *Neusenia*, a Santonian-Campanian fossil from the Neuse River locality in North Carolina (Eklund 2000), and *Potomacanthus lobatus*, a fossil flower from the Puddledock locality in Virginia (Early Cretaceous, Early to Middle Albian) (von Balthazar et al. 2007). *Mauldinia mirabilis* Drinnan, Crane, Friis and Pedersen (1990), a charcoalfied inflorescence, provided unequivocal evidence of Lauraceae in the mid-Cretaceous Potomac Group. A second unnamed species, *Mauldinia* sp., was reported for the Late Santonian of Georgia, USA (Herendeen et al. 1999). Other examples are: *Prisca reynoldsii*, latest Albian to earliest Cenomanian, KS, USA (Retallack and Dilcher 1981), *Perseanthus crossmanensis* (Turonian, of NJ, USA), which was compared to genera in *Perseeae* (Herendeen et al. 1994). Finally, the flower *Neusenia tetrasporangiata* (Early Campanian, NC, USA) compares to flowers of *Neocinnamomum* (tribe *Perseeae*), though it shares anther characteristics of *Cinnamomum* (Eklund 1999 in Friis et al. 2011).

**McRae Group IIIB sp. 4, Cannabaceae? Moraceae? Urticaceae?**

*Clade* – Core Eudicots

*Order* – Rosales

*Families* – Cannabaceae? Moraceae? Urticaceae?

*Genus* – New genus

*Generic diagnosis* – Wood diffuse-porous. Vessels solitary and in short radial multiples (mostly 2), <10 per mm<sup>2</sup>; perforation plates simple; intervessel pits alternate; vessel-ray parenchyma pits predominantly with reduced borders, oval to horizontally elongate. Axial parenchyma predominantly paratracheal, vasicentric, unilateral, lozenge-aliform or irregular or discontinuous confluent areas. Fibers non-septate. Rays 1–6 seriate, multiseriate rays composed of procumbent cells with mostly 1–2 (to 6) marginal rows of square or upright cells; uniseriate and some biseriate rays composed of only square and upright cells.

*Species* – McRae Group IIIB sp. 4

*Specific diagnosis* – Wood diffuse-porous. Vessels solitary and in radial multiples of mostly 2; perforation plates exclusively simple; intervessel pits alternate, medium; vessel-ray parenchyma pits with reduced borders, occasionally bordered, oval to somewhat horizontally elongate. Axial parenchyma nearly vasicentric, lozenge-aliform, unilateral or irregular or discontinuous confluent areas. Fibers non-septate. Rays 1–6 seriate; multiseriate rays composed of procumbent cells with mostly 1–2 (to 6) marginal rows of square or upright cells; uniseriate and some biseriate rays composed of only square and upright cells. Sheath cells not observed. Crystals not observed.

*Holoxylotype* –, TXSTATE 1287 (Fig. 1.5–1.7).

*Stratigraphic horizon* – McRae Formation, Jose Creek Member

*Age* – Late Campanian

*Material* – Description based on one sample collected from the periphery of an *in situ* stump measuring approximately 0.7 m in diameter (Fig. 1.7D)

*Locality* – Texas State University Paleobotanical Locality 2012-48

*Description* – *Growth ring* absent. *Wood* diffuse porous (Fig. 1.5A). *Vessels* solitary (64%) and in radial multiples of 2–3, average 3 (SD 1, range 2–5)/mm<sup>2</sup>, solitary vessels oval in outline, mean tangential diameter 127 (SD 26, range 57–177) µm; vessel element length average 423 (SD 119, range 105–630) (mostly > 300) µm (Fig. 5B); perforation plates exclusively simple (Fig. 1.5C); intervessel pits alternate (Fig. 1.5B), polygonal in outline, medium, 7–10 µm in diameter. *Vessel-ray pits* with reduced borders, oval to horizontally elongate (Fig. 1.5D), occasionally bordered (Fig. 1.5E). *Tyloses* common in wide vessels, bubble-like (Fig. 1.5F). *Fibers* angular in cross section, walls thin to medium-thick, non-septate (Fig. 1.5G). *Axial parenchyma* predominantly paratracheal, vasicentric (or nearly so) (Fig. 1.6A), unilateral (Fig. 1.6B), lozenge-aliform (Fig. 1.6C), occasionally confluent, confluent bands irregular, interrupted, usually only a few cells wide, seldom uniting more than a few pores, thin lines sometimes extending to small, somewhat isolated patches of parenchyma between vessels (Fig. 1.6D), 4–8 cells per parenchyma strand. Multiseriate rays 2–6 (mostly 5–6) seriate (Fig. 1.7A); heterocellular, made up of procumbent cells in the central portion, transitioning to square or upright cells near the margins, with

mostly 1–2 (Fig. 1.7B) (rarely up to 6) uniseriate marginal rows of upright or square cells at one or both ends (Fig. 1.7C), multiseriate regions occasionally vertically fused by short (several cells) uniseriate regions; ray height average 355 (SD 139, range 94–590)  $\mu\text{m}$ ; 23% of rays uniseriate, most uniseriate and some biseriate rays composed of all square and upright cells, uniseriate rays mostly <10 cells tall; all rays 6–11 per mm.

*Description in IAWA Hardwood List codes (IAWA Committee 1989) –*

2 5 13 22 23 26 30v 31 42 46 53 56 66 69 79 80v 81v 83v 84v 86v 93 98 106 107  
108v 115

### **Comparison to extant woods**

A search of the InsideWood database with the combination of anatomical features diffuse-porous wood (5p), vessels without diagonal arrangement (7a) solitary and in short radial multiples (9a 10a), exclusively simple perforation plates (13r 14a), alternate intervessel pitting (22p), intervessel pitting not minute (24a) vessel-ray pits with borders (30p) and with reduced borders (31p), vasicentric tracheids absent (60a), fibers without bordered pits (62e) and non-septate (65a 66p), fibers not very thick-walled (70a), axial parenchyma vasicentric (79p), lozenge-aliform (80p 81p), unilateral (84p), not in bands marginal (89a), axial parenchyma 4-8 cells per strand (90a 91a), multiseriate rays (2-6 cells wide) (98p 99a), not >1mm in height (102a) and heterocellular 104a, without storied structure (118a 122a), without oil cells (124e 125e), without axial or radial canals 127e 128e 129e 130e), without laticifers (132a), without included phloem or cambial variants (133a 134a 135a), selects no woods.

Allowing one or two mismatches in the InsideWood modern database search retrieves species in the monophyletic clade [Cannabaceae + [Moraceae + Urticaceae]]. The McRae fossil wood is most similar to five species of *Celtis* (Cannabaceae) retrieved in the search. The comparison of the fossil with the entire genus *Celtis* shows that some species, like the fossil, have multiseriate rays with several square and upright margin rows and rays < 1 mm tall. Vessel-ray pitting in *Celtis* varies from exclusively reduced borders to a combination of bordered and reduced bordered pitting to all bordered pits, not inconsistent with the fossil, which has predominantly reduced bordered pits with occasional bordered pits. *Celtis* species frequently have aliform and confluent axial parenchyma, with marginal axial parenchyma absent or variable in some species (Sweitzer 1971, InsideWood 2004-onwards).

The search indicated the genera *Cecropia* and *Myrianthus* and *Paurouma* (Urticaceae) which generally have aliform and confluent axial parenchyma as observed in the McRae fossil, but differ by having some marginal parenchyma and only occasionally having the combination of bordered and reduced bordered vessel-ray parenchyma pitting. The two genera of Moraceae (*Helicostylis* and *Morus*) also have aliform and confluent axial parenchyma, but species of *Morus* have marginal parenchyma and species of *Helicostylis* have latex tubes (Metcalf and Chalk 1950, InsideWood 2004-onwards). The combination of bordered and reduced bordered vessel-ray parenchyma pitting occurs in some genera of Moraceae, but is not characteristic of *Helicostylis* or *Morus* (InsideWood 2004-onwards).

The families of other species retrieved by the InsideWood modern database search are less similar to the McRae wood. *Petersianthus macrocarpus* (Lecythidaceae) differs by not having unilateral axial parenchyma. In general, Lecythidaceae species do not have aliform and confluent axial parenchyma and often have very thick-walled fibers (InsideWood 2004-onwards). Species of Anacardiaceae are not characterized by both bordered and reduced border vessel-ray parenchyma pitting and frequently have septate fibers and radial canals (Metcalf and Chalk 1950, InsideWood 2004-onwards). Species of Lauraceae generally have oil cells not found in the McRae wood (Metcalf and Chalk 1950, InsideWood 2004-onwards).

The families Cannabaceae, Moraceae and Urticaceae form a monophyletic clade within Rosales (Zerega et al. 2005, Zhang et al. 2011). Anatomical features shared among McRae Group IIIB sp. 4 and clade families supports association with the clade. However, the fossil anatomical features do not exactly correspond to the characteristics typical of an entire genus, making assignment to a specific family speculative. The fossil could represent a stem lineage below the clade. Uncertainty of placement warrants assignment to a fossil genus.

### **Comparison to fossil woods**

**Comparison to fossil genera attributed to [Cannabaceae [Moraceae + Urticaceae]].** A number of fossil wood genera are attributed to the [Cannabaceae [Moraceae + Urticaceae]] (Table 1.3a). These fossil wood genera share anatomical features with the clade families, but their diagnoses do not accommodate this McRae wood.

*Celtixylon dacicum* Petrescu (1978) and *Moroxylon sturmii* Selmeier (1993) differ from TXSTATE 1287 in having semi-ring-porous wood, larger or smaller vessel diameters ( $\leq 100$  or up to 350, respectively), vessels in clusters and prismatic crystals. In addition, helical thickenings in vessels are reported for *Celtixylon*. *Artocarpoxyylon kartickcherrieansis* Prakash and Lalitha (1978) differs in having some larger diameter vessels, large intervessel pitting, latex tubes and rays with fewer margin rows of square or upright cells. *Cudranioxyylon englismense* Dupéron Laudoueneix 1980 and *Myrianthoxyylon coppensi* Koeniguer 1975 differ in having axial parenchyma in broad, irregular, tangential bands, thick-walled fibers and rays with fewer margin rows of square or upright cells. Unlike TXSTATE 1287, uniseriate rays are reported as rare for *Myrianthoxyylon*. While similar to the fossil wood, *Scottoxyylon eocenicum* Wheeler and Manchester (2002) differs in having more vessels per mm<sup>2</sup>, taller rays, rarer uniseriate rays (compared to 23% uniseriate rays for TXSTATE 1287) and marginal axial parenchyma. Sheath cells (which cannot be confirmed for the McRae fossil) may be present in *S. eocenicum*. The description and illustrations of *Ficoxyylon tropicum* (Schleiden) Felix (1883) do not have enough information for a detailed comparison, but *F. tropicum* differs in having wider rays (up to 10 cells), the vasicentric sheath of axial parenchyma surrounding vessels is broader than TXSTATE 1287, and prismatic crystals are reported as present in axial parenchyma.

**Comparison to similar fossil woods found through a search of the InsideWood database and the subsequent literature review.** A search of the InsideWood database for fossil woods was done using these codes: 5p 7a 9a 10a 13p 14a 20a 21e 22p 30p 49a 50a 60a 62a 65e 75a 83p 89a 98p 99e 102a 107p 118a 124a 125a 130a 300r 301e allowing one mismatch.

Of the many families selected, the wood most consistent with the McRae Group IIIB sp. 4 (Table 1.3b) is from the Farafra Oasis, Egypt described by Kamal El-Din et al. (2006) as having possible affinity to Moraceae, although Kamal El-Din could not rule out affinity to Lauraceae or Anacardiaceae. The wood differs from the McRae fossil in having narrower rays, rays with only 1-2 margin rows of square or upright cells and rare uniseriate rays.

Also similar to TXSTATE 1287 are the Clarno Urticalean Wood Type I and II, two woods described by Wheeler and Manchester (2002) from the Nut Beds of the Eocene Clarno Formation, Oregon (Wheeler and Manchester 2002), which has features found in the (Rosales), either Moraceae, Ulmaceae, or possibly *Celtis* (Cannabaceae). While both woods are similar to McRae Group IIIB sp. 4 in having diffuse porous vessel arrangement, vessels solitary or in short radial multiples, simple perforation plates, alternate intervessel pitting with a range of pit diameters that overlaps the fossil wood, non-septate fibers, rays of similar width and cellular composition, mostly short uniseriate rays and similar ray density, neither Eocene wood is an exact match for TXSTATE 1287. Both have at least some growth ring boundaries (not observed in the McRae fossil), more vessels per mm<sup>2</sup>, and at least occasionally prismatic crystals. The Clarno Urticalean Wood Type I specimen also

has narrower vessels, axial parenchyma in wide bands and rays with sheath cells. The Clarno Urticalean Wood Type II specimen is more similar in that the axial parenchyma distribution is similar to McRae Group IIIB sp. 4, except for some marginal parenchyma. The Clarno Type II (<8 cm diameter) differs in having thicker fiber walls and narrower rays (1-4 cells vs. mostly 4-6), though the ranges overlap McRae Group IIIB sp. 4.

Differences in anatomical features between the McRae wood and existing fossil genera warrant assignment of the Jose Creek wood to a new fossil genus with possible affinity to *Rosales*.

### **Other fossil evidence**

The fossil record documenting Cannabaceae, Moraceae and Urticaceae is mostly Cenozoic. Collinson (1989) lists reports of numerous fruits from Eurasia from the Eocene forward, though some reports warrant reassessment or have been discounted. For example, Collinson suggested that the report by Chandler (1957) of the Moraceae fruit *Moroidea*, from the Eocene of England, was questionable on the basis that it did not have features of Tertiary *Moroidea*, or other Moraceae. Other evidence includes a single flower (Urticaceae) from Upper Eocene or Lower Oligocene Baltic amber (Friis and Crepet 1987), middle Eocene pollen (Moraceae), and multiple records of leaves. Collinson (1989) singled out a report of *figus*-like leaf material (Miocene) as particularly well substantiated (Mathiesen 1975 in Collinson 1989).

Members of the clade are also well represented in the Cenozoic of North America. Collinson (1989) listed reports of lobed leaves attributed to *Morus*, and

*Humulus* (Cannabaceae) from the Florissant flora of Colorado (Eocene) (MacGinitie 1953), though Manchester et al. (2001) in an update of the Florissant flora does not confirm the identifications. MacGinitie (1969) reports *Celtis* in both the Green River (Eocene) and Florissant floras. *Morus*-like or *Broussonetia*-like leaves were described by Manchester (1987) from the Oligocene John Day Formation. Manchester (1981) reported a Moraceae leaf from the middle Eocene Clarno flora of Oregon. Zavada and Crepet (1981) described a flower, *Eoceltis dilcheri*, from the middle Eocene Claiborne Formation of western Tennessee, as potentially an “intermediate reduction sequence” of Celtidoideae; however, Collinson (1989) considered that differences between the fossil and extant Celtidoideae rendered the relationship uncertain. The report by Manchester et al. (2002) of newly discovered endocarps of *Celtis*, found associated with leaves previously attributed to *Viburnum*, but now recognized as *Celtis*, documents a widespread distribution of the genus throughout United States and Canada by the Paleocene.

The fossil record for Urticales extends to the Cretaceous, but some reports have been questioned. The earliest unequivocal fossil records of Cannabaceae, as accepted by Friis et al. (2011), were reported from the latest Cretaceous (Maastrichtian) of Germany. The report included endocarps of two extant genera, *Aphanathe* and *Gironniera* (Knobloch and Mai 1986 in Collinson 1989). Nathorst (1890 in Friis et al. 2011) reported fossil leaves and reproductive structures of *Artocarpus* in Greenland. If confirmed, it would place Moraceae in the Northern Hemisphere during the Late Cretaceous, but the identification has been both accepted (Friis et al. 2011) and questioned (Collinson 1989). Leaf records of

Celtidoideae (*Celtidophyllum cretaceum* and *C. praeaustrale*) from Late Cretaceous Czech Republic, as described in the 1800's, also warrant reevaluation (Friis et al. 2011).

There is substantially less record for Cannabaceae, Moraceae or Urticaceae for the Cretaceous of North America. Collinson (1989) concluded that early reports required reevaluation. Reports of *Artocarpus*-like leaves from the Upper Cretaceous (Berry 1925) of North America were challenged by Wolfe (1973) who questioned the diagnostic value of features used in the initial assessment, as well as the preservation of the specimens. In contrast, Wolfe (1973) accepted a report of *Ulmus* (Ulmaceae) pollen from the Maastrichtian in the Rocky Mountains, USA, and concluded that the family, sister to the Cannabaceae, Moraceae and Urticaceae clade, existed in North America no later than the Campanian.

**McRae Group IIIB sp. 6, Kirkiaceae**

*Clade* – Core Eudicots, Rosid II

*Order* – Sapindales

*Clade* – [Kirkiaceae [Burseraceae + Anacardiaceae]]

*Family* – Kirkiaceae

*Genus* – gen. nov.

*Species* – sp. nov.

*Holoxylotype* – TXSTATE 1236, ST2 (Fig. 1.8–1.10)

*Stratigraphic horizon* – McRae Formation, Jose Creek Member

*Age* – Late Campanian

*Material* – Description based on samples collected from 12 *in situ* stumps and

5 logs, TXSTATE 1230–46 segments, measuring approximately 0.7–2.0 m in diameter (Table 1.4)

*Locality* – Texas State University Paleobotanical Locality 2012-48

*Description* – *Growth rings* absent. *Wood* diffuse porous. *Vessels* solitary (47%) and in radial multiples of 2–3 (rarely up to 5), mean 5 (1), range 4 (1)–7 (2) per mm<sup>2</sup>, solitary vessels oval in outline, mean of tangential diameter means 195 (21) µm, range 173 (49)–234 (41) µm (Fig. 1.8A–B). *Vessel element length* mean of means 507 (62), range 415 (112)–623 (161) µm (Fig. 1.8C); *perforation plates* simple (Fig. 1.8D), *intervessel pits* alternate, polygonal in outline, large, horizontal diameters 15 (3), range 12 (1)–18 (2) µm in diameter (Fig. 1.8E). *Vessel-ray parenchyma pits* with reduced borders to simple, round to oval, the largest extending the full height of the cell (Fig. 1.8F). *Tyloses* common in wide (Fig. 1.9A), *fibers* both non-septate (Fig. 1.9B) and septate (Fig. 1.9C). *Axial parenchyma* scanty paratracheal, occasionally nearly vasicentric (Fig. 1.8B), 8 cells per parenchyma strand (Fig. 1.9D). *Rays* not strongly heterocellular, multiseriate rays 2–4 (mostly 3–4, rarely to 6) seriate; ray height mean 814 (200), range 536 (310)–1184 (536) µm (Fig. 1.9E–F), composed of all procumbent cells or with 1 (rarely up to 5) marginal rows of upright or square cells (Fig. 1.9G); uniseriate rays rare, < 10 cells in height, composed of square and upright cells; average for all rays 8 (1), range 7 (1)–10 (2) per mm. Gum cells occasionally present among ray parenchyma.

*Description in IAWA Hardwood List codes (IAWA Committee 1989)* –

2 5 13 22 23 27 31 42 43 46 47 53 56 65 66 69 78 79v 93 98 102v 104 106 115

## Comparison to extant woods

Samples from twelve stumps and five logs from the McRae Forest of Giants were found to have the following characters: diffuse porous wood (5p), vessels solitary and in short radial multiples (9a 10a), exclusively simple perforation plates (13r 14e), large, alternate intervessel pitting (22r 24a 25a), vessel-ray pits large and simple or with greatly reduced borders (30a 31p), vessel mean tangential diameters medium to large (40a 41a), in low density (48a 49a 50a), libriform fibers without bordered pits (62a), vasicentric / vascular tracheids absent (60a), septate fibers (65p), axial parenchyma scanty paratracheal (or approaching vasicentric) (77e 78p 80a 83a 85a 86a 89a), multiseriate rays primarily (2-4 cells wide) (96a 99a) and weakly heterocellular (105a 106p 108a), storied structure absent (118a 119a 120a), oil cells not present (124e 125e 126e), and radial canals not present (130e).

A search of the InsideWood database (InsideWood 2004-onwards; Wheeler, 2011) using the above code returned species of families in orders, Sapindales (2 genera of Anacardiaceae, 6 genera of Burseraceae and the single genus of Kirkiaceae), and Lamiales (1 genus each of Lamiaceae and Verbenaceae).

*Vitex* (Lamiaceae) and *Viticiremna* (Verbenaceae) were not strong affinity candidates. While the vessel-ray pitting reported for *Vitex ferruginea* and *V. fischei* is consistent with the (without distinct borders), the two species are atypical for the genus *Vitex* in regards to that feature, intervessel pitting in the genus is typically minute to medium in size and most species in *Vitex* have axial parenchyma other than scanty paratracheal or vasicentric (frequently absent or rare, aliform or

mariginal). *Viticipremna novae-pommeraniae* differs by having medium sized intervessel pitting and some bordered vessel ray parenchyma pitting. Verbenaceae genera typically have bordered vessel ray parenchyma pitting and axial parenchyma other than scanty paratracheal or vasicentric. The combination of characters within the genera and families were not as similar to the fossil wood as the individual species returned in the InsideWood search, making the genera and families unlikely affinities for the McRae xylotype.

Three Sapindales families form the monophyletic clade [Kirkiaceae [Burseraceae + Anacardiaceae]] (Fernando et al.1995, Clarkson et al. 2002, Bachelier and Endress 2008, Weeks et al. 2014, Muellner-Riehl and Weeks 2016). Anatomical features usually present in the two genera of Anacardiaceae (*Rhus* and *Toxicodendron*) are less similar to the fossil wood than Burseraceae and Kirkiaceae. Species in the two genera differ by having some combination of features including vessels ring-porous or semi-ring-porous, medium-sized intervessel pitting, helical thickenings in vessel elements, marginal axial parenchyma, rays < 4 cells wide, and greater ray heterogeneity. Radial canals are not common in these genera.

The fossil is more similar to Burseraceae where six genera (*Aucoumea*, *Canarium*, *Dacryodes*, *Haplolobus*, *Protium*, and *Santiria*) were pulled from the InsideWood database, some with multiple species. Within the six genera, there is not an exact match to the McRae wood; rays are narrower (<4 cells) and generally shorter (<1mm in height) than the McRae wood. Also, prismatic crystals (absent from the fossil) are frequently present. As with Anacardiaceae, radial canals are associated with Burseraceae. However, Forman et al. (1989) observed that radial

canals are of sporadic occurrence in some Burseraceae, absent from most *Dacryodes* species, present in only a few species of *Protium* and absent in some other genera (Metcalf and Chalk 1950; InsideWood 2004-forward). The code (130e) used in the InsideWood search excluded radial canals and yet six genera of Burseraceae were retrieved, indicating that association with radial canals does not exclude affinity of the McRae fossil to Burseraceae.

Wood anatomical data for species in the monogeneric family Kirkiaceae are limited (Table 1.5). The fossil wood is similar to *Kirkia acuminata* Oliver which differs from the fossil in having only medium-sized intervessel pitting (Webber 1936), a feature confirmed in a small diameter axis (< 2 cm) of a second species, *K. wilmsii* (Parrott, unpublished data). Ray widths in *K. acuminata* (1-6, mostly 3-4 cells) and *K. leandrii* (1-4 cells) encompass the range of widths observed in the multiple samples of these McRae wood types. Rays of the small axis *K. wilmsii* were narrow (predominantly 1-2 seriate), and many short, uniseriate rays composed of upright cells were observed, anatomical features that may reflect the small axis diameter. Images of larger diameter axis of *K. wilmsii* indicate ray widths of 2-3 (-4) common with few uniseriate rays (Images courtesy Hans Beeckman, Royal Museum for Central Africa). Images suggest uniseriate and biseriate rays are uncommon in *K. acuminata* (Webber 1936, InsideWood 2004-forward, Hans Beeckman, Royal Museum for Central Africa), but commonly uniseriate in *K. leandrii* (Detienne, Pierre. Woods of Madagascar. CIRAD Unpublished, Stannard 2007). Vessels in *Kirkia leandrii* are solitary and radial multiples of 2-3, *K. acuminata* and *K. wilmsii* have short radial multiple, which overlap the range observed among samples of the

McRae xylotype, but the *Kirkia* species also show some small clusters. Radial canals and prismatic crystals are not reported for species of *K. acuminata* or *K. leandrii* (Metcalf and Chalk 1950, InsideWood-2004 onwards) and were not observed in the *K. wilmsii* axis. Rays of *Kirkia acuminata* are reported to have occasional gum cells among the parenchyma (Webber 1936). This is consistent with the McRae xylotype, in which some ray parenchyma have dark content that appears to be trapped against the cell wall in a manner remarkably similar to the extant *Kirkia* cells.

### **Comparison to fossil woods**

**Comparison to fossil woods identified through a search of the InsideWood database.** Those fossil woods identified by an InsideWood search (code: 3a 9a 10a 13r 14e 22r 24a 30a 31p 36a 40a 41a 48a 49a 50a 60a 62a 65p 77e 78p 80a 83a 85a 86a 89a 96a 99a 105a 106p 108e 118a 119a 120a 124e 125a 126a 130e) not already under consideration because of attribution to Burseraceae or *Paraphyllanthoxylon* included genera in the families Combretaceae (*Terminalioxylon*), Euphorbiaceae (now Pyllanthaceae) (*Bridelioxylon*), a possible Lauraceae (*Machilusoxyton*) and Verbenaceae (*Vitexoxyton*), as well as a wood of unknown affinities, Page Group XIA (CASG 60444) (Page 1980).

*Terminalioxylon orangensis* Bamford 2003 differs in having small intervessel pits, mean vessel diameters (118µm) smaller than the range of the fossil, higher (16) vessels per mm<sup>2</sup>, septate fibers rare, and biseriate rays <500 µm in height with up to 4 square margin rows.

One species of *Bridelioxylon* Ramanujam 1956 was among woods identified in the InsideWood search. This is not surprising given Bailey (1924) compared the type species *Paraphyllanthoxylon arizonense* to phyllanthoid types. Ramanujam found his wood most similar to species of *Bridelia*, a genus of Phyllanthaceae (Wurdack et al. 2004). His diagnosis for *Bridelioxylon* differs from the present wood by having distinct growth boundaries, smaller vessel diameters, 20 vessels per mm<sup>2</sup>, vessels in radial multiples up to five or more, vessel-ray pits smaller though simple, like the present fossil), axial parenchyma in vasicentric sheaths one to two cells thick, and rays under 500 μm (Ramanujam 1956).

*Machilusoxylon hindustanensis* Bande 1971 emend. Ingle 1974 differs in having vasicentric parenchyma in narrow sheaths of 1–2 cells and fibers only occasionally septate. Intervessel pit dimensions and vessel-ray pitting type were not reported (Ingle 1974). The species of *Vitexoxylo*n, *V. miocenicum*, differs in having distinct growth rings, minute intervessel pitting, axial parenchyma in vasicentric sheaths mostly 2-3 cells deep, and some uniseriate rays composed of upright cells. Page Group XIA (CASG 60444, Page 1980) is similar to the McRae xylotype, but information about significant features was not reported; vessel-ray pitting is described only as “oval” and septate fibers are not described. It differs in having smaller vessel diameters.

**Comparison to fossil woods and generic diagnoses associated with Burseraceae.** Similarity to woods of fossil genera of Burseraceae was expected, given the results of the “comparison to extant woods.” However, while the McRae fossil shares some features with some of the fossil wood genera attributed to the

Burseraceae, it does not fall within an existing generic diagnosis. *Boswellioxylon* Dayal 1964, 1965, *Tetragastroxylon* Martinez-Cabrera, Cevallos-Ferriz and Poole 2006, *Sumatroxylon* (Kräusel) Berger 1923, and *Lanneoxylon* Srivastava and Guleria 2004 have radial canals. *Burseraceoxylon* Patil and Mhaskar 1971 was proposed without the requisite holotype and therefore not validly published, but the wood as described differs in having bordered vessel-ray pitting similar to intervessel pitting and vasicentric axial parenchyma in sheaths of 1-2 cells.

The InsideWood search selected *Burseroxylon africanum* Bamford 2003 which differs in having small intervessel pits, fewer vessels per mm<sup>2</sup>, shorter vessel elements, mostly biseriate rays <500 µm in height. The *Burseroxylon* Prakash and Tripathi 1973 [75] generic diagnosis and type specimen, *B. preserratum* differ in having fewer vessels per square millimeter, taller rays, and ray cells with prismatic crystals. The Lakhanpal, Prakash and Awasthi 1978 [81] emended diagnosis of *Burseroxylon* includes some very large diameter vessels (to 345 µm), more rays per mm and horizontal gum cells (Vozenin-Serra and Privé-Gill 1991), which added to the disparity between the McRae xylotype and the genus *Burseroxylon*.

The InsideWood search selected *Canarioxylon shahpuraensis* Trivedi and Srivastava (1985), a wood very similar to the generic type species *Canarioxylon ceskobudejovicense* Prakash, Březinová and Awasthi 1974. Woods of *Canarioxylon* show considerable agreement with the McRae xylotype; differences with *Canarioxylon* include bordered vessel-ray pitting similar to the intervessel pitting, somewhat narrower rays and occasional prismatic crystals.

**Comparison to *Paraphyllanthoxylon* species.** Except for the presence of ray gum cells, the fossil wood falls within the generic diagnosis of *Paraphyllanthoxylon* Bailey (1924) and was compared to Cretaceous *Paraphyllanthoxylon* species, as well as Tertiary species identified in the InsideWood database search or the literature (Table 1.6).

Anatomical features of the McRae fossil are generally consistent with *Aplectotremas halistichum* Serlin (1982) from the Edwards Limestone (Albian). Important features of *A. halistichum* (e.g., intervessel pitting and vessel-ray pitting) were not described, but details visible in its transverse section are consistent with *Paraphyllanthoxylon* Wheeler (1991).

The relatively large vessel diameters and low vessel frequency observed for the McRae xylotype invite comparison to *P. abbottii* Wheeler (1991), described from the Black Peaks Formation (Paleocene). Similarities include vessel diameters, vessel-ray parenchyma pit type, and ray width. Both woods have rays with only 1–2 (to 4, some with more in *P. abbottii*) square or upright margin rows. *Paraphyllanthoxylon abbottii* differs in having some samples with more vessels per mm<sup>2</sup> and very scanty or rare to absent axial parenchyma.

*Paraphyllanthoxylon vancouverense* Jud, Wheeler, Rothwell and Stockey (2017), also is very similar to the McRae xylotype, differing in having smaller vessel diameters. Jud et al. report rays with some intermixed square or upright cells, which is not typical of the McRae fossil, but the appearance of “upright” ray cells in the body of the McRae wood seemed to correspond to occasional rows of large procumbent cells (observed in radial view) that might be equivalent to the *P.*

*vancouverense* upright ray cells. Jud et al. also describe some enlarged ray cells with dark content observable in tangential, but not radial view. These differ from the McRae xylotype gum cells in that the gum cells are not enlarged (Fig. 1.9H).

The *Paraphyllanthoxylon marylandense* Herendeen (1991) diagnosis differs from the McRae xylotype in having smaller vessel diameters and relatively high vessel density, opposite to scalariform vessel-ray parenchyma pitting and typically 1–3 (–7) marginal rows of upright cells with common fusion of rays. Herendeen describes “fine helical thickenings” in the mature wood of *P. marylandense*, a feature not observed in the McRae xylotype nor specified in Bailey’s generic diagnosis for *Paraphyllanthoxylon*, but helical thickenings probably would not be observed without the SEM visualization used by Herendeen.

Again, save for presence of ray parenchyma gum cells that correspond to the *Kirkia acuminata* ray type, the McRae xylotype has features most consistent with those of *P. cenomaniana* Takahashi and Suzuki (2003) from the Cretaceous (Cenomanian) Yezo Group in Hokkaido, Japan. *Paraphyllanthoxylon cenomaniana* differs in having greater mean vessel density, though the range of values overlaps with the McRae wood. Takahashi and Suzuki describe the rays as heterocellular; overall, the radial image shows one upright margin row. Takahashi and Suzuki did not report ray parenchyma gum cells in their fossil. However, the similarity of the woods warrants a reexamination of *P. ceomaniana* to confirm presence or absence of gum cells if the quality of preservation in the *P. ceomaniana* specimen is sufficient.

### **Descriptions of *Paraphyllanthoxyon* without attribution to a specific family**

Woods similar to the McRae xylotype are routinely assigned to the form genus *Paraphyllanthoxyon* Bailey (1924) without attribution to a particular family, in part because the combination of wood anatomical features is not uncommon. Indeed, Thayn and Tidwell (1983) provide a list of 14 families to which specimens of *Paraphyllanthoxyon* have been compared, with the most likely family affinities identified very early in the history of the genus.

Bailey (1924) first described the fossil wood *Paraphyllanthoxyon arizonese* as similar to the Phyllanthoideae of the Euphorbiaceae (now Phyllanthaceae). From the beginning, he recognized that conclusive identification of the wood would be problematic as there was “no single, salient structural feature in the fossil which justified its reference to any particular group.” Spackman (1948) described *Paraphyllanthoxylon idahoense* and agreed with Bailey that it was similar to Euphorbiaceae, though “by no means identical,” and added Anacardiaceae and Burseraceae to the list of probable affinities. He also discussed (and discounted) genera from three additional families. Comparable lauraceous genera were eliminated because they have oil cells, *Kirkia acuminata* Oliver was rejected because of its ray type and Verbenaceae because of the vessel arrangement. The possible link between a species of *Paraphyllanthoxyon* and Burseraceae was recognized by Wheeler (1991) and Meijer (2000), who also considered Anacardiaceae and Lauraceae as possible affinities. Orders and families mentioned in connection with *Paraphyllanthoxyon* have included Sapindales (Sapindaceae), Flacourtiaceae – genera now placed in the Salicaceae, Samydaceae, Violaceae) and less commonly

Gentianales (Apocynaceae, Rubiaceae), Lamiales (Verbenaceae), Celestrales (Celestraceae) and Saxifragales (Hamamelidaceae) (Bailey 1924, Spackman 1948, Thayne and Tidwell 1984, Wheeler et al. 1987, Wheeler 1991). While most of the families are not likely affinities for *Paraphyllanthoxyon*, the list of so many families that are not closely related has contributed to the consensus that *Paraphyllanthoxyon* should not be attributed to any modern taxon.

In sharp contrast to the general consensus, the InsideWood database search with codes specific to the McRae xylotype species retrieves a limited number of potential affinities, the most probable of which comprise a monophyletic clade [Kirkiaceae [Burseraceae + Anacardiaceae]]. Like Spackman (1948), this study considered species of Verbenaceae, which were also found inconsistent with the McRae *Paraphyllanthoxylon*. No species of Phyllanthaceae were returned by the InsideWood database search, nor were genera of Lauraceae because, as Spackman (1948) noted, extant lauraceous species with anatomical features similar to Burseraceae and Anacardiaceae (and Kirkiaceae) have oil cells. While there are species in multiple genera of Lauraceae e.g., *Actinodaphne*, *Beilschmiedia*, *Chlorocardium*, *Cryptocarya*, *Endiandra*, *Nectandra*, *Lindera*, *Neolisea*, *Ocotea*, *Oreodaphne* and *Syndiclis* (Metcalf and Chalke 1950, InsideWood 2004 forward) that do not have oil cells, they are generally the exceptions within the genus in not having oil cells and differ from the McRae xylotype in axial parenchyma pattern and/or by having some combination of features including scalariform perforation plates, smaller intervessel pits or narrower ray width (2004 forward).

Spackman (1948) did not elaborate on which aspects of *Kirkia acuminata* ray structure he found inconsistent with *Paraphyllanthoxylon idahoense*. His description of ray structure in *P. idahoense* differs from *Kirkia acuminata* by having both uniseriate rays and multiseriate rays 2-4 cells wide with 1–4 upright marginal rows (as illustrated in the plate photos), whereas *Kirkia acuminata* has few uniseriate rays, predominantly wider rays (4, up to 6 cells) and fewer upright marginal rows (InsideWood, 2004 forward). Ironically, the discrepancies between ray structure in *P. idahoense* and *K. acuminata* represent the similarities between *K. acuminata* and the McRae xylotype. Spackman might have found greater similarity between the ray structure of *P. idahoense* and *K. leandrii*. Slide (AW) 19207 obtained by the Harvard Herbarium in 1934, and very probably the specimen examined by Spackman, has narrow rays (mostly 2, up to 3) and numerous uniseriate rays. The predominantly narrow rays observed in the Harvard specimen may account for Spackman's appraisal of the wood as having the wrong "ray type."

### **Biogeography**

The pantropical families Burseraceae and Anacardiaceae have been shown to share a common stem lineage with Kirkiaceae sister to the pair (Weeks et al. 2005, 2014, Muellner-Riehl et al. 2016). Analyses of the biogeographic history of Burseraceae and Anacardiaceae suggest a Laurasian origin with a most recent common ancestor that was widespread in wet and dry tropical climatic niches (Weeks et al. 2005, 2014). If accepted, the scenario would indicate divergence from other Sapindales lineages occurred during the Aptian, with the Anacardiaceae–Burseraceae split following during the Aptian-Albian. Weeks et al. (2005) placed

early diversification of the Burseraceae in North America, Mexico, or the Caribbean during the Paleocene, with the ancestor of Burseraceae quickly achieving a near pantropical distribution, while that of Anacardiaceae localized in Southeast Asia. Diversification of the stem and crown for both is believed to be in the Early to Late Cretaceous (Muellner-Riehl et al. 2016). The analyses place the most recent common ancestor of the clade and early diverging Burseraceae in the southwestern U.S. at the appropriate time to be consistent with attribution of the fossil wood to the [Kirkiaceae [Burseraceae + Anacardiaceae]] clade. If the bias of biogeographic studies to younger estimated divergence ages (Goswami and Upchurch 2010, Bartish et al. 2011, Heads 2012, Swenson et al. 2012) applies in this instance, the estimate of divergence age would be only more congruous. Techniques used in biogeographic analyses are evolving and results, therefore, may be viewed as tentative, but putting fossil evidence into biogeographic scenarios tests the logic of such analyses and should inform future studies.

If one accepts attribution of at least some *Paraphyllanthoxylon*-like species to Kirkiaceae, conclusions regarding the origins for Burseraceae and Anacardiaceae (and Kirkiaceae, by extension) have potentially intriguing implications for species of *Paraphyllanthoxylon*. Could *Paraphyllanthoxylon*-type woods represent the widespread common ancestor for this clade? Such an assertion would be highly speculative, yet certain findings are at least consistent with the hypothesis.

Right place, right time: *Paraphyllanthoxylon*-like woods are common and have been reported from localities in North and Central American, Europe, Asia and Africa, from the Early Cretaceous (Aptian/Albian, Thayer et al. 1983) through the

Miocene. Specimens with very similar anatomy have been described from remote localities, in the case of the McRae xylotype, Vancouver and Asia. The fossil ages are consistent with the proposed biogeographic origin and radiation of this sapindalean clade. Anatomical variability among species of *Paraphyllanthoxylon* (e.g., vessel mean tangential diameter, vessel density, ray width, number of square or upright margin rows, presence of uniseriate rays, and axial parenchyma distribution) is encompassed by reported values for the Kirkiaceae.

This interpretation clashes with prior supposition based on the Early Cretaceous record of pollen, flowers and leaves (Friis et al. 2011) that diversification of core eudicots was a Late Cretaceous phenomenon (Doyle and Upchurch 2014), and that the Early Cretaceous record of Laurales as both common and diverse would be consistent with interpretation of Early Cretaceous *Paraphyllanthoxylon* as lauralean. Of course, the presence of both in the record does not obligate association. We must suspect there were angiosperm species not preserved in the rather sparse Early Cretaceous fossil wood record that could potentially account for the many lauralean fossils, and it is interesting to note that mature specimens of *Paraphyllanthoxylon* have not been found in association with lauralean leaf or reproductive fossils, despite the prevalence of both in the fossil record. Supporters of the lauralean model refer to Herendeen's (1991) whole plant reconstruction linking *Mauldinia mirabilis* (Laurales) and *Paraphyllanthoxylon marylandense*, an association not without controversy. The description of *P. marylandense* is based on juvenile wood specimens, exceptionally small charcoalfied axes (radius < 2 mm), which likely render the comparison to the *Paraphyllanthoxylon* diagnosis

inconclusive. This conservative interpretation by the present author is inspired by Page (1981) who courageously abandoned the effort to identify affinities in small axis specimens of the Panoche collections because “in many species significant anatomic changes occur during the early stages of growth in the stem.”

In contrast to Laurales, there is no robust record of fossil leaf and reproductive structures to support the sapindalean interpretation of *Paraphyllanthoxylon*-like woods. However, fossil identification is an ongoing process. For example, of more than a hundred morphotypes recognized in the Jose Creek Member leaf macrofossil collections, those tentatively identified as lauralean represent only a small percentage, while the majority of the specimens are of unknown affinity (Contreras 2018).

#### **Rethinking attribution of *Paraphyllanthoxylon*-like woods.**

If the resemblance between Anacardiaceae, Burseraceae (Spackman 1948, Thayne and Tidwell 1984, Wheeler et al. 1987, Wheeler 1991, Meijer 2000) and, less frequently, Kirkiaceae (Spackman 1948) has been recognized since 1948, why was the association not embraced?

Molecular phylogenetic studies have realigned our understanding of familial relationships. In 1948, *Kirkia* was included in Simaouberaceae, so resemblance of *Paraphyllanthoxylon* type woods to *Kirkia* provided further evidence that such woods could align with multiple distantly related families. Now that Kirkiaceae is placed sister to Anacardiaceae and Burseraceae, similarity in the woods supports attribution to a monophyletic clade. Stern (1954) noted (in reference to Lauraceae)

that classification schemes based on the wrong characters led to “unnatural groupings” that complicated identification of fossil woods.

Bailey (1924) reflected on practical limitations to his search process in which he bemoaned that the extremely limited number of descriptions of extant species and genera available at the time (often based on small diameter axis from herbarium specimens) were scattered through the literature, and that the range of anatomical variability was largely unknown. “The only method of determining its [a fossil wood] affinities is the laborious one of searching for similar combinations of [many] anatomical characters in extant Dicotyledons” (Bailey 1924). Compilation of the InsideWood database of wood descriptions and images or the computational power to sort through thousands of woods utilizing large numbers of descriptors simultaneously could not have been foreseen. These tools inspire confidence in the search result, and access to literature online facilitates the search for additional pertinent information.

The McRae xylotype shares some features with *Paraphyllanthoxylon*, but is most similar to species of extant *Kirkia*, a small family comprised of few species that are rare and not well known. The resemblance among the wood types begs the question of a possible connection of *Paraphyllanthoxylon* species to *Kirkia*. This might be explored with detailed study of additional species of *Kirkia*, including some study of the transition of the wood anatomical features from juvenile features through intermediate stages to fully mature wood. Of particular interest would be the extent of gum cells in species of *Kirkia* other than *K. acuminata*. If gum cells are commonly present in all *Kirkia* species, the absence of the feature in

*Paraphyllanthoxylon* would exclude *Kirkia* as the affinity. If some *Kirkia* species lack gum cells, it would be reasonable to compare *Paraphyllanthoxylon*-like woods to *Kirkia* on a case-by-case basis.

In the future, a phylogenetic analysis based on wood characters of fossil *Paraphyllanthoxylon* and the [Kirkiaceae [Anacardiaceae + Burseraceae]] clade should be undertaken to see how the fossil might relate to those families. The molecular phylogeny of extant species of Anacardiaceae, Burseraceae and Kirkiaceae has been studied. It may be possible to superimpose the wood data upon that molecular tree.

### **The competing hypothesis - if it's anything, it's Laurales**

The presence of gum cells in the McRae xylotype and the general agreement of anatomical features with those of *Kirkia* would seem to exclude the fossil from the discussion of whether *Paraphyllanthoxylon* is attributable to Laurales. However, because the McRae xylotype is so similar to *Paraphyllanthoxylon* in most features, it will invite comparison to *P. marylandense* and its link to Laurales. Thus, *Paraphyllanthoxylon marylandense* Herendeen is of particular interest. Herendeen (1991) described *P. marylandense* from a collection of small fragments of charcoalfied axes, two of which bore floral structures of *Mauldinia mirabilis* Drinnan, Crane, Friis and Pederson. *Mauldinia mirabilis* floral structures were originally attributed to Lauraceae (Drinnan et al. 1990), which has been interpreted as linking *Paraphyllanthoxylon* species to that family (Jud et al. 2017). However, after further analysis, Doyle and Endress (2010) concluded that *M. mirabilis* was not Lauraceae, and instead placed the genus sister to Lauraceae and Hernandiaceae or

possibly as sister to a clade of Monimiaceae, Lauraceae and Hernandiaceae. Herendeen had interpreted *P. marylandense* as consistent with woods of some Lauraceae, but the phylogenetic position of *M. mirabilis* as interpreted by Doyle and Endress suggests the wood might share anatomical features with Hernandiaceae or Monimiaceae. Consistent with the suggested placement, the earliest xylem of *P. marylandense*, that closest to the pith, has features that occur in woods of extant Monimiaceae. Helical thickenings, as observed in Herendeen's floral axes, are reported in at least one modern species of Monimiaceae, and other features of the floral axes (e.g., some scalariform perforation plates, round to elliptical to scalariform intervessel pitting and imperforate tracheary elements with large bordered pits) are characteristic of Monimiaceae, in line with the Doyle and Endress (2010) interpretation of *Mauldinia*.

The *P. marylandense* diagnosis and description were not based directly on the wood of the two floral axes. Rather, Herendeen described *P. marylandense* from wood fragments found in association with the floral axes. The wood of one fragment, in particular, had anatomical features similar to the very early xylem (adjacent to the pith) of the floral axes, but also wood that transitioned to somewhat more mature xylem (1–2 mm from the pith). Herendeen provided details of the earliest xylem, but based the description of *P. marylandense* on the more mature xylem. Because the nature of the specimen may have impacted the scope of Herendeen's observations, the diagnosis and description of *P. marylandense* must be interpreted cautiously for the following reasons:

- While the outermost wood described by Herendeen has different character states than the earliest xylem (adjacent to the pith) and may be considered more mature, the axes are very small diameter. Fragments that best illustrated the wood features measured only 3.6 mm in diameter, so that the features may not represent the final mature wood composition. Ray width and height, for example, could be different in a fully mature wood (Barghoorn 1941). It is impossible to know if the final mature wood would have had features (e.g., laticifers or prismatic crystals) not found in juvenile wood or inflorescence axes.

- It cannot be ruled out that anatomical features of the fully mature wood would be found specifically in association with earlywood or latewood. The very small floral axes did not show evidence of repeated growth cycles where such features could be observed.

- The description is based on a limited number of small wood fragments. By chance, some features may not have been observed.

- Because the surfaces of the wood fragments are fractured, fragile features like scalariform perforation plate bars may have been damaged.

- Herendeen (1991) cautioned that some anatomical features of the charcoaled sample likely were altered, particularly those measured quantitatively (e.g., vessel diameter, vessel element length, ray height, rays per mm).

- Large oil cell-like idioblasts that would tie the wood to woods of Lauraceae or some Hernandiaceae were not observed, but oil cells could not be ruled out conclusively. Herendeen noted that volatile compound “cell content” is not preserved in charcoal. While oil cells are usually substantially larger than surrounding cells, this is not always the case; so average-sized cells without the dark “oily content” would not likely be interpreted as oil cells. Furthermore, oil cell-like idioblasts can occur infrequently and might have been missed on the limited fragments of *P. marylandense*.

These specimen limitations complicate comparison of *P. marylandense* to woods of the Lauraceae, Hernandiaceae and Monimiaceae clade and also suggest cautious comparison to mature specimens of *Paraphyllanthoxylon*. Herendeen’s description of *P. marylandense* differs from the earliest xylem of *P. marylandense* by having only simple perforation plates, alternate intervessel pitting and fibers without bordered pits. The features are not unlike the McRae xylotype. However, *P. marylandense* differs by having helical thickenings, albeit reduced to fine lines (observed with SEM) and vessel-ray parenchyma pitting with reduced borders that are smaller than the McRae xylotype pitting, often elongate and sometimes arranged diagonally.

Because the features of *P. marylandense* were observed in charcoaled samples of very small diameter, juvenile wood axes, comparison to fully mature wood features of *Paraphyllanthoxylon* species is somewhat speculative. However, the connection between *P. marylandense* and *Paraphyllanthoxylon*, and therefore the connection of *Paraphyllanthoxylon* to Laurales, would be strengthened if

examination of small diameter (pith adjacent) specimens of *Paraphyllanthoxylon* could be shown to have the anatomical features present in the earliest xylem of *P. marylandense*. If the woods are related, xylem of the McRae xylotype located within a few millimeters of the pith should have scalariform perforation plates, opposite to scalariform vessel-ray parenchyma pitting, ray fusion and possibly helical thickenings. This hypothesis could be tested if appropriate material were available. Numerous stumps and logs are present at the Forest of Giants locality. Due to heart rot, pith and small diameter axis material will not be available for most of them, but at least one (Stump 12, TXSTATE 1242) has an intact central region. A specimen collected from within a few centimeters of the pith of Stump 12 did not show the small axis features reported for *P. marylandense*. However, pith-adjacent material should be examined, as well as material from any other *Paraphyllanthoxylon* species with intact pith, to evaluate this proposed connection.

Notably, neither Monimiaceae nor Hernandiaceae is among the families previously suggested as the possible affinity for *Paraphyllanthoxylon*. The McRae xylotype differs from the woods of Monimiaceae by having exclusively simple perforation plates, alternate intervessel pitting rather than scalariform pitting, large vessel-ray parenchyma pitting with very reduced borders, fibers without bordered pits, and rays only weakly heterocellular. Neither does the McRae wood have features commonly observed in the woods of Hernandiaceae (e.g., septate fibers absent, axial parenchyma aliform to confluent, oil cells in ray or axial parenchyma).

The McRae xylotype shares some anatomical features with select genera of Lauraceae. However, the McRae wood lacks oil cells that characterize most lauraceous genera. Those few species of Lauraceae that lack oil cells have features not typical of *Paraphyllanthoxylon* (e.g., scalariform perforation plates and /or aliform or confluent axial parenchyma). *Ocotea pulchella* represents a notable exception. The description of *O. pulchella* in the Insidewood database (InsideWood 2004-onwards) does not include the presence of oil cells. However, the species is atypical for the genus because oil cells are characteristic of other *Ocotea* species (InsideWood 2004-onwards, Metcalfe and Chalk 1950). Absent oil cells, the McRae xylotype does not fit easily within Lauraceae. The presence of ray gum cells as were reported for *Kirkia acuminata* would support affinity with Kirkiaceae, instead.

### **Other fossil evidence**

Additional fossil evidence that would link *Paraphyllanthoxylon* to a family or clade is unavailable. There are no repeated co-occurrences of *Paraphyllanthoxylon* with direct associations with leaf or pollen fossils. Cretaceous age reproductive fossil evidence for Anacardiaceae and Burseraceae is not known (Friis et al. 2011), and while both families are well represented in the Eocene of North America and England, the leaf record needs reevaluation (Friis et al. 2011). The association of *P. marylandense* with a reproductive structure, *Mauldinia mirabilis* (Lauraceae), while widely accepted as indicating that at least this one species of *Paraphyllanthoxylon* is lauraceous, should be treated circumspectly. The Forest of Giants xylotype is not associated with volcanic tuff outcrops that preserve leaf impressions at other McRae localities. Leaf impressions representing Lauraceae and other taxa of Laurales are

common (Upchurch and Mack 1998, Estrada-Ruiz et al. 2012a, 2012b, 2018) in the McRae exposures where lauraceous woods are preserved as float. Notably, no specimens of the xylotype this author is assigning to Kirkiaceae or any other *Paraphyllanthoxylon*-like wood has been found in those areas to date.

### **Attribution**

Competing hypotheses have evolved as to the possible affinities of *Paraphyllanthoxylon*-like woods. These relatively common woods have been compared to a number of families without conclusive attribution to any. Alternatively, affinity to Lauraceae or Laurales has been proposed.

While *P. marylandense* may have affinities with Laurales and may be grouped with some other *Paraphyllanthoxylon* species, it should not be assumed that all *Paraphyllanthoxylon*-like species have affinities with Lauraceae or Laurales. The McRae xylotype shares anatomical features with woods of some Lauraceae species and genera, but lacks the oil cells that typify those woods, a feature that would also distinguish Lauraceae from Anacardiaceae, Burseraceae and Kirkiaceae. Neither is the McRae xylotype comparable to the woods of Hernandiaceae or Monimiaceae for which a possible link with *P. marylandense* has been proposed.

The search for affinities for the McRae xylotype utilizing the InsideWood database and the literature, without prior assumptions regarding possible affinities, achieves a similar result to that of Spackman (1948). Further evidence of the possible relationship of the fossil to the Kirkiaceae is potentially available through analysis of the juvenile wood of extant and fossil woods. While it is premature to assume sapindalean affinity for all species of *Paraphyllanthoxylon*, the result of this

study provides greater support for attribution of the McRae xylotype to Kirkiaceae than to Lauraceae or Laurales.

**McRae Group IIIB sp. 5, cf. Sapotaceae**

*Clade* – Core Eudicots, Asterids

*Order* – Ericales

*Family* – cf. Sapotaceae

*Genus* – New Genus

*Generic diagnosis* – Diffuse-porous to semi-ring-porous wood with indistinct growth ring boundaries. Vessels mostly solitary and in radial multiples usually of fewer than 4 vessels, with a tendency to diagonal arrangement; perforation plates simple; intervessel pits alternate; vessel-ray parenchyma pits either similar to intervessel pits or with reduced borders. Axial parenchyma diffuse-in-aggregates and in regular lines 1–3 cells wide, scanty paratracheal. Fibers non-septate. Rays 1–4 seriate, heterocellular with many marginal rows of square or upright cells, multiseriate regions occasionally vertically fused by uniseriate regions; uniseriate rays made up of square and upright cells.

*Species* – McRae Group IIIB sp. 5

*Specific diagnosis* – Vessels mostly solitary and in radial multiples of 2–3, with a tendency to diagonal / oblique arrangement. Wood semi-ring-porous; perforation plates simple; intervessel pits alternate, medium to large; vessel-ray parenchyma pits both similar to intervessel pits or with reduced borders, elongate in oblique, vertical or horizontal arrangement. Axial parenchyma diffuse-in-aggregates, sometimes in more or less regularly spaced lines 1–3 cells wide or

scanty paratracheal to nearly vasicentric. Fibers non-septate. Rays 1–4 seriate (mostly uniseriate and 4-seriate), heterocellular, multiseriate portions occasionally vertically fused by uniseriate cells; uniseriate rays composed of square and upright cells.

*Holoxylotype* – TXSTATE 1288 (Fig. 1.10–1.12)

*Stratigraphic horizon* – McRae Formation, Jose Creek Member

*Age* – Late Campanian

*Material* – Description based on sample collected from one *in situ* stump measuring approximately 0.8 m in stem diameter at approximately 1 m height (Fig. 1.10B)

*Locality* – Texas State University Paleobotanical Locality 2012-48

*Description* – *Growth rings* present, but growth boundaries not distinct. *Wood* semi-ring-porous, the transition between sizes gradual (Fig. 1.11A). *Vessels* solitary (63%) and in radial multiples of 2–3 (rarely up to 4), average 6 (SD 2, range 3–10)/mm<sup>2</sup>, solitary vessels oval in outline, tangential diameter average 156 (SD 45, range 99–273) μm. Vessel element length average 692 (SD 194, range 536–1156) μm (Fig. 1.11B); perforation plates simple (Fig. 1.11C–D), intervessel pits alternate, polygonal in outline, medium to large, 7–12 μm in diameter (Fig. 1.11E–F). *Vessel-ray parenchyma pits* with distinct borders (Fig. 1.11G) or with reduced borders, oval to elongated horizontally to vertically, crowded (Fig. 1.11H). Tyloses common, bubble-like (Fig. 1.11I). *Fibers* angular in transverse view, thin-medium-thick-walled, pits not observed, non-septate. *Axial parenchyma* diffuse-in-aggregates, in

lines 1 to 3 cells wide that tend to be regularly spaced, approximately 3–4 per mm, some lines discontinuous (Fig. 1.12A), and occasionally scanty paratracheal to nearly vasicentric (Fig. 1.12B); eight cells per parenchyma strand. *Rays* heterocellular, 1–4 seriate (Fig. 1.12C), multiseriate rays 2–4 (mostly 4) seriate, ray height average 11 (SD 4, range 5–19) cells or average 338 (SD 100, range 96–596)  $\mu\text{m}$ , composed of procumbent cells in the central portion with 1–8 marginal rows of upright or square cells at one or both ends (Fig. 1.12D–E), multiseriate portions occasionally vertically fused by uniseriate cells (Fig. 1.12F); uniseriate rays common (33%) composed of, square and upright cells (Fig. 1.12G), average 6 (SD 2, range 2–14) cells or average 542 (SD 165, range 159–832)  $\mu\text{m}$  tall; range for all rays 4–14 per mm.

*Description in IAWA Hardwood List codes (IAWA Committee 1989) –*

2 4 7v 13 22 23 26 27 30v 32v 42 47 53 56 66 68 69 77 78 86 93 98 106 107 108  
115 116

### **Comparison to extant woods**

The InsideWood database was searched for the following combination of features: diffuse porous wood (3e), vessels solitary and in short radial multiples (9e 10a), in diagonal arrangement (7p), simple perforation plates (13r 14a), alternate intervessel pitting (22r), intervessel pitting medium to large (24a) bordered vessel-ray pits (30p) as well as pits with reduced borders (either 31p or 32p), libriform fibers (60e 61p 62a 63e), non-septate fibers (65a 66r), fibers thin to medium wall thickness (70a), axial parenchyma forming lines one to several cells wide, more or less uniformly spaced (75a 80a 82a 83a 85a 89e), axial parenchyma 8 cells per

strand (90a 91a), multiseriate rays (2-4 cells wide) (96e 99e 100a 101a), not > 1mm in height (102a) and heterocellular (104e 107p 108p 109a), uniseriate rays composed of mostly square and upright cells, without storied structure (118a 119a 120a), without radial canals, included phloem or cambial variants (130e 133a 134a 135a), without prismatic crystals or druses (136a 144a).

The results of that search included six genera of Sapotaceae (*Chrysophyllum*, *Englerophytum*, *Omphalocarpum*, *Pouteria*, *Tieghemella* and *Tsebona*). Conducting the search allowing 1 mismatch identified 7 additional genera of Sapotaceae, 1 genus of Cannabaceae, and 2 genera of Euphorbiaceae. The fossil wood was compared to these individual taxa found in the InsideWood search, but also to their entire genus or family in order to observe trends within those groups and to evaluate the selected taxa in context.

While sharing some features, the wood of *Trema cannabina* (Cannabaceae) does not have axial parenchyma in the narrow lines observed in the fossil. The two Euphorbiaceae species returned by the InsideWood search differed as follows: *Discoclaoxylon hexandrum* (Muell.Arg.) Pax and Hoffm. has some scalariform perforation plates; *Tetrorchidium didymostemon* (Baill.) Pax and K.Hoffm. has rays generally uni- or bi-seriate (InsideWood 2004-onwards). Overall, only a small percentage of woods in Euphorbiaceae have diagonal vessel arrangement, the combination of vessel-ray pitting as both “like intervessel pitting” and “pits with reduced borders” does not occur, many genera have exclusively uniseriate rays, and prismatic crystals are typically present.

Genera of Sapotaceae identified by the InsideWood search segregate into the subfamilies Sapotoideae (*Madhuca*, *Manilkara*, *Palaquium*, *Tieghemella* and *Tsebona*) and Chrysophylloideae (*Aubreginia*, *Breviea*, *Chrysophyllum*, *Englerophytum*, *Micropholis*, *Omphalocarpum*, *Pouteria* and *Synsepalum*) (Swenson and Anderberg 2005, Gautier et al. 2013).

Anatomical features that strongly support affinity of the fossil with Sapotaceae include axial parenchyma arranged in narrow lines (more or less uniformly spaced), two types of vessel-ray parenchyma pits, heterocellular rays < 1 mm in height, and the tendency for vessels to be in diagonal arrangement (Metcalf and Chalk 1950, InsideWood-2004 onwards). Metcalfe and Chalk (1950) report diagonal vessel arrangement to be less pronounced in *Chrysophyllum* than some Sapotaceae genera, consistent with the observed character state in the McRae fossil.

This fossil lacks some common features of many genera of Sapotaceae (e.g., vessel multiples of 4 or more, thick-walled fibers, rays < 4 cells wide and prismatic crystals) (Metcalf and Chalk 1950, Kukachaka 1978, 1979, 1981, 1982, InsideWood-2004 onwards). However, these features are absent or inconsistently present within the genus *Chrysophyllum* (Kukachaka, 1978, InsideWood-2004 onwards). Other anatomical features of the fossil wood (e.g., intervessel pit size and vessel mean tangential diameter) do not exactly match those of the extant family, but overlap in range.

The fossil wood is most similar to *Chrysophyllum*, but affinity to other genera in Chrysophylloideae cannot be excluded. Differences between this McRae fossil and the Sapotoideae genera from the InsideWood search follow: rays of *Madhuca* are

much narrower (1 – 2 seriate), vessel in *Manilkara* and *Palaquium* are often in long radial multiples, axial parenchyma bands in *Tieghemella* are wider, the Malagasy *Tsebona* has predominantly diffuse-in-aggregates parenchyma, without obviously continuous bands of axial parenchyma. Overall, the fossil wood is more similar to genera in the Chrysophylloideae, in particular *Chrysophyllum*, but also *Omphalocarpum*, and the wider-rayed *Pouteria*.

### **Comparison to fossil woods**

McRae Group IIB sp. 5 was compared to fossil genera attributed to Sapotaceae, but also to woods retrieved in an InsideWood search of the fossil wood database to determine if a similar fossil wood might previously have been described and attributed to a family other than Sapotaceae.

**Comparison to fossil woods identified through a search of the InsideWood database.** A search of InsideWood fossil wood database using the codes 3e 7p 9e 10a 13r 14a 22r 24a 30p 60e 61p 62a 65a 75a 80a 83a 85a 89e 96e 99e 100a 101a 102a 104e 107p 108p 118a 119a 120a 130e 133a 134a 136a (banded axial parenchyma) 301p with 1 allowable mismatch did not identify any taxa attributed to Sapotaceae. Excluding wood for which missing description details preclude comparison, the search returned woods in Lecythidaceae, Malvaceae and Juglandaceae.

Species attributed to Lecythidaceae in the genera *Barringtonioxylon* (Kar 2004) and *Careyoxylon* Awasthi (1969) are distinguished by having vessel arrangement other than in diagonal lines and not by showing any tendency to semi-ring-porosity. Species with affinity to Malvaceae in the genus *Bombacoxylon* differ in

having distinct growth boundaries and vessel-ray pitting similar to intervessel pitting. *Bombacacioxylon tertiarum* differs in having some vessels in clusters or radial multiples up to 8, axial parenchyma in closely arranged lines, more rays per mm and thick-walled fibers (Chang et al. 2013).

**Comparison to fossil genera attributed to Juglandaceae.** The InsideWood search of the fossil wood database returned five fossil woods attributed to Juglandaceae. Parallels exist in axial parenchyma arrangement (narrow bands and scanty paratracheal), vessel size, grouping and overall density, and some have similar ray width and height. *Pterocaryoxylon* Müller-Stoll and Mädler (1960) and *Caryojuglandoxylon* Felix (1884) as cited in Müller-Stoll and Mädler 1960) differ in having prismatic crystals in some ray cells, in *Caryojuglandoxylon* the crystals occur in large idioblasts or chambered ray parenchyma.

Wood type DB.D2 Xylotype 5 from the Paleocene and early Eocene of the Denver Basin, CO (Wheeler et al. 2003) and *Clarnoaxylon blanchardii* from the middle Eocene Clarno Formation, Oregon (Wheeler and Manchester 2002) differ in having rays < 4 cells wide, and vessel-ray pitting similar in size and shape to the intervessel pitting. The description of wood type UF 279-Juglandaceae from the John Day Formation of the Upper Eocene, Oregon, is similar to McRae Group IIIB sp. 5, but its vessel-ray parenchyma pits are of similar size to the intervessel pits (Wheeler et al. 2006, Wheeler, Manchester and Wiemann, work in progress, InsideWood 2004-onwards).

**Comparison to fossil genera attributed to Sapotaceae.** While the range of anatomical features present in extant Sapotaceae (Metcalf and Chalk 1950, InsideWood 2004 onwards) encompasses those observed in the McRae fossil, none of the generic and type specimen diagnoses for fossil woods attributed to Sapotaceae (Gregory et al. 2009) have the combination of features observed in the fossil wood. While sapotaceous fossil genera are generally similar to McRae Group IIIB sp. 5 in having diagonal / radial vessel arrangement, simple perforation plates, non-septate fibers and a combination of uniseriate and heterogeneous multi-seriate rays less than 1 mm in height, they differ from the McRae wood in the features discussed below (InsideWood 2004 onwards).

Diagnoses for *Madhucoxylon cacharensense* Prakash and Tripathi (1975), *Manilkaroxylon diluviale* (Hofmann 1948) and *M. crystallophora* Grambast-Fessard (1968) indicate these woods have rays of similar width and margin row composition as the fossil wood, as well as axial parenchyma scanty paratracheal and in narrow bands. However, they have smaller diameter vessels arranged in primarily longer radial multiples, and either vasicentric tracheids or crystals in idioblasts. While the ray margin composition of *Sapotaceoxylon penningtonii* Jud (2017) is similar, rays are narrower (1-2 seriate), the axial parenchyma bands are only 1-cell wide and vessels are narrower and in longer radial multiples. *Arganioxylon sardum* Biondi (1981), *Palaeosideroxylon flammula* Grambast-Fessard (1968) and *Bumelioxylon holleisii* Selmeier (1991) are distinguished by having vessels in “patches” with a dendritic or flame-like arrangement rather than a

diagonal arrangement, narrower vessels and rays. Additionally, *Bumelioxylon* has fine helical thickenings in vessels.

The genus *Chrysophylloxylon*, as proposed by Awasthi (1977) with the type species *Chrysophylloxylon pondicherriense*, includes vessels of comparable diameter to the study wood, also arranged in a diagonal pattern, and comparable ray widths. It differs in having some longer radial vessel multiples (2–8, up to 18), vessel-axial parenchyma pits only similar to the intervessel pitting, vasicentric tracheids, rays with fewer square or upright margin rows and more rays per mm. Muller-Stoll and Madel-Angeliewa (1984) also proposed the name *Chrysophylloxylon*, presumably unaware of the Awasthi publication. The generic and specific diagnoses for their *Chrysophylloxylon* and *C. reticulatum* do not specify paratracheal axial parenchyma, but the narrow bands do contact the vessels; such contact is sometimes, but not always, described as scanty paratracheal. The authors report rays with only a few margin rows, but rays are sometimes fused by up to eight upright cells in uniseriate rows. *Chrysophylloxylon reticulatum* differs by having vessels with narrower diameters in loose radial arrangement, mostly biseriate rays, more rays per mm, and prismatic crystals in chambered parenchyma.

The diagnoses of Awasthi (1977) and Müller-Stoll and Mädél-Angeliewa (1984) accurately reflect a subset of species of extant *Chrysophyllum*, but do not match the features of the McRae fossil. As discussed above, the McRae Group IIIB sp. 5 does not fall within generic diagnoses for other fossil woods attributed to Sapotaceae, warranting a new fossil genus within Sapotaceae.

## Biogeography

A study by Bartish et al. (2011) explored origins and mechanisms for diversification and radiation of the subfamily Chrysophylloideae (Sapotaceae), a taxon likely to encompass McRae Group IIIB sp. 5. The study suggested key points of diversification and radiation with implications for the McRae fossil. The analysis supported an estimated crown node age for Chrysophylloideae of 91.7 Ma (79-105 Ma) with the earliest diversification of Chrysophylloideae proposed to be in the Campanian of Africa between 73 and 83 Ma. Radiation to the Neotropics from Africa was estimated to have occurred between 61 and 72 Ma, possibly resulting from short-distance overseas dispersal via island chains. The ancestral area for the entire subfamily could not be considered due to the study design, but South America was proposed as the ancestral area for a subset of genera (including some species of *Chrysophyllum*) with minimum divergence age of 59 Ma. Their analysis incorporated the fossil pollen *Psilatricolporites maculosus* (*Chrysophyllum*) from Venezuela, age 55 Ma (Eocene), as a calibration fossil. That age and location are consistent with a report of the wood *Sapotaceoxylon penningtonii* from the Cenozoic (Late Paleogene to Early Neogene) of Panama (Jud 2017). However, these hypotheses are at odds with the occurrence of a Late Cretaceous fossil wood with features of the Chrysophylloideae inland from the Western Interior Seaway of North America. To accommodate the McRae fossil, the hypotheses would have to be modified to include earlier radiation of Chrysophylloideae and earlier diversification of *Chrysophyllum*. This is possible. The hypotheses ages are based on “minimum age constraints” imposed by fossils, so radiation of the group could have occurred earlier (Goswami

and Upchurch 2010, Heads 2012, Swenson et al. 2012) when South America was in closer proximity to Africa and dispersal between continents more likely. Propagules of Sapotaceae are capable of long-distance transoceanic dispersal (Armstrong 2010, Stride et al. 2014, Terra-Araujo et al. 2015) and the warm, wet Cretaceous environment could have facilitated transfer and establishment in North America.

The result of a biogeographic analysis by Rose et al. (2018) evaluating phylogenetic relationships within Ericales, including Sapotaceae, largely agrees with Bartish et al. (2011) as to the ancestral range of Chrysophylloideae and mechanisms for radiation. The study postulates the stem of Sapotaceae originating ca.102 Ma and the crown ca. 58 Ma, both in Indo-Malaysia, with the area of origin for Chrysophylloideae in the Neotropics and the subfamily having dispersed to the Neotropics from Afrotropics. However, their study proposes the much more recent divergence age for Chrysophylloideae of approximately 24.4 Ma or younger.

### **Other fossil evidence**

A fossil record of pollen, fruits, seeds, and wood documents the presence of Ericales in Europe, Asia, Africa, Central America and North America by the Eocene (Martínez-Millán 2010). Nixon and Crepet (1993) and Crepet et al. (2013) extend the record to the Turonian (~92 Ma) of New Jersey with descriptions of fossil flowers.

Mehrotra (2000) described an entire-margined, pinnately veined leaf as *Chrysophyllum tertiarum* (Sapotaceae) from the Late Paleocene of India. The attribution to Sapotaceae was accepted by Martínez-Millán (2010), but discounted by Manchester et al. (2015) because the identification did not convincingly establish

unique correspondence with Sapotaceae based on synapomorphies. Wing et al. (2009) describe a sapotaceous leaf in the Cerrejón Formation of Colombia (Late Paleocene), a Neotropical rainforest.

Early descriptions of sapotaceous pollen occurrences worldwide dating from the Paleocene forward were compiled by Muller (1981) and Armstrong (2010). However, many of the early reports have been questioned. The pollen of Sapotaceae is distinctive and can be reliably identified as isolated grains (Harley 1991), but Manchester et al. (2015) caution that examination with SEM is necessary to confirm the identification. Harley (1991) questioned the earliest record for the family, *Sapotaceoidaepollenites robustus*, from Borneo (Maastrichtian to Paleocene) (Muller 1981) as not likely sapotaceous based on wall structure. Harris (1972) described *Sapotaceoidaepollenites rotundus* (middle Eocene) from southern Australia (Martin 1978). Those reports in Muller (1981) and Armstrong (2010) based on LM alone must be interpreted cautiously (Manchester et al. 2015, Hoffman 2018) and might warrant reevaluation with SEM.

Recent reports including SEM study are potentially more reliable. Hofmann (2018) accepts a Santonian / Campanian report of pollen with LM and SEM images (by R. Zetter) from western Hungary. Hoffman describes three Chrysophylleae-types similar to South American *Pouteria / Elaeoluma* (Lower Eocene of Cobham, England and Krappfeld, Austria), corroborating the Bartish et al. (2011) hypotheses that Chrysophylloideae had already split into South American and African lineages by the PETM. Bouchal et al. (2017, 2018) describe pollen from the Eskihisar Formation, Yatağan Basin, Muğla, southwestern Turkey (Middle Miocene).

Fossil woods attributed to Sapotaceae have been reported from Oligocene through the lower Pliocene localities in Europe, Africa, Asia and Central America. This McRae fossil is the first wood report from the Cretaceous and the first from North America. The significance of the report invites intense scrutiny. Future study should include putting this wood in phylogenetic context. If accepted, the identification will impact future biogeographic analyses for the family.

## DISCUSSION

The Late Cretaceous of the southern Western Interior is interpreted as having tropical to warm subtropical temperatures with low seasonality (Wolfe and Upchurch 1987, Upchurch et al. 2015, Estrada-Ruiz et al. 2018). Consistent with that inference, the McRae Formation Forest of Giants fossil woods all have possible affinity to families with modern day tropical and subtropical distributions. McRae Group IA sp. 1 falls within the generic limits of the fossil genus *Laurinoxylon* attributed to Lauraceae and shares anatomical features with the modern genus *Ocotea* in the *Ocotea* clade. Lauraceae are a tropical to subtropical family, with species of *Ocotea* concentrated in South and Central America and to a lesser extent in West Africa and Madagascar (Richter in Metcalfe 1987). McRae Group IIIB sp. 4 shares anatomical features with three families [Cannabaceae + [Urticaceae + Moraceae]], a monophyletic clade within Rosales (Wang et al. 2009, Zhang et al. 2011). Within these three families, the fossil wood is most similar to *Celtis* (Cannabaceae), which has a wide temperate and tropical distribution (Yang et al. 2013). The Moraceae are cosmopolitan and most common in Asia and the Indo-Pacific Islands (Zerega et al. 2005, Clement et al. 2009), and the Urticaceae have a

large concentration of genera and species in tropical Asia (Friis 1989, Wu et al. 2013, Kim et al. 2015, Stevens 2001). McRae Group IIIB sp. 6 is most similar to species of *Kirkiaceae* and shares some features with families in the monophyletic clade [Kirkiaceae [Burseraceae + Anacardiaceae]] (Fernando et al. 1995, Clarkson et al. 2002, Bachelier and Endress 2008, Weeks et al. 2014, Muellner-Riehl and Weeks 2016). The modern distribution of the *Kirkiaceae* is eastern tropical Africa, South Africa and Madagascar (Stannard 2007, Bachelier and Endress 2008). The Burseraceae are found in the tropics of America, Africa and Indo-Asia (Weeks et al. 2005). Anacardiaceae are widely distributed in temperate, seasonally dry or wet tropical forests (Weeks et al. 2014). McRae Group IIIB sp. 5 has possible affinity to *Chrysophyllum*. The pantropic subfamily Chrysophylloideae (Sapotaceae) has the highest species diversity in tropical and subtropical rainforests of Africa, Asia and South America (Swenson et al. 2005, 2008).

### **Climatic evidence**

Paleoclimate proxies throughout the Jose Creek Member sites are available to support climatic inferences for the Forest of Giants locality. The combination of taxa represented by the leaf macrofossils in the Jose Creek Member (palms and cycads, Zingiberaceae, Magnoliidae, and conifers) is consistent with evergreen vegetation that today occurs only where temperatures are consistently above freezing (Upchurch and Mack 1998). This boundary for the minimum temperature is consistent with leaf physiognomy studies that determined the southern Western Interior climate was megathermal (20 – 25°C) and subhumid (precipitation  $\geq 100$  cm yr<sup>-1</sup> in the Holdridge system), with year-round precipitation and little

seasonality (Wolfe and Upchurch 1987, Upchurch and Wolf 1987, Upchurch et al. 2015). The absence of distinct growth rings in many Jose Creek woods (Estrada-Ruiz et al. 2012b) is consistent with those findings, as is the presence of palms and cycads that are susceptible to freezing and require consistent moisture availability (Upchurch and Mack 1998). Paleosols in the Jose Creek Member support the conclusions regarding precipitation, given that modern udalf soils, like those present in the Jose Creek Member, are typically found in areas with annual precipitation greater than 75-100 cm (Buck and Mack 1995).

### **Angiosperm stature**

The Forest of Giants assemblage is dominated by a single species; all but three stumps and logs at the site represent a *Paraphyllanthoxylon*-like wood. These specimens (Table 1.4) were of larger diameter (mean diameter 1.1 m) than the other wood types, 0.6 m, 0.7 and 0.6 m for the Lauraceae, cf. Cannabaceae? Moraceae? Urticaceae and Sapotaceae, respectively. The corresponding estimated heights, using the quantification of Rich et al. (1986), indicate the *Paraphyllanthoxylon*-like trees were also taller than the other taxa with a mean height 43.8 m compared to 29.4 m, 31.8 m and 34.9 for Lauraceae, cf. Cannabaceae? Moraceae? Urticaceae and Sapotaceae. Several of the *Paraphyllanthoxylon*-like stumps represent the largest reported stem diameters for fossil angiosperms worldwide. Large stature angiosperms have been reported from a number of localities, predominantly from the southern Western Interior of North America: *Agujoxylon olacaceoides* and *Metcalfexylon kirtlandense* from the Campanian-Maastrichtian Upper Aguja Formation, Texas, USA (Wheeler and Lehman 2000,

Lehman and Wheeler 2001), *Javelinoxylon multiporosum* from the Javelina Formation, Texas, USA (Wheeler et al. 1994), *Metcalfeoxylon kirtlandense* from Crevasse Canyon (Estrada-Ruiz et al. 2012a), *Paraphyllanthoxylon arizonense* from the Cenomanian Mogollon Rim of Arizona, USA (Bailey 1924), *Paraphyllanthoxylon alabamense* from the Cenomanian-Turonian of the Tuscaloosa Group, Alabama, USA (Cahoon 1972), *Paraphyllanthoxylon* from the Mancos Shale Formation of Utah, USA (Jud et al. 2018), *Quercinium centenoae* (Estrada-Ruiz et al. 2007), *Metcalfeoxylon* and *Javelinoxylon* from the Olmos Formation, Coahuila, Mexico (Estrada-Ruiz et al. 2010) and *Paraphyllanthoxylon arizonense* from the Turonian Moreno Hill Formation (Chin et al. 2019).

These results together support the idea that, by the late Campanian, diverse angiosperm lineages had reached the size of medium to large trees and were a dominant tree form in some sedimentary environments from the warmer regions of North America (cf. Wolfe and Upchurch 1987, Upchurch et al. 2015). They indicate that, by the late Campanian, Lauraceae, some Urticales and Sapotaceae had evolved large tree stature.

### **Biogeography**

The abundance of woods being described from the Jose Creek Member presents an opportunity to explore biogeographic analyses for numerous families, some with multiple species, from the same locality and with a well-constrained age. The proposed affinity of a particular specimen cannot be confirmed by a biogeographic analysis that hypothesizes the existence of a certain family in a particular place and time. Neither does an analysis preclude a specimen affinity

when the theory of diversification and dispersal is inconsistent with the proposed identification. Biogeographic analyses are consistent with some, but not all proposed affinities for the Forest of Giants woods.

### **Lauraceae**

The biogeographic history of the Lauraceae is incompletely understood. Chanderbali et al. (2001) propose a Tertiary radiation of the Perseeae-Laureae clade to Laurasia that would not favor attribution of this Late Campanian, McRae Formation fossil wood to *Ocotea*. Further analysis of the clade with additional fossil evidence may resolve this apparent inconsistency.

### **Kirkiaceae**

The McRae Kirkiaceae-like xylotype is consistent with the diagnosis for *Paraphyllanthoxylon* in all respects except the presence of gum cells in the rays. Woods of all Kirkiaceae have not been described; mature samples of additional *Kirkia* species should be found and the anatomy described in detail. If all Kirkiaceae have gum cells, then perhaps only those *Paraphyllanthoxylon*-like woods with gum cells would possibly relate to Kirkiaceae. However, if some *Kirkia* species lack gum cells, some (or all) *Paraphyllanthoxylon*-like woods may also relate to Kirkiaceae. Could the early *Paraphyllanthoxylon* have given rise to the McRae gum cell producing xylotype?

The biogeographic analysis for Burseraceae and Anacardiaceae proposes a pantropic distribution (Weeks et al. 2005, 2014) early in the Cretaceous and early diversification of Burseraceae in North America beginning in the Albian–Aptian of the Early Cretaceous and into the Cenozoic (Weeks et al. 2005, 2014). The reports of

*Paraphyllanthoxylon* woods from the Cretaceous and Cenozoic are consistent with the pantropic ancestor for the sister families Anacardiaceae and Burseraceae and may be tied to the lineage of Kirkiaceae, as well. Alternatively, the Kirkiaceae lineage may have had a pantropic distribution in North America during the Late Cretaceous entirely independent of *Paraphyllanthoxylon*-like woods.

Similarities between the woods of *Paraphyllanthoxylon* and the families in the [Kirkiaceae [Anacardiaceae + Burseraceae]] clade have been noted since Spackman (1948) and a search of the InsideWood database and the literature for comparable woods supports those observations. An ongoing investigation will explore potential similarities between species of *Paraphyllanthoxylon* and extant Kirkiaceae. When woods of all Kirkiaceae have been described, their features may shed light on the variability reported for species of *Paraphyllanthoxylon*.

Investigation of the relationship between *Paraphyllanthoxylon* and Kirkiaceae should not exclude the search for additional evidence to link at least some species of *Paraphyllanthoxylon* to Laurales by attempting to find pith-adjacent samples of *Paraphyllanthoxylon* species for comparison to the pith-adjacent material describe by Herendeen (1991). If *Paraphyllanthoxylon* represents a polyphyletic genus, both interpretations may have merit.

### **Sapotaceae**

The McRae wood type is the earliest report of Sapotaceae. Neither the Rose et al. (2018) nor the Bartish et al. 2011 biogeographic analyses for Chrysophyllodeae, without some revision, would support the presence of a *Chrysophyllum* stem lineage in North America during the Late Campanian. Adjusting the age of radiation to the

Neotropics from Africa from K-T downward might, in fact, simplify the range expansion hypothesis, but a change in the estimation of the diversification age for the genus would also be necessary.

A biogeographic analysis incorporates fossil evidence to estimate node ages that in turn suggest radiation mechanisms and timeframes, but insufficient fossil evidence or estimates based on minimum age constraints can introduce bias to younger age estimates (Boswami and Upchurch 2010, Bartish et al. 2011, Heads 2012, Swensons et al. 2012). The bounty of McRae fossil woods presents the opportunity to test proposed molecular dates, a process integral to the development or refinement of molecular analyses (Wilf and Escapa 2016). It is hoped that a subset of the McRae woods will be characterized with sufficient certainty to be considered for use as calibration fossils to formulate family radiation hypotheses. This will require evaluation of the fossil beyond that conducted to assign fossil wood affinity. Rather, it will be necessary to identify synapomorphies to resolve the fossil placement within its genus, family or clade phylogenetic tree (Wang and Mao 2016).

#### FUTURE STUDY

##### **Logjam locality associated with the Forest of Giants**

Preliminary examination of specimens from a logjam area discovered near the Forest of Giants locality (lower in the section) reveals the *Paraphyllanthoxylon*-like xylotype was, again, the most represented taxa in the logjam source, with two of the Forest of Giants associated species (*Laurinoxylon* and cf. Sapotaceae) also present. At least one species with probable affinities to *Hypodaphnis* (Lauraceae) or Hernandiaceae, a xylotype not found at the Forest of Giants, is being investigated.

## CONCLUSIONS

The Forest of Giants is a unique locality dominated by a large-stature xylotype with possible affinity to Kirkiaceae. Three associated large stature angiosperm taxa include a new species of *Laurinoxylon*, a wood with features of the “Urticales” families Cannabaceae, Moraceae and Urticaceae (Rosales) and a wood that may be the earliest record for Sapotaceae. Additional species may be identified from an adjacent logjam area. The woods of the large stumps and logs are sufficiently preserved to allow detailed descriptions and illustrations, making possible further study of the phylogenetic relationships of these woods in the future. Given the well-constrained age of the Jose Creek Member, placing the woods in phylogenetic context may enhance their value as potential calibration fossils or independent “test” fossils in biogeographic analyses. All components have a combination of features generally considered derived character states within angiosperms as a whole. Anatomical features for the four woods present in the Forest of Giants generally agree with the much larger sample available from the Jose Creek Member of the McRae Formation indicating a warm subtropical climate with year-round precipitation during the Late Campanian. This assemblage of large, *in situ* angiosperms documents that multiple extant angiosperm lineages had achieved large stature by the end of the Cretaceous in warm climates, with Kirkiaceae a dominant taxon. The Forest of Giants contributes to evidence of graded latitudinal rise of angiosperms in North America during the Cretaceous. This study continues the work of Estrada-Ruiz et al. (2012a, 2012b and 2018) in characterizing the woods of the Jose Creek Member of the McRae Formation.

Table 1.1. Comparison of *Laurinoxylon* sp. 1 McRae Group IA sp. 1, TXSTATE 1250, to fossil woods identified through a search of the InsideWood database.

Taxon	GB	VA	V/ mm <sup>2</sup>	VMTD	PP	IVP ( $\mu$ m)	V-RP	F	AP	RW (cells)	RCC	RH ( $\mu$ m)	Oil Cells
<i>Laurinoxylon</i> sp. 1 Group IA sp. 1, TXSTATE 1250	-	25% sol, 2-3 (-5), mostly 2	12	127	sim	alt, 6-10	rb, r/o/he	s, n-s	scp	2-6 mostly 4-5	1, lg pro	557	large, m (s)
<i>Paraphyllanthoxylon vancouverense</i> Jud, Wheeler, Rothwell & Stockey <sup>1</sup>	I	37% sol, 2-4	7	118	sim	alt, 7-10	rb, o/he	s, n-s	rare, scp	2-4	w, 1-2	658	not confirmed
Page Group XIA CASG 60443 <sup>2</sup>		mostly sol, 2-4		92	sim	alt, small	large	s, n-s	scp	(1) 4-5	1-3		not confirmed
DB.D1 Xylotype 4b <sup>3</sup>	I	sol, 2-4	25-30	134	sim	alt, 7-10		s, n-s	rare, scp	(1) 2-4	h	324	not confirmed
<i>Laurinoxylon neagai</i> Iamandei and Iamandei <sup>4</sup>	-1	rarely sol, 2-3 (4-5)	10	163	sim	alt to opp, large	b	s	d, v, sul	2-4 (to 6)	w, 1-4	500- 2000	s, w
<i>Laurinoxylon ehrendorferi</i> Berger <sup>5</sup>	I	sol, 2 (-3)	12	to 200					nearly v	2-4	1	to 800	m, axp
<i>Laurinoxylon microtracheale</i> Süß <sup>6</sup>	+	mostly sol, 2, rarely 3-6	35	45	sim	alt, minute	b		scp, v	1-5, mostly 3-4	1	50- 320	rays, axp
<i>Laurinoxylon aff. czechense</i> Prakash, Březinová & Bůžek <sup>7</sup>	+	18% sol, 2-4, mostly 2, c	40- 100	60	sim	alt, ~10			scp	2-3	1	280- 520	rays
<i>Laurinoxylon namsangensis</i> Lakhanpal, Prakash & Awasthi <sup>8</sup>	-	sol, 2-5, mostly 2-3	8-10	75-300	sim	alt, sub-alt, 8-12	rb, r/o	s	scp, rarely v	2 (-3)	a		rays
<i>Laurinoxylon perseamimatus</i> Petrescu <sup>9</sup>	-1		5-20		sim	alt, >10			rare, scp, v	1-3	h		rays
<i>Laurinoxylon stichkai</i> Boonchai & Manchester <sup>10</sup>	I	28% sol, 2-4 (-5), c of 3-4 (-6)	8-19	117	sim	alt, 8-12	rb to s, r/sca - h to d	s	scp, v	2-3	1	285	m, w, axp
<i>Ulmium porosum</i> Wheeler, Scott & Barghoorn <sup>11</sup>	+	sol, 2-3 (-5), (diagonal)	32-85	92	sim	alt, med	rb, b, r/o/irr		para	to 5	1-3	140- 1400	m

Table 1.1. Comparison of *Laurinoxylon* sp. 1, McRae Group IA sp. 1, TXSTATE 1250, to fossil woods identified through a search of the InsideWood database.

*Legend:* McRae fossil wood is in boldface. VA = vessel arrangement, (s) = solitary, range represents common radial vessel multiples, range in parentheses represents rare radial multiples; V/mm<sup>2</sup> = average vessel density, range equals range of mean values for multiple samples or range reported by the publication author; VMTD = vessel mean tangential diameter, range represents range of means for multiple samples; PP = perforation plate, (sim) = simple, (sc) = scalariform; IVP = intervessel pits, (alt) = alternate, range of pit diameters (µm); V-RP = vessel-ray parenchyma pits, (b) = bordered, (rb) = reduced borders, (s) = simple, (r) = round, (o) = oval, (e) = elongate, (c) = curved, (h) = horizontal, (d) = diagonal; F = fiber, (s) = septate fibers, (n-s) = non-septate fibers; AP = axial parenchyma, (d) = diffuse, (dia) = diffuse-in-aggregates, (para) = paratracheal, (scp) = scanty paratracheal, (alif) = aliform, (con) = confluent, (v) = vasicentric, (sul) = short uniseriate lines; RW = range of ray widths; RCC = ray cellular composition, number range = number of uniseriate marginal rows of square or upright cells, (w) = square or upright cells mixed within the ray, (h) = heterocellular, (w-h) weakly heterocellular, (lg pro) = marginal row(s) composed of large procumbent cells, (fused) = rays sometimes vertically fused by uniseriate regions; RH = mean ray height, range represents range of means for multiple samples or range reported by the publication author; R/mm = average number of rays per millimeter or range for multiple samples; Oil cells = idioblasts with dark content, (m) = at the ray margin, (s) = at the side of the ray as seen in tangential view, (w) = within the ray as seen in tangential view, (axp) = in axial parenchyma; (f) = among fibers. Nob = Not observed due to quality of sample preservation.

<sup>1</sup>Jud et al. 2017

<sup>2</sup>Page 1980

<sup>3</sup>Wheeler & Michalski 2003

<sup>4</sup>Iamandei and Iamandei. 1997

<sup>5</sup>Berger 1953

<sup>6</sup>Süss 1958

<sup>7</sup>Mantzouka et al. 2016

<sup>8</sup>Lakhanpal et al. 1978

<sup>9</sup>Petrescu 1978

<sup>10</sup>Boonchai and Manchester 2012

<sup>11</sup>Wheeler et al. 1977

Table 1.2. Comparison of *Laurinoxylon* sp. 1, McRae Group IA sp. 1, TXSTATE 1250 to fossil genera and type species of Lauraceae.

Taxon	GB	VA	V/ mm <sup>2</sup>	VMTD	PP	IVP ( $\mu$ m)	V-RP	F	AP	RW (cells)	RCC	RH ( $\mu$ m)	Oil Cells
<b><i>Laurinoxylon</i> sp. 1 Group IA sp. 1, TXSTATE 1250</b>	-	25% sol, 2-3 (-5), mostly 2	12	127	sim	alt, 6-10	rb, r/o/he	s, n-s	scp	2-6 mostly 4-5	1, lg pro	557	large, m (s)
<i>Paraperseoxylon scalariforme</i> Scott & Wheeler emend. Wheeler & Manchester <sup>1</sup>	I	mostly sol, 2-3	14	70-87	sim, sc 4-12	alt, 5	rb, r/he/c	n-s	scp, v, con	1-2 (-3)	1	340- 387	r, f
<i>Ocotoxylon tigurinum</i> Schuster <sup>2</sup>	+	sol, 2-3 (-6)			sc	poly, ellip, 18-21			d	rarely 1, mostly 2 (-3)	1-2	to 630	-
<i>Cinnamoxylon areolosum</i> Gottwald <sup>3</sup>	I	sol, to 3	8-15	80- 100	sim, sc to 4	Alt, 8-12	r to e	few s, n-s	v, alif, con	2-4		250- 450	m, f, axp,
<i>Sassafrasoxylon lipnicense</i> Brezinova & Süss <sup>4</sup>					sim, sc	alt	b, r to he		scp	1-4	w-h		+
<i>Caryodaphnopsylon richteri</i> Gottwald <sup>5</sup>	I	sol, often 2		120- 200	sim	alt, 8-13	r	s	d, weakly v	7-8 (-10)	1	1500- 2000 (-4000 )	axp
<i>Beilschmiedioxylon africanum</i> Dupéron- Laudoueneix and Dupéron <sup>6</sup>	I	75% sol, 2-3	3-6	185	sim	alt, 10-12	he		v, bands	1-6 mostly 3-4	1-4	100- 850	f
<i>Cryptocaryoxylon gippslandicum</i> Leisman <sup>7</sup>					sim, sc	alt	b, r to he		scp	1-4	w-h		+
<i>Machilusoxylon hindusthanensis</i> Bande emend. Ingle <sup>8</sup>	I	mostly sol, 2-4	4-7	90- 180	sim	alt, 5-10	N Ob	s	v	1-4 mostly 2-3	1-5, fused	630 (-820)	

Table 1.2. Continued. Comparison of *Laurinoxylon* sp. 1, McRae Group IA sp. 1, TXSTATE 1250 to fossil genera and type species of Lauraceae.

Taxon	GB	VA	V/ mm <sup>2</sup>	VMTD	PP	IVP ( $\mu$ m)	V-RP	F	AP	RW (cells)	RCC	RH ( $\mu$ m)	Oil Cells
<b><i>Laurinoxylon</i> sp. 1 Group IA sp. 1, TXSTATE 1250</b>	-	25% sol, 2-3 (-5), mostly 2	12	127	sim	alt, 6-10	rb, r/o/he	s, n-s	scp	2-6 mostly 4-5	1, lg pro	557	large, m (s)
<i>Laurinoxylon dituviale</i> Felix emend. Dupéron et al <sup>9</sup>	+	sol, 2-7	9-16	100- 154	sim, sc 6-12	alt, 7-10 to ellip 10-15	he to vertically e	n-s	v	1-5 mostly 3-4	1 (-3)	<1mm (-820)	m
<i>Mezilaurinoxylon eiporosum</i> Wheeler & Manchester <sup>1</sup>	I	sol, 2-3 (-4)	16-38	50-150 84-125	sim	alt, >10	rb, o to window- like	s	scp, v	1-4 (-5)	1	437- 615	m
<i>Olmosoxylon upchurchii</i> Estrada-Ruiz, Martinez-Cabrera, & Cevallos-Ferriz <sup>10</sup>	I	77% sol, 2-3 (-4)	9	109	sim	alt, 5-11	rb, o to he	s, n-s	rarely d, scp	3-7	w-h	990	rays

Table 1.2. Comparison of *Laurinoxylon* sp. 1, McRae Group IA sp. 1, TXSTATE 1250 to fossil genera and type species of Lauraceae.

*Legend:* McRae fossil wood is in boldface. VA = vessel arrangement, (sol) = solitary, range represents common radial vessel multiples, range in parentheses represents rare radial multiples;  $V/mm^2$  = average vessel density, range equals range of mean values for multiple samples or range reported by the publication author; VMTD = vessel mean tangential diameter, range represents range of means for multiple samples; PP = perforation plate, (sim) = simple, (sc) = scalariform; IVP = intervessel pits, (alt) = alternate, range of pit diameters ( $\mu m$ ); V-RP = vessel-ray parenchyma pits, (b) = bordered, (rb) = reduced borders, (s) = simple, (r) = round, (o) = oval, (e) = elongate, (c) = curved, (h) = horizontal, (d) = diagonal; F = fiber, (s) = septate fibers, (n-s) = non-septate fibers; AP = axial parenchyma, (d) = diffuse, (dia) = diffuse-in-aggregates, (scp) = scanty paratracheal, (alif) = aliform, (con) = confluent, (v) = vasicentric, (sul) = short uniseriate lines; RW = range of ray widths; RCC = ray cellular composition, number range = number of uniseriate marginal rows of square or upright cells, (w) = square or upright cells mixed within the ray, (h) = heterocellular, (w-h) weakly heterocellular, (lg pro) = marginal row(s) composed of large procumbent cells, (fused) = rays sometimes vertically fused by uniseriate regions; RH = mean ray height, range represents range of means for multiple samples or range reported by the publication author; R/mm = average number of rays per millimeter or range for multiple samples; Oil cells = idioblasts with dark content, (m) = at the ray margin, (s) = at the side of the ray as seen in tangential view, (w) = within the ray as seen in tangential view, (axp) = in axial parenchyma; (f) = among fibers. Nob = Not observed due to quality of sample preservation.

<sup>1</sup> Wheeler and Manchester 2002

<sup>2</sup> Schuster 1906

<sup>3</sup> Gottwald 1997

<sup>4</sup> In: Poole et al. 2000

<sup>5</sup> Gottwald 1992

<sup>6</sup> Dupéron-Laudoueneix and Dupéron 2005

<sup>7</sup> Leisman 1986

<sup>8</sup> Ingle SR. 1974

<sup>9</sup> Dupéron et al. 2008

<sup>10</sup> Estrada-Ruiz et al. 2010

Table 1.3a. Comparison of McRae Group IIIB sp. 4, TXSTATE 1287 to Urticales (Rosales) fossil genera and woods.

Taxon	Age	GB	VA	IVP ( $\mu\text{m}$ )	VMTD ( $\mu\text{m}$ )	V/ $\text{mm}^2$	FW	AP	RW Uni	RW Multi (cells)	RH ( $\mu\text{m}$ )	RCC	Other
<b>McRae Group IIIB sp.4 TXSTATE 1287 McRae Formation</b>	Ca	-	D, sol, rm 2-3	7-10	127	2-5	T-M	dia, v-ns, al, uni,	23%	1-6 (4-6)	482 (-855)	1-3 (to 8)	
<i>Moroxylon sturmii</i> Selmeier <sup>1</sup> Upper Freshwater Molasse, Southern Germany, Bavaria	Mi	+	R, sol, rm 2-3 (-4), c, b	8-11	170-2 45	14-22	T-Th	v, c	+	1-4	143- 466	p	rhs-v, cr-p
<i>Artocarpoxylon kartickcherrieansis</i> Prakash & Lalitha <sup>2</sup> Tipam sandstones, Assam, India	T	I	sol, rm 2-4	10-1 2	105-3 15	2-3		v, mostly al, rarely c		1-6 (3-5)		1-3	rhs-v, rlt
<i>Cudranioxylon englismense</i> Dupéron- Laudoueneix <sup>3</sup> Babin-Boutin Quarry, Charente, France	Eo		sol, rm, tm, c	NA		14-28	Th	b	+	1-4 (2-3)	400 (-1024)	p	cr-p
<i>Ficoxylon tropicum</i> Felix <sup>4</sup> Kostenblatt, Bohemia	T	-	D, sol, short rm	NA	160			v-ws, al		3-10	tall	pr, 1	cr-p
<i>Celtixylon dacicum</i> (Petrescu) <sup>5</sup> Petrescu <sup>5</sup> Transylvania, Romania	Oli	+	R, sol, rm,c,b	NA	50- 100			v, c		4-10		1-4	cr-p, vht
<i>Myrianthoxylon coppensi</i> Koeniguer <sup>6</sup> Angamma, Chad	Pl		D, sol, rm 2-3	5-7	100-2 00	1-2	Th	b	rare	2-8	100- 900	1-2	
<i>Scottoxylon eocenicum</i> Wheeler & Manchester <sup>7</sup> Clarno Nut Beds	Eo	I, -	D, sol, rm 2-4	5-12	107-1 83	9-21	M	v, al, c, t	rare	1-7 (5-6)	650- 806 (-1,760)	1-3 (to 7)	rhs-p, cr-a

Table 1.3b. Comparison of McRae Group IIIB sp. 4, TXSTATE 1287 to Urticales (Rosales) fossil genera and woods.

Taxon	Age	GB	VA	IVP ( $\mu\text{m}$ )	VMTD ( $\mu\text{m}$ )	V/ $\text{mm}^2$	FW	AP	RW Uni	RW Multi (cells)	RH ( $\mu\text{m}$ )	RCC	Other
<b>McRae Group IIIB sp.4 McRae Formation TXSTATE 1287</b>	Ca	-	D, sol, rm 2-3	7-10	127	2-5	T-M	dia, v-ns, al, uni,	23%	1-6 (4-6)	482 (-855)	1-3 (to 8)	
Clarno Urticalean Wood Type I Clarno Nut Beds <sup>7</sup>	Eo	I, +	D, sol, rm 2-3	8-12	114- 117	9-10	T-M	b (8-10 cells wide)	+	1-8	483 (- 675)	to 5	rhs-p, cr-v
Clarno Urticalean Wood Type II Clarno Nut Beds <sup>7</sup>	Eo	+	D, sol, rm 2	5-8	146	5-10-16	M	v, al, c, m	+	1-4	458 (- 610)	1-4	rhs-v, cr-p
Farafra Oasis Wood 1FO Hefhuf Formation <sup>8</sup>	LC	I	D, sol, rm 2-3	7-10	160	4-7	T-Th	v, al, c	rare	1-4 (3-4)	450- 780	1-2	

Table 1.3a–b. Comparison of McRae Group IIIB sp. 4, TXSTATE 1287 to Urticales (Rosales) fossil genera and woods.

*Legend:* McRae fossil wood is in boldface. Age, (Ca) = Campanian, (Eo) = Eocene, (Ol) = Oligocene, (Mi) = Miocene, (Pl) = Pliocene, (T) = Tertiary; GB = growth boundaries, (-) = absent, (I) = indistinct, (+) = distinct; VA = vessel arrangement, (D) = diffuse-porous, (R) = ring-porous, (sol) = solitary, range represents common vessel multiples, (rm) = radial multiples, (tm) = tangential multiples, (c) = clusters, (b) = vessels in tangential or oblique bands; IVP = intervessel pit size range ( $\mu\text{m}$ ); VMTD = vessel mean tangential vessel diameter from a single specimen, range from multiple;  $V/\text{mm}^2$  = range of vessels per square mm; FW = fiber wall thickness: T = thin, M = medium, Th = thick; AP = axial parenchyma: (dia-sw) = diffuse-in-aggregates short, wide lines, (v) = vasicentric, (v-ns) = vasicentric - narrow sheath, (v-ws) = vasicentric - wide sheath, (al) = aliform, (c) = confluent, (uni) = unilateral, (b) = banded, (t) = terminal, (m) = marginal; RW Uni = uniseriate rays, % = percent uniseriate rays, (+) = present, (-) = absent; RW Multi = multiseriate ray width, range of ray widths, most common range in parentheses; RH = ray height, mean, largest number observed in parentheses, range of means for multiple samples; RCC = ray cellular composition, number range = number of uniseriate margin rows of square or upright cells, (p) = present (exact number unspecified), (pr) = all procumbent cells; Other: (rsh-p) = ray sheath cells present, (rsh-v) = ray sheath cells variable, (cr-p) = prismatic crystals present, (cr-a) = prismatic crystals absent, (cr-v) = prismatic crystals variable, (rlt) = ray latex tubes, (vht) = vessel helical thickenings.

<sup>1</sup> Selmeier 1993

<sup>2</sup> Prakash and Lalitha 1978

<sup>3</sup> Dupéron-Laudoueneix 1980

<sup>4</sup> Felix 1883

<sup>5</sup> Observation from InsideWood 2004-onward image

<sup>6</sup> Koeniguer 1975

<sup>7</sup> Wheeler and Manchester 2002

<sup>8</sup> Kamal El-Din et al. 2006

Table 1.4. Forest of Giants log and stump diameters, and estimated maximum height..

	Stem Diameter (m)	Rich et al 1986 Maximum Height (m)
<b>McRae Group IIB sp. 6</b>		
Log 1	0.7	33.4
Log 3	1.0	39.9
Log 4	0.7	32.6
Log 5	0.9	39.2
ST 1	1.4	52.3
ST 2	1.8	60.0
ST 4	0.9	38.5
ST 5	1.0	42.0
ST 7	0.8	34.1
ST 8	0.8	34.9
ST 12	1.1	42.7
ST 13	1.3	49.2
ST 14	1.0	40.6
ST 15	1.1	43.4
ST 18	2.0	63.9
ST 19	1.6	55.6
Mean	1.1	43.9
SD	0.4	9.6
<b>McRae Group IIB sp. 5, TXSTATE 1288 cf. Sapotaceae</b>		
ST 3	0.8	34.9
<b><i>Laurinoxylon</i> sp. 1, Group IA sp. 1, TXSTATE 1250</b>		
ST 6	0.6	29.4
<b>McRae Group IIB sp.4, cf. Cannabaceae? Moraceae? Urticaceae?</b>		
ST 16	0.7	31.8

Table 1.5. Comparison of McRae Group IIIB sp. 6, TXSTATE 1232-1246 to *Kirkia* species.

Taxon	VA	IVP ( $\mu\text{m}$ )	VMTD	V-RP r/o, med-large	V/ mm <sup>2</sup>	AP	RW Uni	RW Multi (cells)	RH ( $\mu\text{m}$ )	RCC	R/mm
<b>McRae Group IIIB sp. 6</b>	47% sol, 2-3 (5)	alt, 12-18	195 - 234	s, rb, r/o, med-large	4-7	scp, (nearly v)	< 2%	(1) 2-4 (6), mostly 3-4	536 - 1184	all pro, or 1 (-5)	7-10
<i>Kirkia acuminata</i> <sup>2,3,4,7</sup>	sol, 2, (c)	medium; some elongate	126	s, rb, (b), r/o	6-31	rare, scp	3%	1-5 (-6), mostly 3-4	<1 mm	all pro, or 1-several	5-7
<i>Kirkia leandrii</i> <sup>4</sup>	sol, 2-3, (c)					rare, scp	common	1-4, mostly 2-3		all pro, or 1-2	
<i>Kirkia wilmsii</i> <sup>5,6</sup>	sol, 2-3, (c)	medium	76	s, o/e:h-d	31-50		16%, (all sq/upr cells)	1-3, mostly 1-2	326, (mostly <500)	all pro, or 1- several, (ray to ray fusion)	6-8

**Legend:** McRae fossil wood is in boldface. VA = vessel arrangement, (sol) = solitary, number = common radial vessel multiples, c = clusters, rare or uncommon features in parentheses; IVP = intervessel pits, (alt) = alternate, range of pit diameters ( $\mu\text{m}$ ); VMTD = vessel mean tangential diameter, range represents range of means for multiple samples; V-RP = vessel-ray parenchyma pits, (b) = bordered, (rb) = reduced borders, (s) = simple, (r) = round, (o) = oval, (e) = horizontally elongate, (h) = horizontal, (d) = diagonal; V/mm<sup>2</sup> = average vessel density, range equals range of mean values for multiple samples; AP = axial parenchyma, (-) = absent, (scp) = scanty paratracheal, (v) = vascentric; RW Uni = % uniseriate rays; RW Multi = range of multicellular ray widths; RH = mean ray height, range represents range of means for multiple samples; RCC = ray cellular composition, (all pro) = ray parenchyma all procumbent, number range = number of uniseriate marginal rows of square or upright cells; R/mm = average number of rays per millimeter or range for multiple samples.

<sup>1</sup> Takahashi and Suzuki 2003

<sup>5</sup> Parrott, unpublished observations of a small diameter axis

<sup>2</sup> Webber 1936

<sup>6</sup> Images courtesy E. Wheeler - *Kirkia wilmsii* - Tw24046 - xs - 10x.tif; Tw24046 - t1s - 10x.tif

<sup>3</sup> Heimsch 1942

<sup>7</sup> Images courtesy E. Wheeler - *Kirkia acuminata var cordata* - Tw28858 - xs - 10x.tif;

<sup>4</sup> InsideWood, 2004 onward

Tw28858 - t1s - 10x.tif (from EW) and slides

Table 1.6. Comparison of McRae Group IIIB sp. 6, TXSTATE 1232-1246 to similar species of *Paraphyllanthoxylon*.

Taxon	VA	IVP ( $\mu\text{m}$ )	VMTD ( $\mu\text{m}$ )	V/ $\text{mm}^2$	AP	RW Uni	RW Multi (cells)	RH ( $\mu\text{m}$ )	RCC	Other
<b>McRae Group IIIB sp. 6</b>	47% sol, 2-3 (5)	alt, 12-18	195 - 234	4-7	scp, (nearly v)	< 2%	(1) 2-4 (6), mostly 3-4	536 - 1184	all pro, or 1 (-5)	
<i>P. arizonense</i> Wheeler, McClammer & LaPaasha <sup>1</sup>	sol, 2-4		175	4-7 (5)	scp	+	2-4 (-6), mostly 3-4	1018	1-5	
<i>P. marylandense</i> Herendeen <sup>2</sup>	sol, 2-5. mostly 2-3	3-9	81	8-14		+	1-7	220- 1040	1-3 (-7) ray fusion	(fine helical thickenings); scalariform perforation plates in juvenile wood
<i>P. abbottii</i> Wheeler <sup>1</sup>	16-38% sol, 2-4	10-12	141-234	35- 60	absent to rare, scp		1-4, mostly 2-3	474- 763	1-2 (-4)	
<i>P. cenomaniana</i> Takahashi & Suzuki <sup>3</sup>	46% sol, 2-5	13	174	2-16	scp		2-4	300- 2000? (typo)		
<i>P. vancouverense</i> Jud, Wheeler, Rothwell & Stockey <sup>4</sup>	37% sol, 2-4	7-10	118	6-16 (11)	rare, scp		to 5	658	all pro, or 1-2, (w)	enlarged ray cells (tangential view) with dark content

Table 1.6. Comparison of McRae Group IIIB sp. 6, TXSTATE 1232-1246 to similar species of *Paraphyllanthoxylon*.

*Legend:* The study fossil is in bold. VA = vessel arrangement, (%) = percent solitary vessels, (sol) = solitary, range represents common vessel radial multiples; IVP = intervessel pit size range ( $\mu\text{m}$ ), (alt) = alternate; VMTD = vessel mean tangential diameter from a single specimen, range from multiple specimens in  $\mu\text{m}$ ;  $\text{V}/\text{mm}^2$  = range of vessels per square mm; AP = axial parenchyma, (scp) = scanty paratracheal, (v) = vasicentric; RW Uni = % uniseriate rays, (+) = present, (-) = absent; RW Multi = range of multicellular ray widths, uncommon range in parentheses; RH = ray height, range of means for multiple samples, range for a single sample when mean not provided, mean; RCC = ray cellular composition, number range = number of uniseriate marginal rows of square or upright cells, uncommon values in parentheses, (pro) = procumbent cells (w) = square or upright cells within ray; Other = characteristic features.

<sup>1</sup> Bailey 1924, data from Wheeler 1991

<sup>2</sup> Herendeen 1991

<sup>3</sup> Takahashi and Suzuki 2003

<sup>4</sup> Jud et al. 2017

Table 1.7. McRae Formation Forest of Giants woods.

Taxon	ESD (m)	EH (m)	VA	VP	IVP (µm)	VMTD (µm)	V-RP	V/mm <sup>2</sup>
<i>Laurinoxylon</i> sp. 1 McRae Group IA sp. 1, TXSTATE 1250	0.6	29.4	25% sol, 2-3 (4-5)	diffuse porous	alt, 6-10	127	rb, r/o/e	12
McRae Group IIIB sp. 6	mean 1.1, 0.7-2.0	43.8	47% sol, 2-3 (5)	diffuse porous	alt, 12-18	195 - 234	s, r, med- large	4-7
McRae Group IIIB sp.4, TXSTATE 1287 cf. Cannabaceae? Moraceae? Urticaceae?	0.7	31.8	64% sol, 2-3	diffuse porous	alt, 7-10	127	b-rb, o/e	3
McRae Group IIIB sp. 5, TXSTATE 1288 cf. Sapotaceae	0.8	34.9	63% sol, 2-3 (4)	diffuse porous to semi-ring- porous	alt, 7-12	156	b-rb, o/e	6

Taxon	F	AP	RW Uni	RW Multi (cells)	RH (µm)	RCC	R/mm	Oil
<i>Laurinoxylon</i> sp. 1 Group IA sp. 1, TXSTATE 1250	s, n-s	scp	0%	2-6, mostly 4-5	557	all pro, or 1	9	r
McRae Group IIIB sp. 6	s, n-s	scp, (nearly v)	< 2%	(1) 2-4 (6), mostly 3-4	536 - 1184	all pro, or 1 (-5)	7-10	-
McRae Group IIIB sp.4, TXSTATE 1287 cf. Cannabaceae? Moraceae? Urticaceae?	N Ob	dia: lines 1-3 cells wide, v	23%	1-6	505	1-8	9	-
McRae Group IIIB sp. 5, TXSTATE 1288 cf. Sapotaceae	N Ob	dia: lines 1-3 cells wide, scp	33%,	1-4	338	1-8	10	-

Table 1.7. McRae Formation Forest of Giants woods.

*Legend:* McRae fossil wood is in boldface. ESD = estimated stem diameter in m; EH = tree height estimated using the quantification of Rich et al. (1986); VA = vessel arrangement, (sol) = solitary, range represents common radial vessel multiples, range in parentheses represents rare radial multiples; VP = vessel porosity; IVP = intervessel pits, (alt) = alternate, range of pit diameters ( $\mu\text{m}$ ); VMTD = vessel mean tangential diameter, range represents range of means for multiple samples; V-RP = vessel-ray parenchyma pits, (iv) = like intervessel pitting, (b) = bordered, (rb) = reduced borders, (s) = simple, (r) = round, (o) = oval, (e) = horizontally elongate;  $V/\text{mm}^2$  = average vessel density, range equals range of mean values for multiple samples; F = fiber, (s) = septate fibers, (n-s) = non-septate fibers; AP = axial parenchyma, (dia) = diffuse-in-aggregates, (scp) = scanty paratracheal, (v) = vasicentric; RW Uni = % uniseriate rays; RW Multi = range of multicellular ray widths; RH = mean ray height, range represents range of means for multiple samples; RCC = ray cellular composition, (all pro) = ray parenchyma all procumbent, number range = number of uniseriate margin rows of square or upright cells; R/mm = average number of rays per millimeter or range for multiple samples; Oil = idioblasts with dark content, (r) = in rays, N Ob = Not observed due to quality of sample preservation.

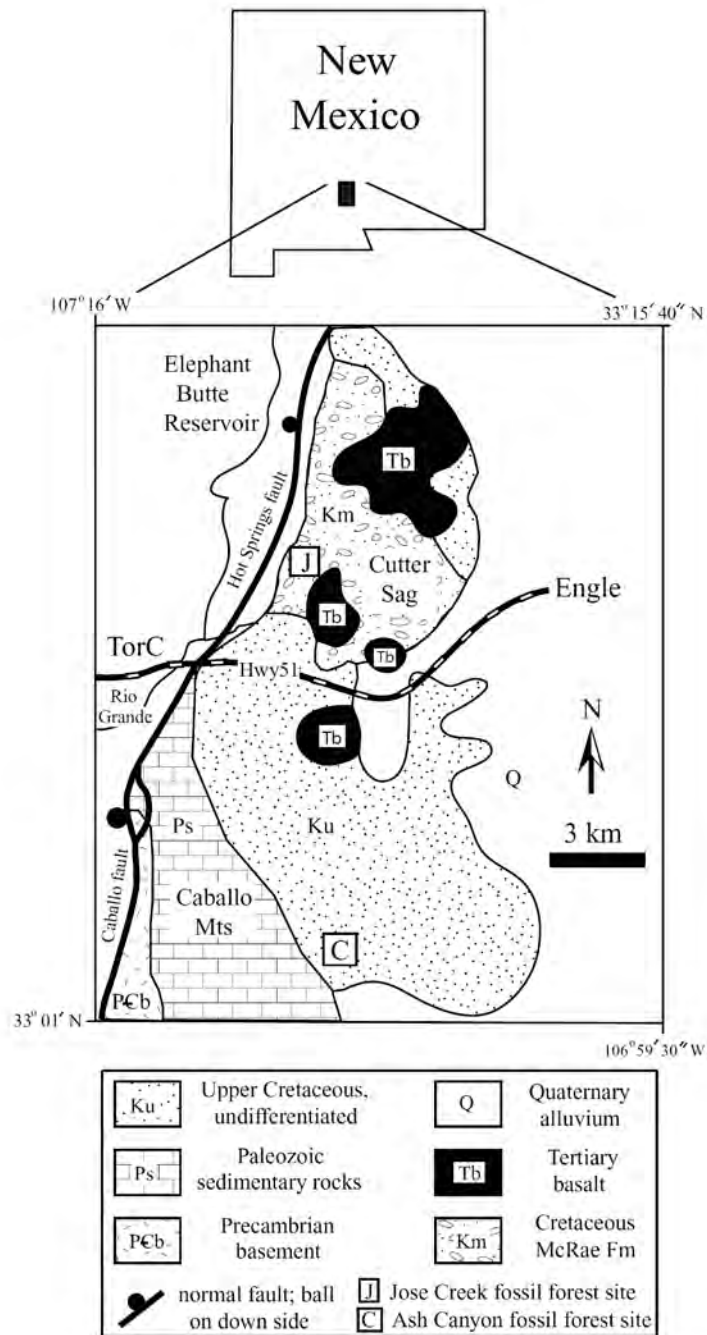


Figure 1.1. Maps showing the location and geology of the McRae Formation, south-central New Mexico (Estrada-Ruiz et al. 2018).



Figure 1.2. McRae wood holoxylotype Group IA sp. 1 (TXSTATE 1250) Lauraceae.  
- A: Fragmented stump. - B: Area near Stump 6 (Group IA sp. 1 ).

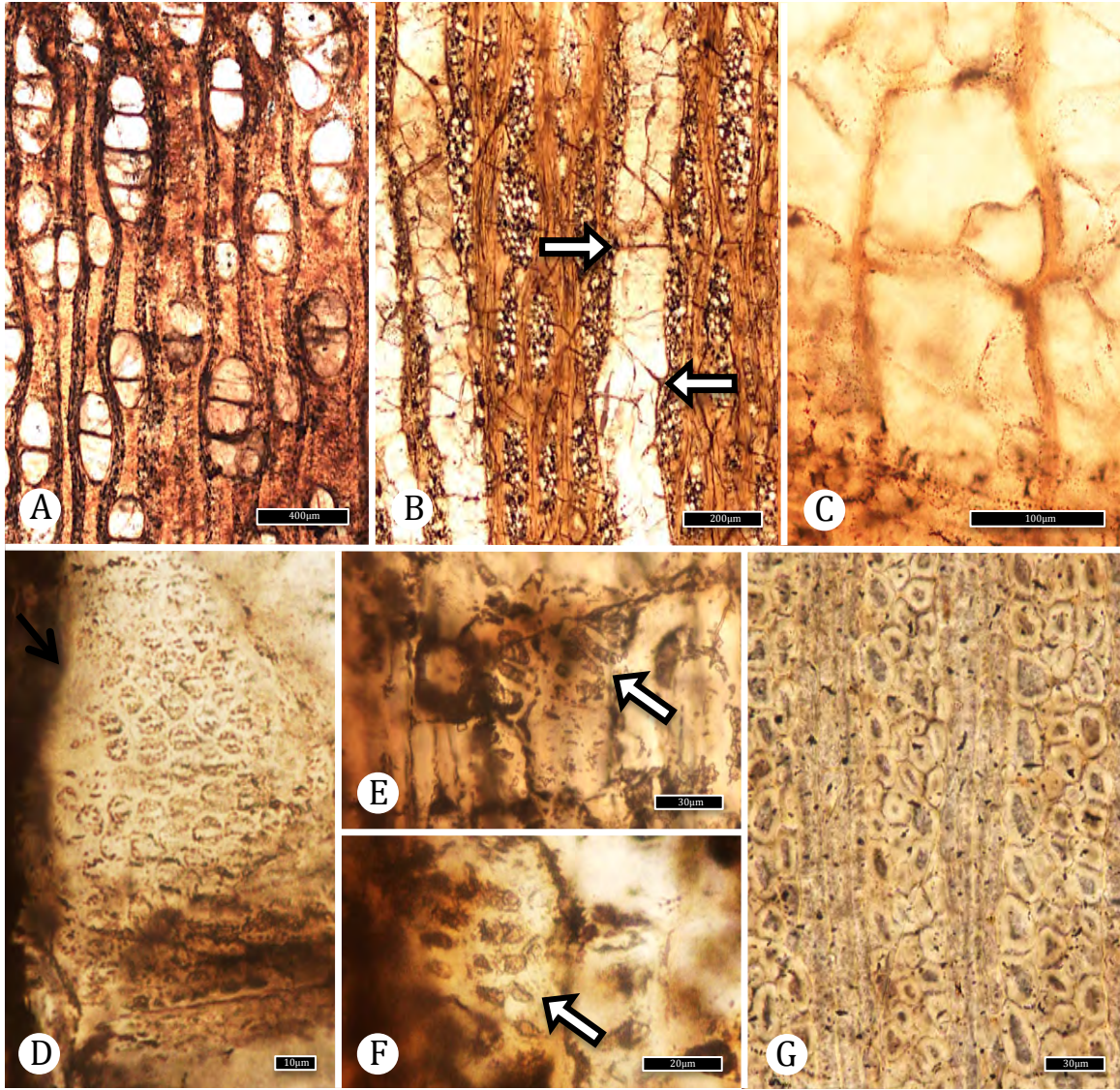


Figure 1.3. McRae wood holoxylotype Group IA sp. 1 (TXSTATE 1250) Lauraceae. – A: TS. Wood diffuse-porous. TXSTATE 1250, X-4. Scale bar = 400  $\mu\text{m}$ . – B: TLS Vessel element (arrows at end walls). TXSTATE 1250, T-1. Scale bar = 200  $\mu\text{m}$ . – C: RLS: Tyloses thin-walled. TXSTATE 1250, R-1. Scale bar = 100  $\mu\text{m}$ . – D: TLS. Alternate intervessel pits rounded in outline. TXSTATE 1250, T-2. Scale bar = 10  $\mu\text{m}$ . – E: RLS. Vessel-ray parenchyma pits with reduced borders, horizontally elongate (arrow). TXSTATE 1250, R-7. Scale bar = 30  $\mu\text{m}$ . – F: RLS. Vessel-ray pits with reduced borders, horizontally elongate (arrow). TXSTATE 1250, R-1. Scale bar = 20  $\mu\text{m}$ . – G: TS. Fibers angular in cross section, thin-walled to thick-walled. TXSTATE 1250, X-3. Scale bar = 30  $\mu\text{m}$ .

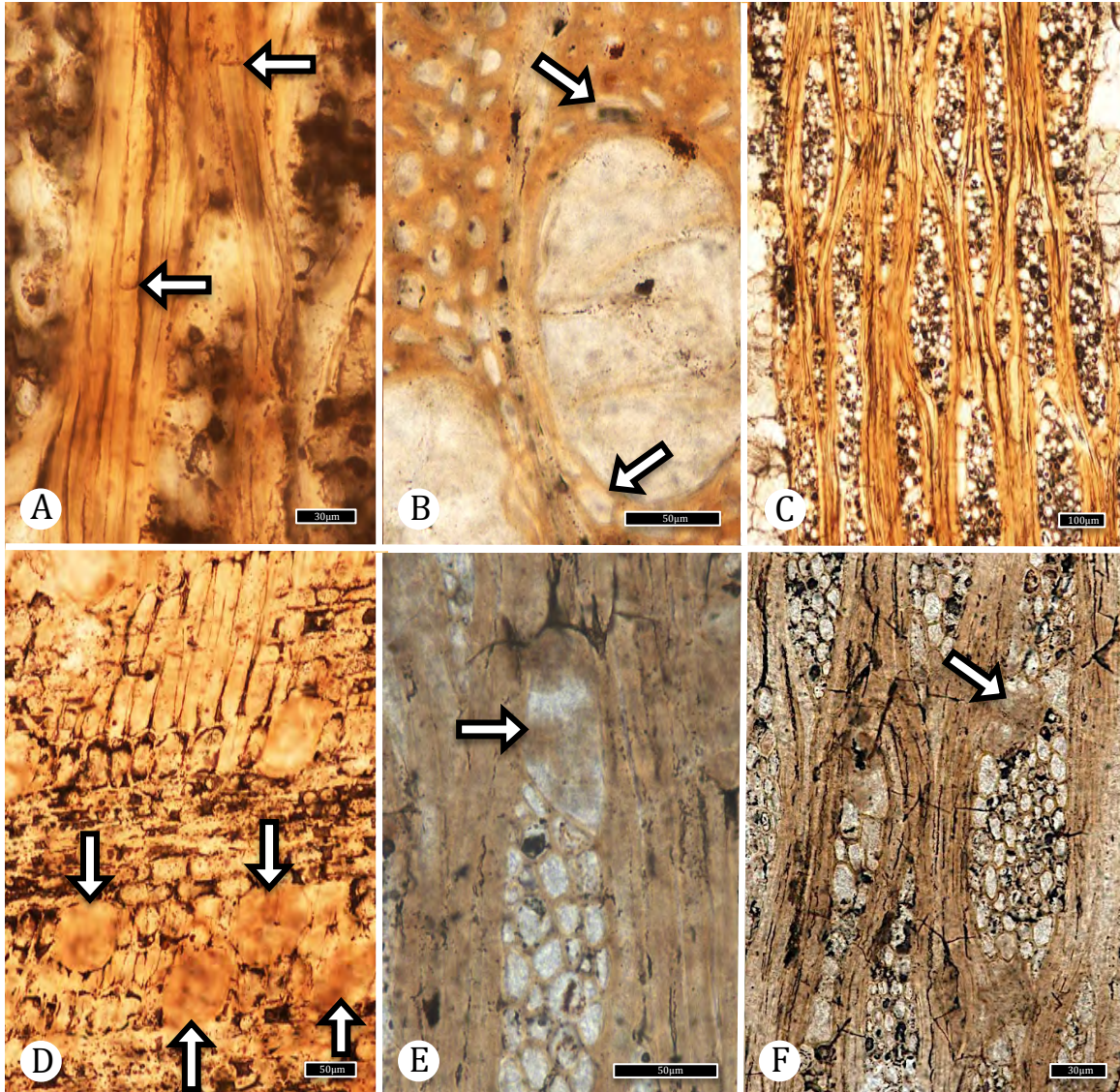


Figure 1.4. McRae wood holoxylotype Group IA sp. 1 (TXSTATE 1250) Lauraceae.  
 – A: TLS. At least some fibers septate (arrow). TXSTATE 1250, T-2. Scale bar = 30  $\mu\text{m}$ .  
 – B: TS. Axial parenchyma scanty paratracheal (arrows). TXSTATE 1250, X-2. Scale bar = 50  $\mu\text{m}$ .  
 C: TLS. Rays 2 – 6 seriate, cells all procumbent or with one row of square or upright margin cells. TXSTATE T-1. Scale bar = 100  $\mu\text{m}$ .  
 – D: RLS. Large idioblasts from one ray margin in close proximity to idioblasts at the margin of the ray below it (arrows). TXSTATE 1250, R-2. Scale bar = 50  $\mu\text{m}$ .  
 – E: TLS. Ray with large idioblast at the margin (arrow). TXSTATE 1250, T-1. Scale bar = 50  $\mu\text{m}$ .  
 – F: TLS. Ray with idioblasts at the ray edge (arrow). TXSTATE 1250, T-1. Scale bar = 30  $\mu\text{m}$ .

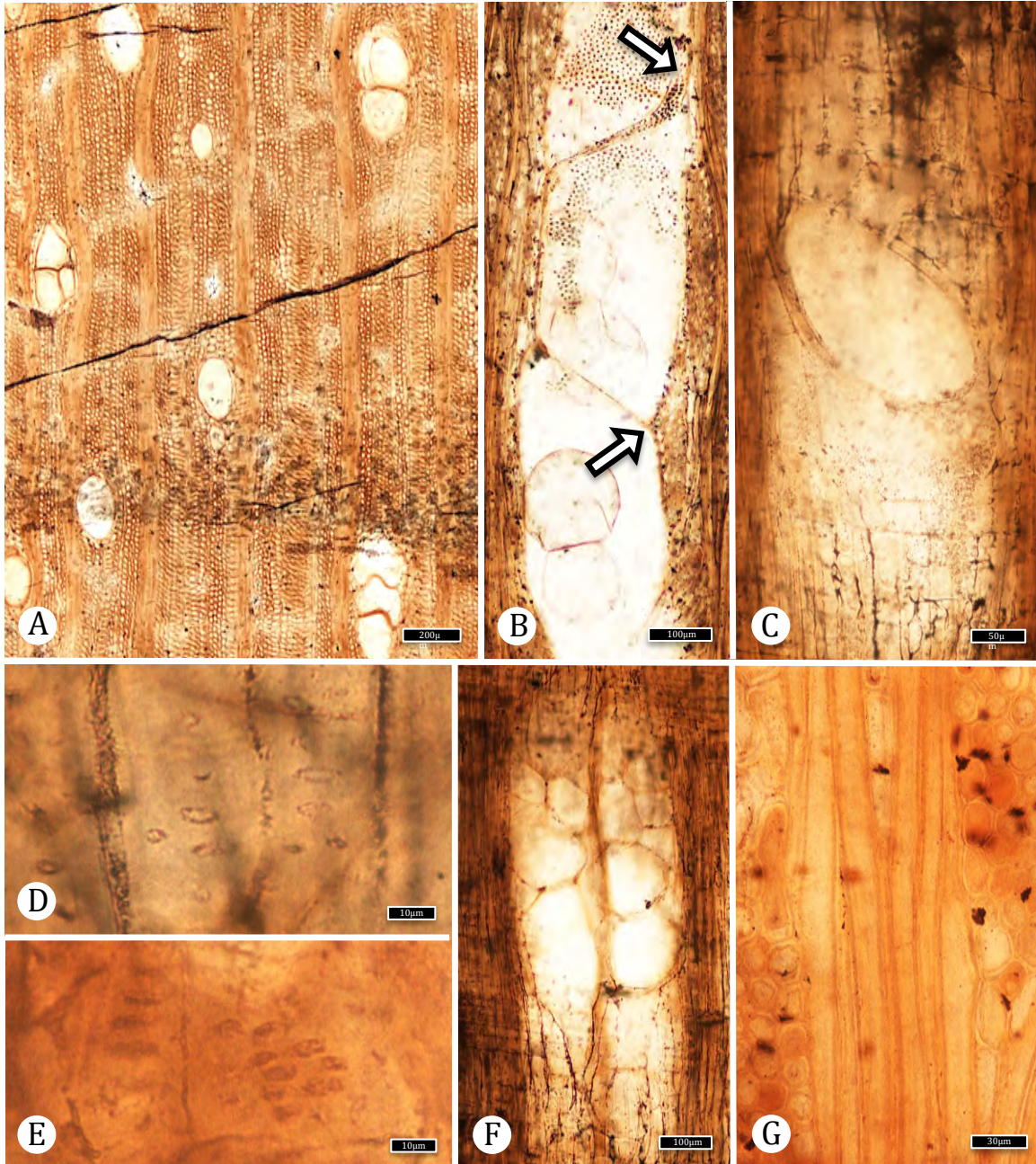


Figure 1.5. McRae wood holoxylotype Group IIIB sp. 4 (TXSTATE 1287) cf. Cannabaceae? Moraceae? Urticaceae? – A: TS. Wood diffuse-porous, vessels solitary or in radial multiples of 2–3. TXSTATE 1287, X-1. Scale bar = 200  $\mu\text{m}$ . – B: TLS. Vessel element (arrows at end walls). TXSTATE 1287, T-5. Scale bar = 100  $\mu\text{m}$ . – C: RLS. Simple perforation plate. TXSTATE 1287, R-1. Scale bar = 50  $\mu\text{m}$ . – D: Vessel-ray parenchyma pitting with reduced borders, horizontally elongate. TXSTATE 1287, R-5. Scale bar = 10  $\mu\text{m}$ . – E: RLS. Bordered vessel-ray parenchyma pits. TXSTATE 1287, R-1. Scale bar = 10  $\mu\text{m}$ . – F: RLS. Tyloses bubble-like. TXSTATE 1287, R-1. Scale bar = 100  $\mu\text{m}$ . – G: TS. Fiber walls thin to medium-thick, non-septate. TXSTATE T-1. Scale bar = 30  $\mu\text{m}$ .

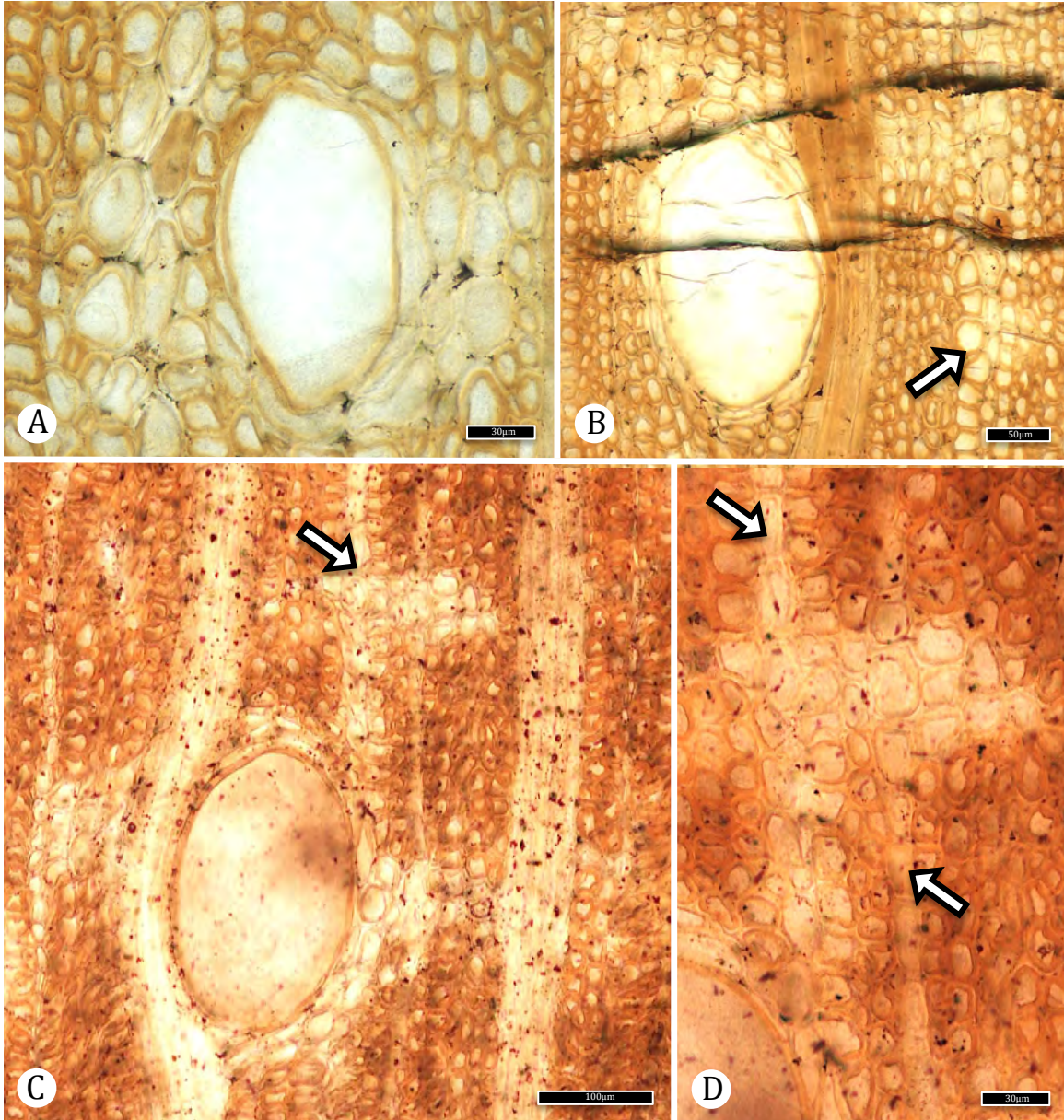


Figure 1.6. McRae wood holoxylotype Group IIIB sp. 4 (TXSTATE 1287) cf. Cannabaceae? Moraceae? Urticaceae? – A: TS. Axial parenchyma vasicentric, or nearly so. TXSTATE 1287, X-1. Scale bar = 30  $\mu\text{m}$ . – B: TS. Axial parenchyma unilateral, extending tangentially and radially (arrow). TXSTATE 1287, X-1. Scale bar = 50  $\mu\text{m}$ . – C: TS. Axial parenchyma aliform and in a small patch (arrow) connected to the vessel by a narrow unilateral extension of parenchyma adjacent to a ray. TXSTATE 1287, X-4. Scale bar = 100  $\mu\text{m}$ . – D: TS. Detail of Fig. 9C showing rays (arrows) passing through axial parenchyma patch. TXSTATE 1287, X-4. Scale bar = 30  $\mu\text{m}$

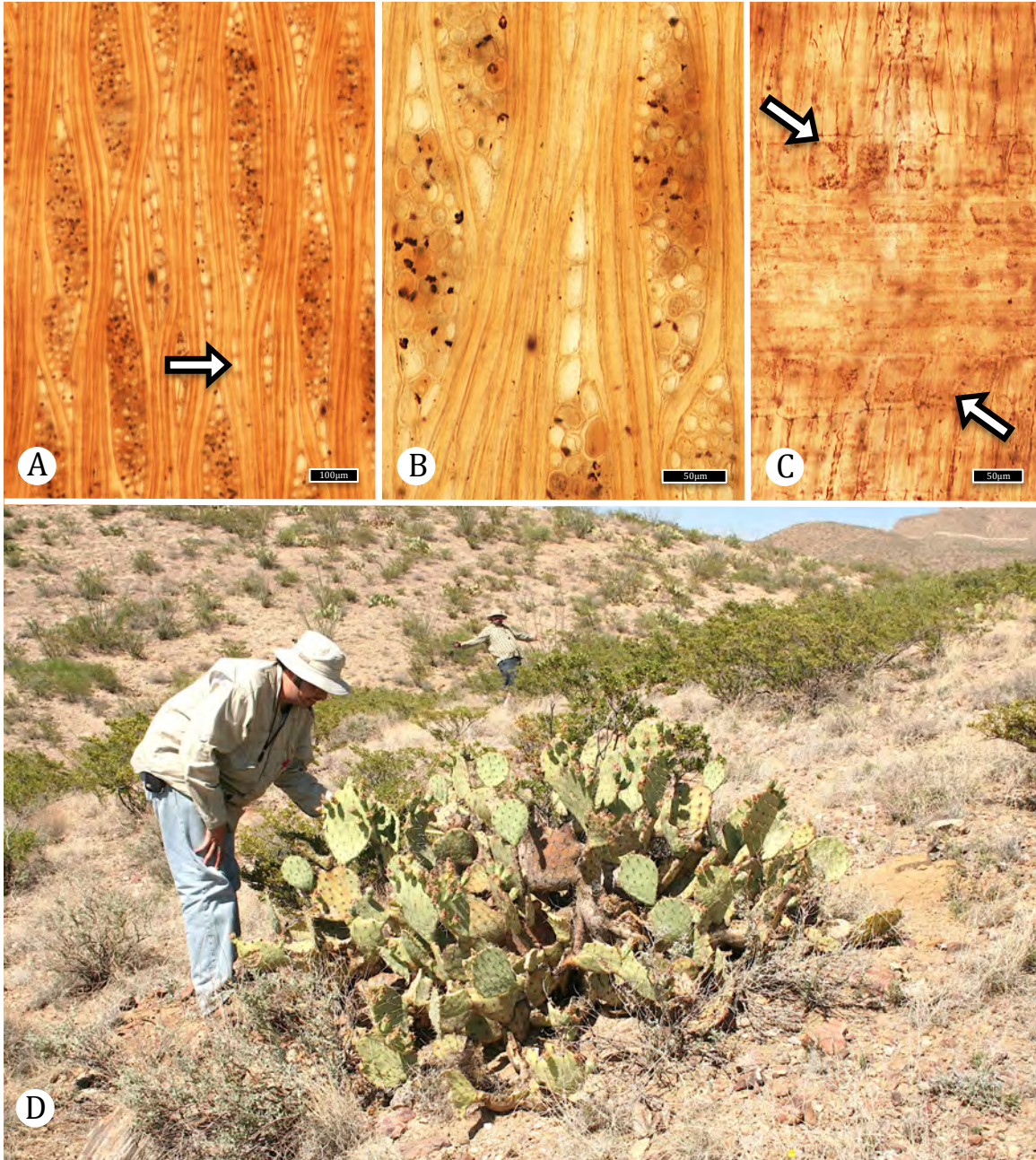


Figure 1.7. McRae wood holoxylotype Group IIIB sp. 4 (TXSTATE 1287) cf. Cannabaceae? Moraceae? Urticaceae? – A: TLS. Multiseriate rays 2-6 (mostly 5-6) cells wide; uniseriate rays mostly <10 cells tall (arrow). TXSTATE 1287, T-1. Scale bar = 100 μm. – B: TLS. Rays composed of all procumbent cells or with 1-2 (here shown with 4) marginal rows of square or upright cells. TXSTATE 1287, T-1. Scale bar = 50 μm. – C: Ray composed of procumbent cells with 1 marginal row square or upright cells (arrows). TXSTATE 1287, R-5. Scale bar = 50 μm. – D: Group IIIB sp.4 (TXSTATE 1287) Discovered under a clump of *Opuntia*.

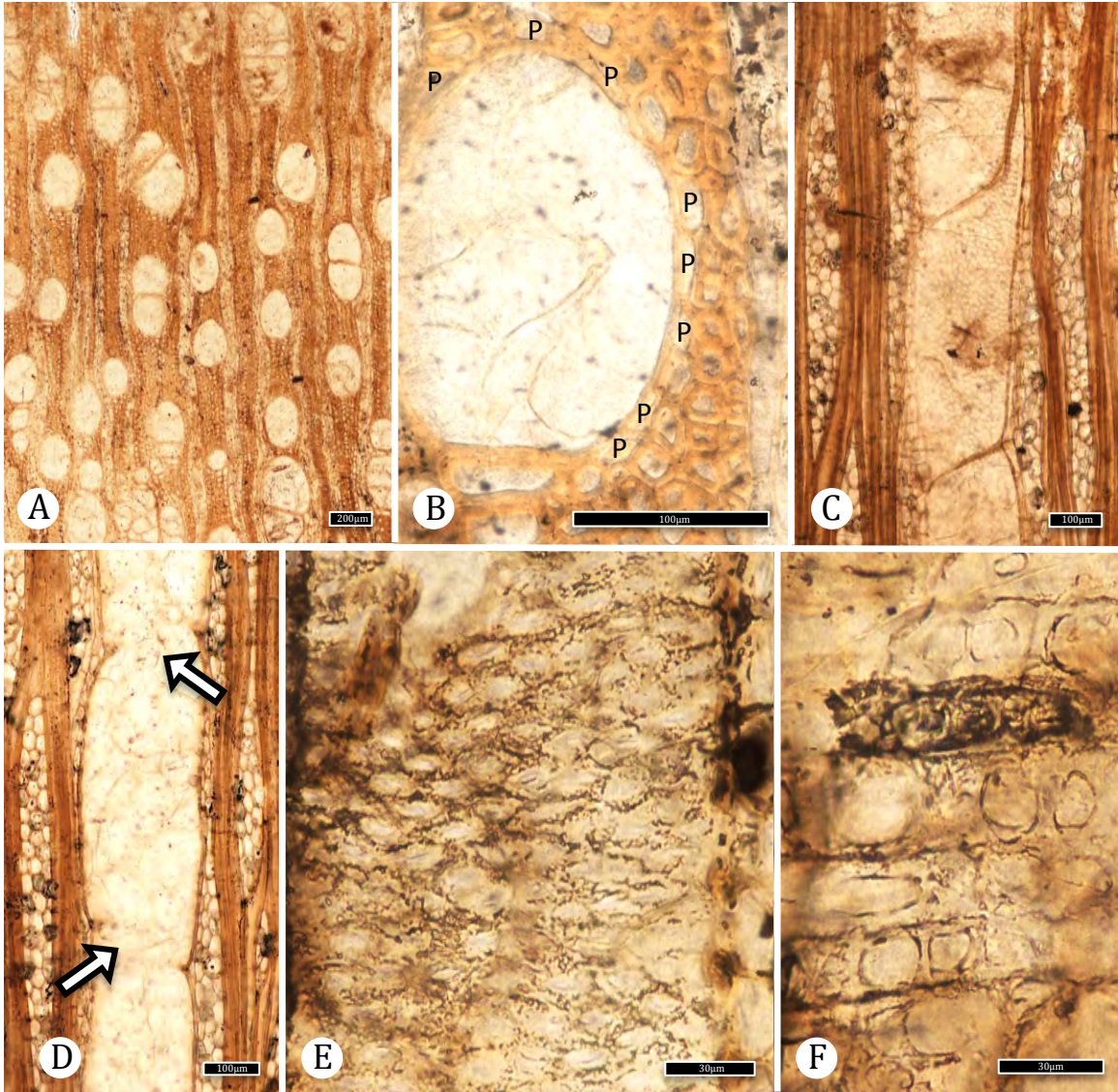


Figure 1.8. Group IIIB sp. 6 holoxylotype (TXSTATE 1232) Kirkiaceae.  
 – A: TLS. Vessels solitary and in radial multiples of 2 or 3. TXSTATE 1232, X-2. Scale bar = 200 µm. – B: TS. Axial parenchyma (P) paratracheal. TXSTATE 1232, X-2. Scale bar = 100 µm. – C: TLS. Vessel element. TXSTATE 1232, T-2. Scale bar = 100 µm. – D: TLS. Simple perforation plates (arrows). TXSTATE 1232, T-2. Scale bar = 100 µm. – E: TLS. Alternate intervessel pits, polygonal. TXSTATE 1232, T-2. Scale bar = 30 µm. – F: RLS. Vessel-ray parenchyma pits with reduced borders or simple, large and round. TXSTATE 1232, R-3. Scale bar = 30 µm.

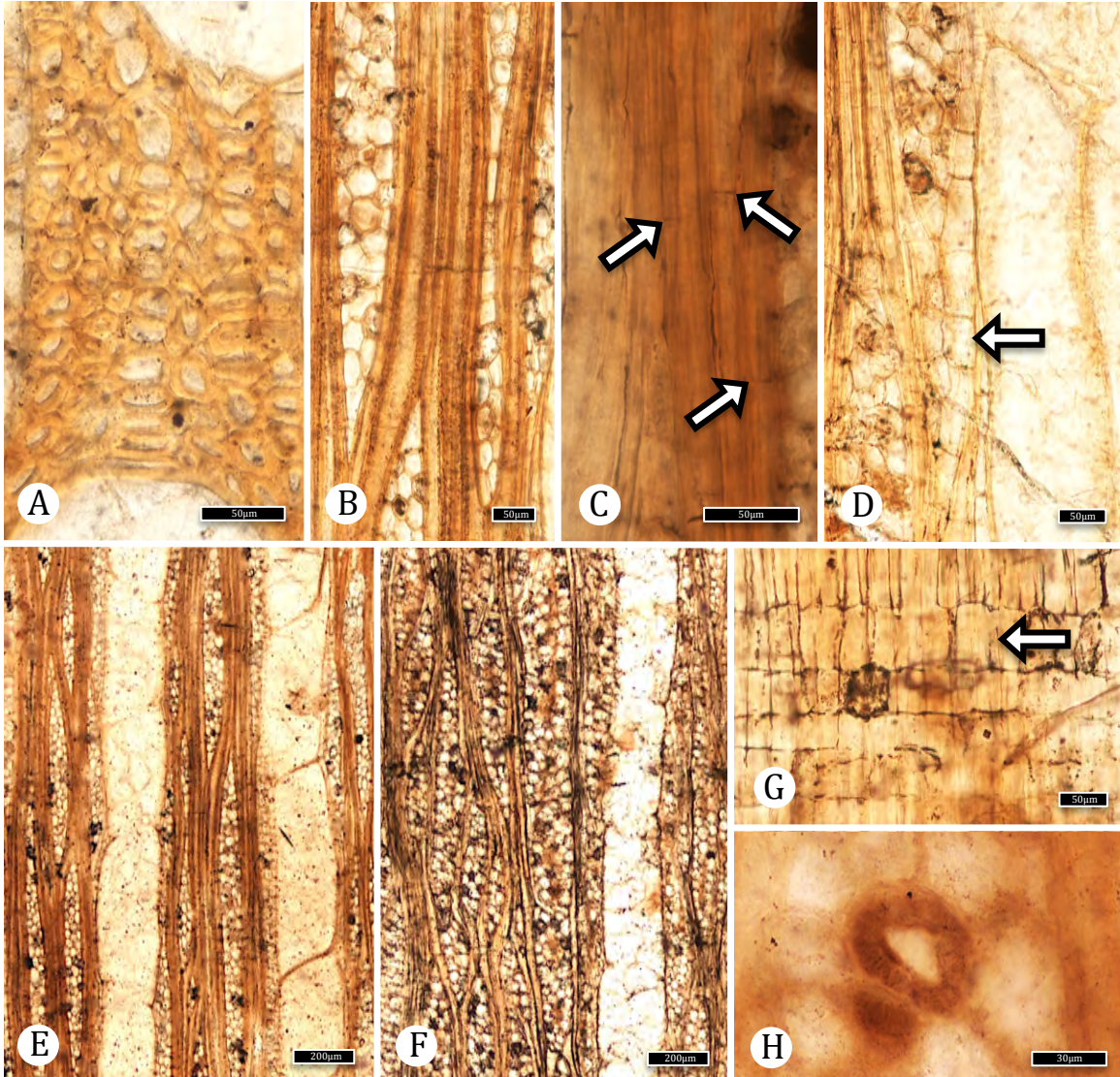


Figure 1.9. Group IIIB sp. 6 holoxylotype (TXSTATE 1232) Kirkiaceae.

- A: TS. Fibers angular in outline, thin to thick-walled. TXSTATE 1232, X-2. Scale bar = 50  $\mu\text{m}$ .
- B: TLS. Non-septate fibers. TXSTATE 1232, T-2. Scale bar = 50  $\mu\text{m}$ .
- C: TLS. Septate fibers (arrows). TXSTATE 1232, T-2. Scale bar = 50  $\mu\text{m}$ .
- D: TLS. Axial parenchyma paratracheal with 8 cells per strand (arrow). TXSTATE 1232, T-2. Scale bar = 50  $\mu\text{m}$ .
- E: TLS. Rays 3-4 seriate, some >1000  $\mu\text{m}$  high. TXSTATE 1232, T-2. Scale bar = 200  $\mu\text{m}$ .
- F: TLS. Rays mostly 3-4 seriate (to 5 seriate) and mostly <1000  $\mu\text{m}$  high. TXSTATE 1238, T-1. Scale bar = 200  $\mu\text{m}$ .
- G: RLS. Ray cells procumbent with one marginal row square or upright cells (arrow). TXSTATE 1232, R-3. Scale bar = 50  $\mu\text{m}$ .
- H: TLS. Thick-walled ray cell interpreted as artifact. TXSTATE 1244, T-1. Scale bar = 30  $\mu\text{m}$ .



Figure 1.10. Forest of Giants *in situ* stumps. – A. Group IIIB sp. 6 holoxylotype (TXSTATE 1232) Kirkiaceae. “Stump 2,” estimated stem diameter of 1.8 m, measuring 3.7 m at the base of the buttress roots. – B. McRae wood holoxylotype Group IIIB sp.5 (TXSTATE 1288) cf. Sapotaceae. The most intact stump in the Forest of Giants.

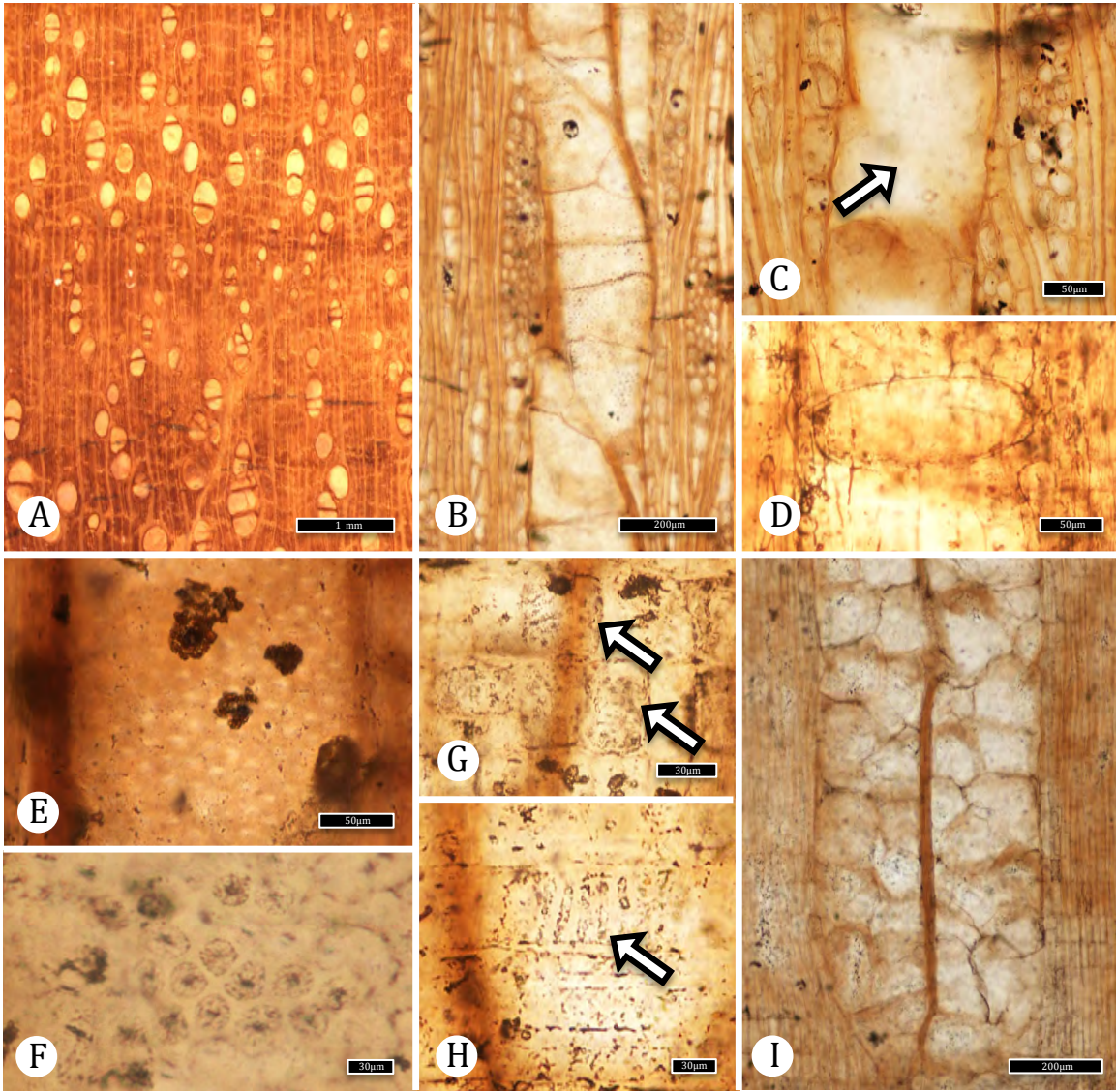


Figure 1.11. McRae wood holoxylotype Group IIIB sp. 5 (TXSTATE 1288) cf. Sapotaceae. – A: TS. Wood semi-ring-porous, vessels diffuse and in a radial or diagonal pattern. TXSTATE 1288, X-7. Scale bar = 1 mm.– B: TLS. Vessel element. TXSTATE 1288, T-5. Scale bar = 200  $\mu$ m. – C: TLS. Simple perforation plate (arrow). TXSTATE 1288, T-5. Scale bar = 50  $\mu$ m. – D: RLS. Simple perforation plate. TXSTATE 1288, R-1. Scale bar = 50  $\mu$ m. – E: TLS. Alternate intervessel pitting. TXSTATE 1288, T-7. Scale bar = 50  $\mu$ m. – F: TLS. Alternate intervessel pitting. TXSTATE 1288, T-7. Scale bar = 30  $\mu$ m. – G: RLS. Bordered vessel-ray parenchyma pits (arrows). TXSTATE 1288, R-18. Scale bar = 30  $\mu$ m. – H: RLS. Vessel-ray parenchyma pitting with reduced borders, vertically elongate (arrow). TXSTATE 1288, R-18. Scale bar = 30  $\mu$ m. – I: RLS. Tyloses bubble-like. TXSTATE 1288, R-5. Scale bar = 200  $\mu$ m.

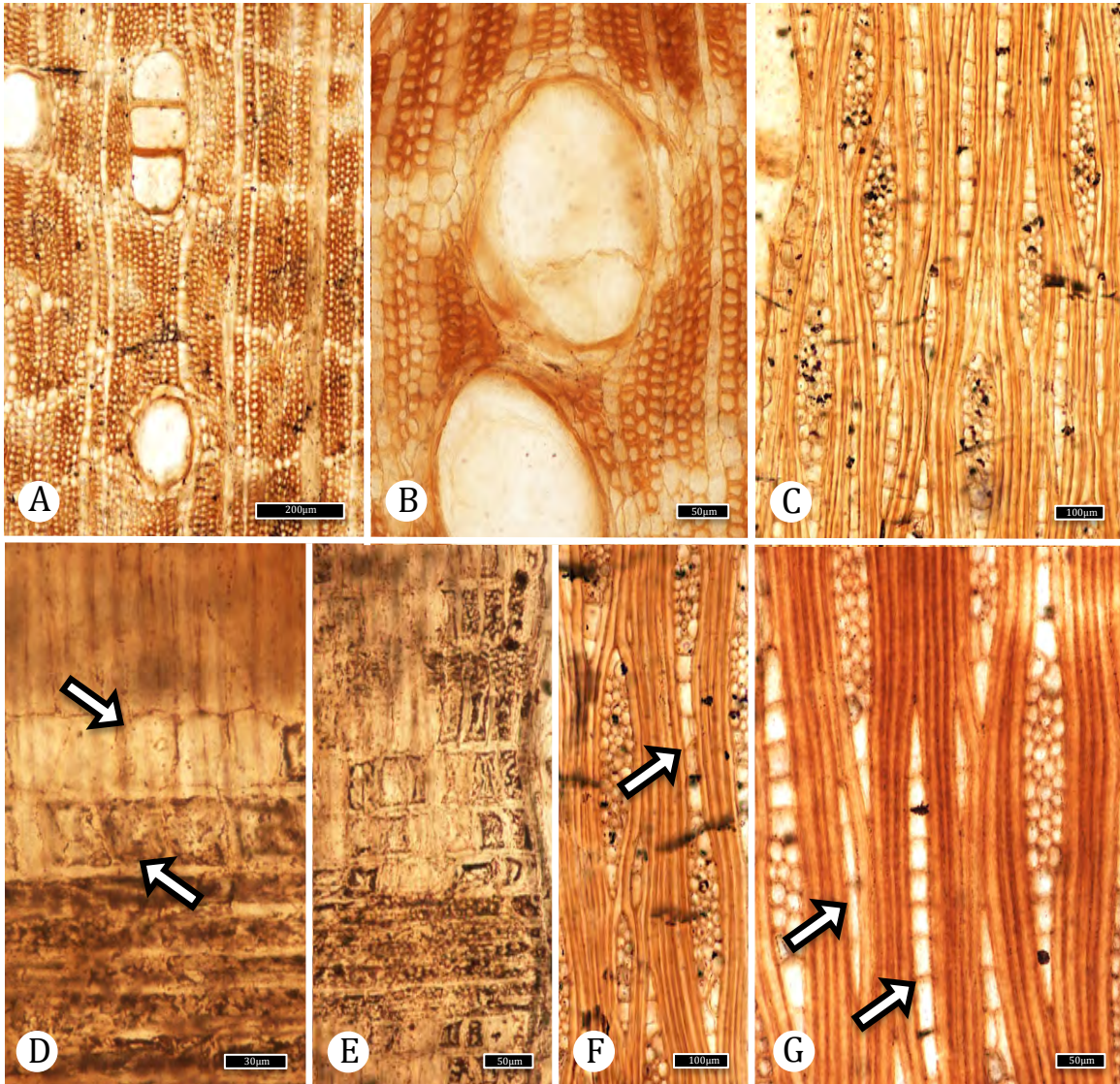


Figure 1.12. McRae wood holoxylotype Group IIIB sp. 5 (TXSTATE 1288) cf. Sapotaceae. – A: TS. Lines of axial parenchyma more-or-less regularly spaced. TXSTATE 1288, X-5. Scale bar = 200  $\mu\text{m}$ . – B: TS. Axial parenchyma vasicentric and diffuse-in-aggregates forming lines up to several cells wide. TXSTATE 1288, X-7. Scale bar = 50  $\mu\text{m}$ . – C: TLS. Uniseriate rays common, multiseriate rays mostly 3–4 cells wide. TXSTATE 1288, T-5. Scale bar = 100  $\mu\text{m}$ . – D: RLS. Ray composed of procumbent cells with 2 marginal rows square or upright cells. (arrows). TXSTATE 1288, R-8. Scale bar = 50  $\mu\text{m}$ . – E: RLS. Ray composed of procumbent cells with many rows square or upright cells. TXSTATE 1288, R-8. Scale bar = 50  $\mu\text{m}$ . – F: TLS. Multiseriate regions of rays occasionally vertically fused by uniseriate regions. TXSTATE 1288, T-5. Scale bar = 100  $\mu\text{m}$ . – G: TLS. Uniseriate rays composed of square or upright cells. (arrow). TXSTATE 1288, T-7. Scale bar = 50  $\mu\text{m}$ .

## REFERENCES

- Amato JM, Mack GH, Jonell TN, Seager WR, Upchurch GR. 2017. Onset of the Laramide orogeny and associated magmatism in southern New Mexico based on U-Pb geochronology. *GSA Bull.* 129: 1209-1226.
- Armstrong K. 2010. Systematics and biogeography of the pantropical genus *Manilkara* Adans. (Sapotaceae), Doctoral Thesis.
- Armstrong KE, Stone GN, Nicholls JA, Valderrama E, Anderberg AA, Smedmark J, Gautier L, Naciri Y, Milne R, Richardson JE. 2014. Patterns of diversification amongst tropical regions compared: a case study in Sapotaceae. *Front. Genet.* 5: 362.
- Awasthi N. 1975. [1977]. On two new fossil woods resembling *Chrysophyllum* and *Holoptelea* from the Cuddalore Series near Pondicherry. *Palaeobotanist* 24: 21–25.
- Awasthi N. 1977. On two New fossil woods reesembling *Chrysophyllum* and *Holoptelea* from the Cuddalore Series near Pondicherry. *Palaeobotanist* 24: 21–25.
- Awasthi N, Srivastava R. 1990 [1992]. Additions to the Neogene flora of Kerala coast, India. *Geophytology* 20: 148–154
- Bachelier JB, Endress PK. 2008. Floral structure of *Kirkia* (Kirkiaceae) and its position in Sapindales. *Ann. Bot.* 102: 539–550.
- Bailey IW. 1924. The problem of identifying the wood of Cretaceous and later dicotyledons: *Paraphyllanthoxylon arizonense*. *Ann. Bot.* 38: 439–451.

- Bamford MK. 2003. Fossil woods from Auchas and their palaeoenvironment. *Memoir Geol. Surv. Namibia* 19: 23–34.
- Bande MB, Dechamps R, Lakhanpal RN, Prakash U. 1987. Some new fossil woods from the Cenozoic of Zaire. *Mus. Roy. Afr. Cent. Tervuren, Dépt. Géol. Min., Rapp. Ann.* 1985–6: 113–140.
- Barghoorn ES. 1941. The ontogenetic development and phylogenetic specialization of rays in the xylem of dicotyledons. II. Modification of the multiseriate and uniseriate rays. *Am. J. Bot.* 28: 273–282.
- Bartish IV, Antonelli A, Richardson JE, Swenson U. 2011 [= 2010]. Vicariance or long-distance dispersal: Historical biogeography of the pantropical subfamily Chrysophylloideae (Sapotaceae). *J. Biogeogr.* 38: 177–190.
- Bell CD, Donoghue MJ. 2005. Dating the Dipsacales- comparing models, genes, and evolutionary implications. *Am. J. Bot.* 92: 284–296.
- Berger LG den. 1923. Fossiele houtsoorten uit het Tertiair van Zuid-Sumatra. *Verh. Geol. Mijnb. Genoot. Ned. (Geol. ser.)* 7: 143–148.
- Berger W. 1953. Jungtertiäre Pflanzenreste aus dem Gebiete der Ägäis (Lemnos, Thessaloniki). *Ann. Géol. Pays Hellén.* 5: 34–64.
- Biondi E. 1981. *Arganioxylon sardum* n. gen., n. sp., et *Sclerocaryoxylon chiarugii* n. gen., n. sp.- bois fossiles de Miocène de la Sardaigne (Italie). *Rev. Palaeobot. Palynol.* 34: 301–320.
- Bonsen KJ, Ter Welle BJH. 1984. Systematic wood anatomy and affinities of the Urticaceae. *Botanische Jahrbücher für Systematik*, 105: 49–71.

- Boonchai N, Manchester SR. 2012. Systematic affinities of early Eocene petrified woods from Big Sandy Reservoir, Southwestern Wyoming. *Int. J. Plant Sci.* 173: 209–227.
- Bouchal JM, Mayda S, Zetter R, Grímsson F, Akgün F, Denk T. 2017. Miocene palynofloras of the Tınaz lignite mine, Muğla, southwest Anatolia- taxonomy, palaeoecology and local vegetation change. *Rev. Palaeobot. Palynol.* 243: 1–36.
- Bouchal JM. 2018. The middle Miocene palynofloras of the Salihpaşalar lignite mine (Yatağan Basin, southwest Anatolia)- environmental characterisation and comparison with palynofloras from adjacent basins. *Palaeobiodiversity Palaeoenviron.* 1–46.
- Březinová D, Süss H. 1988. Nadel- und Laubholzreste aus miozänen Hornsteinen von Lipnice, CSSR. *Feddes Repert.* 99: 279–289.
- Buck BJ, Mack GH. 1995. Latest Cretaceous (Maastrichtian) aridity indicated by paleosols in the McRae Formation, south-central New Mexico. *Cretaceous Res.* 16: 559–572.
- Cahoon EJ. 1972. *Paraphyllanthoxylon alabamense*: a new species of fossil dicotyledonous wood. *Am. J. Bot.* 59: 5–11.
- Cantino PD, Doyle JA, Graham SW, Judd WS, Olmstead RG, Soltis DE, Soltis PS, Donoghue MJ. 2007. Towards a phylogenetic nomenclature of *Tracheophyta*. *Taxon.* 56: 1E–44E.

- Chanderbali AS, van der Werff H, Renner SS. 2001. Phylogeny and historical biogeography of Lauraceae: evidence from the chloroplast and nuclear genomes. *Ann. Mo. Bot. Gard.* 88: 104–134.
- Chandler MEJ. 1957. The Oligocene flora of the Bovey Tracey lake basin, Devonshire. *Bull. Br. Mus. (Natural History), (Geology)* 3, 71–123.
- Chang CY, Cao CX, Wang Q. 2013. Further contribution to the Neogene petrified wood forest of Mizoram, India. *Chin. Sci. Bull.* 58.
- Chase MW, Christenhusz MJM, Fay MF, Byng JW, Judd WS, Soltis DE, Soltis PS, Stevens PF, Stevens PF. 2016. An update of the Angiosperm Phylogeny Group classification for the orders and families of flowering plants: APG IV. *Bot. J. Linn. Soc.* 181: 1–20.
- Chin K, Estrada-Ruiz E, Wheeler EA, Upchurch Jr GR, Wolfe DG. 2019. Early angiosperm woods from the mid-Cretaceous (Turonian) of New Mexico, USA: *Paraphyllanthoxylon*, two new taxa, and unusual preservation. *Cretac. Res.* 98: 292–304.
- Christophel DC, Kerrigan R, Rowett AI. 1996. The use of cuticular features in the taxonomy of the Lauraceae. *Ann. Mo. Bot. Gard.* 419–432.
- Clarkson JJ, Chase MW, Harley MM. 2002. Phylogenetic relationships in Burseraceae based on plastid rps16 intron sequences. *Kew Bull.* 183–193.
- Clement WL, Weiblen GD. 2009. Morphological evolution in the mulberry family (Moraceae). *Syst. Bot.* 34: 530–552.

- Coiffard C, Gomez B, Thiébaud M, KVAČEK J, Thévenard F, Neraudeau D. 2009. Intramarginal veined Lauraceae leaves from the Albian–Cenomanian of Charente–Maritime (Western France). *Palaeontology*. 52: 323-336.
- Collinson ME. 1989. The fossil history of the Moraceae, Urticaceae (including Cecropiaceae), and Cannabaceae. *Crane, P, R., Blackmore, S ed (s). Evolution, systematics, and fossil history of the Hamamelidae 2*: 319–39.
- Contreras DL. 2018. Conifer evolution and the ecological expansion of flowering plants in the Mesozoic. PhD. Thesis, University of California, Berkeley.
- Crane PR. 1987. Vegetational consequences of the angiosperm diversification. *Origins of angiosperms and their biological consequences/edited by EM Friis, WG Chaloner, and PR Crane*.
- Crawley M. 2001. Angiosperm Woods from British Lower Cretaceous and Palaeogene Deposits. *Special Papers in Palaeontology* 66. The Palaeontological Association, 100 pp.
- Crepet WL, Nixon KC, Daghighian CP. 2013. Fossil Ericales from the Upper Cretaceous of New Jersey. *Int. J. Plant Sci.* 174: 572–584.
- Dayal R. 1964. Occurrence of *Boswellia* in the Deccan Intertrappean beds of Keria, Madhya Pradesh. *Curr. Sci.* 33: 683–684.
- Dayal R. 1965 [1966]. Occurrence of *Boswellia* in the Deccan Intertrappean beds of Keria, Madhya Pradesh. *Palaeobotanist* 14: 185–190.
- De Faria AD, Pirani JR, Ribeiro JELDS, Nylinder S, Terra-Araujo MH, Vieira PP, Swenson U. 2017. Towards a natural classification of Sapotaceae subfamily Chrysophylloideae in the Neotropics. *Bot. J. Linnean Soc.* 185: 27–55.

- Detienne, Pierre. Woods of Madagascar. CIRAD Unpublished.
- Dilcher DL. 1974. Approaches to the identification of angiosperm leaf remains. Bot. Rev. 40: 1–157.
- Doweld AB. (2017). (2533–2534) Proposals to conserve the name *Laurinoxylon* against *Ulminium* and to reject the name *Laurinium* (fossil Lauraceae). Taxon 66: 764–765.
- Doyle JA, Endress PK. 2010. Integrating Early Cretaceous fossils into the phylogeny of living angiosperms- Magnoliidae and eudicots. J. Syst. Evol. 48: 1–35.
- Drinnan AN, Crane PR, Friis EM, Pedersen KR. 1990. Lauraceous flowers from the Potomac Group (mid-Cretaceous) of eastern North America. Bot. Gaz. 151: 370–384.
- Dupéron -Laudoueneix M. 1980. Presence d'un bois fossile de Moraceae dans l'Eocene de la Charente. Cr 105e Congr. Nat. Soc. Sav., Caen, Sci. 1: 117–29.
- Dupéron-Laudoueneix M, Dupéron J. 2005. Bois fossiles de Lauraceae: nouvelle découverte au Cameroun, inventaire et discussion. In Ann. Paléontol. 91: 127–151.
- Dupéron J, Dupéron -Laudoueneix M, Sakala J, De Franceschi D. 2008. *Ulminium diluviale* Unger: historical data on the discovery and new study. Ann. Paléontol. 94 (2008) 1–12.
- El-Din MMK. 2003. Petrified wood from the Farafra Oasis, Egypt. IAWA J. 24: 163–172.
- El-Din MMK, Wheeler EA, Bartlett JA. 2006. Cretaceous woods from the Farafra Oasis, Egypt. IAWA J. 27: 137–143.

- Eklund H. 1999. *Big survivors with small flowers: fossil history and evolution of Laurales and Chloranthaceae* (Doctoral dissertation, Acta Universitatis Upsaliensis).
- Eklund H. 2000. Lauraceous flowers from the Late Cretaceous of North Carolina, U.S.A. *Bot. J. Linn. Soc.* 132: 397–428.
- Estrada-Ruiz E, Martínez-Cabrera HI, Cevallos-Ferriz SRS. 2007. Fossil woods from the late Campanian–early Maastrichtian Olmos Formation, Coahuila, Mexico. *Rev. Palaeobot. Palynol.* 145: 123–133.
- Estrada-Ruiz E, Martínez-Cabrera HI, Cevallos-Ferriz SRS. 2010. Fossil woods from the Olmos Formation (late Campanian-early Maastrichtian), Coahuila, Mexico. *Am. J. Bot.* 97: 1179–1194.
- Estrada-Ruiz E, Upchurch GR, Wolfe JA, Cevallos-Ferriz SRS. 2011. Comparative morphology of fossil and extant leaves of Nelumbonaceae, including a new genus from the Late Cretaceous of Western North America. *Bot.* 32: 337–351.
- Estrada-Ruiz E, Upchurch GR, Wheeler EA, Mack GH. 2012a. Late Cretaceous angiosperm woods from the Crevasse Canyon and McRae formations, south-central New Mexico, USA: part 1. *Int. J. Plant Sci.* 173: 412–428.
- Estrada-Ruiz E, Parrott JM, Upchurch GR, Wheeler EA, Thompson DL, Mack G, Mindy MM. 2012b. The wood flora from the Upper Cretaceous Crevasse Canyon and McRae formations, south-central New Mexico, USA: A progress report. In *New Mexico Geological Society Guidebook, 63rd Field Conference, Warm Springs Region.* 503–518.

- Estrada-Ruiz E, Wheeler EA, Upchurch GR, Mack GH. 2018. Late Cretaceous angiosperm woods from the McRae Formation, South-central New Mexico, USA-part 2. *Int. J. Plant Sci.* 179: 136–150.
- Feldpausch TR, Banin L, Phillips OL, Baker TR, Lewis SL, Quesada CA, Affum-Baffoe K *et al.* 2011. Height-diameter allometry of tropical forest trees. *Biogeosciences* 8: 1081–1106.
- Felix J. 1883. Untersuchungen über fossile Hölzer. I. Tertiäre Laubhölzer. II Fossile Hölzer mit Wurzeleinschlüssen. *Z. Dtsch. Geol. Ges.* 35: 59–91.
- Fernando ES, Gadek PA, Quinn CJ. 1995. Simaroubaceae, an artificial construct-evidence from rbcL sequence variation. *Am. J. Bot.* 92–103.
- Forman LL, Brandham PE, Harley MM, Lawrence TJ. 1989. *Beiselia mexicana* (Burseraceae) and its affinities. *Kew Bull.* 1–31.
- Friis EM, Crepet WL. 1987. Time of appearance of floral features. *Friis, E, M,, Chaloner, W, G, Crane, P, R ed (s). The origins of angiosperms and their biological consequences. Cambridge Univ. Press: Cambridge, etc*, 145–79.
- Friis I, 1989. The Urticaceae: a systematic review. In: Crane, P.R., Blackmore, S. (Eds.), *Evolution, Systematics, and Fossil History of the Hamamelidae*. Clarendon Press, Oxford, pp. 285–308.
- Friis EM, Crane PR, Pedersen KR. 2011. *Early flowers and angiosperm evolution*. Cambridge University Press, Oxford.
- Gautier L, Naciri Y, Anderberg AA, Smedmark JE, Randrianaivo R, Swenson U. 2013. A new species, genus and tribe of Sapotaceae, endemic to Madagascar. *Taxon* 62: 972–983.

- Gillette DD, Wolbert DB, Hunt AP. 1986. Tyrannosaurus Rex from the McRae Formation (Lancian, Upper Cretaceous), Elephant Butte Reservoir, Sierra County, New Mexico. New Mexico Geological Society Guidebook, 37th Field Conference, Truth or Consequences. 235–238.
- Goswami A, Upchurch P. 2010. The dating game: a reply to. Zool. Scr. 39: 406–409.
- Gottwald H. 1992. Holzzer aus marinen Sanden des oberen Eozan von Helmstedt (Niedersachsen). Palaeontographica B (Niedersachsen), 225, 27–103.
- Gottwald H. 1997. Alttertiare Kieselholzer aus miozanen Schottern der ostbayerischen Molasse bei Ortenburg. Documentae naturae 109: 1–83.
- Graham A. 2012. Catalog and literature guide for Cretaceous and Cenozoic vascular plants of the New World. Ann. Mo. Bot. Gard. 98: 539–541.
- Grambast-Fessard N. 1968. Contribution a l'etude des flores tertiaires des regions provencales et alpines: IV-Deux structures ligneuses nouvelles de Sapotacees. Nat. monspel. Bot. 19: 57–74.
- Gazeau-Koeniguer F, Le gisement de Nucourt CV. 1975. Etude d'un bois hétéroxylé de l'Eocène du Vexin français. Biologie végétale- Biologie animale 2: 75.
- Gregory M, Poole I, Wheeler EA. 2009. *Fossil dicot wood names: an annotated list with full bibliography*. Published for the International Association of Wood Anatomists at the National Herbarium Nederland.
- Harley MM. 1991. The pollen morphology of the Sapotaceae. Kew Bull. 379–491.
- Harris WK. 1972. New form species of pollen from southern Australian early Tertiary sediments. Roy. Soc. S. Australia Trans. 96: 53–61.

- Heads M. 2012. Bayesian transmogrification of clade divergence dates: a critique. *J. Biogeogr.* 39: 1749–1756.
- Heimsch C. 1942. Comparative anatomy of the secondary xylem in the 'Gruinales' and 'Terebinthales' of Wettstein with reference to taxonomic grouping. *Lilloa.* 8: 83–198.
- Herendeen PS. 1991a. Lauraceous wood from the mid-Cretaceous Potomac group of eastern North America: *Paraphyllanthoxylon marylandense* sp. nov. *Rev. Palaeobot. Palynol.* 69:277–290.
- Herendeen PS, Crepet WL, Nixon KC. 1994. Fossil flowers and pollen of Lauraceae from the Upper Cretaceous of New Jersey. *Plant Syst. Evol.* 189: 29–40.
- Herendeen PS, Magallon-Puebla S, Lupia R, Crane PR, Kobylinska J. 1999. A preliminary conspectus of the Allon flora from the Late Cretaceous (late Santonian) of central Georgia, USA. *Ann. Mo. Bot. Gard.* 407–471.
- Hofmann E. 1948. *Manilkaroxylon diluviale* n. sp. ein fossiles Sapotaceen Holz aus dem Quartar von Sta. Paula in Ekuador. *Paläobiologica*, 8, 280–2.
- Hofmann CC. 2018. Light and scanning electron microscopic investigations of pollen of Ericales (Ericaceae, Sapotaceae, Ebenaceae, Styracaceae and Theaceae) from five lower and mid-Eocene localities. *Bot. J. Linnean Soc.* 187: 550–578.
- Iamandei E, Iamandei S. 1997. Xylotomical study of some fossil dicot trunks of Techereu in the Metalliferous Carpathians. *Acta Palaeontologica Romaniae.* 1. The First Romanian National Symposium on Palaeontology, Bucharest, 107–112.
- Ingle SR. 1974. Revision of the genus *Machilusoxydon* Bande. *Botanique* 5: 53–56.

- IAWA Committee. 1989. IAWA list of microscopic features for hardwood identification. *IAWA Bull.* n.s. 10: 219–332.
- InsideWood. 2004-onwards. Published on the Internet:  
<http://insidewood.lib.ncsu.edu/search> [accessed August 7, 2018].
- Jud NA, Wheeler EA, Rothwell GW, Stockey RA. 2017. Angiosperm wood from the Upper Cretaceous (Coniacian) of British Columbia, Canada, *IAWA J.* 38: 141–161.
- Jud NA, Dunham JI. 2017. Fossil woods from the Cenozoic of Panama (Azucero Peninsula) reveal an ancient neotropical rainforest. *IAWA J.* 38: 366–S2.
- Jud NA, D’Emic MD, Williams SA, Mathews JC, Tremaine KM, Bhattacharya J. 2018. A new fossil assemblage shows that large angiosperm trees grew in North America by the Turonian (Late Cretaceous). *Sci. Adv.* 4: eaar8568.
- Kamal El-Din MM, Wheeler EA, Bartlett JA. 2006. Cretaceous woods from the Farafra Oases, Egypt. *IAWA J.* 27: 137–143.
- Kar RK, Mohabey DM, Srivastava R. 2004. Angiospermous fossil woods from the Lameta Formation (Maastrichtian), Maharashtra, India. *Geophytology* 33: 21–27.
- Kim C, Deng T, Chase M, Zhang DG, Nie ZL, Sun H. 2015. Generic phylogeny and character evolution in Urticeae (Urticaceae) inferred from nuclear and plastid DNA regions. *Taxon*, 64: 65–78.
- Koeniguer JC. 1975. Expéditions paléontologiques au Tchad. I. Les bois plio-quadernaires du Nord-Tchad (Kolinga, Koro Toro, Angamma). *Ann. Paléont. Invert.* 61: 177–214.

- Kostermans AJGH. 1957. Lauraceae. *Reinwardtia* 4: 193–256.
- Kramer K. 1974. Die Tertiären Hölzer südost-Asiens (unter Ausschluss der Dipterocarpaceae. *Palaeontographica* 145B: 1–150.
- Kribs DA. 1935. Salient lines of structural specialization in the wood rays of dicotyledons. *Bot. Gaz.* 96: 547–557.
- Kribs DA. 1937. Salient lines of structural specialization in the wood parenchyma of dicotyledons. *Bulletin of the Torrey Botanical Club*, 64: 177–187.
- Kukachka BF. 1978. *Wood anatomy of the neotropical Sapotaceae. VII. Chrysophyllum*. USDA For. Serv. Res. Pap. FPL 331. For. Prod. Lab., Madison, Wis.
- Kukachka BF. 1979. *Wood Anatomy of the Neotropical Sapotaceae VIII. Diploon*. USDA For. Serv. Res. Pap. FPL 349. For. Prod. Lab., Madison, Wis.
- Kukachka BF. 1981. *Wood Anatomy of the Neotropical Sapotaceae. XXIV. Ecclinusa*. USDA For. Serv. Res. Pap. FPL 395. For. Prod. Lab., Madison, Wis.
- Kukachka BF. 1982. *Wood Anatomy of the Neotropical Sapotaceae. XXXI. Pouteria*. USDA For. Serv. Res. Pap. FPL 419. For. Prod. Lab., Madison, Wis.
- Lakhanpal RN, Prakash U, Awasthi N. 1981. Some more dicotyledonous woods from the Tertiary of Deomali, Arunachal Pradesh, India. *The Palaeobotanist* 27: 232–252.
- Leisman GA. 1986. *Cryptocaryoxylon gippslandicum* gen, et sp. nov., from the Tertiary of eastern Victoria, Alcheringa-An Australasian J. Palaeontol. 10: 1986.

- Lemoigne Y, Beauchamp J, Samuel E. 1974. Étude paleobotanique des depots volcaniques d'age Tertiaire des Bordures est et Ouest du Systeme des Rifts Ethiopiens. *Geobios* 7: 267–288.
- Lemoigne Y. 1978. Flores Tertiares de la Haute Vallee de l'Omo (Ethiopie). *Palaeontographica* 165B: 80–157.
- Lozinsky RP, Hunt AP, Wolberg DL, Lucas SG. 1984. Late Cretaceous (Lancian) dinosaurs from the McRae Formation, Sierra County, New Mexico. *N. M. Geol.* 6: 72–77.
- MacGinitie HD. 1953. *Fossil plants of the Florissant beds, Colorado* (Vol. 599). Carnegie institution of Washington Publications 599, 1–198.
- MacGinitie HD. 1969. *The Eocene Green River flora of northwestern Colorado and northeastern Utah*. University of California Press.
- Mack GH, Kottlowski FE, Seager WR. 1998. The stratigraphy of South-Central New Mexico, New Mexico Geological Society Guidebook, 49<sup>th</sup> Field Conference, Las Cruces Country II.
- Mack G, Amato JM, Upchurch GR. 2015. U-Pb Geochronology of Ash Fall Tuffs in the McRae Formation (Upper Cretaceous), South-Central New Mexico, 2015 New Mexico Geological Society Annual Spring Meeting.
- Mädel-Angeliowa E, Müller-Stoll WR. 1973. Kritische Studien über fossile Combretaceen-Hölzer: über Hölzer von Typus Terminalioxylon G. Schönfeld mit einer Revision der bisher zu Evodioxylon Chiarugi gestellten Arten. *Palaeontographica* 142B: 117–136.

- Manchester SR. 1981. Fossil plants of the Eocene Clarno Nut Beds. Oregon Geol. 43: 75–81.
- Manchester SR. 1987. Oligocene fossil plants of the John Day Formation, Fossil, Oregon. Oregon Geol. 49: 115–26.
- Manchester SR, Akhmetiev MA, Kodrul TM. 2002. Leaves and fruits of *Celtis aspera* (Newberry) comb. nov.(Celtidaceae) from the Paleocene of North America and Eastern Asia. Int. J. Plant Sci. 163: 725–736.
- Manchester SR, Grímsson F, Zetter R. 2015. Assessing the fossil record of asterids in the context of our current phylogenetic framework. Ann. Missouri Bot. Gard. 100: 329–363.
- Mantzouka D, Karakitsios V, Sakala J, Wheeler EA. 2016. Using idioblasts to group *Laurinoxylon* species: case study from the Oligoo-Miocene of Europe. IAWA J. 37: 459–488.
- Martin HA. 1978. Evolution of the Australian flora and vegetation through the Tertiary- evidence from pollen. Alcheringa, 2: 181–202.
- Martinez-Cabrera HI, Cevallos-Ferriz SRS, Poole I. 2006. Fossil woods from Early Miocene sediments of the El Cien formation, Baja California Sur, Mexico. Rev. Palaeobot. Palynol. 138: 141–294.
- Martínez-Millán M. 2010. Fossil record and age of the Asteridae. Bot. Rev. 76: 83–135.
- Mehrotra RC. 2000. Study of plant megafossils from the Tura Formation of Nangwalbibra, Garo Hills, Meghalaya, India. Palaeobotanist 49: 225–237.

- Meijer JFF. 2000. Fossil woods from the late Cretaceous Aachen Formation. Rev. Palaeobot. Palynol. 112: 297-336.
- Metcalf CR, Chalk L. 1950. Anatomy of the dicotyledons. Vols. 1 and 2. Clarendon Press, Oxford.
- Muellner-Riehl AN, Weeks A, Clayton JW, Buerki S, Nauheimer L, Chiang YC, Cody S, Pell SK. 2016. Molecular phylogenetics and molecular clock dating of Sapindales based on plastid *rbcl*, *atpB* and *trnL* DNA sequences. Taxon 65: 1019–1036.
- Muller J. 1981. Fossil pollen records of extant angiosperms. Bot. Rev. 47: 1–142.
- Müller-Stoll WR, Madel E. 1960. Juglandaceen-Hölzer aus dem Tertiär des pannonischen Beckens. Senckenbergiana Lethaea 41: 255–295.
- Muller-Stoll WR, Madel-Angeliewa E. 1983. Fossile Holzer mit schmalen apotrachealen Parenchymbandern. I. Arten aus der Gattung *Eucaryoxylon* Muller-Stoll and Madel. Feddes Repert. 94: 655–657.
- Mueller-Stoll WR, Maedel-Angeliewa E. 1984. Fossile Hölzer mit schmalen apotrachealen Parenchymabändern. III. Die Sapotaceae-Gattung *Chrysophylloxylon* gen. nov. Feddes Repert. 95: 169–181.
- Nishida S, van der Werff H. 2007. Are cuticular characters useful in solving generic relationships of problematic species of Lauraceae?. Taxon. 56: 1229–1229.
- Nishida S, van der Werff H. 2011. An evaluation of classification by cuticular characters of the Lauraceae: a comparison to molecular phylogeny. Ann. Mo. Bot. Gard. 348–357.

- Nixon KC, Crepet WL. 1993. Late Cretaceous fossil flowers of ericalean affinity. *Am. J. Bot.* 80: 616–623.
- Page VM 1967. Angiosperm Wood from the Upper Cretaceous of Central California  
Part I. *Am. J. Bot.* 54: 510–514.
- Page VM. 1980. Dicotyledonous wood from the Upper Cretaceous of central  
California, II. *J. Arnold Arbor.* 61: 723–748.
- Parham JF, Donoghue PC, Bell CJ, Calway TD, Head JJ, Holroyd PA, Inoue JG et al.  
2011. Best practices for justifying fossil calibrations. *Syst. Biol.* 61: 346–359.
- Patil GV, Mhaskar DN. 1971. *Burseraceoxylon mohgaense* gen. et sp. nov., a fossil  
wood from Mohgaon Kalan. *Proc. 58th Indian Sci. Congr.* 459.
- Petrescu J. 1978. Etudes sur les flores paléogènes du nord-ouest de la Transsylvanie  
et de la Moldavie Central. *Bucarest.: Univ. Cluj-Napoca.*
- Pole M. 2007. Lauraceae macrofossils and dispersed cuticle from the Miocene of  
southern New Zealand. *Palaeontol. Electronica.* 10: 3A.
- Poole I, Richter HG, Francis JE. 2000. Evidence for Gondwanan origins for *Sassafras*  
(Lauraceae)? Late Cretaceous fossil wood of Antarctica. *IAWA J.* 21: 463–475.
- Prakash U, Awasthi N. 1969 [1970]. Fossil woods from the Tertiary of eastern India.  
1. *Palaeobotanist* 18: 32–44.
- Prakash U, Tripathi PP. 1973 [1975]. Fossil dicotyledonous woods from the Tertiary  
of eastern India. *Palaeobotanist* 22: 51–62.
- Prakash U, Březinová D, Awasthi N. 1974. Fossil woods from the Tertiary of south  
Bohemia. *Palaeontographica* 147B: 107–123.

- Prakash U, Tripathi PP. 1975 [1977]. Fossil woods of *Ougenia* and *Madhuca* from the Tertiary of Assam. *The Palaeobotanist* 24: 140–145.
- Prakash U, Lalitha C. 1978. Fossil wood of *Artocarpus* from the Tertiary of Assam. *Geophytology* 8: 132–3.
- Prakash U, Awasthi N, Lemoigne Y. 1981 [1982]. Fossil dicotyledonous woods from the Tertiary of Blue Nile Valley, Ethiopia. *Palaeobotanist* 30: 43–59.
- Privé-Gill C, Cao N, Legrand P. 2008. Fossil wood from alluvial deposits (reworked Oligocene) of Limagne at Bussieres (Puy-de-Dome, France). *Rev. Palaeobot. Palynol.* 149: 73–84.
- Ramanujam CKG. 1956. Fossil woods from the Euphorbiaceae from the Tertiary rocks of South Arcot District, Madras. *J. Ind. Bot. Soc.* 35: 285–307.
- Renner SS. 2005. Relaxed molecular clocks for dating historical plant dispersal events. *Trends in Plant Science.* 10: 550–558.
- Retallack G, Dilcher DL. 1981. Early angiosperm reproduction: *Prisca reynoldsii*, gen. et sp. nov. from mid-Cretaceous coastal deposits in Kansas, USA. *Palaeontographica Abteilung B*, 179: 103–137.
- Rich PM, Helenum K, Kearns D, Morse SR, Palmer MW, Short L. 1986. Height and stem diameter relationships for dicotyledonous trees and arborescent palms of Costa Rican tropical wet forest *Bulletin of the Torrey Botanical Club* 113: 241–246
- Richter HG. 1981. Anatomie des sekundären xylems und der rinde der Lauraceae. *Sonderbände Naturwiss. Vereins Hamburg* 5: 1–148.

- Richter HG. 1987. Lauraceae. Mature secondary xylem. In: Metcalfe CR (ed.), Anatomy of the dicotyledons. Ed. 2. Vol. III: 167–171. Oxford Science Publications.
- Richter HG. 1990. Wood and bark anatomy of Lauraceae. III. *Aspidostemon Rohwer* Richter, IAWA Bulletin n.s. 11: 47–56.
- Roberts LNR, Kirschbaum MA. 1995. Paleogeography of the Late Cretaceous of the Western Interior of Middle North America—coal distribution and sediment accumulation: U. S. Geological Survey, Professional Paper 1561: 116.
- Rohwer JG, Rudolph B. 2005. Jumping genera: the phylogenetic positions of *Cassytha*, *Hypodaphnis*, and *Neocinnamomum* (Lauraceae) based on different analyses of trnK intron sequences. *Ann. Missouri Bot. Gard.* 92: 153–178.
- Rose JP, Kleist TJ, Lofstrand SD, Drew BT, Schönenberger J, Sytsma KJ. 2018. Phylogeny, historical biogeography, and diversification of angiosperm order Ericales suggest ancient Neotropical and East Asian connections. *Mol. Phylogenet. Evol.* 122: 59–79.
- Schönfeld G. 1947. Hölzer aus dem Tertiär von Kolumbien. *Abh. Senckenberg. Naturf. Ges.* 475: 1–53.
- Schuster J. 1906. Über ein fossiles Holz aus dem Flysch des Tegernseer Gebietes. *Geognostische Jahreshefte* 19: 139–52.
- Seager WR, Mack GH, Raimonde MS, Ryan RG. 1986. Laramide basement-cored uplift and basins in south-central New Mexico. *New Mexico Geological Society Guidebook, 37th Field Conference, Truth or Consequences.* 123–130.

- Seager WR, Mack GH, Lawton TF. 1997. Structural kinematics and depositional history of a Laramide uplift-basin pair in southern New Mexico: Implications for development of intraforeland basins. *Geol. Soc. Am. Bull.* 109: 1389–1401.
- Selmeier A. 1991. Ein verkieseltes Sapotaceae-Holz, *Bumelioxylon holleisii* n. gen., n. sp., aus jungtertiären Schichten der Südlichen Frankenalb (Bayern). *Archaeopteryx* 9: 55–72.
- Selmeier A. 1993. *Moroxylon* nov. gen. (Moraceae), ein verkieseltes Maulbeerholz aus jungtertiären Schichten Bayerns (Hallertau). *Mitt. Bayer. Staatsslg. Palaont. Hist. Geol.* 33: 209–226.
- Serlin BS. 1982. An Early Cretaceous fossil flora from northwest Texas: its composition and implications. *Palaeontograph. Abt. B* 182: 52–86.
- Spackman W. 1948. A dicotyledonous wood found associated with the Idaho *Tempskyas*. *Ann. Mo. Bot. Gard.* 35: 107–115.
- Srivastava R, Guleria JS. 2004. Fossil wood of Anacardiaceae from the Deccan Intertrappean sediments of Betul district, Madhya Pradesh, India. *Geophyloogy* 33: 53–56.
- Stannard BL. 2007. The inclusion of *Pleiokirkia* in *Kirkia* (Kirkiaceae), and corresponding combination. *Kew Bull.* 62: 151–152.
- Stern WL. 1954. Comparative anatomy of xylem and phylogeny of Lauraceae. *Trop. Woods* 100: 1–73.
- Stevens PF. (2001 onwards). Angiosperm Phylogeny Website. Version 14, July 2017 [and more or less continuously updated since].

- Stride G, Nylinder S, Swenson U. 2014. Revisiting the biogeography of *Sideroxylon* (Sapotaceae) and an evaluation of the taxonomic status of *Argania* and *Spiniluma*. *Australian Syst. Bot.* 27: 104–118.
- Süss H. 1958. Anatomische Untersuchungen über die Lonbeerholzer aus dem Tertiär des Hasenbergers bei Wiesa in Sachsen. *Abh. dt. Akad. Wiss. Berlin, Chem. Geol. Biol. Kl.* (1956) 8: 1–59.
- Sweitzer EM. 1971. Comparative anatomy of Ulmaceae. *J. Arbor.* 52: 523–585.
- Swenson U, Anderberg AA. 2005. Phylogeny, character evolution, and classification of Sapotaceae (Ericales). *Cladistics* 21: 101–130.
- Swenson U, Richardson JE, Bartish IV. 2008. Multi-gene phylogeny of the pantropical subfamily Chrysophylloideae (Sapotaceae)- evidence of generic polyphyly and extensive morphological homoplasy. *Cladistics* 24: 1006–1031.
- Swenson U, Nylinder S, Wagstaff SJ. 2012. Are Asteraceae 1.5 billion years old? A reply to Heads. *Syst. Bio.* 61: 522–532.
- Swenson U, Nylinder S, Munzinger J. 2014. Sapotaceae biogeography supports New Caledonia being an old Darwinian island. *J. Biogeogr.* 41: 797–809.
- Takahashi KI, Suzuki M. 2003. Dicotyledonous fossil wood flora and early evolution of wood characters in the Cretaceous of Hokkaido, Japan. *IAWA J.* 24: 269–309.
- Taylor DW. 1988. Eocene floral evidence of Lauraceae: corroboration of the North American megafossil record. *Am. J. Bot.* 948–957.

- Terra-Araujo MH, de Faria AD, Vicentini A, Nylinder S, Swenson U. 2015. Species tree phylogeny and biogeography of the Neotropical genus *Pradosia* (Sapotaceae, Chrysophylloideae). *Mol. Phylogenet. Evol.* 87: 1–13.
- Thayn GF, Tidwell WD. 1984. A review of the genus *Paraphyllanthoxylon*. *Rev. Palaeobot. Palynol.* 43: 321–335.
- Thayne GF, Tidwell WD, Stokes WL. 1983. Flora of the Lower Cretaceous Cedar Mountain Formation of Utah and Colorado, Part I. *Paraphyllanthoxylon utahense*. *Great Basin Nat.* 43: 3.
- Trivedi BS, Srivastava, KIRAN. 1985. *Canarioxylon shahpuraensis* sp. nov. from the Deccan Intertrappean beds of Shahpura, District Mandla (MP). India. *Geophytology*, 15: 27–32.
- Unger F. 1842 - in Endlicher, Stephano. 1840. *Genera Plantarum Secundum Ordines Naturales Disposita*, Volume I. Suppl. II, Appendix, S. 100 bis 102. Wien. 1942a.
- Unger F. 1847. *Chloris protogaea: Beitrage zur Flora der Vorwelt*. in Commission bei Wilhelm Engelmann.
- Upchurch GR, Wolfe JA. 1987. Mid-Cretaceous to Early Tertiary vegetation and climate: evidence from fossil leaves and woods. *Origins of angiosperms and their biological consequences*/edited by EM Friis, WG Chaloner, and PR Crane.
- Upchurch GR, Askin RA. 1989. Latest Cretaceous and earliest Tertiary dispersed plant cuticles from Seymour Island. *Antarct. J. US.* 1989 Review p. 7-10.

- Upchurch GR, Dilcher DL. 1990. Cenomanian angiosperm leaf megafossils, Dakota Formation, Rose Creek Locality, Jefferson County, Southeastern Nebraska. Dept. Bio. Faculty Publications-Biology, Texas State University.
- Upchurch GR, Crane PR, Drinnan AN. 1994. The megaflora from the Quantico locality (upper Albian), Lower Cretaceous Potomac Group of Virginia. Virginia Museum of Natural History, Memoir 4: 1–57.
- Upchurch GR. 1995. Dispersed angiosperm cuticles-their history, preparation, and application to the rise of angiosperms in Cretaceous and Paleocene coals, southern western interior of North America. *Inter. J. Coal Geol.* 28: 161–227.
- Upchurch GR, Mack GH. 1998. Latest Cretaceous leaf megafloras from the Jose Creek Member, McRae Formation of New Mexico. *N. M. Geol. Soc. Guide.* 49: 209–222.
- Upchurch GR, Kiehl J, Shields C, Scherer J, Scotese C. 2015. Latitudinal temperature gradients and high-latitude temperatures during the latest Cretaceous: congruence of geologic data and climate models. *Geology* 43: 683–686.  
Supplementary material: GSA Data Repository item 2015238.
- van der Werf H, Richter HG. 1985. *Caryodaphnopsis* Airy-Shaw (Lauraceae), a genus new to the Neotropics. *Sys. Bot.* 10: 166–173.
- van der Werff H, Richter HG. 1996. Toward an Improved Classification of Lauraceae, *Ann. Mo. Bot. Gard.* 83: 409–418.

- von Balthazar M, Pedersen KR, Crane PR, Stampanoni M, Friis EM. 2007.  
*Potomacanthus lobatus* gen. et sp. nov.: a new flower of probable Lauraceae  
from the Early Cretaceous (Early to Middle Albian) of Eastern North America.  
Am. J. Bot. 94: 2041–2053.
- Vozenin-Serra C, Privé-Gill C. 1991. Les terrasses alluviales pléistocènes du Mékong  
(Cambodge). II. Bois silicifiés hétéroxylés récoltés entre Stung-Treng et  
Snoul. Rev. Palaeobot. Palynol. 68: 87–117.
- Wang H, Moore MJ, Soltis PS, Bell CD, Brockington SF, Alexandre R, Davis CC, Latvis  
M, Manchester SR, Soltis DE. 2009. Rosid radiation and the rapid rise of  
angiosperm-dominated forests. Proc. Natl. Acad. Sci. U.S.A. 106: 3853–3858.
- Wang Q, Mao KS. 2016. Puzzling rocks and complicated clocks: how to optimize  
molecular dating approaches in historical phytogeography. New Phytol. 209:  
1353–1358.
- Webber IE. 1936. Systematic anatomy of the woods of the Simarubaceae. Am. J. Bot.  
23: 577–587.
- Weeks A, Daly DC, Simpson BB. 2005. The phylogenetic history and biogeography of  
the frankincense and myrrh family (Burseraceae) based on nuclear and  
chloroplast sequence data. Mol. Phylogenet. Evol. 35: 85–101.
- Weeks A, Zapata F, Pell SK, Daly DC, Mitchell JD, Fine PV. 2014. To move or to  
evolve- contrasting patterns of intercontinental connectivity and climatic  
niche evolution in “Terebinthaceae” (Anacardiaceae and Burseraceae). Front.  
Genet. 5: 409.

- Wheeler E, Scott RA, Barghoorn ES. 1977. Fossil dicotyledonous woods from Yellowstone National Park. *J. Arnold Arbor*, 58: 280–306.
- Wheeler EA, Lee M, Matten LC. 1987. Dicotyledonous woods from the Upper Cretaceous of southern Illinois. *Bot. J. Linn. Soc.* 95: 77–100.
- Wheeler EA. 1991. Paleocene dicotyledonous trees from Big Bend National Park, Texas: variability in wood types common in the Late Cretaceous and Early Tertiary, and ecological inferences. *Am. J. Bot.* 658–671.
- Wheeler EA, Lehman TM, Gasson PE. 1994. *Javelinoxylon*, an Upper Cretaceous dicotyledonous tree from Big Bend National Park, Texas, with presumed Malvacean affinities. *Am. J. Bot.*, 81: 703-710.
- Wheeler EA, Lehman TM. 2000. Late Cretaceous woody dicots from the Aguja and Javelina Formations, Big Bend National Park, Texas, USA. *IAWA J.* 21: 83–120.
- Wheeler EA, Manchester SR. 2002. Woods of the middle Eocene nut beds flora, Clarno Formation, Oregon, USA. *IAWA J. Suppl*, 3, 1–188.
- Wheeler EA, Michalski TM. 2003. Paleocene and Eocene woods of the Denver Basin, Colorado. *Rocky Mountain Geology* 38: 29–43.
- Wheeler EA. 2011. Inside Wood—A web resource for hardwood anatomy. *IAWA J.* 32: 199–211.
- Wheeler EA, Srivastava R, Manchester SR, Baas P. 2017. Surprisingly modern Latest Cretaceous–earliest Paleocene woods of India. *IAWA J.* 38: 456–542.
- Wiemann MC, Wheeler EA, Manchester SR, Portier KM. 1998. Dicotyledonous wood anatomical characters as predictors of climate. *Palaeogeogr. Palaeoclim. Palaeoecol.* 139: 83–100.

- Wiemann MC, Manchester SR, Wheeler EA. 1999. Paleotemperature estimation from dicotyledonous wood anatomical characters. *Palaios* 14: 459–474.
- Wiemann MC, Williamson GB. 2002. Geographic variation in wood specific gravity: effects of latitude, temperature, and precipitation. *Wood Fiber Sci.* 34: 96–107.
- Wilf P, Escapa IH. 2015. Green Web or megabiased clock? Plant fossils from Gondwanan Patagonia speak on evolutionary radiations. *New Phytol.* 207: 283–290.
- Wilf P, Escapa IH. 2016. Molecular dates require geologic testing. *New Phytol.* 209: 1359–1362.
- Wing SL, Herrera F, Jaramillo CA, Gómez-Navarro C, Wilf P, Labandeira CC. 2009. Late Paleocene fossils from the Cerrejón Formation, Colombia, are the earliest record of Neotropical rainforest. [pnas-0905130106](https://doi.org/10.1073/pnas.0905130106).
- Wing SL, Hickey LJ, Swisher CC. 1993. Implications of an exceptional fossil flora for Late Cretaceous vegetation. *Nature* 363: 342–344.
- Wing SL, Strömberg CAE, Hickey LJ, Tiver F, Willis B, Burnham RJ, Behrensmeyer AK. 2012. Floral and environmental gradients on a Late Cretaceous landscape. *Ecol. Monogr.* 82: 23–47.
- Wing SL, Boucher LD. 1998. Ecological aspects of the Cretaceous flowering plant radiation. *Annu. Rev. Earth Planet. Sci.* 26: 379–421.
- Wolfe JA. 1973. Fossil forms of Amentiferae. *Brittonia* 25: 334–355.
- Wolfe JA. 1977. Paleogene floras from the Gulf of Alaska region. *U.S. Geol. Surv. Prof. Pap.* 997: 1–108.

- Wolfe JA, Upchurch GR. 1987. North American nonmarine climates and vegetation during the Late Cretaceous. *Palaeogeogr., Palaeoclim., Palaeoecol.* 61: 33–77.
- Wu ZY, Monro AK, Milne RI, Wang H, Yi TS, Liu J, Li DZ. 2013. Molecular phylogeny of the nettle family (Urticaceae) inferred from multiple loci of three genomes and extensive generic sampling. *Mol. Phylogenet. Evol.* 69: 814–827.
- Wurdack KJ, Hoffmann P, Samuel R, de Bruijn A, van der Bank M, Chase MW. 2004. Molecular phylogenetic analysis of Phyllanthaceae (Phyllanthoideae pro parte, Euphorbiaceae sensu lato) using plastid *rbcl* DNA sequences. *Am. J. Bot.* 91: 1882–1900.
- Yang MQ, van Velzen R, Bakker FT, Sattarian A, Li DZ, Yi TS. 2013. Molecular phylogenetics and character evolution of Cannabaceae. *Taxon* 62: 473–485.
- Zavada MS, Crepet WL. 1981. Investigations of angiosperms from the Middle Eocene of North America: flowers of the Celtidoideae. *Am. J. Bot.* 68: 924–933.
- Zerega NJ, Clement WL, Datwyler SL, Weiblen GD. 2005. Biogeography and divergence times in the mulberry family (Moraceae). *Mol. Phylogenet. Evol.* 37: 402–416.
- Zhang SD, Soltis DE, Yang Y, Li DZ, Yi TS. 2011. Multi-gene analysis provides a well-supported phylogeny of Rosales. *Mol. Phylogenet. Evol.* 60: 21–28.

## II. SIGNIFICANCE AND SYSTEMATIC ASSIGNMENT OF LATE CRETACEOUS

### *PLATANUS*-LIKE FOSSIL WOODS FROM THE MCRAE FORMATION

#### (LATE CAMPANIAN) OF SOUTH-CENTRAL NEW MEXICO, USA

##### ABSTRACT

Extant Platanaceae are composed of a single genus, *Platanus*, with 6–11 species native to North America, Europe, and Asia. Fossil woods indistinguishable from extant *Platanus* are assigned to the extant genus. *Platanus*-like woods reported from the mid- to late Cenozoic differ sufficiently from *Platanus* by the incidence of solitary vs. grouped vessels, the incidence of simple vs. scalariform perforation plates and/or the distinctness of the growth boundaries to be assigned to the fossil genus *Platanoxylon*. *Platanus*-like woods from the Late Cretaceous to early Cenozoic have been related to Platanaceae but differ from *Platanoxylon* and *Platanus* in having exclusively solitary vessels and exclusively scalariform perforation plates. *Platanus*-like woods from the McRae Formation, south-central New Mexico, of Late Campanian age (76.5 to >72.5 Ma) are compared to Cretaceous, Cenozoic and extant *Platanus*-like woods to assess their evolutionary significance and relationship within Platanaceae. Woods from the crown group, *Platanus*, as well as probable members of the stem lineage (fossils), are assigned to Platanaceae on the basis of opposite intervessel pits, a combination of some exceptionally wide rays (>10 cells wide) along with very few or no uniseriate rays, and rays that are nearly homocellular. McRae *Platanus*-like woods differ from *Platanus* and *Platanoxylon* by generally having exclusively solitary vessels and scalariform perforation plates, features considered ancestral, as well as an absence of growth rings. However,

several xylo types show one or more intermediate features. One xylo type has weakly developed growth boundary structure, while another has areas with somewhat narrower fibers and smaller vessels, neither forming a continuous, uninterrupted ring. The one xylo type where vessels are not exclusively solitary (71-85% solitary) has a tendency for vessels to occur in tangential groups. Another xylo type has simple to scalariform combination perforation plates (i.e., a simple perforation plate interfacing with a scalariform perforation plate). The McRae woods fall outside the generic limits of *Platanoxylon* and do not have the exact combination of features of *Platanus*, warranting assignment to a new genus. The creation of a new genus for these *Platanus*-like woods is also supported by the extensive and diverse record of fossil leaves, flowers and fruits, which document a major radiation of Platanaceae during the mid- to Late Cretaceous.

*Keywords* – Platanaceae, *Platanus*, *Platanoxylon*, *Plataninium*, McRae Formation, New Mexico, Late Campanian, fossil wood

## INTRODUCTION

Extant Platanaceae are remnants of a lineage that was much more diverse during the Cretaceous and Paleogene (e.g., Süss and Müller-Stoll 1977, Manchester 1986, Friis and Crane 1989, Magallon-Puebla et al. 1997, Friis et al. 2011). Today, Platanaceae comprise a single genus, *Platanus* native to North America, Europe, and Asia (Nixon and Poole 2003). The genus is restricted to the Northern Hemisphere, and species are found primarily in riparian habitats with continuous moisture availability. *Platanus kerrii* (subgenus *Castaneophyllum*) is recognized as distinct in its leaf, inflorescence and wood anatomy from the remaining species, which are

assigned to the subgenus *Platanus* (Nixon and Poole 2003). Determination of the number of species is complicated by a history of interspecific or interlineage hybridization. Based on morphological details, Nixon and Poole (2003) recognized 7 species, Grimm and Denk (2007) recognized 6, but the other treatments list 8 to 11 species (Chen and Craven 2007, Mabberley 2008).

All woods of Platanaceae, including extant *Platanus* and probable fossil relatives, have exceptionally wide rays (>10 cells wide), very few or no uniseriate rays, rays that are nearly homocellular, and opposite intervessel pits (Brush 1917, Metcalfe and Chalk 1950). Woods assigned to Platanaceae are well represented in the fossil record and have been reported from numerous sites that date from mid-Cretaceous through the Cenozoic (Gregory et al. 2009). Fossil woods from the Neogene that are indistinguishable from extant *Platanus* have been assigned to the genus (Süss and Müller-Stoll 1977, Gregory et al. 2009). Some *Platanus*-like woods reported from the Eocene or earlier differ from extant *Platanus* in certain anatomical features, including the degree of vessel grouping, incidence of scalariform perforation plates, and growth ring distinctiveness (Süss and Müller-Stoll 1977, Herendeen et al. 1999). *Platanus*-like fossil woods have been assigned to two genera, *Plataninium* and *Platanoxylon* (Gregory et al. 2009).

In this chapter, I describe 4 species of wood from the Upper Cretaceous Jose Creek Member, McRae Formation, south-central New Mexico that have intervessel pitting and ray structure characteristic of Platanaceae, but differ in having exclusively solitary vessels, exclusively scalariform perforation plates, and/or an absence of growth boundaries. I compare the McRae material to species of extant

*Platanus*, particularly *P. kerrii*, and Cenozoic species of *Platanoxylon*, and propose a new genus for Cretaceous *Platanus*-like woods that accommodates their anatomical differences from *Platanus* and *Platanoxylon*.

#### GEOLOGIC SETTING

Silicified fossil woods, conifer and angiosperm, are common as *in situ* stumps and float in the Jose Creek Member of the McRae Formation (Upper Cretaceous) in south-central New Mexico (Fig. 2.1).

The age of the McRae Formation was originally based on Lancian age dinosaur fossils present in the Hall Lake Member, which indicated a minimum Maastrichtian age for the underlying Jose Creek Member (Lozinsky et al. 1984, Gillette et al. 1986, Wolberg et al. 1986, Lucas et al. 1998, Upchurch and Mack 1998). The age was subsequently revised to Late Campanian based on U-Pb dates from zircon crystals obtained from a volcanic clast from the base of the Jose Creek Member, three volcanic ash beds in the mid- to upper Jose Creek Member, and volcanic ashes in the lower Hall Lake Member, which together give an age range of 76.1 to >72.5 Ma for the Jose Creek Member when accounting for  $\pm 2 \sigma$  statistical uncertainty (Amato et al. 2017). Amato et al. (2017) attributed the apparent contradiction in ages to uncertainty in the position of the dinosaur fossils relative to the Hall Lake Member volcanic tuff.

The McRae represents terra firma 200 km inland from the Western Interior Seaway (Molenaar 1983, Roberts and Kirschbaum 1995, Estrada-Ruiz et al. 2012a, 2012b) at approximately 39° paleolatitude (Upchurch et al. 2015). The formation is fluvial in origin and consists of volcanic sediments, with some localized areas of

granite and Precambrian quartzite clasts (Seager et al. 1986, 1997, Amato et al. 2017). The formation comprises the first basin fill in the Laramide Love Ranch Basin of south-central New Mexico, USA (Seager et al. 1986, 1997, Amato et al. 2017). Carbonaceous beds indicative of swamp conditions are virtually absent from the McRae Formation and are restricted to the lowermost part of the unit.

Fluvial strata of the Jose Creek Member, particularly the volcanic ashes, are a rich source of fossil leaf impressions in addition to fossil woods. The virtual absence of fossil plant materials in the Hall Lake member has been attributed to semi-arid conditions, as indicated by the fossil soils (Upchurch and Mack 1998).

#### MATERIALS AND METHODS

Permineralized woods were collected from the Jose Creek Member on the Armendaris Ranch near Truth or Consequences, New Mexico. Woods were collected mostly as float through the thickness of the Jose Creek Member, but one specimen comes from an *in situ* stump 40 cm diameter located 65 m above the base of the formation, in an assemblage of stumps referred to as Fossil Forest 1. Float material was found in relatively close proximity (often within ~150 m), but situated along various slopes, such that specimens with different locality numbers may not represent parts of the same tree.

In this study, the minimum diameters of small axes with intact pith were measured directly from the axes. Where float specimens represented fragments of larger axes, the minimum diameter was calculated by measuring on a transverse surface along widely separated rays to the point where the rays would converge and doubling that estimated radius. The 40 cm diameter *in situ* stump was measured in

the field and represents maximum diameter at the top of the buttress roots. Specimen diameters are given because some anatomical features (e.g., ray width, height and cellular composition, vessel diameter and frequency) generally vary with increase in axis diameter (i.e. vary between juvenile and mature wood (e.g., Panshin and Zeeuw 1980) and because a minimum diameter of 10 cm indicates that the parent plant represents a tree. In an effort to examine the most mature wood possible, slides were prepared from the largest diameter portion of each specimen with acceptable preservation.

Slides were prepared by cutting blocks (transverse, tangential and radial) using a Hillquist trim saw model SF-8 or tile saw. Blocks were polished with 320 grit powders before being affixed to 1" x 3" Hillquist Thin Section Glass slides using Norland optical adhesive 72. Exposing the adhesive to UV light (standard black light bulb) for 16 hours was sufficient to hold blocks in place while removing excess material and initial grinding with a Hillquist thin section machine. The final desired thickness of the section was achieved by hand grinding on a glass plate with 120, 240, 320 or 400 grit powder. Coverslips were affixed with the same Norland optical adhesive 72 to avoid optical problems that might arise from using different adhesive and mounting mediums. Slides were observed using a Nikon Eclipse 50i microscope and measurements and photographs taken with a Nikon DS-Fi1 camera head and Nikon DS-L2 camera control unit. Observations were made and recorded following the recommendations of an International Association of Wood Anatomists Committee (1989). Possible affinities were initially determined by searching the InsideWood online database (InsideWood 2004–onward, Wheeler 2011). Higher-

level systematics follows APG IV (Chase et al. 2016) and Cantino et al. (2007).

Taxonomic names follow those proposed by Chase and Reveal (2009).

The number of vessels per square millimeter was measured in two ways, 1) considering only the area between the wide rays, with no ray area included in the calculation and 2) “overall,” including the ray area in the calculation.

The fossil woods are archived in the paleobotanical collections of Texas State University, San Marcos. Individual pieces of wood are given a specimen number preceded by the abbreviation TXSTATE. The specific slide used for each illustration is given in the figure captions with the notation X-, T- or R- to identify the slide as transverse, tangential or radial, respectively, and followed by a number indicating the particular slide in each series that was photographed. Individual wood localities have a two-part number preceded by “Texas State University Paleobotanical Locality”; this number consists of the collection year (four digits) followed by a two-digit identifier. Specimens and locality data are archived in the Texas State University Paleobotanical Collections. Detailed locality data are not provided here because the localities occur on private land and looting of fossil wood localities is a common practice in the western United States.

Following the example of the leaf architecture working group in its use of the term morphotype, woods are referred to as xylotypes. A xylotype is a wood with a combination of anatomical features thought to represent a potential species that is differentiated from other woods under consideration. A holoxylotype is a specimen that best illustrates anatomical features of the xylotype; a paraxylotype is a specimen thought to represent the same taxon as a holoxylotype and may be used to

confirm anatomical features of the holoxylotype or to provide additional detail to a description.

Woods are not given formal taxonomic recognition with Linnaean nomenclature in this dissertation because it would not constitute valid and effective publication. Rather, woods are referred to by their TXSTATE accession number and an organizational scheme proposed for McRae xylotypes. A new genus and new species names will be proposed at the time of publication in compliance with the International Code of Nomenclature for algae, fungi and plants (Turland et al. 2018).

#### DESCRIPTIONS

*Clade* – Eudicots

*Order* – Proteales

*Family* – Platanaceae

*Genus* – New genus

*Generic diagnosis* – Growth boundaries absent or indistinct. Wood diffuse porous. Vessels predominantly solitary (>80%) and occasionally in radial, oblique or tangential multiples; mean tangential diameters usually narrow (some vessels up to approximately 140  $\mu\text{m}$ ); perforation plates exclusively scalariform or occasionally simple to scalariform combination; intervessel pitting predominantly opposite, often scalariform in vessel element tails or narrow vessels; vessel-ray parenchyma pits with reduced borders, oval to horizontally elongate. Tyloses present (bubble-like or segmenting the vessel horizontally) or absent. Axial parenchyma diffuse or diffuse-in-aggregates, sometimes forming short lines, incidentally contacting vessels. Rays frequently >20–30 cells wide (uniseriate rays

rare) and frequently several mm to over one cm in height; predominantly homocellular, composed of procumbent cells, some rays heterocellular with one to several rows of square or upright margin cells. Ray parenchyma with bordered pits sometimes present, predominantly on tangential walls. Imperforate elements with distinctly bordered pits on both radial and tangential walls. Vasicentric tracheids present. Prismatic crystals sometimes present in procumbent or upright ray parenchyma cells.

### **McRae Group IIC sp. 1**

*Species* – McRae Group IIC sp. 1, (Fig. 2.2–2.5). Basis for the genus

*Specific diagnosis* – Growth boundaries absent. Vessels predominantly solitary (>90%) and rarely in radial, oblique or tangential multiples of 2–3, about 30 per mm<sup>2</sup> overall (including the larger ray area in the calculation); exclusively scalariform or simple to scalariform combination perforation plates. Tyloses, when present, bubble-like or horizontally segmenting the vessels. Rays generally in two size classes, narrow rays 2–6 cells wide, wider rays 15–40 cells wide. Axial parenchyma diffuse, diffuse-in-aggregates or sometimes forming short lines, incidentally contacting vessels.

*Holoxylotype* – TXSTATE 1212

*Synonymy* – *Platanoxylon* species 2, Estrada-Ruiz et al. (2012b), Figs. 2.3A–E

*Stratigraphic horizon* – McRae Formation, Jose Creek Member

*Age* – Late Campanian

*Material* – *In situ* stump with a maximum diameter of 40 cm at the top of the buttress roots

*Locality* – Texas State University Paleobotanical Locality 1992-01, known as Fossil Forest 1

*Paraxylotype* – TXSTATE 1267

*Stratigraphic horizon* – McRae Formation, Jose Creek Member

*Age* – Late Campanian

*Material* – Estimated minimum stem diameter of 5–8 cm, collected as float

*Locality* – Texas State University Paleobotanical Locality 2013-18

*Paraxylotype* – TXSTATE 1268

*Stratigraphic horizon* – McRae Formation, Jose Creek Member

*Age* – Late Campanian

*Material* – Estimated minimum stem diameter of 14 cm, collected as float

*Locality* – Texas State University Paleobotanical Locality 2013-19

*Paraxylotype* – TXSTATE 1269

*Stratigraphic horizon* – McRae Formation, Jose Creek Member

*Age* – Late Campanian

*Material* – Estimated minimum stem diameter of 30 cm, collected as float

*Locality* – Texas State University Paleobotanical Locality 2013-19

*Paraxylotype* – TXSTATE 1270

*Stratigraphic horizon* – McRae Formation, Jose Creek Member

*Age* – Late Campanian

*Material* – Estimated minimum stem diameter of 5 cm, collected as float

*Locality* – Texas State University Paleobotanical Locality 2013-19

*Description* – *Growth rings* absent. *Wood* diffuse porous (Fig. 2.3A). *Vessels* solitary (89–99%), rarely in radial, oblique or tangential multiples of 2, mean of means 63 (6), range 53 (10)–68 (11) per mm<sup>2</sup> in the area between rays, mean of means 31 (13), range 21 (2)–55 (13)/mm<sup>2</sup> overall, solitary vessels round to oval in outline, tangential diameter mean of means 72 (3) μm, range 68 (2)–77 (20) μm; vessel element length mean of means 527 (88), range of means 433 (70)–645 (134) μm; perforation plates either exclusively scalariform, 10 (5)–14 (4), mostly <15 bars per plate (Fig. 2.3B–C), sometimes bars forked, occasional simple to scalariform combination plates (Fig. 2.3D); intervessel pits crowded opposite (Fig. 2.3E), small to medium, 7–8 μm in diameter, (Fig. 2.3G) to scalariform on vessel element tails or narrow vessels (Fig. 2.3F). *Vessel-ray parenchyma pits* with reduced borders, round, oval or horizontally elongate (Fig. 2.4B) to nearly scalariform (Fig. 2.4C). *Vessel-axial parenchyma pits* with reduced borders, round, horizontally elongate ovals to nearly scalariform. *Tyloses* bubble-like (Fig. 2.4D), or horizontally segmenting vessel (Fig. 2.4E), or not observed. *Fibers* angular in cross section, thin-walled to medium-thick-walled, fibers with 1 row of bordered pits visible on radial and tangential walls (Fig. 2.4F), non-septate. Vasicentric tracheids with two or three rows of pits common (Fig. 2.4G). *Axial parenchyma* diffuse, (Fig. 2.5A), diffuse-in-aggregates forming short one-celled lines (Fig. 2.5B), incidentally contacting vessels, parenchyma strand

length not observed. *Rays* mean of means 16 (4), range 12 (5)–21 (10) cells wide (50% 16–37 cells wide) (Fig. 2.5C–D), homocellular composed of procumbent cells or heterocellular composed of procumbent cells in the central portion with 1–4 marginal rows of upright or square cells at one or both ends (Fig. 2.5E–F); ray height mean of means 3196 (456), range 2666 (2779)–3639 (1512)  $\mu\text{m}$ ; 3 (1)–4 (1) per mm; uniseriate rays not observed. Prismatic crystals not observed.

*Description in IAWA Hardwood List codes (IAWA Committee 1989) –*

2 5 9v 13v 14 15 16 17 20v 21 25 26 31 32 41 48 (overall) 49 (between large rays)  
53 60 62 63 66 69 76 77 78v 86v 99 102 103v 104 106 107 114

*Remarks* – TXSTATE 1212, from a horizon known as Fossil Forest 1, (Fig. 2.2) was selected as the holoxylotype for the species and genus because of its significance as a large *in situ* stump with a maximum diameter of 40 cm at the top of the buttress roots. The specimen was sampled cautiously to preserve the stump integrity, which resulted in a contorted hand sample from which it was difficult to obtain true radial and tangential views. Specimens TXSTATE 1268 and TXSTATE 1269 (float material that appears to be derived from the same bed) were very similar and provided better images and more anatomical information. Data from specimens TXSTATE 1268, TXSTATE 1269, TXSTATE 1270 and TXSTATE 1267 were incorporated into the xylotype description, though the latter two specimens showed considerably more variability than the type specimen.

Vessel density in specimen TXSTATE 1270 is approximately twice that of other specimens when rays are included in the calculation, but very similar to other specimens in the area between rays. This reflects the fact that rays in TXSTATE

1270 are spaced farther apart. In tangential sections, the rays of specimen TXSTATE 1270 are more tapered than in other specimens and have a continuous distribution of ray widths, while more than half the rays of specimen TXSTATE 1267 are <10 cells in width, the largest (up to 37 cells), exceeding all other McRae *Platanus*-like specimens. Süss and Müller-Stoll (1977) expressed the opinion that diversity in ray dimensions would have been greater for fossil (ancestral) species than extant (derived) *Platanus* because ray forms were evolving and many forms seen in the fossil record no longer occur in *Platanus*. They favored use of ray shape and dimensions to delimit species. However, they also cautioned that ray characteristics could be dependent on location within the tree as is the case for many species (Barghoorn 1940, 1941). A thorough survey of extant *Platanus* species is needed to establish norms and patterns for within species and within tree variability in ray characteristics.

The axial parenchyma of specimen TXSTATE 1270 forms distinct uniseriate lines, while the parenchyma in other specimens is diffuse or diffuse-in-aggregates (not forming distinct lines). Variability in this character is seen in extant species; *Platanus kerrii* has an axial parenchyma distribution similar to that of TXSTATE 1270 (Wheeler 1995, InsideWood 2004-onward) in that diffuse-in-aggregate axial parenchyma sometimes form short lines.

Specimen TXSTATE 1267 is the only McRae *Platanus*-like wood where simple to scalariform combination perforation plates are observed, occurring commonly and seen as misaligned paired-plates. The transition from exclusively scalariform perforation plate types to species with a combination of scalariform and simple

perforation plates in the Cenozoic might warrant recognition of the specimen as a separate xylotype. Considering these specimens to represent a single species reflects a “lumper” approach that might need to be modified should additional specimens or statistical analysis support recognition of more than one species.

### **McRae Group IIC sp. 2**

*Species* – McRae Group IIC sp. 2, (Fig. 2.6–7).

*Specific diagnosis* – Growth boundaries absent. Vessels predominantly solitary (>70%) and in oblique multiples of 2–3, with a strong tendency for tangential arrangement; mean tangential diameters approximately 100 µm; perforation plates exclusively scalariform. Tyloses segmenting vessels horizontally. Axial parenchyma diffuse or diffuse-in-aggregates, incidentally contacting vessels. Rays frequently 15–30 cells wide and mostly 0.1–1.3 cm in height.

*Holoxylotype* –TXSTATE 1203

*Synonymy* – *Platanoxylon* sp. Estrada-Ruiz et al. (2012a), p. 423 Figs. 8a–i.

*Synonymy* – *Platanoxylon* sp. 1, Estrada-Ruiz et al. (2012b), Figs. 3F–G.

*Stratigraphic horizon* – McRae Formation, Jose Creek Member

*Age* – Late Campanian

*Material* – Estimated minimum stem diameter of 5–6 cm, collected as float

*Locality* – Texas State University Paleobotanical Locality 1992-01, float below the fossil forest horizon

*Paraxylotype* – TXSTATE 1271

*Stratigraphic horizon* – McRae Formation, Jose Creek Member

*Age* – Late Campanian

*Material* – Estimated minimum stem diameter of 5 cm, collected as float

*Locality* – Texas State University Paleobotanical Locality 2013-19

*Paraxylotype* – TXSTATE 1272

*Stratigraphic horizon* – McRae Formation, Jose Creek Member

*Age* – Late Campanian

*Material* – Estimated minimum stem diameter of 11 cm, collected as float

*Locality* – Texas State University Paleobotanical Locality 1992-01, float below the fossil forest horizon

*Description* – *Growth rings* indistinct, some areas with radially narrowed fibers, sometimes accompanied by a difference in vessel diameter across a weakly defined boundary and slight flaring of the rays. *Wood* diffuse porous (Fig. 2.6A–B). *Vessels* solitary (71–85%) and in tangential or oblique multiples of 2–3 (Fig. 2.6B), mean of means 77 (10), range 69 (20)–88 (21) per mm<sup>2</sup> in the area between rays, mean of means 47 (2), range 46 (26)–49 (4) per mm<sup>2</sup> overall, solitary vessels round to oval in outline, tangential diameter mean of means 104 (6) μm, range 98 (26)–110 (23) μm; vessel element length mean of means 647 (95), range 555 (95)–744 (117) μm; perforation plates exclusively scalariform, 4–20, mostly <10 bars per plate (Fig. 2.6C), bars of perforation plate sometimes forked (Fig. 2.6D); intervessel pits opposite (Fig. 2.6E), individual pits sometimes coalescing, scalariform in narrow vessels (Fig. 2.6F). *Vessel-ray parenchyma pits* with much reduced borders, pits

rounded to horizontal oval (Fig. 2.6G). *Vessel-axial parenchyma pits* with reduced borders, horizontally elongate to scalariform. *Tyloses* horizontally segmenting vessels (Fig. 2.7A). *Fibers* medium-thick walled with distinctly bordered pits visible in both radial and tangential walls (Fig. 2.7B); vasicentric tracheids present (Fig. 2.7C); fibers non-septate. *Axial parenchyma* diffuse, or diffuse-in-aggregates, incidentally contacting vessels. *Rays* mean of means 15 (2), range 13 (7)–17 (7) cells wide (frequently 15–30 cells wide) (Fig. 2.7D), homocellular composed of procumbent cells or weakly heterocellular composed of cells of variable size and wall thickness, wide rays at times dissected by vessels, ray height mostly 0.1–1.3 cm; 2–3 per mm; uniseriate rays not observed. Secondary phloem present, poorly preserved. Prismatic crystals not observed.

*Description in IAWA Hardwood List codes (IAWA Committee 1989) –*

2 5 9v 14 15 16 20v 21 31 32 42 49 53 56 60 62 63 66 69 76 77 78v 99 102 104 106  
107 114

*Remarks* – Estrada-Ruiz et al. (2012b) described specimen TXSTATE 1203 as *Platanoxylon* sp. 1. Subsequently, this specimen was determined to be indistinguishable from specimens TXSTATE 1271 and TXSTATE 1272. Based on all the specimens, the description of Estrada-Ruiz et al. is here emended to include fibers with distinctly bordered pits and vessel-ray parenchyma pitting with much reduced borders, pits rounded to horizontal oval. The presence of vessel-ray parenchyma pits with distinct borders, as reported by Estrada-Ruiz et al. (2012b), could not be confirmed.

This species differs from other McRae woods in having much larger vessel diameters and a strong tendency for some vessels to be in tangential multiples. Axial parenchyma was not observed to form short lines as in other McRae *Platanus*-like woods.

All specimens show structures interpreted as root penetrations, so this xylotype may represent root material. Because the specimens were collected at or near the same localities as McRae Group IIC sp. 1, it cannot conclusively be stated that McRae Group IIC sp. 2 is not part of the same plant as McRae Group IIC sp. 1.

### **McRae Group IIC sp. 3**

*Species* – McRae Group IIC sp. 3, (Fig. 2.8–2.10).

*Specific diagnosis* – Growth boundaries intermediate between distinct and indistinct. Vessels predominantly solitary (>90%) occasional radial, oblique or in tangential multiples of 2; mean tangential diameters about 60 µm; perforation plates exclusively scalariform. Tyloses bubble-like. Axial parenchyma diffuse or diffuse-in-aggregates forming short lines, incidentally contacting vessels. Rays mostly 3–4 cells wide (larger rays 10–21 cells wide) and mostly 1–9 mm in height; occasional square and upright cells in the ray body. Bordered pits (sensu Carlquist 2007) on ray parenchyma common, predominantly on tangential walls. Prismatic crystals in ray parenchyma.

*Holoxylotype* – TXSTATE 1273

*Stratigraphic horizon* – McRae Formation, Jose Creek Member

*Age* – Late Campanian

*Material* – Estimated minimum stem diameter of 9.6 cm, collected as float

*Locality* – Texas State University Paleobotanical Locality 2013-40

*Description* – *Growth boundaries* intermediate between distinct and indistinct (Fig. 2.8A), delineated by slightly radially narrowed fibers (Fig. 2.8B), a difference in vessel diameter between latewood and earlywood, and a slight tangential flaring of rays (Fig. 2.8C). *Wood* diffuse porous. *Vessels* solitary (95%), radial, oblique or in tangential multiples of 2 (rarely 3) usually in the earlywood, especially the earliest earlywood (Fig. 2.8C), average 107 (SD 39, range 78–180)/mm<sup>2</sup> in areas between large rays, solitary vessels oval in outline, mean tangential diameter 62 (SD 12, range 37–90) µm; vessel element length average 596 (SD 133, range 308–594) µm; perforation plates exclusively scalariform (Fig. 2.8D), 4–14 bars per plate, sometimes forked; intervessel pits opposite (Fig. 2.8E, 10E), predominantly medium, 6–11 µm in diameter to scalariform on vessel element tails, narrower vessels often with scalariform intervessel pitting. *Vessel-ray parenchyma pits* with reduced borders, round or oval to horizontally elongate (Fig. 2.8F–G). *Vessel-axial parenchyma pits* with reduced borders, horizontally elongate ovals to nearly scalariform (Fig. 2.8H). *Tyloses* infrequent, segmenting vessel elements (Fig. 2.9A). *Fibers* angular in cross section, thin-walled to thick-walled, with one or two rows of bordered pits visible in radial and tangential walls (Fig. 2.9B), pits 2–3.5 µm in diameter, vasicentric tracheids with two to several rows of pits present (Fig. 2.9C), fibers non-septate. *Axial parenchyma* diffuse, diffuse-in-aggregates often forming short uniseriate lines (Fig. 2.9D), incidentally contacting vessels, number of cells per parenchyma strand not observed due to quality of preservation. *Rays* 2–25 (mostly

3–4) seriate (Fig. 2.9E), 23% of rays >10 cells in width, multiseriate rays homocellular composed of procumbent cells to heterocellular composed of procumbent cells and occasional isolated square or upright cells, or with occasional rows of square or upright cells in the ray body especially in narrower rays, some rays with 1–3 marginal rows of upright or square cells at one or both ends (Fig. 2.10A–B); ray height 0.3–12.1 mm, rays ≤4 cells wide (63%) mostly <2 mm in height; rays predominantly 4–7 per mm; uniseriate rays rare, <400 μm in height. Bordered pits, predominantly on tangential ray parenchyma walls, common (Fig. 2.10C). Solitary prismatic crystals occasionally present in procumbent or upright / square ray parenchyma (Fig. 2.10D).

*Description in IAWA Hardwood List codes (IAWA Committee 1989) –*

1v 2 5 9 14 15 16 20 21 26 31 32 41 49 50 (between large rays) 53 60 62 63 66 69  
76 77 78v 99 102 104 106 107 115 136 137 138

*Remarks –* This wood differs from other McRae *Platanus*-like woods by having intermediate growth boundaries, albeit indistinct and often discontinuous. The wood exhibits a combination of tangential vessel multiples and flared rays at the growth boundary, features found in extant *Platanus* and described by Süss and Müller-Stoll (1977) for many mid- to late Cenozoic *Platanoxylon* species. The factor/s causing the growth interruption in this wood are not known. While several woods described from the Jose Creek have occasional areas of radially narrowed fibers, the majority of woods, both angiosperm and conifer, show no growth boundaries, suggesting that the cause of the growth interruption may have been specific to this wood, possibly relating to water availability.

Vessel density is high (mean = 107/ mm<sup>2</sup> in the area between rays) and the rays narrow compared to other McRae *Platanus*-like woods (76% <10 cells wide, mostly 3-4 cells wide). The rays are notable for the presence of occasional square or upright cells in the body of the rays (especially the narrower rays). Other features that distinguish this wood are the common occurrence of pronounced bordered pits (Carlquist 2007) on ray parenchyma walls and occasional prismatic crystals in the procumbent or upright ray parenchyma.

#### **McRae Group IIC sp. 4**

Species – McRae Group IIC sp. 4, (Fig. 2.11–2.12).

*Specific diagnosis* – Growth boundaries absent. Vessels predominantly solitary (>90%) and occasionally in oblique multiples of 2; mean tangential diameter about 50 µm; perforation plates exclusively scalariform. Tyloses horizontally segmenting vessels. Axial parenchyma diffuse or diffuse-in aggregates forming short lines, incidentally contacting vessels. Rays up to 30 cells wide, 0.2–3.5 mm in height; with occasional larger cells dispersed throughout the ray and an irregularly distributed layer (up to several cells thick) of larger cells at the ray edge.

*Holoxylotype* – TXSTATE 1274

*Stratigraphic horizon* – McRae Formation, Jose Creek Member

*Age* – Late Campanian

*Material* – Estimated minimum stem diameter of 20 cm, collected as float

*Locality* – Texas State University Paleobotanical Locality 2013-7

*Description* – *Growth rings* absent. *Wood* diffuse porous (Fig. 2.11A). *Vessels* solitary (94%) and in oblique multiples of 2, average 94 (SD 20, range 60–180) per mm<sup>2</sup> in areas between large rays, solitary vessels oval in outline, mean tangential diameter 46 (SD 16, range 37–60) µm; vessel element length average 379 (SD 66, range 240–466) µm; perforation plates scalariform (Fig. 2.11B), 7–23 bars per plate (Fig. 2.11C), bars of perforation plate widely spaced, occasionally pushed apart to produce larger gaps, occasionally forked; intervessel pits opposite (Fig. 2.11D), medium, 6–8 µm in diameter to scalariform. *Vessel-ray pits* with reduced borders to simple, round or oval (Fig. 2.11E) to horizontally elongate (Fig. 2.11F). *Vessel-axial parenchyma pits* with reduced borders, round to oval, scattered (Fig. 2.11G). *Tyloses* common, horizontally segmenting vessels. *Fibers* angular in outline in cross section, thin-walled to medium-thick walled, fibers with one or two rows of bordered pits visible in radial and tangential walls (Fig. 2.11H), vasicentric tracheids present, fibers non-septate. *Axial parenchyma* diffuse (Fig. 2.12A), diffuse-in-aggregates often forming short one-celled lines (not extending ray-to-ray) (Fig. 2.12B), incidentally contacting vessels, 2–4 cells per parenchyma strand. *Rays* 2–29 seriate (biseriate rare) (Fig. 2.12C), homocellular composed of procumbent cells to heterocellular composed of procumbent cells in the central portion with 1–3 marginal rows of upright or square cells at one or both ends (Fig. 2.12D–E), with occasional larger cells dispersed throughout the ray and an irregularly distributed layer (up to several cells thick) of larger cells at the ray edge; ray height 0.2–3.5 mm, rays ≤4 cells wide (17%) up to 1.1 mm; 4–5 per mm; uniseriate rays not observed. Pith preserved (Fig. 2.12F). Prismatic crystals not observed.

*Description in IAWA Hardwood List codes (IAWA Committee 1989) –*

2 5 9 14 15 16 17 20 21 26 31 32 40 49 50 (between large rays) 53 56 62 63 66 69  
76 77 78v 91 92 99 102 104 106 114 115

*Remarks* – Specimen TXSTATE 1274 represents stem wood with well-preserved pith and what appear to be the remains of primary vascular bundles (Fig. 2.12F). Vessel diameters (mean 46  $\mu\text{m}$ ) measured from slides prepared from the specimen periphery (mature wood) are the smallest of all the McRae *Platanus*-like woods. Ray width is similar to the McRae wide-ray types (TXSTATE 1203 and TXSTATE 1212), but the rays are less than half as tall. A series of tangential sections was prepared at increasing radii (i.e., 2, 3, 4, 6, 7, 8 cm) to evaluate ontogeny as an influence on ray dimension, particularly ray height. Examination of the serial tangential sections reveals that ray height in the specimen is uniform through the entire available radius range, confirming that ray height distinguishes this xylotype from other McRae *Platanus*-like woods (i.e., other McRae *Platanus*-like woods have significantly taller rays at similar stem position). The specimen differs from other McRae *Platanus*-like woods in that rays have occasional large cells intermixed within the ray body, as well as a layer (one to several cells deep) at the ray edges in some areas. In addition to the reduced bordered, oval to horizontally elongate vessel-ray pits, some pits appear to be simple and are noticeably larger elongate ovals than other McRae *Platanus*-like species. Vessel-axial parenchyma pitting on larger parenchyma cells tends to be smaller, round to oval and scattered on the cell surface, rather than oval to scalariform.

## DISCUSSION

### **InsideWood database search code**

**Comparison to extant woods.** The first step in an InsideWood search for a potential modern affinity for the McRae “wide ray” fossil woods focused on anatomical features shared by all four of the xylotypes. This search included solitary vessels (exclusively solitary in most of the woods) (9p), scalariform perforation plates (14p), opposite intervessel pits (21p), vessel-ray pitting with reduced borders (30a), vasicentric tracheids (60p), fibers with distinctly bordered pits (62p), rays frequently greater than 10 cells wide (99r) and >1 mm in height (102r), with procumbent cells in the ray body (105e). Another important feature of the McRae woods, the rarity or absence of uniseriate rays, could not be directly included in the search because it is not in the IAWA Hardwood List. This is reflected in a search result that included individual species in *Tetracera* (Dilleniaceae), *Berberidopsis* (Berberidopsidaceae) and *Fagus* (Fagaceae), all of which are excluded by having rays of two sizes, including numerous uniseriate rays. Furthermore, *Fagus* species always have some simple perforation plates.

The result of the “first step” search did not suggest family affinity. Notably, it did not indicate Platanaceae as a possible affinity due to specific anatomical feature mismatches seen in *Platanus* (e.g. vessels frequently in multiples and a combination of simple and scalariform perforation plates). Yet, in spite of the mismatches, woods similar to the McRae woods have been compared to the family Platanaceae, primarily on the basis of shared features (e.g., very wide and tall, nearly

homocellular rays, rare or absent uniseriate rays, and opposite intervessel pitting) (Page 1968, Brett 1972, Crawley 1989, Wheeler et al. 1995).

A second search was conducted to see if families other than Platanaceae would be retrieved if the search code allowed the mismatches present in *Platanus*. The code for the second search included diffuse-porous wood (5p), vessels solitary or in tangential multiples, but not in long radial multiples or clusters (10a, 11a), allowing simple perforation plates, but with at least some scalariform perforation plates (14p), intervessel pits opposite (21p, 22a), fibers non-septate (65a), rays >10 cells wide (99r) and >1 mm in height (102r), rays not of two distinct sizes (103a) not composed of exclusively square and upright cells (105a) and without oil cells (124a). The search yielded not only Platanaceae, but genera in six other families. These families are Aquifoliaceae, Cardiopteridaceae and Stemonuraceae (Aquifoliales, Kårehed 2001), Cornaceae (Cornales) and two genera found to be sister by Stull et al. 2015, *Ottoschulzia* (Icacaceae) and *Metteniusa* (Metteniusaceae).

Species of *Ilex* (Aquifoliaceae), Cornaceae, *Ottoschulzia* and *Metteniusa* are excluded by having common uniseriate rays (Metcalf and Chalk 1950, InsideWood 2004-onwards, Lens et al. 2008). *Medusanthera* (Stemonuraceae) does not have uniseriate rays, but its multiseriate rays are narrower than those in the fossil woods (9–11 seriate) and the perforation plates are >94% simple (Lens et al. 2008, Metcalfe and Chalk 1950). Species of *Pseudobotrys* (Cardiopteridaceae) are similar to the McRae fossil wood in that uniseriate rays are not present, the multiseriate rays (11–19 seriate) are of similar proportion, vessels are primarily solitary,

perforation plates are exclusively scalariform, intervessel pitting is predominantly opposite, fibers have distinctly bordered pits, and axial parenchyma is diffuse-in-aggregates or scanty paratracheal. However, *Pseudobotrys* differs in having vessel-ray pitting similar to intervessel pitting and rays composed of procumbent cells with square and upright cells mixed throughout (Lens et al. 2008, InsideWood 2004-onward).

The Jose Creek *Platanus*-like woods most closely resemble Platanaceae in having exceptionally wide rays, some exceeding 30 cells in width, and few or no uniseriate rays. The rays are nearly homocellular and the massive ray bodies generally composed of all procumbent cells or with only a few rows of square or upright cells at the margins, structure consistent with that reported for *Platanus racemosa*, *P. orientalis*, *P. wrightii*, and *P. kerrii* (Brush 1917, Page 1968, Wheeler 1995). Intervessel pitting in the Jose Creek fossils is opposite, except for some vessel element tails and occasional, usually narrow, vessels where it transitions to scalariform, consistent with descriptions of extant *Platanus* (Wheeler 1995). Axial parenchyma in both extant *Platanus* and the Jose Creek fossils is generally diffuse or diffuse-in-aggregates, often forming short lines that contact vessels. The term “scanty paratracheal” might apply, however, since the axial parenchyma-vessel contact in the fossil woods appears to result from random distribution of apotracheal parenchyma, the phrase “scanty paratracheal” axial parenchyma was not used in the descriptions.

All the Jose Creek fossil *Platanus*-like woods have vessel-ray parenchyma pitting that generally is oval to very elongated horizontal oval with reduced borders.

Vessel-ray parenchyma pitting in extant *Platanus* was described as similar to intervessel pitting (Metcalf and Chalk 1950), which would distinguish the McRae *Platanus*-like woods from extant *Platanus* species. However, *Platanus* pitting has also been reported with reduced borders (or simple). Baas (1969) described the pits of *P. kerrii* twig wood as “large and simple, in scalariform or opposite arrangement,” and Wheeler (1995) described vessel to marginal ray cell pits in mature *P. kerrii* wood as having narrow borders and sometimes elongated. *Platanus kerrii* is sister to the remaining crown group species (Feng et al. 2005, Grimm and Denk 2007), and as such may retain some vessel-parenchyma pitting characteristics seen in the fossil woods.

While strong similarities to Platanaceae exist, the Jose Creek *Platanus*-like woods differ from extant *Platanus* species (Table 2.1). The fossils have vessels that are exclusively or predominantly solitary, exclusively or predominantly scalariform perforation plates, rays often wider than *Platanus* (*P. kerrii* the exception) and vessel-ray parenchyma pitting with reduced borders, not similar to intervessel pitting as is typical (or predominant) in most *Platanus* species. The vasicentric tracheids in the Jose Creek *Platanus*-like woods twist around vessels and have multiple rows of pitting that differ from that of fibers. Brush (1917) reported tracheids adjacent to vessels in *Platanus*, but it is not clear from his description whether they are equivalent to the fossil wood vasicentric tracheids. The differences in these anatomical features warrant assignment of the Jose Creek woods to a fossil genus.

**Comparison to fossil woods.** A search of the InsideWood database was conducted to see if fossil woods with similar anatomical features could be attributed to a family other than Platanaceae or had been described without assignment to a particular family. A search was conducted for woods with exclusively solitary vessels (9p), exclusively scalariform perforation plates (13a 14p), intervessel pitting opposite (21p), vessel-ray pitting with reduced borders (30a), fibers with distinctly bordered pits (62p), rays commonly >10 seriate (99r), ray height >1 mm (102r), rays composed of procumbent cells in the body and with <4 margin rows of square or upright cells (105e 108a). None of the woods exhibited vasicentric tracheids; a search including the vasicentric code (60p) had a null result. However, the feature was not used to rule out a potential match because vasicentric tracheids might not be observable in poorly preserved specimens.

Several woods were superficially similar but could be excluded by some combination of features. *Hythia elgari* Stopes (Crawley 2001) and *Mulleroxylon eupomatioides* (Page 1970) were excluded for having common uniseriate rays composed of upright cells. Scott and Barghoorn (1955) and Wheeler and Manchester (2002) noted a general similarity of *Euptelea baileyana* to *Platanus*, but described *Euptelea* as having predominantly scalariform intervessel pits, axial parenchyma rare to diffuse, more heterocellular rays, and commonly occurring uniseriate rays. This last feature is the most obvious difference between these McRae woods and *Euptelea*.

*Spiroplatanoxylon hortobágyii* (Greguss) Süss (Süss 2007) was given special consideration because vessels in some McRae *Platanus*-like woods had markings

that superficially resembled helical thickenings, a key characteristic of *Spiroplatanoxydon*. In particular, fine horizontal lines cover the entire length of some vessels (Fig. 2.13A,C,E). Upon close inspection, these do not appear to be helical thickenings because the markings are not observed to circle around the vessels. Neither are the markings interpreted as large scalariform perforation plates. Perforation plates in the specimens are well-defined and have robust, widely spaced bars (Fig. 2.13B,D,F). The fine lines are not a result of coalescent intervessel pit apertures (Fig. 2.3G) or narrow, closely spaced scalariform intervessel pits (Fig. 2.3F). The exact nature of some of the lines is difficult to determine and may represent some structure akin to the intermediate forms of tracheids described by Brush (1917). Whatever explanation there is for the fine horizontal lines in the McRae woods, the images of helical thickenings in *Spiroplatanoxydon hortobágyii* provided in Süß (2007) do not match any vessel feature seen in the McRae woods. *Spiroplatanoxydon hortobágyii* further differs by having crystals in chambered parenchyma.

The anatomical features of fossil woods similar to the McRae *Platanus*-like woods are summarized in Table 2. 2. The McRae woods differ from the other species in having vasicentric tracheids and reduced bordered vessel-ray parenchyma pitting. Each of the McRae woods is also distinguished from the other woods by some combination of very wide rays (frequently >30 cells), the absence of uniseriate rays, the arrangement of axial parenchyma in short lines or the presence of prismatic crystals.

### ***Plataninium* or *Platanoxylon*?**

*Platanus*-like fossil woods typically have been assigned to *Plataninium* or *Platanoxylon*, genera dating back to the mid-1800's and mid-1900's. As with many genera originally proposed at that time, the history of these genera is confusing, and some nomenclatural issues cannot be conclusively resolved.

Unger (in Endlicher 1840) proposed the genus *Plataninium* for a wood he thought most comparable to that of *Platanus occidentalis*. His description included features consistent with Platanaceae (e.g., distinct annual rings; vessels solitary and in multiples; and broad and tall, nearly homocellular rays (Metcalf and Chalk 1950)). However, he described scalariform perforation plates, not the co-occurrence of simple and scalariform plates typical of extant *Platanus*, and he referred to "poroso-spiralia" in the Latin diagnosis, a phrase often interpreted to mean vessels with spiral thickenings. However, "poroso" could also refer to alternate intervessel pits (pores) that more-or-less spiral down a vessel. In a comment following the diagnosis Unger indicated he thought the vessels were like those of *Acer*, a wood with both helical thickenings and alternate intervessel pitting, while *Platanus* has neither (Metcalf and Chalk, 1950). Unger's (1847) line drawings of the wood appear to show helical thickenings, but the drawing is schematic, and his description "Die Gefässwand war spiralg gestreift, nicht selten mit einander kreuzenden Fasern, in deren Maschen sich kleine, kaum zu unterscheidende Tüpfel befinden," could alternatively refer to vasicentric tracheids wrapping around the vessels, rather than spiral thickenings. Unfortunately, the specimen and slides are not available, so that his description cannot be evaluated.

Vater (1884) emended the diagnosis of *Plataninium* to include round and scalariform intervessel pitting, imperforate longitudinal elements intermediate between fibers and vessels, axial parenchyma in short uniseriate lines, and rays that expand at the growth boundaries. Page (1968) further emended the diagnosis to make *Plataninium* a form genus for woods “whose familial relationships cannot be determined with certainty” (e.g., Fagaceae, Platanaceae, Eupteleaceae and Icacinaceae), but she did not mention spiral thickenings. Brett (1972) further emended the diagnosis to include woods with rays with square or upright cells in the marginal rows. As emended by Page and Brett, Süss & Müller-Stoll (1977) found the genus too broadly defined to be useful for true *Platanus*-like woods, declaring *Plataninium* a *nomen ambiguum*. This left unresolved the correct generic assignment for wide-ray fossil woods with spiral thickenings, prompting Süss (2007) to propose the genus *Spiroplatanoxylon* for fossil woods with those features.

In 1951, Andreánszky described a fossil wood from Mikofalva, Hungary, and proposed using the name *Platanoxylon* for *Platanus*-like woods, but did not provide a generic diagnosis, holotype or type species, so the genus was not validly published. Independently of Andreánszky, Hofmann (1952) used the name *Platanoxylon* sp. for a wood described as similar to *Platanus occidentalis*, also without validly publishing the genus name and with no reference to the earlier use of the name by Andreánszky. Prakash et al. (1971) were first to designate a species of *Platanoxylon*, *P. bohemicum*. The authors cited *Platanoxylon* Andreánszky 1951 as the generic authority, perhaps unaware of the invalid status of the genus. Since 1951, the name *Platanoxylon* has commonly been applied to *Platanus*-like woods (see lists in

Gregory et al. 2009).

In an attempt to resolve this nomenclatural ambiguity, Süss and Müller-Stoll (1977) returned to Mikofalva to collect *Platanus*-like wood specimens comparable to material described as *Platanoxylon* by Andreánszky in 1951. Based on that material (in particular, a conspicuous log segment thought to be Andreánszky's source material), Süss and Müller-Stoll provided a generic diagnosis that closely allied the wood species to extant *Platanus*, designated a type species (*Platanoxylon andreánszkyi*), selected a holotype and proposed that Andreánszky be the accepted authority, thus validly publishing the name. Any assertion of valid publication by Hofmann (1952) was dismissed on the basis that the diagram accompanying her article included numerous narrow rays that distinguished her wood from *Platanus*. Süss did not accept publication by Prakash et al. (1971) of *Platanoxylon bohemicum* Prakash, Březinová and Bužek as valid, in part because he questioned the affinity of *P. bohemicum* with *Platanus*. The fossil had spiral thickenings (not mentioned in the description), as well as exclusively scalariform perforation plates. Süss later (Süss 2007) proposed the new genus *Spiroplatanoxylon* to accommodate woods with spiral thickenings and the new combination of *S. bohemicum*.

Article 46.2 of the International Code of Nomenclature for algae, fungi and plants (Turland et al. 2018) allows the name of a new taxon to be attributed to an author other than the author of publication, but the date of effective publication is not retroactive (ICN, Article 31). Had Hofmann or Prakash et al. validly published a name for their woods, *Platanoxylon* would not have been used for *Platanus*-like woods. However, Süss and Müller-Stoll appear to have validly published the genus

name.

While the circumstances surrounding previous references to the name *Platanoxylon* by Hofmann and Prakash et al. might be viewed differently, Süss and Müller-Stoll's pragmatic solution of declaring Andreánszky the authority for *Platanoxylon*, thus legitimizing "common practice" and linking the fossil name to its intended affinity, was sensible. Furthermore, the *Platanoxylon* diagnosis circumscribed a logical subset of *Platanus*-like species, primarily from the Cenozoic, with features consistent with extant *Platanus*, but that are sufficiently different to warrant assignment to a fossil genus. Süss and Müller-Stoll provided the following diagnosis for *Platanoxylon* Andreánszky.

***Platanoxylon* Andreánszky**

**Generic diagnosis.** Growth zones present, sometimes indistinct and difficult to recognize, vessels in cross-section angular to round, single and in short radial, tangential or oblique rows and in irregular groups, distributed more or less evenly over the growth zone, diameter small to medium, radially 60 to 110  $\mu\text{m}$ , tangentially 45 to 80  $\mu\text{m}$ , in the root wood radially to 135  $\mu\text{m}$ , tangentially 110  $\mu\text{m}$ , without spiral thickenings, vessel perforations simple and scalariform or sometimes only scalariform, bordered pits opposite. Wood fibers irregularly arranged, axial parenchyma apotracheal, diffuse and short uniseriate lines, single cells attached to the vessels, medullary rays predominantly very high and broad, often flared at the growth boundary, uniseriate and low-rank (narrow) medullary rays rare, homocellular, sometimes weakly heterocellular, ray cells on average 20 to 30  $\mu\text{m}$  high.

### **Rationale for a new genus of Cretaceous and some early Cenozoic**

***Platanus*-like woods.** The diagnosis for *Platanoxylon* as emended by Süss and Müller-Stoll (1977) includes distinct or indistinct growth rings, a combination of simple and scalariform perforation plates and vessels solitary and in multiples. Many Cretaceous and early Cenozoic *Platanus*-like woods, including the McRae woods described herein, have anatomical features that fall outside those generic limits, yet the woods share other anatomical features that tie them to Platanaceae. A new genus within Platanaceae is needed to accommodate Cretaceous and early Cenozoic woods that do not align with *Platanoxylon*.

Süss and Müller-Stoll (1977) asserted that woods assigned to *Platanoxylon* should relate specifically to *Platanus* and offered a narrow interpretation of *Platanoxylon*, citing precise reasons for excluding previously described *Platanus*-like species from the genus. In their view, species with exclusively scalariform perforation plates were to be retained in *Platanoxylon* when certain key features were also present (e.g., growth boundaries and vessels in tangential multiples or clusters not uncommon), and excluded when those features were absent, suggesting the authors viewed the “exclusively scalariform perforation plates” as exclusionary only when combined with other disqualifying features (e.g., growth boundaries absent, exclusively solitary vessels). The presence of some “weakly heterocellular rays” was included in the *Platanoxylon* generic diagnosis, supported by descriptions of various *Platanus* species having rays with a few square or upright margin rows (Brush 1917, Page 1968, Baas 1969), a feature later confirmed in *P. kerrii* (Wheeler 1995). Nonetheless, Süss and Müller-Stoll suggested the presence of

rays with marginal rows of square or upright cells was among the reasons for questioning the affinity of certain woods to *Platanus*.

In 1977, Süss and Müller-Stoll identified several species of *Plataninium* or *Platanoxylon* that fell outside their *Platanoxylon* diagnosis. The woods described by Page (1968), *Plataninium platanooides* and *P. californicum* from the Maastrichtian Panoche Formation of California, were excluded due to their lack of growth rings, primarily solitary vessels, and heterocellular rays (one to several rows of square or upright cells at the margins). Süss and Müller-Stoll also noted that *P. californicum* had relatively large diameter vessels at 130 µm (radial diameter) and long vessel elements. *Plataninium decipiens* Brett (1972), an Eocene *Platanus*-like wood with exclusively scalariform perforation plates, mostly solitary vessels (some tangential multiples) and obscure growth rings was questioned because it also had opposite to scalariform intervessel pitting and some square or upright cells at the ray margins. While not consistent with the *Platanoxylon* diagnosis, these woods, like the McRae *Platanus*-like woods, align with Platanaceae and will require a separate genus.

Following the Süss and Müller-Stoll interpretation, the Crawley (1989) wood from Reading Beds, UK, *Plataninium decipiens* (Upper Paleocene) and *Plataninium piercei* (Wheeler et al. 1995) from Kirtland, San Juan Basin, NM (Early Maastrichtian) with exclusively scalariform perforation plates, exclusively solitary vessels (predominantly solitary in the case of *P. piercei*) and growth rings absent would also fall outside the *Platanoxylon* generic diagnosis, as would the McRae *Platanus*-like woods. Specimens TXSTATE 1212 and TXSTATE 1274 typify the McRae woods in that they have exclusively scalariform perforation plates and

exclusively solitary vessels (>90%) with only occasional radial, oblique or tangential multiples, as well as growth rings absent. Also, these woods have rays with one to several rows of square and upright cells. Specimen TXSTATE 1267 differs from TXSTATE 1212 and TXSTATE 1274 by having a small percentage of simple to scalariform perforation plates, perhaps a transitional form (Meylan and Butterfield 1975) that indicates a degree of advancement in the wood with a step towards true simple perforation plates as specified in the diagnosis for *Platanoxylon*. Nonetheless, because the wood has exclusively solitary vessels and no growth rings, it remains outside *Platanoxylon*. Specimen TXSTATE 1273 has occasional growth boundaries with somewhat radially narrowed fibers, a difference in vessel diameter across the boundary in some places and flaring of rays at the growth boundaries, all features observed in *Platanus* that tie this specimen to Platanaceae while falling outside the generic limits of *Platanoxylon*. Specimen TXSTATE 1203 has exclusively scalariform perforation plates, 83% solitary vessels or tangential multiples of 2–3 and some weakly defined growth boundaries. This combination of features approaches the spirit of the *Platanoxylon* diagnosis, but because the percentage of solitary vessels is still very high and vessel clusters not present, and the growth ring boundaries are indistinct, this wood is more consistent with the new genus than species assigned to *Platanoxylon*.

Süss and Müller-Stoll (1977) expressed reluctance to attribute the Cretaceous woods to Platanaceae because of the disparity between the features of both the Cretaceous and early Cenozoic woods and *Platanus*. However, a relationship to Platanaceae becomes more apparent when species are listed in

chronological order to allow following the transition of character states through time (Table 2. 3). Perforation plates are exclusively scalariform in the Cretaceous and early Cenozoic (with the exception of the single McRae specimen with some simple-to-scalariform combination plates), whereafter simple perforation plates are observed, eventually becoming predominant over scalariform plates in extant woods. Vessels are exclusively solitary (>90%) in most early woods, with the incidence of multiples (usually tangential) and clusters increasing through time. The exceptions, *Plataninium ogasawarae* and *P. jezoensis* are noteworthy for having vessel multiples in the early to mid- Late Cretaceous. The species also have indistinct growth boundaries that are not observed in some Cretaceous and early Cenozoic *Platanus*-like woods.

Were the early *Platanus*-like woods not already known, their features would be predicted in that the pattern of character state transition parallels general angiosperm trends for anatomical features observed by Wheeler and Baas (1991). The character states of *Platanus*-like woods stagger-step from the Cretaceous through the Cenozoic to the present, “ancestral” features shifting to more “advanced” features, each feature at its own pace, and with no distinct “line” between genera. Thus, the early woods are connected to Platanaceae, but are different than both fossil *Platanoxylon* and extant *Platanus*. The new genus is therefore proposed to accommodate the anatomical differences present in the early *Platanus*-like woods.

### **Estimation of *Platanus* divergence time**

A phylogenetic and historical biogeographic study by Feng et al. (2005) exploring divergence times for the crown group subgenus *Platanus* (excluding *Platanus kerrii*) employed two calibration fossils. The first fossil, the earliest known report of *Platanus*-like dispersal hairs on achenes (Crane 1989), was used to set the most recent common ancestor (MRCA) for the *Platanus* crown group at 45 Ma, based on the presence of these hairs in all living species of Platanaceae and their absence from many Cenozoic and all Cretaceous species. This resulted in divergence date estimates for the crown species of subgenus *Platanus* from 16.5 to 4.8 Ma. The second calculation used fossils with an enlarged petiole base that encloses the bud, a character common to *Platanus*-like fossils in the Paleocene that is present in subgenus *Platanus* but absent from *P. kerrii*. This set the MRCA for the crown group at 60 Ma, resulting in estimated divergence dates for the crown species from 21.9 to 6.5 Ma. The enlarged petiole base character distinguishes subgenus *Platanus* from subgenus *Castaneophyllum* (*P. kerrii*), which is sister to all other *Platanus* species (Feng et al. 2005, Grimm and Denk 2007), establishing a minimum divergence estimate for *P. kerrii*. A more accurate estimate of divergence age for *P. kerrii* proved unfeasible with the data and techniques employed in the Feng et al. (2005) analysis.

The position of *P. kerrii* as sister to the remaining crown species may explain why the McRae fossil woods, and fossil *Platanus*-like woods in general, more closely resemble *P. kerrii* than species of the subgenus *Platanus* (Wheeler et al. 1995). *Platanus kerrii* is distinguished from species of subgenus *Platanus* by having wider

rays, some vessel-ray pitting with reduced borders (Wheeler 1995) and a higher percentage of scalariform perforation plates (53%) (Baas 1969).

### **Other fossil evidence**

The fossil record for Platanaceae in the mid- to Late Cretaceous is plentiful in the Northern Hemisphere. Fossil evidence indicates the family was more diverse and more widespread than it is today, as evidenced by the small number of species and single genus in Platanaceae. Fossil leaves referred to platanoids include lobate forms, entire leaves with pinnate venation, compound leaves and compound and pinnatifid leaves (e.g., Crane 1989, Friis et al. 2011 and references therein). From the Jose Creek Member of the McRae, Upchurch and Mack (1998) reported palmately veined leaves (*Platanus raynoldsii*, Platanaceae), as well as leaves that may represent extinct genera in the family, and Estrada-Ruiz et al. (2012b) reported leaves similar to *Platanites marginatus*. At other North American localities, fossil leaf forms that contrast with the typical extant *Platanus* type leaves have been reported. Compound leaves, referred to *Erlingdorgia montana* and *Platanites marginata*, were described from the Hell Creek formation of Montana and North Dakota, USA (Maastrichtian) (Johnson 1996 in Friis et al. 2011). Pinnatifid leaves of *Sapindopsis* were reported in association with *Aquia brookensis*, a staminate inflorescence (with pollen) found to be similar to *Platanus* described from Virginia, USA (Early-Middle Albian) (Crane et al. 1993). *Friisicarpus brookensis*, pistillate flowers resembling *P. kerrii*, were found in association with the *Sapindopsis* and *A. brookensis*. Additional North American inflorescence types include *Hamatia elkneckensis*, also staminate and with *in situ* pollen reported from Bull Mountain locality, Maryland, USA (latest

Albian or early Cenomanian) which was found in association with a pistillate species, *Friisicarpus elkneckensis* (Pedersen et al. 1994). Species of *Platananthus*, a fossil genus for some pistillate inflorescences described by Manchester (1986) have been reported from the West Brothers locality, Maryland, USA (Late Albian) and the Neuse River locality, North Carolina, USA (Early Campanian). *Quadriplatanus georgianus* from the Upatoi Creek locality, Georgia, USA (Coniacian) comprises both staminate and pistillate flowers (Magallon-Puebla et al. 1997). All of the fossil Platanaceae flowers from the Cretaceous have characteristics distinct from extant *Platanus* (e.g., five vs. four or variable number of floral parts, fruit morphology, tricolporate pollen) that suggest different pollination and dispersal strategies in the older species (Crane et al. 1993, Pederson et al. 1994, Magallón-Puebla et al. 1997, Friis et al. 2011).

It is not surprising that the considerable diversity seen in Cretaceous platanaceous leaves and reproductive structures would be matched by diversity in Cretaceous *Platanus*-like woods. In the McRae Formation, multiple platanaceous specimens have been examined and sorted into xylo types. However, the delimitation of species is complicated by the nature of anatomical structure observed in extant *Platanus*, in particular, variability in ray structure.

Süss and Müller-Stoll (1977) contended that fossil *Platanus*-like woods from the Cretaceous through the Cenozoic included transitional forms of ray structure (Kribs Heterogeneous Type I to Heterogeneous Type II to Homogeneous Type II) (Kribs 1935), and that greater species-to-species variation was likely during early platanoid diversification than exists today, including forms not observed in extant

species. They proposed that evolving ray forms are illustrated in fossil wood species that may represent extinct lineages. Therefore, ray characters could be used to delimit fossil species.

A recent taxonomic treatment of New World *Platanus* recognized that interfertility and the resulting gene flow among extant species may contribute to morphological overlap, particularly within the subgenus *Platanus*, that influences the usefulness of morphological characters in delimiting species for some taxa (Nixon and Poole 2003). The solution was to recognize as species the morphologically well-defined taxa and as varieties taxa with broadly overlapping character states. The treatment recognized seven distinct species, three of which had two varieties each. *Platanus kerrii* was among the species without ambiguous morphological overlap. Grimm and Denk (2007) confirmed that *Platanus kerrii* is sister to the subgenus *Platanus* (Feng et al. 2005) and is distinctly different at both the molecular and morphologic levels. Results of that study suggested that boundaries of extant species may be recently established or still in flux; it was hypothesized that gene pools in fossil lineages may have been similarly impacted.

The possibility that extinct species of *Platanus* may have shared the modern tendency for interfertility might inform our interpretation of taxa that overlap in some anatomical features (Nixon and Poole 2003, Feng et al. 2005, Grimm and Denk 2007). There is a reasonable expectation that distinct species could show considerable overlap of some features and yet be distinguishable by a set of others. In some cases, small differences might be significant and specimens should not be uncritically “lumped,” if, as Süss and Müller-Stoll (1977) postulated, greater

interspecies variability of Platanaceae anatomical features existed in the Cretaceous. If additional evidence becomes available, species that have been too narrowly defined can be placed in synonymy with no loss of information. As a practical matter, individual specimens that have been “lumped” and described as a single taxon are less likely to receive critical review. In this study, data from specimens TXSTATE 1203, 1271 and 1272 were confidently incorporated into a single xylotype. Specimens TXSTATE 1212 and 1267-1270 were also incorporated in a xylotype, but the specimen descriptions showed considerable variability and this group may warrant reevaluation. The task of delimitating species would be informed by a comprehensive study of the variability present within individual trees of *Platanus* species, including comparison of anatomical features at various positions within the tree (i.e., radial distance from pith, stem vs. branch vs. root). Additional studies might explore variability within species, as well as addressing the influence of environmental factors on anatomical variability.

## CONCLUSIONS

A new genus is proposed for fossil *Platanus*-like woods having the combination of exclusively or primarily solitary vessels and exclusively scalariform perforation plates, vessel-ray parenchyma pits with reduced borders that are round to oval or horizontally elongate, and vasicentric tracheids. Four new species of *Platanus*-like woods from the Jose Creek Member of the McRae Formation are proposed.

Table 2.1.1. Comparison of McRae Group IIB, *Platanus*-like woods and *Platanus*.

Taxon	GR	VA	PP	IVP	VMTD ( $\mu\text{m}$ )	V-RP	V-AP	VT	AP	RW Uni	RW Multi (cells)	RH ( $\mu\text{m}$ )	RCC	Cr
<i>P. occidentalis</i> <sup>3</sup>	+	sol, tm, c	s, sc	o	83	iv <sup>5</sup>	s, o, e	+	dia, sl		14	1450		+
<i>P. wrightii</i> <sup>3</sup>	+	sol, tm, c	s, sc	o	76	iv <sup>6</sup>	s, o, e	+	dia, sl		$\leq 12^5$	1920	2-3 <sup>4</sup>	
<i>P. racemosa</i> <sup>3</sup>	+	sol, tm, c	s, sc	o	73	iv <sup>6</sup>	s, o, e	+	dia, sl		$\leq 12^5$	2340	2-3 <sup>4</sup>	
<i>P. lindeniana</i> <sup>1</sup>	I	sol, dm	s, sc	o, sc	50-100	iv, (rb) <sup>5</sup>			d	+	$\leq 11$	> 1mm		+
<i>P. orientalis</i>	+	sol, tm, dm	s, sc	o		rb, r/o, e			d, dia, sl	-	$\leq 16^5$		2-3	
<i>P. mexicana</i> <sup>1</sup>		sol, rm, dm	s, sc	o, sc					d	-	$\leq 17^5$			
<i>P. kerrii</i> <sup>2</sup>	I	sol, (tm)	s, sc	o, (sc)	94	iv, (rb, e)	rb	-	d, dia		12 ( $\leq 34$ )	1372 ( $\leq 2873$ )	1-3	+
Group IIC sp. 1 TXSTATE 1212, 1267-1270	-	sol (>90%), (rm, dm, tm)	sc	o, (sc)	68-77	rb, r/o, e, (sc)	rb, r/o, e, (sc)	+	d, dia, sl	-	12-21 ( $\leq 37$ )	2666- 3639	1-4	-
Group IIC sp. 2 TXSTATE 1203, 1271-1272	I	sol (71-85%), dm, tm	sc	o	98-110	rb, r/o, e	rb, r/o, e, (sc)	+	d, dia	-	13-17 ( $\leq 30$ )	1000- 13000	NA	-
Group IIC sp. 3 TXSTATE 1273	Int	sol (>90%), (rm, dm, tm)	sc	o, (sc)	62	rb, r/o, e	rb, r/o, e, (sc)	+	d, dia, sl	rare	8 ( $\leq 21$ )	2722 ( $\leq 12141$ )	1-3, w	+
Group IIC sp. 4 TXSTATE 1274	-	sol (>90%), (dm)	sc	o, sc	46	rb, r/o, (s, large)	rb, o	+	d, dia, sl	-	15 ( $\leq 29$ )	1409 ( $\leq 3480$ )	1-3, w, e	-

Table 2.1. Comparison of McRae Group IIB, *Platanus*-like woods and *Platanus*.

*Legend:* McRae fossil woods are in boldface. GR = growth rings, (-) = absent, (I) = indistinct, (Int) = intermediate, (+) = distinct; VA = vessel arrangement, (sol) = solitary, (tm) = tangential multiples, (rm) = radial multiples, (dm) = diagonal or oblique multiples, (c) = clusters; PP = perforation plate, (s) = simple, (sc) = scalariform; IVP = intervessel pits, (o) = opposite, (sc) = scalariform, infrequent character states indicated by parentheses; VMTD = vessel mean tangential diameter, mean value, range of means for multiple samples; V-RP = vessel-ray parenchyma pits, (iv) = like intervessel pitting, (rb) = reduced borders, (s) = simple, (r/o) = round or oval, (e) = horizontally elongate, (sc) = nearly scalariform (infrequent character states indicated by parentheses); V-AP = vessel-axial parenchyma pits, (rb) = reduced borders, (s) = simple, (r) = round, (o) = oval, (e) = horizontally elongate; VT = vasicentric tracheids (+) = vasicentric tracheids present, (-) = vasicentric tracheids absent; AP = axial parenchyma, (d) = diffuse, (dia) = diffuse-in-aggregates, (sl) = short lines; RW Uni = uniseriate rays, (+) = present, (-) = absent; RW Multi = multiseriate ray width, mean, largest number observed in parentheses; RH = ray height, mean, largest number observed in parentheses, range of means for multiple samples; RCC = ray cellular composition, number range = number of uniseriate margin rows of square or upright cells, (w) = square or upright cells within ray, (e) = large or square / upright cells along edge; Cr = crystals in ray parenchyma, (+) = present, (-) = not observed. Blank spaces indicate unavailable information.

<sup>1</sup>Camacho Uribe D. 1988

<sup>2</sup>Wheeler EA. 1995

<sup>3</sup>Brush WD. 1917

<sup>4</sup>Page VM. 1968

<sup>5</sup>Observation from InsideWood 2004-onward image

<sup>6</sup>Metcalf CR, Chalk L. 1950

Table 2.2. Comparison of McRae Group IIB, *Platanus*-like woods and similar fossil species.

Age Location	Taxon	GR	VA	PP	IVP	VMTD (µm)	V-RP	VT	AP	RW Uni	RW Multi (cells)	RH (µm)	RCC	Cr
Late Campanian McRae	Group IIC sp. 1 TXSTATE 1212, 1267-1270	-	sol, (rm, dm, tm)	sc 10-14	o, (sc)	68-77	rb,r/o, e, (sc)	+	d, dia, sl	-	12-21 (≤ 37)	2666- 3639	1-4	-
Late Campanian McRae	Group IIC sp. 2 TXSTATE 1203, 1271-1272	I	sol, dm, tm	sc 4-20	o	98-110	rb,r/o, e	+	d, dia	-	13-17 (≤ 30)	1000- 13000		-
Late Campanian McRae	Group IIC sp. 3 TXSTATE 1273	Int	sol, (rm, dm, tm)	sc 4-14	o, (sc)	62	rb,r/o, e	+	d, dia, sl	rare	8 (≤ 21)	2722 (≤12141)	1-3, w	+
Late Campanian McRae	Group IIC sp. 4 TXSTATE 1274	-	sol, (dm)	sc 7-23	o, sc	46	rb, r/o, (s, large)	+	d, dia, sl	-	15 (≤ 29)	1409 (≤ 3480)	1-3, w, e	-
Maastrichtian Del Puerto Creek, CA	Group IIC, CASG 60421 <sup>1</sup>		sol	sc 40-50		171	o, sc		sc-p, d, sl	+	≤ 15	1700 (≤ 2700)	1-5	+
Campanian Aguja Formation Big Bend, TX	Platanoid- Icacinoid Type II <sup>2</sup>		sol	sc 10-15	sc	74			dia	-	≤ 25	2582	few	
Early Middle Eocene Specimen Ridge	<i>Platanoxylon haydenii</i> <sup>3</sup>	+	sol, tm	sc 3-28	sc, o, sub-o,	74	e, sc	-	d, sl	rare	≤ 22	≤6000	2-3	
Middle Eocene Clarno Nut Beds	<i>Platanoxylon haydenii</i> <sup>4</sup>	+	sol, tm	sc 4-27	o	91	o, sc	-	d, dia, sl	rare	to 27	≤5000	2-3	+
Upper Paleocene Reading Beds, UK	<i>Plataninium brettii</i> <sup>5</sup>	+	sol, tm, (rm)	sc 4-40	o to a, r to sc	35	o to a, r to sc	-	dia	+	≤ 14	≤6000	1-4+	
Maastrichtian Panoche, CA	<i>Plataninium platanoides</i> <sup>6</sup>	-	sol, (m)	sc 4-22	o, sc	60-70	o, sc	-	d, sl, (v)	rare	15+	2000+	2-3	
Paleocene Black Peaks, Big Bend, TX	cf. <i>Platanoxylon haydenii</i> <sup>7</sup>	-	sol, tm	sc 12-24		88		-	d, dia	very rare	11 ≤22	3800 ≤7000	1-3	
Upper Paleocene Reading Beds, UK	<i>Plataninium decipiens</i> <sup>5</sup>	-	sol	sc 14-24	o, sc	75	sc	-	dia, sl	-	20 ≤30	5000, (≤10000)	1-3	

Table 2.2. Continued. Comparison of McRae Group IIB, *Platanus*-like woods and similar fossil species.

Age Location	Taxon	GR	VA	PP	IVP	VMTD ( $\mu\text{m}$ )	V-RP	VT	AP	RW Uni	RW Multi (cells)	RH ( $\mu\text{m}$ )	RCC	Cr
Maastrichtian Panoche, CA	<i>Plataninium californicum</i> <sup>6</sup>	-	sol	sc, s? < 30	o, sc	(Radial) 130	o, sc	-	d, sl, (v)	rare	$\leq 20$	$\leq 7000$	1-2	
Eocene London Clay, Kent, Britain	<i>Plataninium decipiens</i> <sup>8</sup>	I	sol, (tm)	sc 13-25	o, sc	80 $\leq 105$	sc	-	d, sl		$\leq 18$	$\leq 6000$	1-2	+
Coniacian to Santonian Hokkaido, Japan	<i>Plataninium ogasawarae</i> <sup>9</sup>	I	sol, r/tm	sc 6-37	o, e	63	iv, o, e	-	d	rare	$\leq 27$	10000	0	-
Cenomanian Hokkaido, Japan	<i>Plataninium jezoensis</i> <sup>9</sup>	I	sol, r/tm	sc 9-29	o, r	83	iv, r	-	dia	rare	$\leq 30$	6300	0	-
Early Maastrichtian Kirtland, San Juan Basin, NM	<i>Plataninium piercei</i> <sup>10</sup>	-	sol, (m)	sc 6-9	o, sub-a	48		-	d, dia	very rare	$\leq 25$	4230 ( $\leq 7910$ )	1-2 (4-6)	+

Table 2.2. Comparison of McRae Group IIB, *Platanus*-like woods and similar fossil species.

*Legend:* McRae fossil woods are in boldface. GR = growth rings, (-) = absent, (I) = indistinct, (Int) = intermediate, (+) = distinct; VA = vessel arrangement, (sol) = solitary, (tm) = tangential multiples, (rm) = radial multiples, (dm) = diagonal or oblique multiples, (c) = clusters; PP = perforation plate, (s) = simple, (sc) = scalariform; IVP = intervessel pits, (o) = opposite, (sc) = scalariform, infrequent character states indicated by parentheses, (a) = alternate, (r) = round, (e) = elongate; VMTD = vessel mean tangential diameter, mean value, range of means for multiple samples; V-RP = vessel-ray parenchyma pits, (iv) = like intervessel pitting, (rb) = reduced borders, (s) = simple, (r/o) = round or oval, (e) = horizontally elongate, (sc) = nearly scalariform, infrequent character states indicated by parentheses; VT = vasicentric tracheids (+) = vasicentric tracheids present, (-) = vasicentric tracheids absent; AP = axial parenchyma, (d) = diffuse, (dia) = diffuse-in-aggregates, (sl) = short lines (sc-p) = scanty paratracheal, (v) = vasicentric; ; RW Uni = uniseriate rays, (+) = present, (-) = absent; RW Multi = multiseriate ray width, mean, largest number observed in parentheses; RH = ray height, mean, largest number observed in parentheses, range of means for multiple samples; RCC = ray cellular composition, number range = number of uniseriate margin rows of square or upright cells, (w) = square or upright cells within ray, (e) = large or square / upright cells along edge; Cr = crystals in ray parenchyma, (+) = present, (-) = not observed. Blank spaces indicate unavailable information.

<sup>1</sup>Page VM. 1980

<sup>2</sup>Wheeler EA, Lehman TM. 2000

<sup>3</sup>Wheeler EA, Scott RA, Barghoorn ES. 1977

<sup>4</sup>Scott RA, Wheeler EA. 1982

<sup>5</sup>Crawley M. 1989

<sup>6</sup>Page VM. 1968

<sup>7</sup>Wheeler EA. 1991

<sup>8</sup>Brett DW. 1972

<sup>9</sup>Takahashi KI, Suzuki M. 2003

<sup>10</sup>Wheeler EA, McClammer J, LaPasha CA. 1995

Table 2.3. Transitions in anatomical features through time.

Age	Locality	Taxon	Growth Boundaries	Vessel Grouping	Perforation Plates
Extant	Eastern to south central USA, NE Mexico	<i>Platanus occidentalis</i>			
	California, USA, N. Baja California, Mexico	<i>Platanus racemosa</i>			
	SW USA, NW Mexico	<i>Platanus wrightii</i>			
	Thailand, Laos, Vietnam, Cambodia	<i>Platanus kerrii</i>			
Upper Miocene	Mikfalva, HUN	<i>Platanoxylon andreanszkyi</i> <sup>1</sup>			
Upper Miocene	Columbia Basalts, Washington State, USA	<i>Platanus americana</i> <sup>2</sup>			
Oligocene	Tsuyazaki Formation Kyushu, JPN	<i>Platanus tsuyazakiensis</i> <sup>3</sup>			
Eocene	Clarno Nut Beds, Oregon, USA	<i>Platanoxylon haydenii</i> <sup>5</sup>			
Eocene	Nevada County California, USA	<i>Platanoxylon pacificum</i> <sup>1</sup>			
	<i>Yellowstone NP, USA</i>	<i>Platanoxylon platenii</i> <sup>1</sup>			
Middle Eocene	Amethyst Mountain, Yellowstone NP, USA	<i>Platanoxylon catenatum</i> <sup>1</sup>			
	Amethyst Mountain, Yellowstone NP, USA	<i>Platanoxylon knowltonii</i> <sup>1</sup>			
	Amethyst Mountain, Yellowstone NP, USA	<i>Platanoxylon haydenii</i> <sup>1</sup>			
	Specimen Ridge, Yellowstone NP, USA	<i>Platanoxylon haydenii</i> <sup>4</sup>			
Lower Eocene	London Clay, Kent, Britain	<i>Plataninium decipiens</i> <sup>6</sup>			
Upper Paleocene	Reading Beds, UK	<i>Plataninium decipiens</i> <sup>7</sup>			
Middle Paleocene	Black Peaks, Big Bend, Texas, USA	<i>Plataninium haydenii</i> <sup>8</sup>			
Paleocene	Interbasaltic Beds, UK	<i>Plataninium brettii</i> <sup>7</sup>			
	Panoche, California, USA	<i>Plataninium platanoides</i> <sup>10</sup>			
Maastrichtian	Panoche, California, USA	<i>Plataninium californicum</i> <sup>10</sup>			
Early Maastrichtian	Kirtland; San Juan Basin, New Mexico, USA	<i>Plataninium piercei</i> <sup>9</sup>			
		<b>McRae Group IIC sp. 1*</b>			
		<b>McRae Group IIC sp. 1</b>			
		<b>McRae Group IIC sp. 2</b>			
<b>Late Campanian</b>		<b>McRae Group IIC sp. 3</b>			
		<b>McRae Group IIC sp. 4</b>			
		<i>Plataninium decipiens</i> <sup>11</sup>			
		<i>Plataninium ogasawarae</i> <sup>12</sup>			
Santonian	Aachen Formation BEL, NLD, DEU				
Coniacian to Santonian	Obirashibe River, Hokkaido, JPN				
Cenomanian & Turonian	mid-Yezo Group, Hokkaido, JPN				

Table 2.3. Continued. Transitions in anatomical features through time..

*Legend:*

<b>Growth Boundaries</b>	<b>Vessel Grouping</b>	<b>Perforation Plates</b>
<b>Distinct</b>	<b>Mostly groups, some solitary</b>	<b>Mostly simple</b>
<b>Indistinct</b>	<b>Solitary, some groups</b>	<b>Scalariform and simple</b>
<b>Absent</b>	<b>Exclusively solitary</b>	<b>Exclusively scalariform</b>

\*TXSTATE 1267, the only McRae wood Group IIC sp. 1 specimen with occasional simple to scalariform combination perforation plates.

- <sup>1</sup> Süss H, Müller-Stoll WR. 1977
- <sup>2</sup> Prakash U, Barghoorn ES. 1961
- <sup>3</sup> Suzuki M. 1976
- <sup>4</sup> Wheeler EA, Scott RA, Barghoorn ES. 1977
- <sup>5</sup> Scott RA, Wheeler EA. 1982
- <sup>6</sup> Brett DW. 1972
- <sup>7</sup> Crawley M. 1989
- <sup>8</sup> Wheeler EA. 1991
- <sup>9</sup> Wheeler EA, McClammer J, LaPasha CA. 1995
- <sup>10</sup> Page VM. 1968
- <sup>11</sup> Meijer J. 2000
- <sup>12</sup> Takahashi KI, Suzuki M. 2003

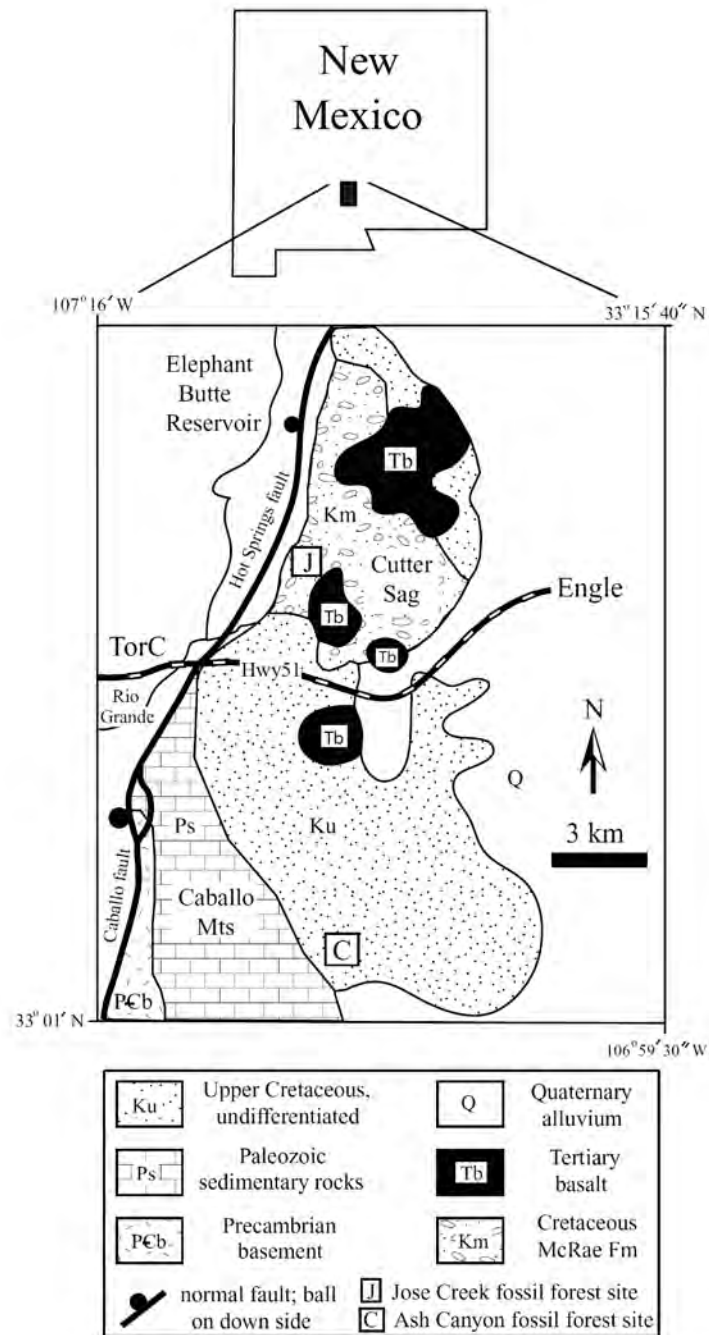


Figure 2.1. Map showing the location and geology of the McRae Formation, south-central New Mexico (Estrada-Ruiz et al. 2018).



Figure 2.2. Holoxylotype of McRae wood Group IIB sp. 2 (TXSTATE 1212) Platanaceae. - *In situ* stump with a maximum diameter of 40 cm at the top of the buttress roots.

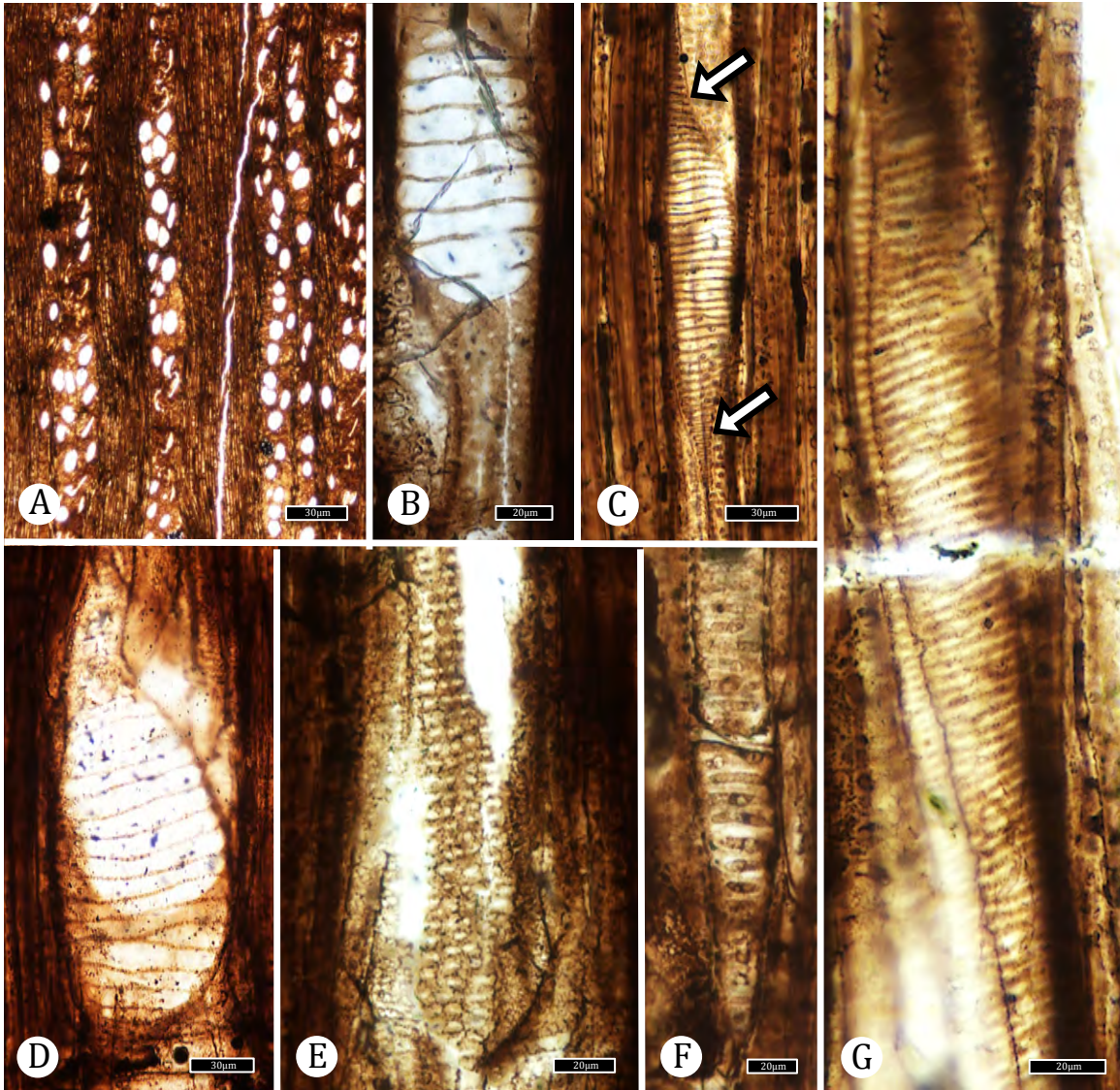


Figure 2.3. McRae wood Group IIC sp. 1 (TXSTATE 1212, 1267-1270) Platanaceae. – A: TS. Vessels diffuse-porous, solitary, or occasionally in short radial multiples. TXSTATE 1268, X-1. Scale bar = 30  $\mu\text{m}$ . – B: RLS. Scalariform perforation plate. TXSTATE 1268, R-3. Scale bar = 20  $\mu\text{m}$ . – C: RLS. Scalariform pitting on vessel element tails intergrading with the scalariform perforation plate. TXSTATE 1270, R-2. Scale bar = 30  $\mu\text{m}$ . – D: RLS. Misaligned simple to scalariform perforation plate. TXSTATE 1267, R-2. Scale bar = 30  $\mu\text{m}$ . – E: RLS. Opposite intervessel pitting. TXSTATE 1268, R-3. Scale bar = 20  $\mu\text{m}$ . – F: TLS. Narrow vessel with scalariform pitting. TXSTATE 1270, T-1. Scale bar = 20  $\mu\text{m}$ . – G: RLS. Opposite intervessel pits horizontally merged. TXSTATE 1270, R-3. Scale bar = 20  $\mu\text{m}$ .

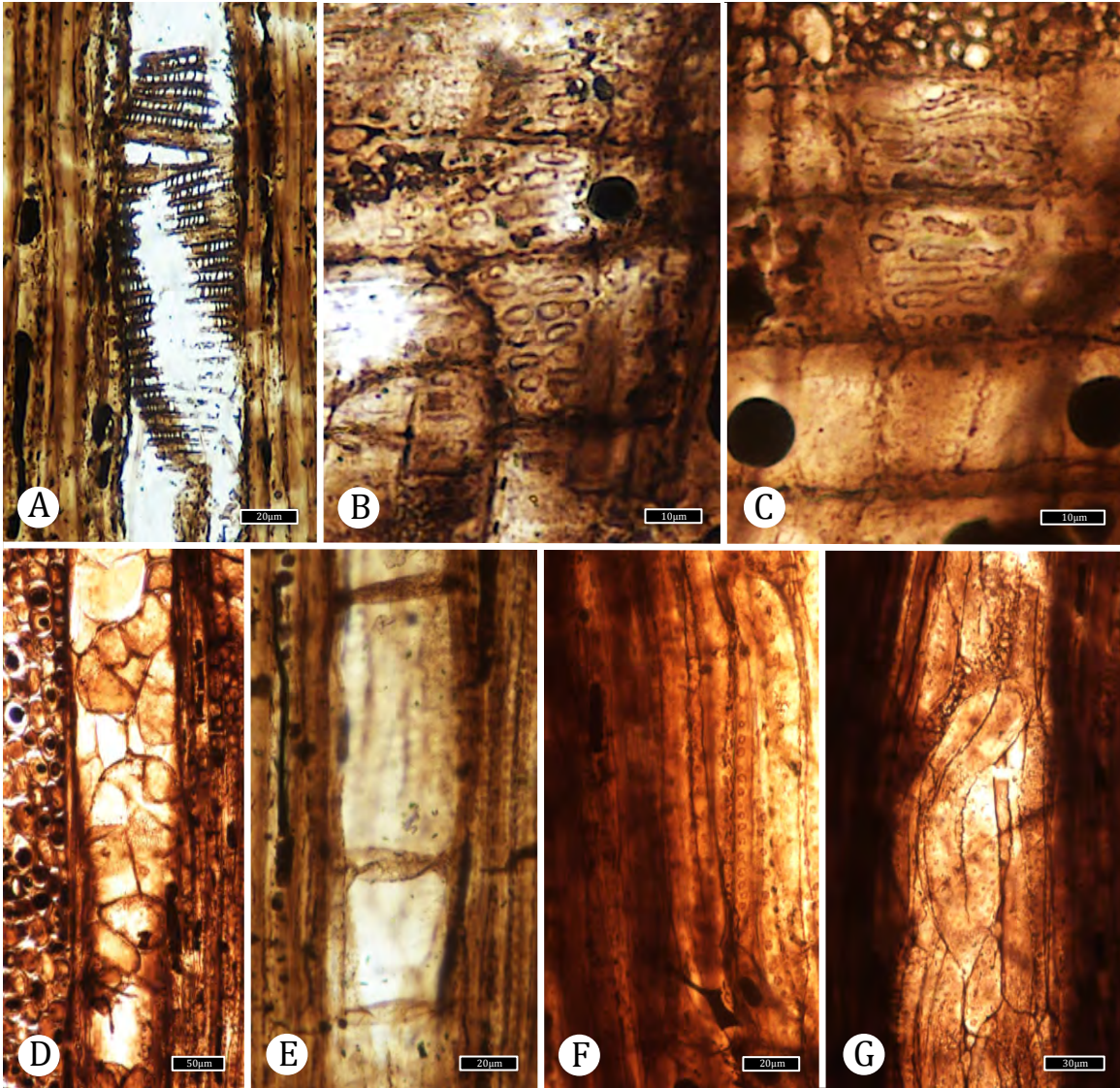


Figure 2.4. McRae wood Group IIC sp. 1 (TXSTATE 1212, 1267-1270) Platanaceae. – A: RLS. Rare scalariform perforation plate with incomplete openings between bars. TXSTATE 1270, R-1. Scale bar = 20  $\mu\text{m}$ . – B – C: Vessel-ray parenchyma pits with reduced borders. – B: RLS. Pits round, oval or horizontally elongate. TXSTATE 1267, R-2. Scale bar = 10  $\mu\text{m}$ . – C: RLS. Pits joined horizontally or nearly scalariform. TXSTATE 1267, R-2. Scale bar = 10  $\mu\text{m}$ . – D: TLS. Tyloses bubble-like. TXSTATE 1270, T-1. Scale bar = 50  $\mu\text{m}$ . – E: RLS. Tyloses segmenting vessel horizontally. TXSTATE 1270, R-2. Scale bar = 20  $\mu\text{m}$ . – F: RLS. Fibers with bordered pits. TXSTATE 1268, R-3. Scale bar = 20  $\mu\text{m}$ . – G: RLS. Vasicentric tracheids with 2–3 rows of pits. TXSTATE 1267, R-2. Scale bar = 30  $\mu\text{m}$ .

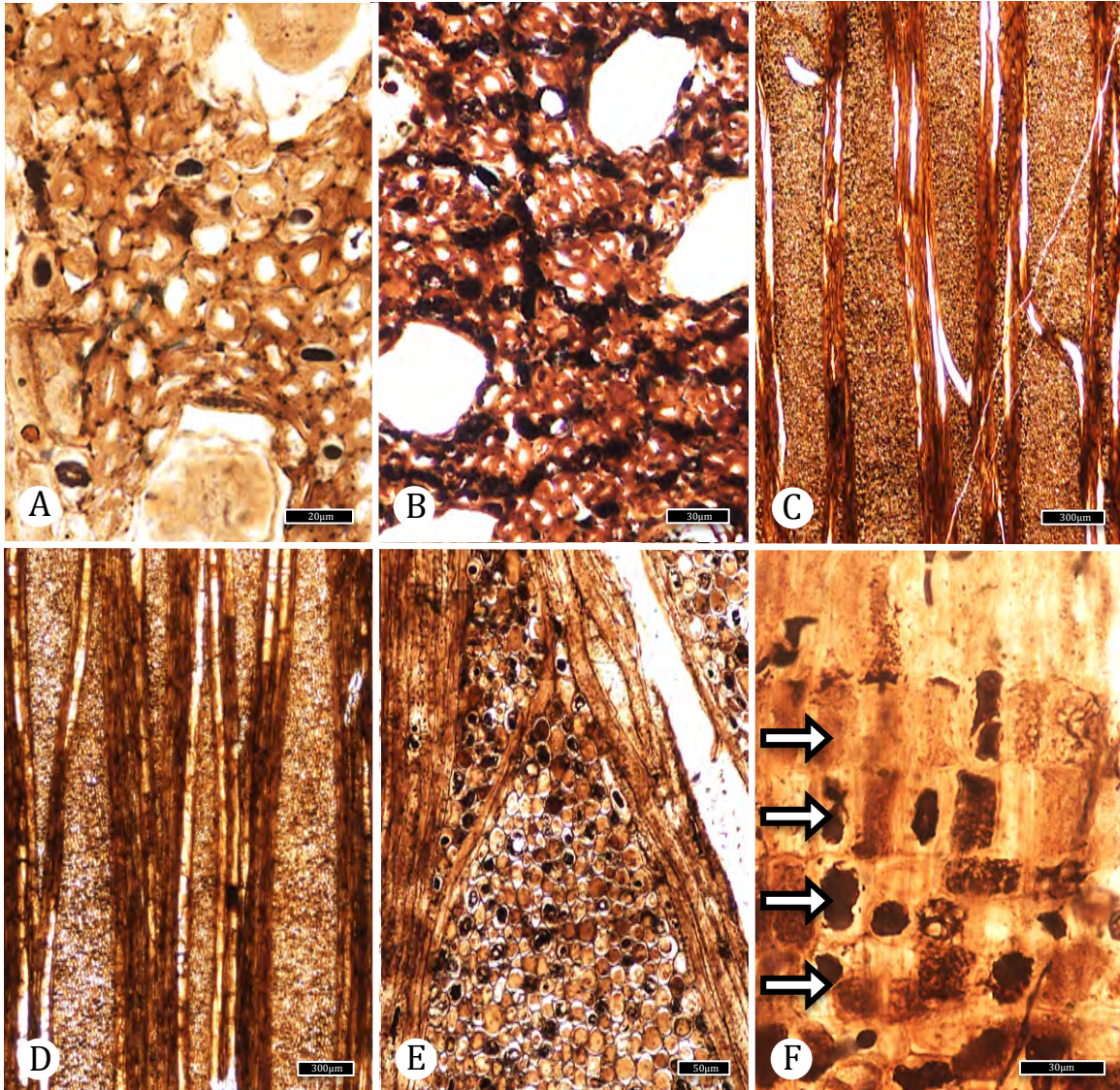


Figure 2.5. McRae wood Group IIC sp. 1 (TXSTATE 1212, 1267-1270)  
 Platanaceae. – A: TS. Axial parenchyma diffuse or diffuse-in-aggregates. TXSTATE 1267, X-5. Scale bar = 20  $\mu\text{m}$ . – B: TS. Axial parenchyma apotracheal in short lines. TXSTATE 1270, X-3. Scale bar = 30  $\mu\text{m}$ . – C–D: Rays > 10 cells wide. – C: TLS. Rays nearly homocellular, frequently 20 cells wide, dissected by vessels. TXSTATE 1268, T-4 . Scale bar = 300  $\mu\text{m}$ . – D: TLS. Rays tall and tapered. TXSTATE 1270, T-1. Scale bar = 300  $\mu\text{m}$ . – E: TLS. Rays nearly homocellular, composed of procumbent cells. TXSTATE 1267, T-3. Scale bar = 50  $\mu\text{m}$ . – F: RLS. Ray with 4 rows square or upright cells (arrows). TXSTATE 1267, R-4. Scale bar = 30  $\mu\text{m}$ .

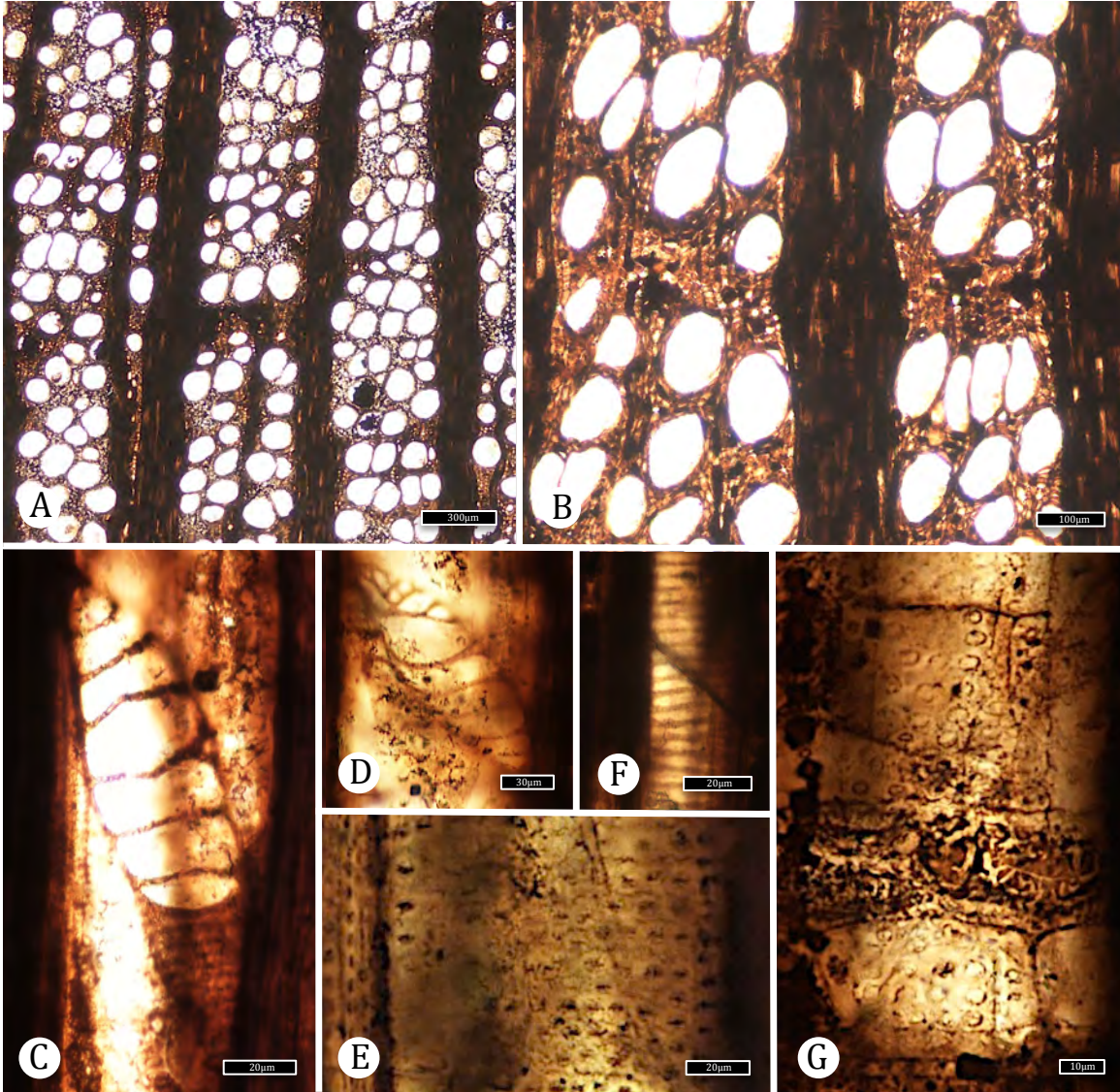


Figure 2.6. McRae wood Group IIC sp. 2 (TXSTATE 1203, 1271-1272) Platanaceae. – A: TS. Wood diffuse porous, slight tendency to tangential arrangement. TXSTATE 1203. S1. Scale bar = 300  $\mu\text{m}$ . – B: TS. Vessels predominantly solitary, less frequently in oblique or tangential multiples. Growth boundaries indistinct or absent. TXSTATE 1203. S1. Scale bar = 100  $\mu\text{m}$ . – C: RLS. Scalariform perforation plates. TXSTATE 1271, R-1. Scale bar = 20  $\mu\text{m}$ . – D: RLS. Rare partially reticulate perforation plate. TXSTATE 1271, R-1. Scale bar = 30  $\mu\text{m}$ . – E: RLS. Opposite intervessel pits. TXSTATE 1271, R-1. Scale bar = 20  $\mu\text{m}$ . – F: RLS. Narrow vessel with scalariform pitting. TXSTATE 1203, S6. Scale bar = 20  $\mu\text{m}$ . – G: RLS. Vessel-ray parenchyma pitting with reduced borders, round to oval. TXSTATE 1203, S7. Scale bar = 10  $\mu\text{m}$ .

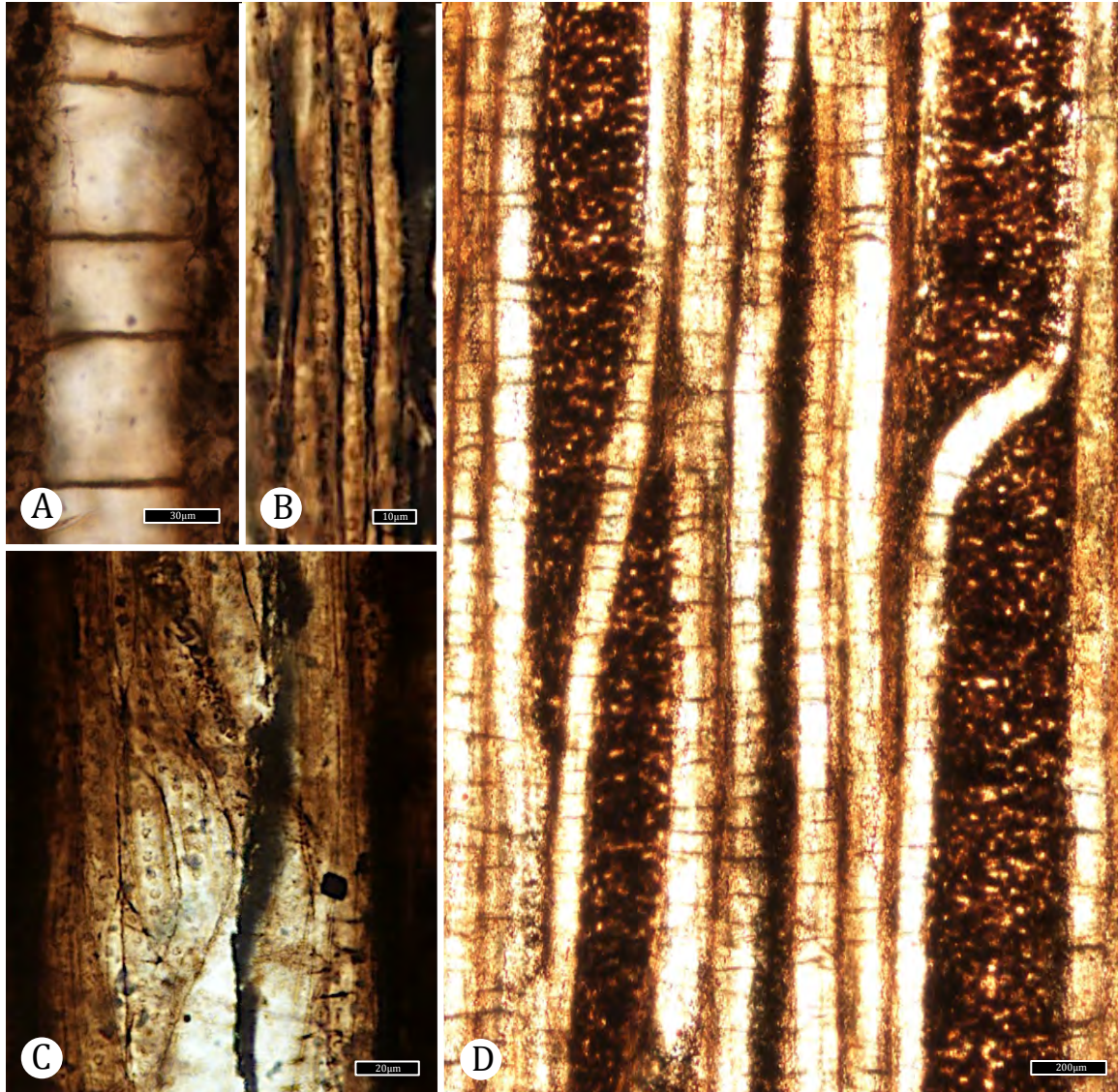


Figure 2.7. McRae wood Group IIC sp. 2 (TXSTATE 1203, 1271-1272)  
 Platanaceae. – A: TLS. Tyloses horizontally segmenting vessels. TXSTATE 1272,  
 R-1. Scale bar = 30  $\mu\text{m}$ . – B: TLS. Fibers with distinctly bordered pits. TXSTATE  
 1203, S4. Scale bar = 10  $\mu\text{m}$ . – C: RLS. Vasicentric tracheids with several rows of  
 bordered pits. TXSTATE 1203, S7. Scale bar = 20  $\mu\text{m}$ . – D: TLS. Rays not strongly  
 heterocellular, dissected by vessels. TXSTATE 1272, T-1. Scale bar = 200  $\mu\text{m}$ .

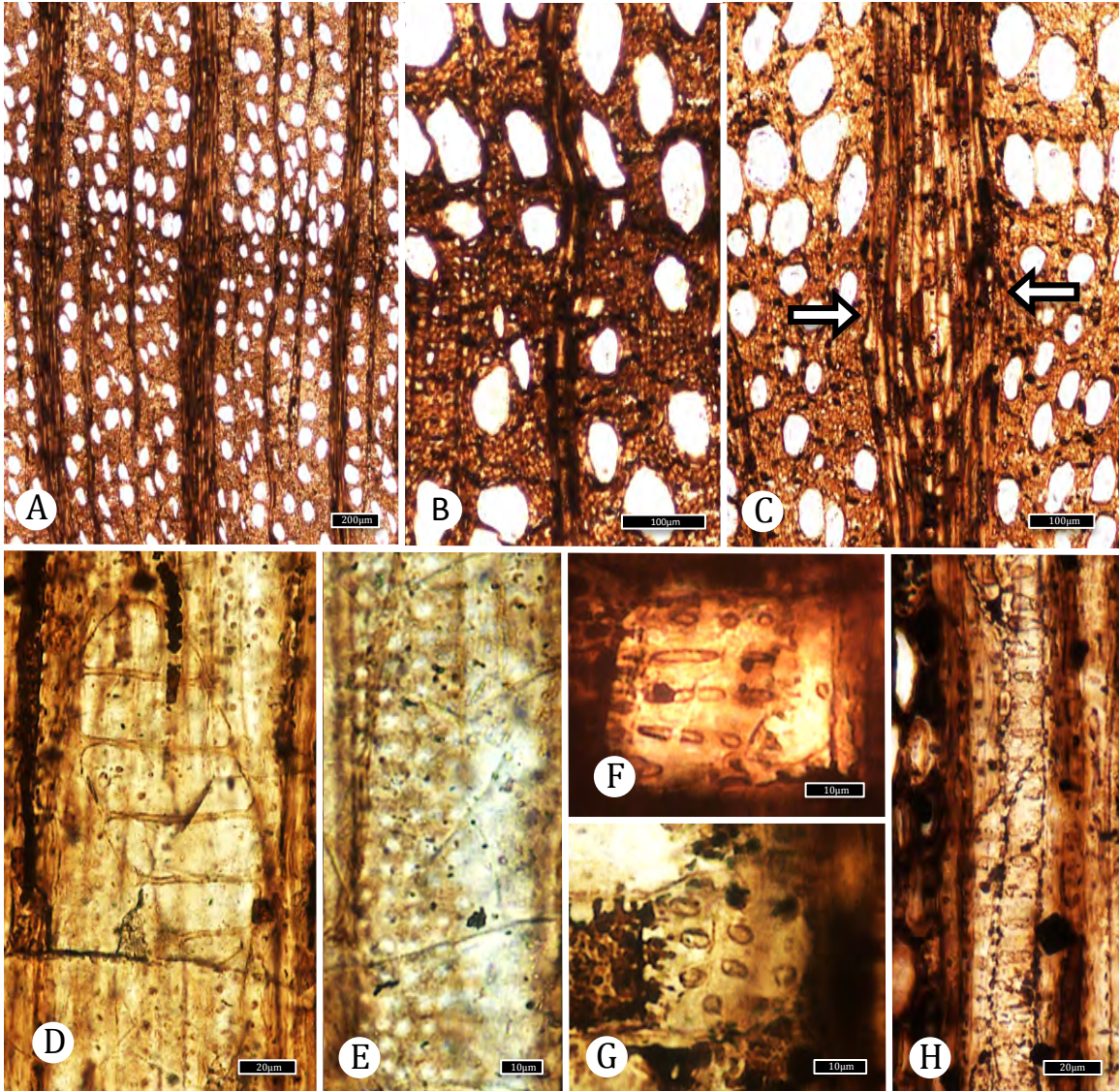


Figure 2.8. McRae wood Group IIC sp. 3 (TXSTATE 1273) Platanaceae. – A: TS. Growth ring boundaries intermediate (between distinct and indistinct), wood diffuse-porous, vessels solitary. TXSTATE 1273, X-3. Scale bar = 200  $\mu\text{m}$ . – B: TS. Growth boundary delineated by radially narrowed fibers and a difference in vessel diameter between latewood and earlywood of subsequent rings. TXSTATE 1273, X-3. Scale bar = 100  $\mu\text{m}$ . – C: TS. Rays flaring at the growth boundary (arrows). TXSTATE 1273, X-4. Scale bar = 100. – D: RLS. Scalariform perforation plate with five widely spaced bars. TXSTATE 1273, R-2. Scale bar = 20  $\mu\text{m}$ . – E: Opposite intervessel pitting. TXSTATE 1273, R-2. Scale bar = 10  $\mu\text{m}$ . – F–G: Vessel-ray parenchyma pits with much reduced borders. – F: RLS. Vessel-ray parenchyma pitting oval to horizontally elongate. TXSTATE 1273, R-2. Scale bar = 10  $\mu\text{m}$ . – G: RLS. Vessel-ray parenchyma pitting round to oval. TXSTATE 1273, R-2. Scale bar = 10  $\mu\text{m}$ . – H: RLS. Vessel-axial parenchyma pitting horizontally elongate to nearly scalariform. TXSTATE 1273, T-5. Scale bar = 20  $\mu\text{m}$ .

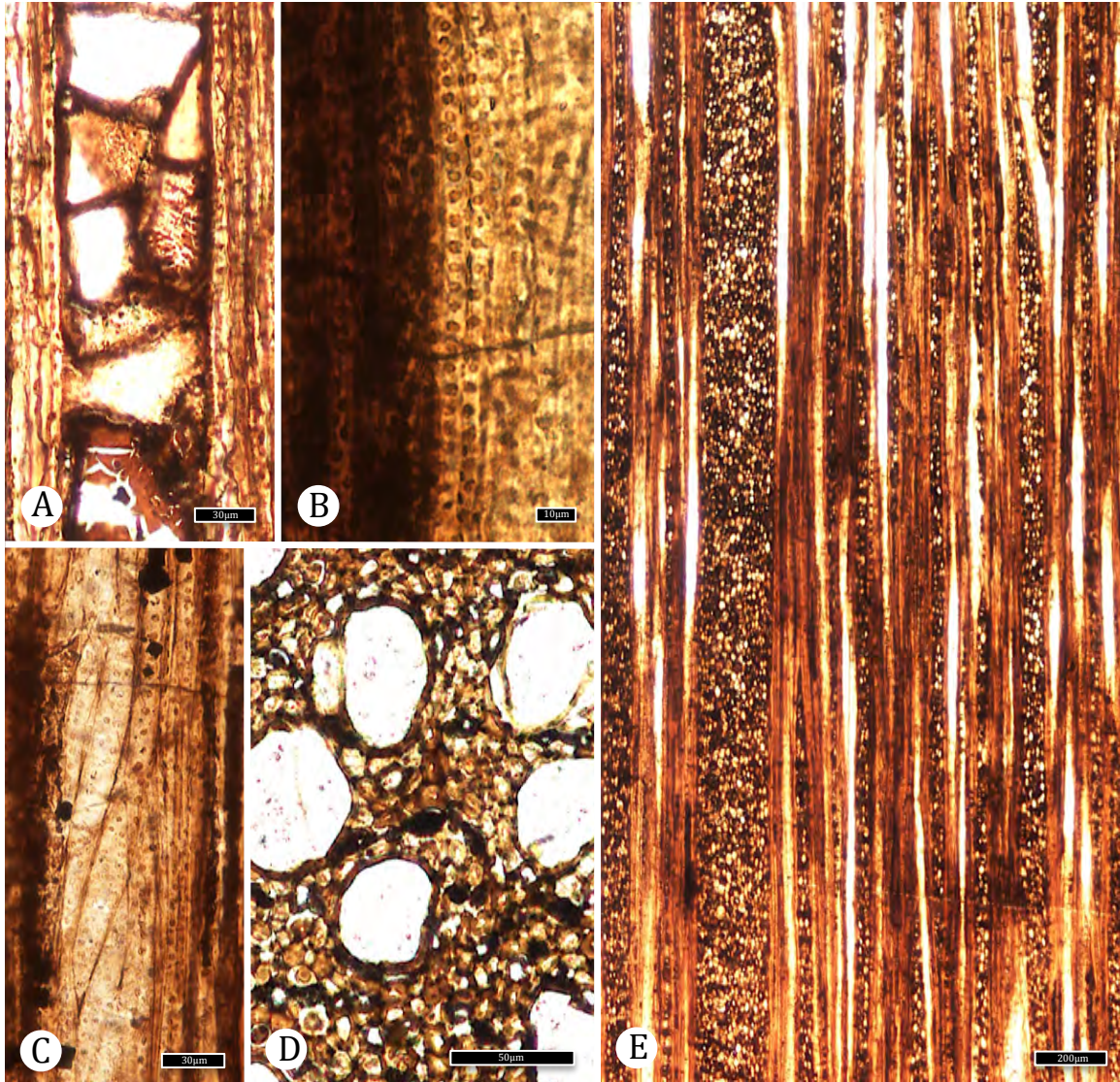


Figure 2.9. McRae wood Group IIC sp. 3 (TXSTATE 1273) Platanaceae. – A: TLS. Tyloses present. TXSTATE 1273, T-4. Scale bar = 30 µm.– B: Fibers with one row of bordered pits. TXSTATE 1273, R-2. Scale bar = 10 µm. – C: RLS. Vasicentric tracheids. TXSTATE 1273, R-2. Scale bar = 30 µm. – D: TS. Axial parenchyma diffuse, diffuse-in-aggregates forming short lines, and sometimes adjacent to vessels. TXSTATE 1273, X-1. Scale bar = 50 µm. – E: TLS. Larger rays >10-seriate, commonly > 5 mm in height; majority of rays ≤ 6-seriate, commonly >1 mm in height. TXSTATE 1273, T-5. Scale bar = 200 µm.

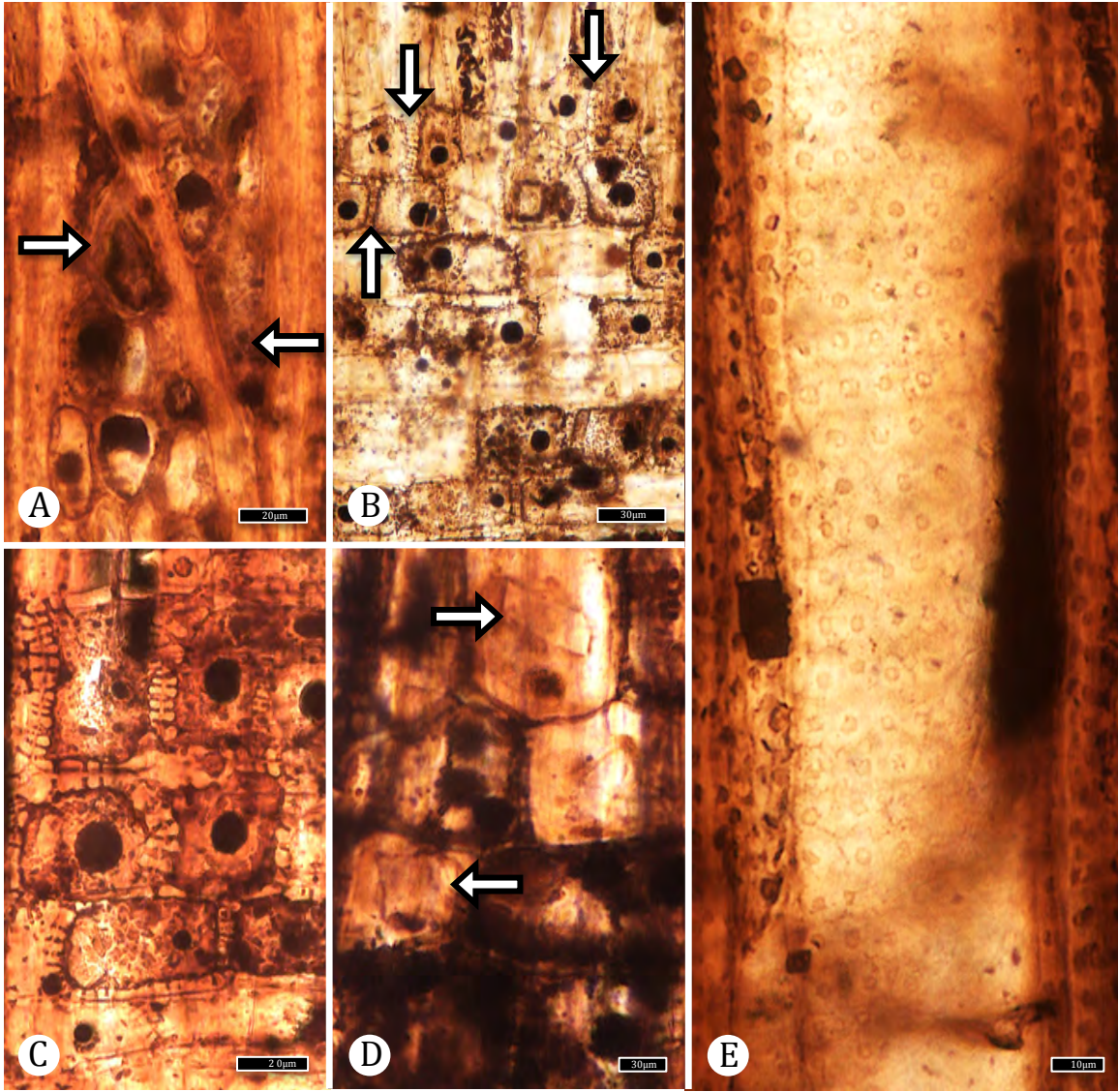


Figure 2.10. McRae wood Group IIC sp. 3 (TXSTATE 1273) Platanaceae. – A: TLS. Ray margin with one square or upright row of cells (arrows). TXSTATE 1273, T-5. Scale bar = 20  $\mu\text{m}$ . – B: RLS. Three rows of square or upright cells at the ray margin (arrows). TXSTATE 1273, R-2. Scale bar = 30  $\mu\text{m}$ . – C: RLS. Ray parenchyma cells with thick walls and bordered pits. TXSTATE 1273, R-2. Scale bar = 20  $\mu\text{m}$  – D: RLS. Prismatic crystals in ray parenchyma (arrows). TXSTATE 1273, R-2. Scale bar = 30  $\mu\text{m}$ . – E: RLS. Vessel with thickenings between intervessel pits. TXSTATE 1273, R-2. Scale bar = 10  $\mu\text{m}$  .

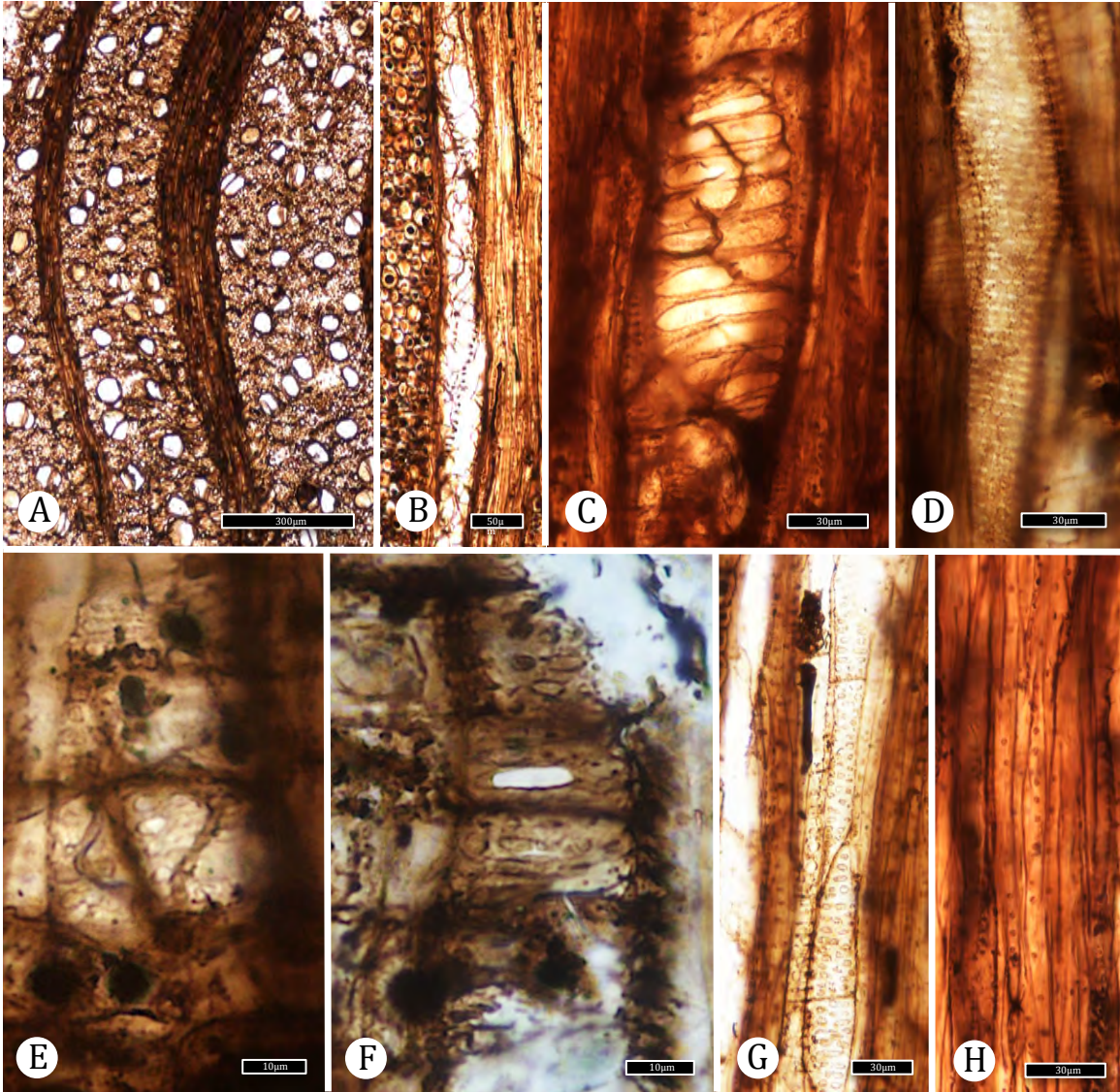


Figure 2.11. McRae wood Group IIC sp. 4 (TXSTATE 1274) Platanaceae. – A: TS. Growth ring boundaries absent, diffuse-porous. TXSTATE 1274, X-6. Scale bar = 300  $\mu\text{m}$ . – B: TLS. Vessel element with scalariform perforation plates. TXSTATE 1274, T-1. Scale bar = 50  $\mu\text{m}$ . – C: RLS. Scalariform perforation plate. TXSTATE 1274, R-5. Scale bar = 30  $\mu\text{m}$ . – D: TLS. Opposite intervessel pitting. TXSTATE 1274, T-1. Scale bar = 30  $\mu\text{m}$ . – E-F: Vessel-ray parenchyma pits with much reduced borders to apparently simple. – E: RLS. Pits oval. TXSTATE 1274, R-1. Scale bar = 10  $\mu\text{m}$ . – F: RLS. Pits oval or horizontal elongate. TXSTATE 1274, R-2. Scale bar = 10  $\mu\text{m}$ . – G: TLS. Vessel-axial parenchyma pits simple or with reduced borders, oval in shape. TXSTATE 1274, T-1. Scale bar = 30  $\mu\text{m}$ . – H: RLS. Non-septate fibers with distinctly bordered pits. TXSTATE 1274, R-5. Scale bar = 30  $\mu\text{m}$ .

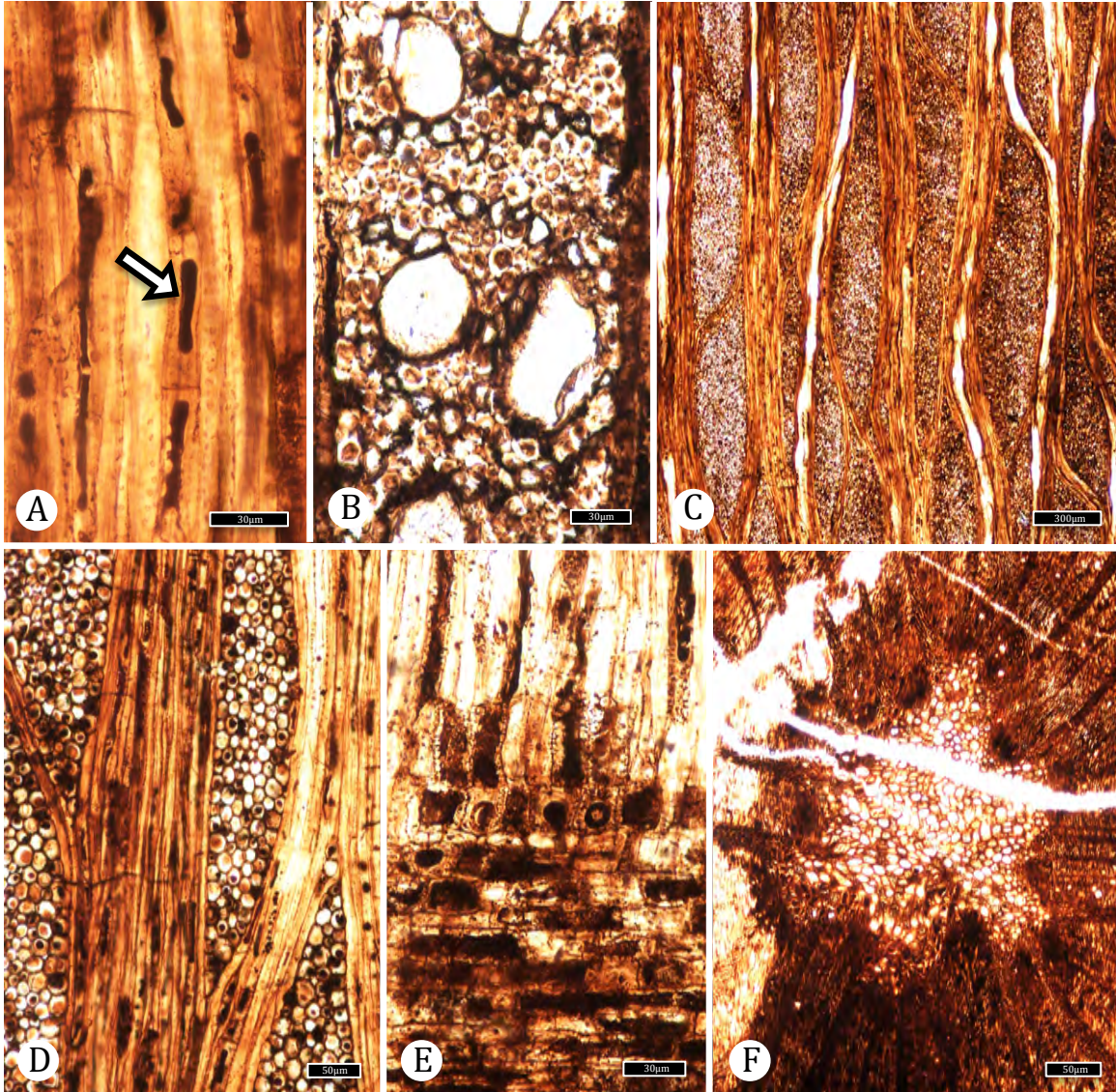


Figure 2.12. McRae wood Group IIC sp. 4 (TXSTATE 1274) Platanaceae. – A: TLS. Axial parenchyma strands among fibers (arrow). TXSTATE 1274, T-2. Scale bar = 30  $\mu\text{m}$ . – B: TS. Solitary vessels. Axial parenchyma forming short, more-or-less tangential lines. TXSTATE 1274, X-5. Scale bar = 30  $\mu\text{m}$ . – C: TLS. Larger rays commonly >10-seriate and up to 3.5 mm in height. TXSTATE 1274, T-1. Scale bar = 300  $\mu\text{m}$ . – D: TLS. Ray body composed of procumbent cells, with few square or upright marginal cells. TXSTATE 1274, T-2. Scale bar = 50  $\mu\text{m}$ . – E: RLS. Ray with one marginal row of upright cells and one row of square cells. TXSTATE 1274, R-3. Scale bar = 30  $\mu\text{m}$ . – F: TS. Pith. TXSTATE 1274, X-7. Scale bar = 50  $\mu\text{m}$ .

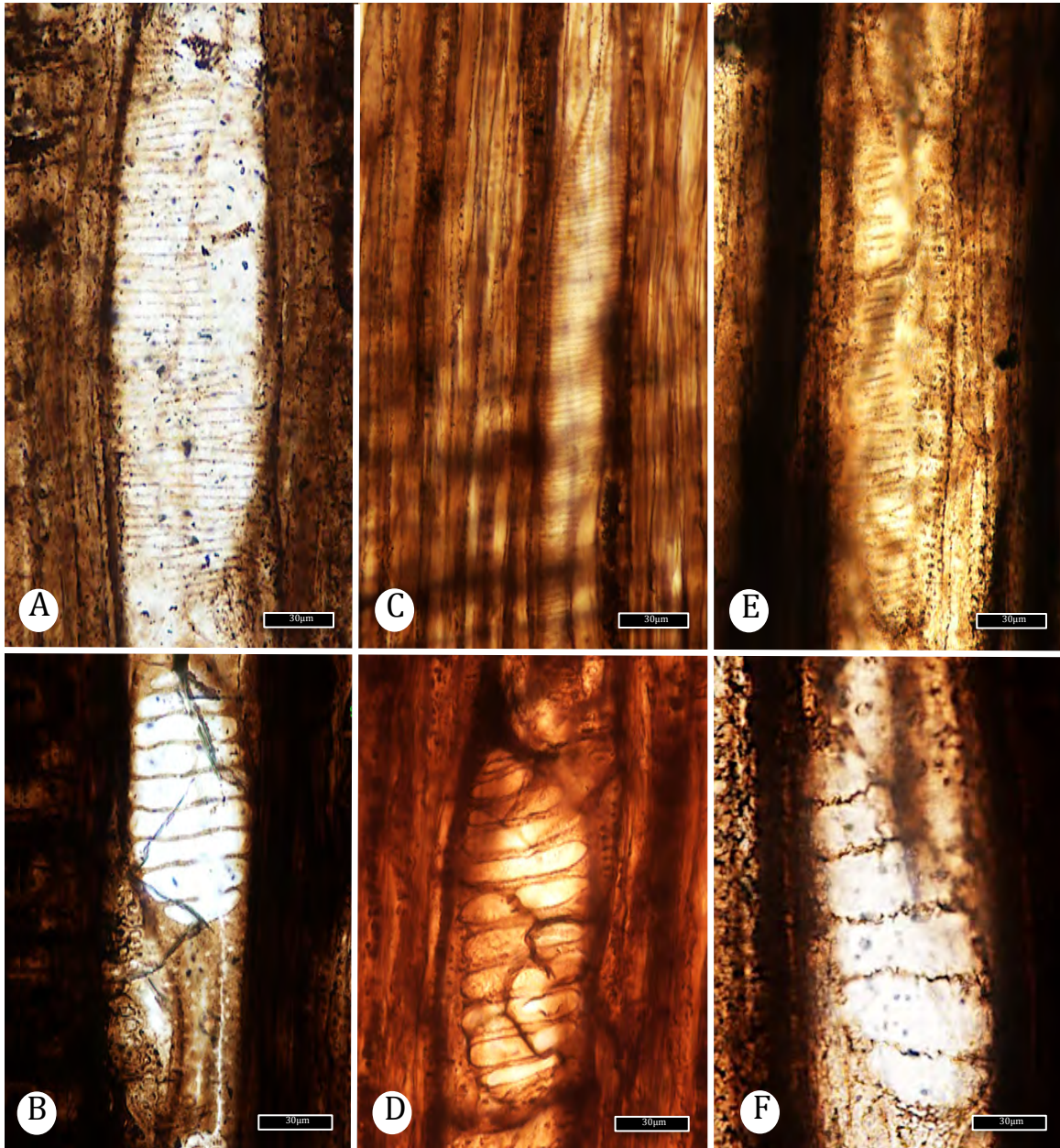


Figure 2.13. Unexplained fine bars silhouetted against vessels. A, C, E: Examples of “fine, horizontal lines” observed to cover the entire surface of some vessels that are not interpreted as helical thickenings, coalesced opposite intervessel pits or perforation plates, but for which there is not a clear explanation. B, D, F: Typical perforation plates for the specimens illustrated in A, C, and E. – A: TLS. TXSTATE 1268, R-3. – B: Typical perforation plate for specimen TXSTATE 1268, R-3. – C: TLS. TXSTATE 1274, R-5. – D: RLS: Typical perforation plate for specimen TXSTATE 1274, R-5. – E: RLS. TXSTATE 1203, S6. – F: RLS. Typical perforation plate for specimen TXSTATE 1203, S2. All scale bars = 30 µm.

## REFERENCES

- Amato JM, Mack GH, Jonell TN, Seager WR, Upchurch GR. 2017. Onset of the Laramide orogeny and associated magmatism in southern New Mexico based on U-Pb geochronology. *GSA Bull.* 129: 1209–1226.
- Andreánszky G. 1951. Der versteinerte Wald von Mikofalva und einige andere verkieselte Baumstämme aus Ungarn. *Ann. Biol. Univ. Hung.* 1: 15–24.
- Baas P. 1969. Comparative anatomy of *Platanus kerrii* Gagnep. *Bot. J. Soc.* 62: 413–421.
- Barghoorn ES. 1940. The ontogenetic development and phylogenetic specialization of rays in the xylem of dicotyledons. I. The primitive ray structure. *Am. J. Bot.* 27: 918–928.
- Barghoorn ES. 1941. The ontogenetic development and phylogenetic specialization of rays in the xylem of dicotyledons. II. Modification of the multiseriate and uniseriate rays. *Am. J. Bot.* 28: 273–282.
- Brett DW. 1972. Fossil Wood of *Platanus* from the British Eocene. *Palaeontology* 15: 496–500.
- Brush WD. 1917. Distinguishing characters of North American sycamore woods. *Bot. Gaz.* 64: 480–496.
- Camacho Uribe D. 1988. *La madera: estudio anatómico y catálogo de especies mexicanas* 168. Dirección de Restauración del Patrimonio Cultural, Instituto Nacional de Antropología e Historia.

- Cantino PD, Doyle JA, Graham SW, Judd WS, Olmstead RG, Soltis DE, Soltis PS, Donoghue MJ. 2007. Towards a phylogenetic nomenclature of *Tracheophyta*. *Taxon*. 56: 1E–44E.
- Carlquist S. 2007. Bordered pits in ray cells and axial parenchyma: the histology of conduction, storage, and strength in living wood cells. *Bot. J. Linn. Soc.* 153: 157–168.
- Chase MW, Christenhusz MJM, Fay MF, Byng JW, Judd WS, Soltis DE, Soltis PS, Stevens PF, Stevens PF. 2016. An update of the Angiosperm Phylogeny Group classification for the orders and families of flowering plants: APG IV. *Bot. J. Linn. Soc.* 181: 1–20.
- Chen J, Craven LA. 2007. Flora of China. *Flora of China* 13: 321–328.
- Crane PR. 1989. Paleobotanical evidence on the early radiation of nonmagnoliid dicotyledons. In *Woody plants—evolution and distribution since the Tertiary* (pp. 165–191). Springer, Vienna.
- Crane PR, Pedersen KR, Friis EM, Drinnan AN. 1993. Early Cretaceous (early to middle Albian) platanoid inflorescences associated with *Sapindopsis* leaves from the Potomac Group of eastern North America. *Sys. Bot.* 18: 328–344.
- Crawley M. 1989. Dicotyledonous wood from the lower Tertiary of Britain. *Palaeontology*. 32: 597–622.
- Crawley M. 2001. Angiosperm Woods from British Lower Cretaceous and Palaeogene Deposits. Special Papers in Palaeontology 66. The Palaeontological Association, 100 pp.

- Endlicher S. 1840. *Genera Plantarum Secundum Ordines Naturales Disposita*, Volume I. Suppl. II, Appendix, S. 100 bis 102. Wien. 1942.
- Estrada-Ruiz E, Upchurch GR, Wheeler EA, Mack GH. 2012a. Late Cretaceous angiosperm woods from the Crevasse Canyon and McRae formations, south-central New Mexico, USA: part 1. *Intern. J. Plant Sci.* 173: 412–428.
- Estrada-Ruiz E, Parrott JM, Upchurch GR, Wheeler EA, Thompson DL, Mack G, Mindy MM. 2012b. The wood flora from the Upper Cretaceous Crevasse Canyon and McRae formations, south-central New Mexico, USA: A progress report. In *New Mexico Geological Society Guidebook, 63rd Field Conference, Warm Springs Region*. 503–518.
- Feng Y, Oh SH, Manos PS. 2005. Phylogeny and historical biogeography of the genus *Platanus* as inferred from nuclear and chloroplast DNA. *Sys. Bot.* 30: 786–799.
- Friis E M, Crane PR. 1989. Reproductive structures of Cretaceous Hamamelidae. *Crane, P, R., Blackmore, S ed (s). Evolution, systematics, and fossil history of the Hamamelidae 1*, 155–74.
- Friis EM, Crane PR, Pedersen KR. 2011. *Early flowers and angiosperm evolution*. Cambridge University Press, Oxford.
- Gillette DD, Wolbert DB, Hunt AP. 1986. *Tyrannosaurus rex* from the McRae Formation (Lancian, Upper Cretaceous), Elephant Butte Reservoir, Sierra County, New Mexico. *New Mexico Geological Society Guidebook, 37th Field Conference, Truth or Consequences*. 235–238.

- Gregory M, Poole I, Wheeler EA. 2009. Fossil dicot wood names - an annotated list with full bibliography. *IAWA J. Suppl.* 6: 1–220.
- Grimm GW, Denk T. 2007. ITS evolution in *Platanus* (Platanaceae): homoeologues, pseudogenes and ancient hybridization. *Ann. Bot.* 101: 403–419.
- Herendeen PS, Wheeler EA, Baas P. 1999. Angiosperm wood evolution and the potential contribution of paleontological data. *Bot. Review.* 65: 278–300.
- Hofmann E. 1952. Pflanzenreste aus dem Phosphoritvorkommen von Prambachkirchen in Oberösterreich. II. Teil, *Palaeontographica*, 92 B, 121–182.
- InsideWood. 2004-onwards. Published on the Internet:  
<http://insidewood.lib.ncsu.edu/search> [accessed August 7, 2018].
- Johnson KR. 1996. Description of seven common plant megafossils from the Hell Creek Formation (Late Cretaceous: late Maastrichtian), North Dakota, South Dakota, and Montana. In *Proceedings of the Denver Museum of Natural History, series 3*: 1–48.
- Kårehed J. 2001. Multiple origin of the tropical forest tree family Icacinaceae. *Am. J. Bot.* 88: 2259–2274.
- Kribs DA. 1935. Salient lines of structural specialization in the wood rays of dicotyledons. *Bot. Gaz.* 96: 547–557.
- Lens F, Kårehed J, Baas P, Jansen S, Rabaey D, Huysmans S, Hamann T, Smets E. 2008. The wood anatomy of the polyphyletic Icacinaceae s.l. and their relationships within asterids. *Taxon.* 57: 525–552.

- Lozinsky RP, Hunt AP, Wolberg DL, Lucas SG. 1984. Late Cretaceous (Lancian) dinosaurs from the McRae Formation, Sierra County, New Mexico. *N. M. Geol.* 6: 72–77.
- Lucas SG, Mack GH, Estep JW. 1998. The ceratopsian dinosaur *Torosaurus* from the Upper Cretaceous McRae Formation, Sierra County, New Mexico. In *Las Cruces Country II, New Mexico Geological Society, 49th Annual Field Conference Guidebook*, 223–227.
- Mabberley DJ. 2008. *Mabberley's plant-book: a portable dictionary of plants, their classifications and uses* (No. Ed. 3). Cambridge University Press.
- Magallón-Puebla S, Herendeen PS, Crane PR. 1997. *Quadriplatanus georgianus* gen. et sp. nov.: staminate and pistillate platanaceous flowers from the Late Cretaceous (Coniacian-Santonian) of Georgia, USA. *Intern. J. Plant Sci.* 158: 373–394.
- Manchester SR. 1986. Vegetative and reproductive morphology of an extinct plane tree (Platanaceae) from the Eocene of western North America. *Bot. Gaz.* 147: 200–226.
- Meijer JFF. 2000. Fossil woods from the Late Cretaceous Aachen Formation. *Rev. Palaeobot. Palynol.* 112: 297–336.
- Metcalfe CR, Chalk L. 1950. *Anatomy of the Dicotyledons*. Vols. 1 & 2. Clarendon Press, Oxford.
- Meylan BA, Butterfield BG. 1975. Occurrence of simple, multiple, and combination perforation plates in the vessels of New Zealand woods. *New Zealand J. Bot.* 13: 1–18.

- Molenaar CM. 1983. Major depositional cycles and regional correlations of Upper Cretaceous rocks, southern Colorado Plateau and adjacent areas. *Rocky Mountain Section (SEPM)*.
- Nixon KC, Poole JM. 2003. Revision of the Mexican and Guatemalan species of *Platanus* (Platanaceae). *Lundellia* 6: 103–137.
- Page VM. 1968. Angiosperm wood from the Upper Cretaceous of Central California: Part II. *Am. J. Bot.* 55: 168–172.
- Page VM. 1970. Angiosperm wood from the Upper Cretaceous of central California. III. *Am. J. Bot.* 57: 1139–1144.
- Page VM. 1980. Dicotyledonous wood from the Upper Cretaceous of central California, II. *J. Arnold Arbor.* 61: 723–748.
- Panshin AJ, Zeeuw CD. 1980. *Textbook of wood technology*. McGraw-Hill Book Co.
- Pedersen KR, Friis EM, Crane PR, Drinnan AN. 1994. Reproductive structures of an extinct platanoid from the Early Cretaceous (latest Albian) of eastern North America. *Rev. Palaeobot. Palynol.* 80: 291–303.
- Prakash U, Barghoorn ES. 1961. Miocene fossil woods from the Columbia Basalts of central Washington. *J. Arnold Arbor.* 42: 165–203.
- Prakash U, Březinová D, Bužek C. 1971. Fossil woods from the Doupovské hory and České stredohorí Mountains in Northern Bohemia. *Palaeontographica B.* 133: 103–28.
- Roberts LNR, Kirschbaum MA. 1995. Paleogeography of the Late Cretaceous of the Western Interior of Middle North America—coal distribution and sediment accumulation: U. S. Geological Survey, Professional Paper 1561: 116.

- Scott RA, Barghoorn ES. 1955. The occurrence of *Euptelea* in the Cenozoic of Western North America. *J. Arnold Arbor.* 36: 259–265.
- Scott RA, Wheeler EA. 1982. Fossil woods from the Eocene Clarno Formation of Oregon. *IAWA Bull.* 3: 135–154.
- Seager WR, Mack GH, Raimonde MS, Ryan RG. 1986. Laramide basement-cored uplift and basins in south-central New Mexico. *Truth or Consequences Region New Mexico. NM Geol. Soc. Guide.* 37: 123–130.
- Seager WR, Mack GH, Lawton TF. 1997. Structural kinematics and depositional history of a Laramide uplift-basin pair in southern New Mexico: Implications for development of intraforeland basins. *Geol. Soc. Am. Bull.* 109: 1389–1401.
- Stevens PF. 2001 onwards. Angiosperm Phylogeny Website. Version 14, July 2017 [and more or less continuously updated since].
- Stull GW, Duno de Stefano R, Soltis DE, Soltis PS. 2015. Resolving basal lamiid phylogeny and the circumscription of Icacinaceae with a plastome-scale data set. *Am. J. Bot.* 102: 1794–1813.
- Süss H. 2007. Holzfossilien der Morphogattung *Spiroplatanoxylon* gen. nov. aus dem Tertiär von Europa und Vorderasien, *Feddes Repert.* 118: 1–19.
- Süss H, Müller-Stoll WR. 1977. Untersuchungen über fossile platanenhölzer beiträge zu einer monographie der gattung *Platanoxylon* Andreánszky. *Feddes Repert.* 88: 1–62.
- Suzuki M. 1976. Some fossil woods from the Palaeogene of northern Kyushu. *The botanical magazine= Shokubutsu-gaku-zasshi* 89: 59–71.

- Takahashi KI, Suzuki M. 2003. Dicotyledonous fossil wood flora and early evolution of wood characters in the Cretaceous of Hokkaido, Japan. *IAWA J.* 24: 269–309.
- Turland NJ, Wiersema JH, Barrie FR, Greuter W, Hawksworth DL, Herendeen PS, Knapp S, Kusber W-H, Li D-Z, Marhold K, May TW, McNeill J, Monro AM, Prado J, Price MJ, Smith GF (eds.) 2018: International Code of Nomenclature for algae, fungi, and plants (Shenzhen Code) adopted by the Nineteenth International Botanical Congress Shenzhen, China, July 2017. *Regnum Vegetabile* 159. Glashütten: Koeltz Botanical Books. DOI <https://doi.org/10.12705/Code.2018>
- Unger F. 1847. *Chloris protogaea: Beiträge zur Flora der Vorwelt.* in Commission bei Wilhelm Engelmann.
- Upchurch GR, Mack GH. 1998. Latest Cretaceous leaf megafloras from the Jose Creek Member, McRae Formation of New Mexico. *N. M. Geol. Soc. Guide.* 49: 209–222.
- Upchurch GR, Kiehl J, Shields C, Scherer J, Scotese C. 2015. Latitudinal temperature gradients and high-latitude temperatures during the latest Cretaceous: congruence of geologic data and climate models. *Geology* 43: 683–686. Supplementary material: GSA Data Repository item 2015238.
- Vater H. 1884. Die fossilen Hölzer der Phosphoritlager des Herzogtums Braunschweig. *Zeitschrift der Deutschen Geologischen Gesellschaft*, 783–853.

- Wheeler EA. 1991. Paleocene dicotyledonous trees from Big Bend National Park, Texas: variability in wood types common in the Late Cretaceous and Early Tertiary, and ecological inferences. *Am. J. Bot.* 658–671.
- Wheeler EA. 1995. Wood of *Platanus kerrii*. *IAWA J.* 16: 127–132.
- Wheeler EA. 2011. Inside Wood—A web resource for hardwood anatomy. *IAWA J.* 32: 199–211.
- Wheeler EA, Baas P, Gasson PE. 1989. IAWA list of microscopic features for hardwood identification. *IAWA Bull.* n.s. 10: 219–332.
- Wheeler EA, Baas P. 1991. A survey of the fossil record for dicotyledonous wood and its significance for evolutionary and ecological wood anatomy. *IAWA Bull.* n.s. 12: 275–332.
- Wheeler EA, Lehman TM. 2000. Late Cretaceous woody dicots from the Aguja and Javelina Formations, Big Bend National Park, Texas, USA. *IAWA J.* 21: 83–120.
- Wheeler EA, Manchester SR. 2002. Woods of the middle Eocene nut beds flora, Clarno Formation, Oregon, USA. *IAWA J. Suppl.* 3, 1–188.
- Wheeler EA, McClammer J, LaPasha CA. 1995. Similarities and differences in dicotyledonous woods of the Cretaceous and Paleocene. San Juan Basin, New Mexico, USA. *IAWA J.* 16: 223–254.
- Wolberg DL, Lozinsky RP, Hunt AP. 1986. Late Cretaceous (Maastrichtian-Lancian) vertebrate paleontology of the McRae Formation, Elephant Butte area, Sierra County, New Mexico. *N. M. Geol. Soc. Guide.* 37, 227–334.

### III. THE ANGIOSPERM WOOD FLORA OF THE UPPER CRETACEOUS (CAMPANIAN) MCRÆ FORMATION, SOUTH-CENTRAL NEW MEXICO: DIVERSITY AND SIGNIFICANCE

#### ABSTRACT

The Jose Creek Member of the McRae Formation, south-central New Mexico, preserves a diverse angiosperm flora of Late Campanian (76.5 to >72.5 Ma) age. This flora is of special interest because it provides an abundance of fossil evidence in the form of leaves, reproductive structures, and silicified woods found *in situ* and as float. The wood flora, as currently understood, is one of the three most diverse Cretaceous wood floras in the world, and the only one where the majority of wood types represent mature wood. To date, thirty-four species of non-monocot angiosperms have been recognized, representing both members of the magnoliid clade and eudicots. Many of the McRae xylo types are common elements in other Cretaceous wood assemblages. Most magnoliids represent Lauraceae (~seven wood types), a dominant element in modern Asian tropical and subtropical vegetation. Two genera (*Agujoxylon* and *Metcalfexylon*) with exclusively scalariform perforation plates co-occur in assemblages from the southwest of North America. Four wide-rayed *Platanus*-like types (see Chapter 2) have a combination of wood anatomical features considered ancestral to extant Platanaceae (e.g., exclusively solitary vessels and scalariform perforation plates), warranting a new genus. An assemblage of exceptionally large angiosperms (Forest of Giants) consisting of *in situ* stumps and logs (four wood types) is dominated by one species of *Paraphyllanthoxylon*, with one stump being the largest Cretaceous angiosperm yet recorded worldwide (2 m in diameter at the top of the buttress roots). The

remaining three wood types (representing Lauraceae, Sapotaceae and cf. Rosales, possibly relating to Cannabaceae? Moraceae? or Urticaceae?) are represented by individual stumps (see Chapter 1). The affinities of most woods with simple perforation plates are, as yet, unidentified. The McRae Formation flora provides unique insight into the stature and diversification of angiosperms at a critical period in their radiation.

*Keywords* – South-central New Mexico, McRae Formation, Jose Creek Member, Campanian, Cretaceous, fossil angiosperm wood.

## INTRODUCTION

Reports of fossils from the McRae Formation of south-central New Mexico, USA, are found in Lee's 1906 description of the Engle coal region in which he recounts the discovery of *Triceratops* remains in "red strata" above the coal beds, a reference to the Hall Lake Member of the McRae Formation. Neither leaf nor wood megafossils have been observed in association with the dinosaur bones, to date, and the only record of vegetation from the Hall Lake Member is of concretions representing possible coprolites (Upchurch et al. 2012). In sharp contrast to the Hall Lake Member, Lee mentioned large quantities of petrified wood in the layers below the dinosaur-bearing layer, corresponding to the Jose Creek Member, the lower unit of the McRae Formation. Lozinsky et al. (1984) also noted the abundance of petrified wood in the Jose Creek Member, sometimes as *in situ* stumps  $\pm$  1 m in diameter, along with leaf remains in the finer grained sediments. Subsequent exploration of Jose Creek localities in the mid-1980's by Greg Mack and early 1990's by Garland Upchurch and Greg Mack confirmed the accessibility of well-preserved plant

megafossils and yielded fossil collections that were the basis of the first reports of the the leaf and wood floras of the McRae Formation (Upchurch and Mack 1998, Estrada-Ruiz et al. 2011, 2012a, 2012b, 2018). More recent fieldwork (2012–2016) by members of the Upchurch lab added substantially to the silicified wood specimen collection, resulting in the wood flora described in this work.

The emerging profile is that of a diverse wood flora for the Jose Creek Member, composed of angiosperms and conifers found in varying combinations, including one locality with exclusively large angiosperms and others with a mixture of angiosperms (dicot and monocot) and conifers. The wood flora is significant not only for its diversity, but also for the high quality of preservation of the wood specimens and the high percentage of mature specimens (approximately 70% with stem diameter >10 cm). It represents a major wood flora described from a southern Western Interior locality well inland from the Western Interior Seaway, the value of which is enhanced by the presence of an extensive leaf flora, reproductive structures and multiple sources of evidence on paleoclimate (paleosols, palm wood fossils and statistically significant samples of dicot silicified wood xylotypes and leaf impression). Radiometric dating of volcanic ashes and a volcanic clast indicate a Late Campanian age of 76.5 – 72.5 Ma (Amato et al. 2017).

This report summarizes current understanding of the Jose Creek wood flora (Fig. 3.1). Reference is made to seven published McRae angiosperm woods (Estrada-Ruiz et al. 2012a, 2012b, 2018). Chapter 2 of this dissertation considers ten specimens with “wide rays” that were sorted into four xylotypes, two of which were previously described informally (Estrada-Ruiz et al. 2012a, 2012b) and two of

which are new xyloids, all of which will be assigned to a new genus in Platanaceae. Chapter 1 of this dissertation pertains to a large assemblage of very large *in situ* stumps and logs dubbed the Forest of Giants that yielded four xyloids, all with exclusively simple perforation plates. The majority of stumps and logs at the Forest of Giants are *Paraphyllanthoxylon*-like with probable affinity to Kirkiaceae. Individual stumps are tentatively assigned to Lauraceae Sapotaceae, and Rosales (with characteristics of the families Cannabaceae, Moraceae and Urticaceae).

Described and illustrated in this chapter are nineteen additional xyloids of angiosperm wood from the Jose Creek Member, including four woods tentatively assigned to Lauraceae, specimens identified as *Agujoxylon olacaceoides* Wheeler and Lehman (2000), *Metcalfeoxylon kirtlandense* Wheeler, McClammer and LaPasha (1995), and a wood with “rays of two sizes” compared to the type species of *Ilacinoxylon*. Three additional xyloids with exclusively scalariform perforation plates remain unassigned to genus. A single Jose Creek specimen with both simple and scalariform perforation plates remains unassigned to genus. Among the woods with exclusively simple perforation plates, there is a new species of *Fulleroxylon* Estrada-Ruiz, Upchurch, Wheeler and Mack (2012b) and seven xyloids that are unassigned to family or genus.

## GEOLOGIC SETTING

This study is based on fossil angiosperm woods collected at various sites in the Jose Creek Member of the McRae Formation (Late Campanian), which is currently exposed in the northwestern part of the Love Ranch Basin (Amato et al. 2017, Seager et al. 1997, Seager et al. 1986) in the southern San Andres Mountains near

Truth or Consequences, New Mexico (Mack et al. 1998). During the Cretaceous, the site was situated approximately 200 km inland from the Western Interior Seaway at an estimated 39° paleolatitude in an alluvial plain to piedmont environment (Roberts and Kirschbaum 1995; Estrada-Ruiz et al. 2012b).

The McRae Formation is fluvial in origin and consists of volcanic sediments, with some localized areas of granite and Precambrian quartzite clasts (Seager et al. 1997, Amato et al. 2017). The formation is divided into an upper Hall Lake Member and a lower Jose Creek Member (Seager et al. 1997; Mack et al. 1998). The virtual absence of fossil plant materials in the Hall Lake Member has been attributed to semi-arid conditions, as indicated by the predominantly calcic paleosols and an abundance of oxidized iron (Mack et al. 1998), conditions that may have limited fossilization opportunities (Upchurch and Mack 1998). To date, the plant fossil record for the Hall Lake is limited to concretions that possibly represent coprolites (Upchurch et al. 2012). In contrast, the strata of the lower Jose Creek Member are a rich source of fossil angiosperm and conifer woods, found both as *in situ* stumps and float material. Volcanic sediments are thought to have contributed to the high quality of preservation observed in much of the study material by providing a ready source of silica integral to the preservation of these fossil angiosperm woods.

The age of the McRae Formation was first estimated after the discovery of Lancian age dinosaur fossils in the Hall Lake Member, the presence of which constrained the minimum age of the underlying Jose Creek Member to late Maastrichtian (Lozinsky et al. 1984, Gillette et al. 1986, Lucas et al. 1998, Upchurch and Mack 1998). Uncertainty as to the exact stratigraphic position of dinosaur

fossils within the Hall Lake Member contributed to uncertainty of the age estimate (Upchurch and Mack 1998). A more precise age has been derived from U-Pb dates obtained from zircon crystals found in volcanic ash beds, one in the basal Hall Lake Member and three in the middle to upper Jose Creek Member, as well as a volcanic clast from the base of the Jose Creek Member. Together these dates give an age range for the Jose Creek Member of 76.5–72.5 Ma (statistical uncertainty  $\pm 2 \sigma$ ) (Amato et al. 2017) which indicates a Late Campanian age for the Jose Creek Member.

## MATERIALS AND METHODS

Fieldwork protocol for collecting wood specimens included labeling each specimen and specimen bag with the collection site number and collection date. A GPS sequence number (allowing later retrieval of coordinates) was recorded on the collection bag and in a notebook along with measurements of stumps or logs. Metal tags were affixed aside stumps and logs for future identification. Photographs of stumps and logs included a written notation of the collection locality and date.

Each permineralized specimen was assessed for quality of preservation. Stem diameter of *in situ* stumps and log segments were measured in the field. Measurements cannot reflect the outermost portions of specimens that were not preserved. Minimum stem diameter of small axes with intact pith collected as float were estimated by measuring along the longest ray observed in transverse view and then multiplying by two. Where float specimens represented fragments of larger axes, the minimum diameter was calculated by measuring on a transverse surface along widely separated rays to the point where the rays would converge and

doubling that estimated radius. It is likely that estimates understate the source tree diameter because the amount of material beyond the radial position of a specimen cannot be determined, so the actual diameter of the source tree could be substantially larger than the estimate. Slides were prepared from the most mature wood available that was likely to provide anatomical information. Transverse (X), tangential (T) and radial (R) block faces were affixed to slides with Norland Optical Adhesive 72 by curing the adhesive in UV light for approximately 16 hours. Excess fossil material was removed with a Hillquist Thin Section Machine and final slide thickness achieved by polishing with 320-400 grit powder. Coverslips were affixed with the same Norland Optical Adhesive 72 to maximize resolution. Slides were labeled as to the type and sequence of the cut (e.g., T-1, T-2; R-1; X-1), and a unique identifier (i.e., collection site and specimen number). A sequential "TXSTATE" number was assigned to specimens found to have preservation adequate for study. Measurements and photographs of anatomical features were taken with a Nikon Eclipse 50i microscope and a Nikon DS-Fi1 camera head and Nikon DS-L2 camera control unit. Recommendations of an International Association of Wood Anatomists Committee (1989) were followed as to the collection of anatomical data. Specimens and locality data are archived in the Texas State University Paleobotanical Collections. Exact locations of collection sites are not indicated because the localities are on private land and because looting of fossil wood is common in the American southwest.

The term xylotype is used in reference to these woods in much the same way that leaves and seeds are informally called morphotypes while they are being

studied. Like morphotypes, a xylo type represents a combination of diagnostic anatomical features thought to delimit a potential species and differentiated from other woods under consideration until such time as the wood is identified as a known species or formally recognized as a new species. The specimen that best illustrates the anatomical features of the xylo type is designated as the holoxylo type. The term paraxylo type is used for specimens examined and cited in the description as representing the same taxon. Observations of paraxylo type anatomy were used to confirm a holoxylo type anatomical feature or to complete the description when a feature was not observed in the holoxylo type.

This report includes descriptions and illustrations for previously unreported xylo types, with tentative identification of select, readily recognizable specimens and specimens for which an InsideWood database search was undertaken. Identification and naming of all unknown specimens is beyond the scope of this dissertation. The systematic search for affinity for the remaining specimens using the InsideWood database (InsideWood 2004–onward, Wheeler 2011) and the literature will be conducted in the future. Formal identifications will be proposed in journal articles to assure valid publication in compliance with the International Code of Nomenclature for algae, fungi and plants (Turland et al. 2018). Herein, woods are referred to by their TXSTATE accession number, and are organized into groups with shared anatomical features as illustrated below. The organizational scheme utilizes some of the same anatomical features used by Page (1979) (e.g., perforation plate type, vessel grouping, axial parenchyma pattern). It differs from Page in that the format reflects anatomical features relevant to specific groups of McRae xylo types.

Names of formal taxonomic groups and major clades follow APG IV (Chase et al. 2016) and Cantino et al. (2007).

#### ORGANIZATION OF MCRAE FORMATION ANGIOSPERM WOODS

McRae Group I: Idioblasts (probable oil cells) present

1. Group IA: Simple perforation plates, axial parenchyma scanty paratracheal
  - a. Vessel-ray pitting with reduced borders, round to oval to horizontally elongate
    - *Laurinoxylon* sp. 1, McRae Group IA sp. 1 TXSTATE 1250
    - *Laurinoxylon* sp. 2, McRae Group IA sp. 2 TXSTATE 1251
    - *Pygmaeoxyton paucipora* Estrada-Ruiz, Upchurch, Wheeler and Mack (2012b)
  - b. Vessel-ray parenchyma pitting of two types - 1) large, simple, 2) reduced border oval to elongate, horizontal, diagonal or curved
    - *Laurinoxylon* sp. 3, McRae Group IA sp. 3 TXSTATE 1252–1253
    - *Laurinoxylon* sp. 4, McRae Group IA sp. 4 TXSTATE 1254
2. Group IB: Simple perforation plates, axial parenchyma aliform to confluent
  - McRae Group IB sp. 1 TXSTATE 1255–1256
3. Group IC: Simple and scalariform perforation plates
  - *Laurinoxylon rennerae* Estrada-Ruiz, Wheeler, Upchurch and Mack (2018)

McRae Groups II, III, and IV: Idioblasts absent

McRae Group II: Exclusively scalariform perforation plates

1. Group IIA: Rays < 10 cells wide
  - a. Axial parenchyma common
    - i. Vessel-ray parenchyma pits of two types
      - *Agujoxylon olacaceoides* TXSTATE 1257
    - ii. Vessel-ray parenchyma pits of one type, small
      - McRae Group IIA sp. 1 TXSTATE 1259
      - McRae Group IIA sp. 2 TXSTATE 1260
      - *Metcalfexylon kirtlandense* TXSTATE 1261
  - b. Axial parenchyma not common
    - McRae Group IIA sp. 3 TXSTATE 1262–1264
    - *Turneroxylon newmexicoensis* Estrada-Ruiz, Wheeler, Upchurch and Mack (2018)
    - *Baasia armendarisense* Estrada-Ruiz, Upchurch, Wheeler and Mack (2012b)
    - McRae Angiosperm Wood Type 1 Estrada-Ruiz, Upchurch, Wheeler and Mack (2012b, 2018)
2. Group IIB: Rays >10 cells wide
  - a. Uniseriate rays common (rays of two sizes)
    - Cf. *Icacinoxylon* sp. 1 TXSTATE 1265–1266
  - b. Uniseriate rays few or absent (Platanaceae)
    - McRae Group IIB sp. 1 TXSTATE 1212, 1267–1270
    - McRae Group IIB sp. 2 TXSTATE 1203, 1271–1272
    - McRae Group IIB sp. 3 TXSTATE 1273

- McRae Group IIB sp. 4 TXSTATE 1274

McRae Group III: Exclusively simple perforation plates

1. Group IIIA: Vessels exclusively solitary

a. Axial parenchyma rare, vasicentric tracheids, rays 1-2 seriate

i. Vessels diameter >100  $\mu\text{m}$ , septate fibers

- *Fulleroxylon armendarisense* Estrada-Ruiz, Upchurch, Wheeler, et Mack (2012b)
- *Fulleroxylon* sp. 1 TXSTATE 1275–1277

ii. Vessels diameter <100  $\mu\text{m}$ , non-septate fibers

- *Mcraeoxyton waddellii* Estrada-Ruiz, Wheeler, Upchurch, et Mack (2018)
- McRae Group IIIA sp. 1 TXSTATE 1278

b. Axial parenchyma common, vasicentric tracheids not present

i. Rays >10 cells wide

- McRae Group IIIA sp. 2 TXSTATE 1279

ii. Rays <10 cells wide

- McRae Group IIIA sp. 3 TXSTATE 1280
- McRae Group IIIA sp. 4 TXSTATE 1281–1282

2. Group IIIB: Vessels both solitary and in radial multiples

a. Axial parenchyma rare to scanty paratracheal

- McRae Group IIIB sp. 1 TXSTATE 1283
- McRae Group IIIB sp. 2 TXSTATE 1284–1285
- McRae Group IIIB sp. 6 TXSTATE 1230–1246

b. Axial parenchyma common (vasicentric to lozenge-aliform)

- McRae Group IIIB sp. 3 TXSTATE 1286
- McRae Group IIIB sp. 4 TXSTATE 1287
- McRae Group IIIB sp. 5 TXSTATE 1288

McRae Group IV: Simple and scalariform perforation plates in the same wood

- McRae Group IV sp. 1 TXSTATE 1289

#### SYSTEMATIC DESCRIPTIONS

##### **McRae Group I: Idioblasts (probable oil cells) present**

There are four xylootypes that have idioblasts presumed to be oil cells, simple perforation plates, alternate intervessel pits, rays typically <10 cells in width and no laticifers or tanniferous tubes, a combination of anatomical features typical of Lauraceae. A fifth wood (TXSTATE 1250 from the Forest of Giants) with these features is described in Chapter 1 (Table 3.1). The woods are presented as xylootypes new to the McRae. Analysis of and search for affinities is ongoing, and it has not yet been determined if they represent new species or can be assigned to existing species. Many species (~ 100) of lauraceous fossil woods have been described; detailed comparisons to all of them is beyond the scope of this dissertation (see lists of Süß and Mädler 1958, Dupéron-Laudoueneix and Dupéron 2005, Gregory et al. 2009). Three of these woods, as well as the Forest of Giants xylotype, are tentatively placed in the form genus *Laurinoxylon* because the generic diagnosis, as emended by Dupéron et al. (2008), is sufficiently broad to encompass a wide range of anatomical features consistent with numerous extant genera without

phylogenetic inference. In addition to these new McRae Group I types, two McRae woods with idioblasts were described previously. *Pygmaeoxyton paucipora* Estrada-Ruiz, Upchurch, Wheeler and Mack (2012b) falls within Group IA with the “axial parenchyma scanty paratracheal – vessel-ray pitting Richter Type II” xylotypes and *Laurinoxylon rennerae* Estrada-Ruiz, Wheeler, Upchurch and Mack (2018) is the sole representative of Group IC, a wood with both simple and scalariform perforation plates.

Group I is characterized by diffuse porous wood without growth boundaries, exclusively simple perforation plates and uniseriate rays absent or very rare. The size, frequency and position of idioblasts varies, but their presence was confirmed in both tangential and radial views for all xylotypes. There are differences in the volume and distribution of axial parenchyma, the type of vessel-ray parenchyma pitting, intervessel pit size, vessel diameter and the presence or absence of septate fibers.

**Group IA: Axial parenchyma scanty paratracheal**

**a. Vessel-ray pitting with reduced borders, round to oval to horizontally elongate (Richter Type II)**

*Clade* – Magnoliids

*Order* – Laurales

*Family* – Lauraceae

*Genus* – *Laurinoxylon* Felix

*Species* – *Laurinoxylon* sp. 2, McRae Group IA sp. 2

*Holoxylotype* – TXSTATE 1251 (Fig. 3.2–3.3).

*Stratigraphic horizon* – McRae Formation, Jose Creek Member

*Age* – Late Campanian

*Material* – Estimated minimum stem diameter of 20 cm, collected as float

*Locality* – Texas State University Paleobotanical Locality 2014-12

*Description* – *Growth rings* absent. *Wood* diffuse porous. *Vessels* solitary (47%) and in radial multiples of 2–3 (up to 4) (Fig. 3.2A), mean 18 (SD 9, range 7–34)/mm<sup>2</sup>, average tangential diameter 65 (SD 15, range 37–81) µm; average vessel element length 266 (SD 66, range 163–388) µm (Fig. 3.2B); perforation plates simple (Fig. 3.2B,C); intervessel pits alternate, polygonal in outline (Fig. 3.2B, D), minute to small, 3–6 µm in diameter. *Vessel-ray pits* with reduced borders, round to horizontal or vertical elongate, some curved, several per cell (Richter Type II) (Richter 1981) (Fig. 3.2E, F). *Tyloses* not common, thin-walled, bubble-like. *Fibers* septate (Fig. 3.2G) and non-septate, angular in cross section, thin-walled to thick-walled, pits not observed. *Axial parenchyma* scanty paratracheal to narrow vasicentric (Fig. 3.2H), 2–8 cells per parenchyma strand (Fig. 3.2I, 3.3A). *Rays* (2) 3–6 (mostly 5) seriate (Fig. 3.3B), multiseriate rays homocellular composed of procumbent cells or heterocellular with 1 to several margin rows composed of square cells (Fig. 3.3C, D), sometimes intermixed with oil cells (Fig. 3.3D), or sometimes large procumbent cells (Fig. 3.3E), some short rays composed of primarily square or upright cells (Fig. 3.3F); ray height average 22 (SD 10, range 5–45) cells or average 336 (SD 61, range 69–676) µm high; average 13 (SD 3, range 8–16) per mm; uniseriate rays not observed. *Oil cells* only slightly larger than typical

ray cells along the side of ray (Fig. 3.3G), at the ray margin (Fig. 3.3H) or nested within the rays (Fig. 3.3H-I).

*Description in IAWA Hardwood List codes (IAWA Committee 1989):*

2 5 13 22 23v 24 25 31 32 41 47 52 56 65 66 69 78 79v 98 104v 105v 106 115 116  
124

*Remarks* – This wood is the second Group IA wood with Type II vessel-ray pitting. It differs from TXSTATE 1250 (described in Chapter 1) by having more solitary vessels, narrower vessels, higher vessel density, minute to small intervessel pitting, shorter rays, marginal rows composed of square cells and usually smaller oil cells, which, at times, occur at the sides of rays as seen in tangential view.

**Group IA: Axial parenchyma scanty paratracheal,**

**b. Vessel-ray pitting of two types - 1) reduced border oval to elongate, horizontal, diagonal or curved (Richter Type II), 2) large, simple**

Two woods in Group IA have vessel-ray pitting of two types, 1) Richter Type II where pits are reduced bordered to simple, round to oval, elongated (horizontally or diagonally) to kidney shaped, and 2) large simple pits that individually fill a substantial portion of the cell wall, sometimes occurring along with some Type II pits. The large simple pits are sometimes elliptical in shape (Fig. 3.7F), rather than being round or oval (Fig. 3.6F or Fig. 3.4G) as Richter describes his Type IV pits, and therefore do not consistently and exactly fit into the Richter scheme.

*Clade* – Magnoliids

*Order* – Laurales

*Family* – Lauraceae

*Genus* – *Laurinoxylon* Felix

*Species* – *Laurinoxylon* sp. 3, McRae Group IA sp. 3

*Holoxylotype* – TXSTATE 1252 (Fig. 3.4–3.5).

*Stratigraphic horizon* – McRae Formation, Jose Creek Member

*Age* – Late Campanian

*Material* – Estimated minimum stem diameter of 35 cm, collected as float

*Locality* – Texas State University Paleobotanical Locality 1991-15

*Paraxylotype* – TXSTATE 1253 (Fig. 3.6).

*Stratigraphic horizon* – McRae Formation, Jose Creek Member

*Age* – Late Campanian

*Material* – Estimated minimum stem diameter of 15 cm, material collected as float

*Locality* – Texas State University Paleobotanical Locality 2014-3

*Description* – *Growth rings* absent. *Wood* diffuse porous (Fig. 3.4A). *Vessels* solitary (24–33%) and in radial multiples of predominantly 2–3 (4–5 or more not uncommon) (Fig. 3.4B), mean of means 24 (2), range 22 (5)–25 (7)/mm<sup>2</sup>, solitary vessels tending to be angular in outline, tangential diameter mean of means 89 (6), range 85 (23)–92 (15) μm; vessel element length mean of means 355 (60), range 312 (74)–397 (101) μm (Fig. 3.4C); perforation plates simple (Fig. 3.4D); intervessel pits alternate (Fig. 3.4E), polygonal in outline, small to large, 5–12 μm in diameter.

*Vessel-ray pits* of two types, smaller pits with reduced borders to simple, round, elongated horizontally or vertically (Fig. 3.4F), some irregular-shaped, several to many per cell (consistent with Richter type II), other pits large, simple, rounded, window-like (more similar to Richter Type “IV”) (Fig. 3.4G). *Tyloses* common, thin-walled. *Fibers* angular in cross section, thin-walled to medium thick-walled, septate, pits not observed (Fig. 3.4H). *Axial parenchyma* scanty paratracheal (Fig. 3.5A) and diffuse (Fig. 3.5B), 4–8 cells per parenchyma strand (Fig. 3.5A). *Rays* (1) 3–7 seriate, mostly 3-6 (mostly 4-6 seriate in larger diameter axis) (Fig. 3.5B); multiseriate rays homocellular composed of procumbent cells or heterocellular with 1–2 (to 3) square or upright marginal rows (Fig. 3.5C), ray height 9–55 cells, mean of means 545 (95), range 477 (274)–612 (326)  $\mu\text{m}$ , mostly < 1000  $\mu\text{m}$  high; uniseriate and biseriate rays uncommon (<10 cells tall); range of means for all rays 9–13 per mm. *Oil cells* small, slightly larger than other ray cells at the ray margin (sometimes in clusters (Fig. 3.5E), along the side of rays (Fig. 3.5D,E) (not extending into fibers) or less frequently nested within rays (Fig. 3.5F).

*Description in IAWA Hardwood List codes (IAWA Committee 1989) –*

2 5 10v 12v 13 22 23 25 26 27 31 32 33 41 48 53 56 65 69 76 78 92 93 98 102v 104  
106 107v 115 116v 124

*Remarks –* Data from two specimens were combined to describe this xylotype. While sample TXSTATE 1253 strongly resembles TXSTATE 1252, it differs in having larger intervessel pits (Fig. 3.6C), shorter vessel elements and somewhat narrower and shorter rays (Fig. 3.6B, G). This variation may reflect the difference in axis diameter with the larger axis (TXSTATE 1252) having larger rays. In addition,

the difference in quality of preservation of the two specimens may account for the disparate appearance of the oil cells (Fig. 3.6H) and vessel-ray pits (Fig. 3.6E, F).

This wood differs from TXSTATE 1254, the second wood in group IA–vessel-ray pits of two types, by having more solitary vessels, larger intervessel pits, fewer vessels per square millimeter, taller rays and oil cells occurring within rays or along the sides of rays more frequently than TXSTATE 1254.

This xylotype resembles the McRae wood *Laurinoxylon rennerae* previously described by Estrada-Ruiz et al. (2018) (Table 3.1). However, the diagnosis for *L. rennerae* includes the occurrence of some scalariform perforation plates, a feature Richter found important in differentiating extant Lauraceae (Richter in Metcalfe 1987). The *L. rennerae* diagnosis also includes septate fibers as rare and vessel-ray pits as Richter Type II, with no mention of larger simple pits. Further, the rays in *L. rennerae* are narrower and shorter than those observed in sample TXSTATE 1252. *Laurinoxylon rennerae* was described from a sample with an estimated stem diameter of 50 cm, larger than either specimen attributed to this xylotype; therefore, the smaller ray width and height of *L. rennerae* run counter to what might be expected for a larger axis.

*Clade* – Magnoliids

*Order* – Laurales

*Family* – Lauraceae

*Genus* – *Laurinoxylon* Felix

*Species* – *Laurinoxylon* sp. 4, McRae Group IA sp. 4

*Holoxylotype* – TXSTATE 1254 (Fig. 3.7–3.8).

*Stratigraphic horizon* – McRae Formation, Jose Creek Member

*Age* – Late Campanian

*Material* – Estimated minimum stem diameter of 15 cm, collected as float

*Locality* – Texas State University Paleobotanical Locality 2012-36

*Description* – *Growth rings* absent. *Wood* diffuse porous (Fig. 3.7A). *Vessels* solitary (15%) and in radial or oblique multiples of mostly 2, up to 4–5), average 58 (SD 15, range 29–80)/mm<sup>2</sup>, solitary vessels oval in outline, average tangential diameter 83 (SD 14, range 62–110) μm; vessel element length not observed; perforation plates simple (Fig. 3.7B); intervessel pits alternate (Fig. 3.7C), polygonal in outline, minute to small, 3–5 μm in diameter. *Vessel-ray pits* of two types, reduced border to simple, round, oval, elongate or curved, multiple pits per cell (Fig. 3.7E) (Richter Type II), or one large simple pit per cell in addition to smaller pits (Fig. 3.7F) (approaching Richter Type IV). *Vessel-axial parenchyma pits* with slightly reduced borders (Fig. 3.7D). *Tyloses* common. *Fibers* angular in cross section, thin-walled to thick-walled, with minutely bordered pits, non-septate. *Axial parenchyma* not common, scanty paratracheal (Fig. 3.7G) and rarely diffuse, number of cells per parenchyma strand not observed. *Rays* (1) 3–5 (mostly 4) seriate (Fig. 3.8A), multiseriate rays homocellular composed of procumbent cells, the marginal row sometimes enlarged, or heterocellular composed of all uniformly sized procumbent cells with 1 marginal row of square or upright cells (Fig. 3.8B–C); ray height average 319 (SD 130, range 90–674, mostly 200–400) μm; uniseriate rays rare (<5 cells tall), range for all rays 6–12 per mm. *Oil cells* not common, primarily at the ray margins

(Fig. 3.8D–E), occasionally at the side of rays, often only slightly larger than surrounding adjacent ray parenchyma, sometimes larger (Fig. 3.8F).

*Description in IAWA Hardwood List codes (IAWA Committee 1989) –*

2 5 10v 13 22 23 24 25 31 32 33 41 48 49 56 61 66 69 76v 78 98 104 106 115 124

*Remarks –* This Group IA wood (Type II & IV vessel-ray pitting) differs from *Laurinoxylon rennerae* by having exclusively simple perforation plates, whereas *L. rennerae* has both simple and scalariform perforation plates. It differs from TXSTATE 1252 and *Laurinoxylon rennerae* by having fewer solitary vessels and more vessels in oblique multiples of 4–5, minute to small intervessel pits, more vessels per square millimeter, non-septate fibers, axial parenchyma very scanty paratracheal, shorter rays and oil cells that are small and primarily at the ray margins.

**Group IB: Axial parenchyma aliform to confluent**

*Clade –* Magnoliids

*Order –* Laurales

*Family –* Lauraceae

*Species –* McRae Group IB sp. 1

*Holoxylotype –* TXSTATE 1255 (Fig. 3.9–3.10).

*Stratigraphic horizon –* McRae Formation, Jose Creek Member

*Age –* Late Campanian

*Material –* Estimated minimum stem diameter of 17 cm, collected as float

*Locality –* Texas State University Paleobotanical Locality 2013-19

*Paraxylotype* – TXSTATE 1256 (Fig. 3.11)

*Stratigraphic horizon* – McRae Formation, Jose Creek Member

*Age* – Late Campanian

*Material* – Estimated stem diameter of 30 cm, material collected as float

*Locality* – Texas State University Paleobotanical Locality 2014-2

*Description* – *Growth rings* absent. *Wood* diffuse porous (Fig. 3.9A). *Vessels* solitary (47–56%) and in radial, oblique or tangential multiples of 2–3 (up to 4) (Fig. 3.9B), mean of means 13 (1), range 12 (9)–14 (5)/mm<sup>2</sup>, solitary vessels oval to angular in outline, tangential diameter mean of means 59 (8), range 53 (13)–65 (8) μm; vessel element length mean of means 199 (1), range 198 (62)–200 (57) μm (Fig. 3.9C); perforation plates simple (Fig. 3.9D); intervessel pits alternate (Fig. 3.9E), polygonal in outline, small to medium, means 6–8 μm in horizontal diameter. *Vessel-ray pits* bordered (Fig. 3.9F) or with slightly reduced borders, oval and some horizontally elongate (Fig. 3.9G). *Vessel-axial parenchyma pits* large, elliptical, reduced borders to simple, often extending across full diameter of cells, crowded or similar to vessel-ray pitting. *Tyloses* rarely observed. *Fibers* angular in outline, non-septate, thin-walled (Fig. 3.10A), pits not observed. *Axial parenchyma* common, lozenge-aliform to confluent (Fig. 3.9A), 2–4 cells per parenchyma strand. *Rays* 1–5 (up to 7) (mostly 3–4) seriate (Fig. 3.10B), multiseriate rays composed of procumbent cells of variable size, marginal row sometimes large procumbent or barely procumbent cells (Fig. 3.10C) homocellular or heterocellular with one row of square or upright marginal cells (Fig. 3.10D); ray height mean of means 303 (62),

range 259 (118)–347 (160)  $\mu\text{m}$ ; uniseriate rays uncommon, < 5 cells tall; mean for all rays 12 (1) per mm. *Oil cells* common in axial parenchyma (Fig. 3.10E), less frequently within rays (Fig. 3.10F) or at ray margins (Fig. 3.10G).

*Description in IAWA Hardwood List codes (IAWA Committee 1989) –*

2 5 12v 13 22 23 25v 26v 30v 31v 41 47 52 66 69 80 81 83 91 92 97 98 104 106  
115v 116v 124 125

*Remarks* – The description is based on two samples that are the only McRae Lauraceae woods with aliform or confluent axial parenchyma. Oil cells are present in ray margin cells or occasionally within the body of rays but are primarily concentrated in the confluent axial parenchyma. The samples have been tentatively combined into one xylotype because the anatomical features of the two samples are similar. The axial parenchyma in sample TXSTATE 1256 is primarily aliform and not confluent (Fig. 3.11A), only bordered vessel-ray pits were observed (Fig. 3.11D) and oil cells occur less frequently (Fig. 3.11E, G) than in TXSTATE 1255. These differences were not used to “split” the specimens into two xylotypes in this study. These specimens will be compared to extant genera within Lauraceae that have aliform and confluent axial parenchyma. If species in those genera are delimited by differences in aliform vs. confluent parenchyma, exclusively bordered vessel-ray pitting or oil cell location, these specimens will be reexamined and, if appropriate, named as two separate xylotypes.

## **McRae Groups II, III, and IV: Idioblasts absent**

### **McRae Group II: Exclusively Scalariform Perforation Plates**

Ten xylootypes with exclusively scalariform perforation plates are included in this group. These woods also share the features opposite intervessel pits and fibers with distinctly bordered pits. Differences are found in vessel diameter and density, the number of bars per perforation plate, the presence or absence of vasicentric tracheids, axial parenchyma distribution, ray width, the frequency of uniseriate rays and the occurrence of prismatic crystals.

#### **Group IIA: Rays <10 cells wide**

##### **a. Axial parenchyma common**

Five woods with exclusively scalariform perforation plates and rays <10 cells wide are described (Tables 3). Estrada-Ruiz et al. (2012a, 2018) previously reported *Baasia aremendarisense* (Estrada-Ruiz et al. 2012a) and *Turneroxylon newmexicoensis* (Estrada-Ruiz et al. 2018), which also fall within this grouping of McRae woods.

#### **Group IIA: Rays <10 cells wide**

##### **a. Axial parenchyma common**

##### **i. Vessel-ray parenchyma pits of two types**

*Clade* – Core Eudicots, Pentapetales

*Order* – Santalales

*Family* – cf. Olacaceae

*Genus* – *Agujoxylon* Wheeler and Lehman (2000)

*Species* – *Agujoxylon olacaceoides* Wheeler and Lehman (2000)

*Holoxylotype* – TXSTATE 1257 (Fig. 3.12–3.13)

*Stratigraphic horizon* – McRae Formation, Jose Creek Member

*Age* – Late Campanian

*Material* – Parallel rays indicate a mature specimen of undetermined diameter

*Locality* – Texas State University Paleobotanical Locality 2013-26

*Description* – *Growth rings* absent. *Wood* diffuse porous. *Vessels* solitary (85%) and in radial multiples of 2 (up to 3) (Fig. 3.12A), tendency toward radial arrangement, average 36 (SD 12, range 13–60)/mm<sup>2</sup>, solitary vessels angular in outline, tangential diameter average 71 (SD 13, range 32–92) μm. Vessel element length average 1130 (SD 264, range 772–1788) μm (Fig. 3.12B); perforation plates scalariform, 20–55 bars per plate (Fig. 3.12C), bars of perforation plate only occasionally forked, intervessel pits opposite to scalariform, oval to horizontally elongate in outline (Fig. 3.12D), small to medium, 6–10 μm in diameter, not crowded. *Vessel-ray parenchyma pits* of two types: simple or reduced borders, round to horizontal elongate (Fig. 3.12E), and large, simple or reduced borders, occupying most of the cross field (Fig. 3.12F) or occurring in the same cell with smaller pits. *Vessel-axial parenchyma pitting* with reduced borders oval to horizontally elongate (Fig. 3.12G). *Tyloses* common, thin-walled and segmenting vessels or tending to bubble-like (Fig. 3.13B). *Fibers* probably angular in cross section, thin-walled to thick-walled, one continuous row of bordered pits visible in radial and tangential walls (Fig. 3.12H), closely spaced, fibers non-septate (Fig.

3.13A). *Axial parenchyma* abundant, diffuse and scanty paratracheal, parenchyma often alternating with fibers (Fig. 3.13B–C), more than eight cells per parenchyma strand (Fig. 3.13D). *Rays* (1) 2–7 (mostly 3–5) seriate (Fig. 3.13D), multiseriate rays heterocellular, composed of generally procumbent cells in the body, cell size variable, some barely procumbent, rays generally ending with one to many (<25) uniseriate square or upright marginal rows one or both ends, occasional square and upright cells intermixed throughout the ray (Fig. 3.13E), multiseriate regions occasionally vertically fused by uniseriate (<50 cells) regions; ray height 400–4500 µm, uniseriate rays rare; all rays mostly 10–14 per mm.

*Description in IAWA Hardwood List codes (IAWA Committee 1989) –*

2 5 7v 12 14 17 18 21 25 26 31 32 33 41 47 48 49 54 56 62 63 66 69 76 78 94 98  
102 106 107 108 109 115 116

*Remarks* – Features of this wood are consistent with *Agujoxylon olacaceoides* as first described from the upper Campanian to lower Maastrichtian Aguja Formation of Big Bend National Park, Texas, USA (Wheeler and Lehman 2000). These features include predominantly solitary vessels with some radial multiples, scalariform perforation plates, opposite to scalariform intervessel pits, vessel-ray pits of two sizes, small pits with reduced borders and large pits with reduced borders to simple that nearly fill the cross field, fibers with bordered pits in both radial and tangential view, and abundant apotracheal axial parenchyma that tend to alternate with fibers radially. Prismatic crystals are not observed in this specimen, but this may reflect the quality of preservation (Tables 3.3).

**Group IIA: Rays <10 cells wide**

**a. Axial parenchyma common**

**ii. Vessel-ray parenchyma pits of one type, small**

*Family* – unknown

*Species* – McRae Group IIA sp.1

*Holoxylotype* – TXSTATE 1259 (Fig. 3.14–3.15).

*Stratigraphic horizon* – McRae Formation, Jose Creek Member

*Age* – Late Campanian

*Material* – Estimated minimum axis diameter of 3.3 cm, collected as float

*Locality* – Texas State University Paleobotanical Locality 1992-3

*Description* – *Growth rings* absent. *Wood* diffuse porous. *Vessels* solitary (92%) and in oblique multiples of 2 (Fig. 3.14A), average 52 (SD 17, range 28–83)/mm<sup>2</sup>, solitary vessels oval to slightly angular in outline, tangential diameter average 39 (SD 9, range 18–61) μm; vessel element length average 580 (SD 114, range 349–681) μm (Fig. 3.14B); perforation plates scalariform, average 46 (SD 11, range 34–72) thin bars per plate, bars of perforation plate only occasionally forked (Fig. 3.14C); intervessel pits opposite, oval, some horizontally elongated, < 4 μm in vertical diameter, crowded (Fig. 3.14D); pits on vessel element tails often horizontally elongate to scalariform (Fig. 3.14E). *Vessel-ray pits* with distinct borders, very small, similar to intervessel pits in shape, very crowded, covering the entire cross field (Fig. 3.14F). *Tyloses* not observed. *Fibers* angular in cross section, thin-walled to thick-walled, with one row of bordered pits visible on radial and

tangential walls, rows of pits continuous (Fig. 3.14G), fibers non-septate. *Axial parenchyma* common, diffuse, diffuse-in-aggregates (Fig. 3.14H, 3.15A), scanty paratracheal (Fig. 3.15B), 2–4 cells per strand. *Rays* heterocellular, 1–5 (mostly 1–2) seriate, multiseriate rays (Fig. 3.15D) made up of predominantly square, upright or barely procumbent rows with only a few rows of truly procumbent cells together in the ray body (most <5, up to 10 rows) (Fig. 3.15E), one to many (<13 observed) square or upright uniseriate marginal rows one or both ends, ray bodies of inconsistent width, tapering in places, but usually 2 or more cells wide, rarely alternating uniseriate and multiseriate portions in a ray, then only a few uniseriate rows (rare exceptions); ray height average 52 (SD 32, range 17–113) cells, average 544 (SD 275, range 349–681)  $\mu\text{m}$ . Uniseriate rays common (33% of rays), appearing to be all square and upright cells (Fig. 3.15F), uniseriate ray height 312–658  $\mu\text{m}$  tall; average for all rays 34 (SD 5, range 24–49) per mm.

*Description in IAWA Hardwood List codes (IAWA Committee 1989) –*

2 5 9 14 17 18 21 24 30 40 48 49 53 62 63 66 69 76 77 78 91 92 97 98 106 107 108  
109 116

*Remarks* – This wood has predominantly narrow rays (mostly 1-2 cells wide) and small vessels at high density compared to other McRae woods with exclusively scalariform perforation plates. The features, alone, do not conclusively distinguish the wood from other types because the sample is a small diameter axis (estimated diameter 3.3 cm), so the ray dimensions and cellular composition as well as quantitative vessel features in a mature wood of the same species could be different. However, considering this sample as a separate type is supported by other

anatomical differences (Table 3.2) including perforation plates with more bars, vessel-ray pits that are opposite, very small and crowded over the entire cross field, vasicentric tracheids not present and fibers with one row of pits that extends the length of the fiber. Multiseriate rays are made up of predominantly square, upright or barely procumbent rows with only a few rows of truly procumbent cells together in the ray body (most <5, up to 10 rows), one to many (<13) square or upright uniseriate marginal rows one or both ends; and multiseriate regions only rarely joined by uniseriate regions, then only a few uniseriate cells (rare exceptions). At present, this wood will be treated as a separate McRae type. If in the future evidence links this type to a mature wood, the type can be placed in synonymy.

*Family* – unknown

*Species* – McRae Group IIA sp. 2

*Holoxylotype* – TXSTATE 1260 (Fig. 3.16–3.17).

*Stratigraphic horizon* – McRae Formation, Jose Creek Member

*Age* – Late Campanian

*Material* – Estimated minimum stem diameter of 7 cm, collected as float

*Locality* – Texas State University Paleobotanical Locality 2016-6

*Description* – *Growth rings* absent. *Wood* diffuse porous (Fig. 3.16A). *Vessels* exclusively solitary (100%), average 48 (SD 9, range 35–59)/mm<sup>2</sup>, solitary vessels round to oval in outline, tangential diameter average 47 (SD 9, range 31–67) μm; vessel element length 600–800 μm; perforation plates scalariform, 20–28 bars per plate (Fig. 3.16B), bars of perforation plate sometimes forked; intervessel pits

opposite, oval or occasionally horizontally elongate (Fig. 3.16C–D). *Vessel-ray pits* with reduced borders, round to oval, small, throughout the cross field, not crowded (Fig. 3.16E). *Vessel-axial parenchyma pitting* oval, with borders (Fig. 3.16F). *Tyloses* not observed. *Fibers* medium to thick-walled with one row distinctly bordered pits present in both radial and tangential walls (Fig. 3.17A), nonseptate. Vasicentric tracheids with 2-3 rows of pits (Fig. 3.17B). *Axial parenchyma* not uncommon, diffuse, occasionally adjacent to vessels (Fig. 3.17C). *Rays* 2–6 cells wide, multiseriate rays heterocellular, composed of procumbent cells in the central portion with marginal rows of square or upright cells (as few as 1, mostly <5, occasionally many, up to 15 observed) (Fig. 3.17E–F), sheath cells present; multi-seriate portions of tallest rays >1 mm in height (Fig. 3.17D); uniseriate rays 23%; range for all rays 4–17 per mm.

*Description in IAWA Hardwood List codes (IAWA Committee 1989) –*

2 5 9 14 17 21 31 40 48 49 53 60 62 63 66 69 76 97 98 102 106 107 108 110 115  
116

*Remarks* – This wood is distinguished from other McRae woods by the combination of vasicentric tracheids with 2-3 rows of small pits, fibers with a single continuous row of pits, the presence of sheath cells and rays where multiseriate portions are not vertically fused by uniseriate regions (Table 3.2). The specimen was small and not well preserved, which limited the number and quality of slides and complicated the search for affinity. It is hoped that additional material will be found.

*Clade:* Eudicots, Pentapetalae

*Order:* Malpighiales (?)

*Family* – unknown

*Genus* – *Metcalfeoxylon* Wheeler, McClammer and LaPasha (1995)

*Species* – *Metcalfeoxylon kirtlandense* Wheeler, McClammer and LaPasha (1995)

*Holotype* – TXSTATE 1261 (Fig. 3.18–3.19).

*Stratigraphic horizon* – McRae Formation, Jose Creek Member

*Age* – Late Campanian

*Material* – Estimated minimum stem diameter of 20 cm, collected as float

*Locality* – Texas State University Paleobotanical Locality 2016-16

*Description:* *Growth rings* absent. *Wood* diffuse porous. *Vessels* solitary (93%) and rarely in radial multiples of 2; average 2 (SD 1, range 1–6)/ mm<sup>2</sup>; areas with few or no vessels alternating with irregular tangential bands of vessels (Fig. 3.18A), solitary vessels oval to angular in outline, tangential diameter average 133 (SD 31, mean 89–208) μm; vessel element length average 997 (SD 193, mean 676–1374) μm (Fig. 3.18B); perforation plates scalariform (Fig. 3.18C), average 15 (SD 5, range 11–28) bars per plate, bars of perforation plate sometimes forked; intervessel pits rounded in outline, opposite to alternate, small, 5–8 μm in diameter (Fig. 3.18D). *Vessel-ray pits* with distinct borders, smaller than intervessel pits, throughout the ray cell (Fig. 3.18E). *Tyloses* occasionally present, bubble-like (Fig. 3.18F). *Fibers* angular in cross section, medium to thick-walled (Fig. 3.18G), fiber-tracheids with one continuous row of distinctly bordered pits present in both radial and tangential

walls, fibers non-septate (Fig. 3.18H). Vascentric tracheids with several rows of crowded pits observed (Fig. 3.19A). *Axial parenchyma* abundant, diffuse (Fig. 3.19B–C) and diffuse-in-aggregates, sometimes forming short, irregular tangential or diagonal rows (1–3 cells wide) (Fig. 3.19A), scanty paratracheal, over eight cells per parenchyma strand. *Rays* 2–5 (mostly 3–4) cells wide, multi-seriate rays heterocellular, composed of procumbent cells in the central portion, cell size variable, square and upright rows intermixed among procumbent areas (Fig. 3.19D), rays with one to many (up to 26 observed) uniseriate square or upright marginal rows, alternating uniseriate (<30 cells) and multiseriate portions in a ray (Fig. 3.19E); multiseriate ray height 440–3,700 µm. Uniseriate rays composed of square and upright cells, uniseriate ray height 4–18 cells or 190–760 µm; average for all rays 14 (SD 2, range 10–17) per mm.

*Description in IAWA Hardwood List codes (IAWA Committee 1989) –*

2 5 9 12 14 16 17 21v 25 26 30 42 46 54 60 62 63 66 69 76 77 78 94 97 98 102 106  
107 108 109 116

*Remarks* – This wood is very similar to previously reported *Metcalfeoxylon kirtlandense* woods (Wheeler et al. 1995, Wheeler and Lehman 2000, Estrada-Ruiz et al. 2010, Estrada-Ruiz et al. 2012a, 2012b) (Table 3.3). The McRae wood, as seen in transverse view, has areas (tangential “bands”) that have no vessels, possibly reflecting some seasonality in water availability. This differs from the San Juan Basin (Wheeler et al. 1995), Crevasse Canyon (Estrada-Ruiz et al. 2012a, 2012b) and Olmos (Estrada-Ruiz et al. 2010) *Metcalfeoxylon* woods, where the vessels are uniformly distributed. However, the Big Bend Aguja Formation *Metcalfeoxylon*

sometimes has vessels in a diagonal pattern (Wheeler and Lehman 2000), suggesting some variability in vessel arrangement. The McRae wood could represent a new species of *Metcalfeoxylon* or additional within-species variability in vessel arrangement.

*Metcalfeoxylon* may represent Malpichiales (Wheeler, personal communication). Like other occurrences of *Metcalfeoxylon*, the Jose Creek specimen represents the wood of a tree. Stumps of *Metcalfeoxylon* measure up to 1.4 m in diameter in the upper Campanian to lower Maastrichtian Aguja Formation of Big Bend (Lehman and Wheeler, 2000) and up to 0.75 m in diameter in the Campanian Crevasse Canyon Formation of New Mexico (Estrada-Ruiz et al. 2012a).

**Group IIA: Rays <10 cells wide**

**b. Axial parenchyma not common, vessel diameter <100 µm,  
fiber pits “discontinuous”**

*Family* – unknown

*Species* – McRae Group IIA sp. 3

*Holoxylotype* – TXSTATE 1262 (Fig. 3.20–3.21).

*Stratigraphic horizon* – McRae Formation, Jose Creek Member

*Age* – Late Campanian

*Material* – Estimated minimum stem diameter of 17 cm, collected as float

*Locality* – Texas State University Paleobotanical Locality 2014-7

*Paraxylotype* – TXSTATE 1263 (Fig. 3.22)

*Stratigraphic horizon* – McRae Formation, Jose Creek Member

*Age* – Late Campanian

*Material* – Estimated minimum stem diameter of 60 cm, collected as float

*Locality* – Texas State University Paleobotanical Locality 2014-10

*Paraxylotype* – TXSTATE 1264 (Fig. 3.23–3.24)

*Stratigraphic horizon* – McRae Formation, Jose Creek Member

*Age* – Late Campanian

*Material* – Estimated minimum stem diameter of 7 cm, collected as float

*Locality* – Texas State University Paleobotanical Locality 2016-6

*Description* – *Growth rings* absent. *Wood* diffuse porous (Fig. 3.20A). *Vessels* solitary (97–100%), rarely in radial or oblique multiples of 2, mean of means 26 (12), range 16 (3)–39 (7)/mm<sup>2</sup>, solitary vessels oval in outline (Fig. 3.20B), tangential diameter mean of means 62 (5), range 56 (9)–66 (10) μm; vessel element length average 959 (SD 159, range 682–1291) μm (Fig. 3.20C); perforation plates scalariform (Fig. 3.20D), 15–45 (mostly 20–40) bars per plate, bars of perforation plate only occasionally forked; intervessel pits opposite (Fig. 3.20E), oval to horizontally elongated in outline, not crowded, vessel element tail pitting opposite to scalariform (Fig. 3.20F). *Vessel-ray pits* with distinct borders, similar to intervessel pits in size and shape throughout the ray cell (Fig. 3.20G). *Vessel-axial parenchyma pitting* similar to intervessel pitting (Fig. 3.20H). *Tyloses* common, segmenting the vessel and/or bubble-like. *Fibers* thin-walled to thick-walled, fibers with one row of bordered pits visible in radial and tangential walls, rows of pits (Fig.

3.21A) in a “discontinuous” pattern with stretches of usually 3-10 pits (single row) alternating with stretches without pits, non-septate. Vasicentric tracheids with a single row of bordered pits (“continuous” and larger than pits on fibers located between vessels) present in most samples. *Axial parenchyma* not common, diffuse and scanty paratracheal (Fig. 3.21B) observed as 2 cells per parenchyma strand (Fig. 3.21C), but larger strands probably present. *Rays* 1–6 seriate, multiseriate rays heterocellular, composed of procumbent cells in the body, uniform in size (much longer horizontally than vertically tall), occasionally large and sometimes irregularly shaped cells intermixed in the ray body forming biseriate or uniseriate rows within the ray body (tangential view), more commonly irregular and/or large cells adjacent to the uniseriate marginal rows, in radial view these cells appearing as square and upright rows intermixed among procumbent cells (Fig. 3.21E), rays often with one to many (up to 30 observed) uniseriate square or upright marginal rows. Multiseriate regions occasionally vertically fused by uniseriate or biseriate regions of <20 cells (Fig. 3.21D). Tendency to sheath cells. Body of the multiseriate rays (excluding uniseriate margins) <1 mm high; uniseriate rays common (20–25%) in smaller axes, less common (6%) in large axis, composed of square and upright cells with occasional procumbent rows (Fig. 3.21F), usually <500 µm (up to 1 mm) tall; mean of means for all rays 22 (5), range 18 (3)–27 (4) per mm.

*Description in IAWA Hardwood List codes (IAWA Committee 1989) –*

2 5 9 14 16 17 21 25 30 31 41 47 48 54 56 62 63 66 69 76 78 91 97 98 106 107 108  
109 110 116

*Remarks* – Specimens TXSTATE 1262, 1263 and 1264 (Table 3.4) are grouped together because of their shared ray structure and fiber pitting. The striking appearance of the rays results from large, often irregularly shaped, “blocky” cells inserted in various areas of the ray (Fig. 3. 21, 3.22, 3.24). Multiseriate portions of rays range from 248–453  $\mu\text{m}$ , while the uniseriate margins or uniseriate regions that vertically fuse multiseriate regions are often very long. Sheath cells are present. Fiber pits are bordered and “discontinuous” (i.e., usually 3-10 pits (single row) alternating with areas without pits). Vasicentric tracheids have a single uninterrupted row of larger bordered pits.

Vasicentric tracheids were not observed in specimen TXSTATE 1262. Crystals were not observed in the ray parenchyma, which may reflect the quality of preservation. Specimen TXSTATE 1263 has wider and somewhat taller rays (Fig. 3.22A) than TXSTATE 1262 and 1264, with fewer uniseriate rays (6%). This may reflect its larger diameter axis.

Sample TXSTATE 1264 differs from TXSTATE 1262 and 1263 in having smaller diameter vessels; rays occur in higher density (Fig. 3.23A) than TXSTATE 1263. Rays are narrow (mostly 3 cells wide) and close-set (Fig. 3.24C). The smaller vessels and narrower rays may reflect the smaller axis (estimated diameter 7 cm) of TXSTATE 1264. Sheath cells are not observed in TXSTATE 1264 and crystals are present in the ray parenchyma (Fig. 3.24B). Like TXSTATE 1263, TXSTATE 1264 has vasicentric tracheids with a single, continuous row of bordered pits that are larger than pits on fibers located between vessels (Fig. 3.23H).

**Group IIB: Rays >10 cells wide, uniseriate rays common (rays of two sizes)**

*Family* – cf. Icacinaceae

*Genus* – cf. *Icacinoxylon* Shilkina (1956)

*Species* – cf. *Icacinoxylon* sp. 1

*Holoxylotype* – TXSTATE 1265 (Fig. 3.25–3.26).

*Stratigraphic horizon* – McRae Formation, Jose Creek Member

*Age* – Late Campanian

*Material* – Estimated minimum stem diameter of 9 cm, collected as float

*Locality* – Texas State University Paleobotanical Locality 2014-14

*Paraxylotype* – TXSTATE 1266

*Stratigraphic horizon* – McRae Formation, Jose Creek Member

*Age* – Late Campanian

*Material* – Estimated minimum stem diameter of 3cm, collected as float

*Locality* – Texas State University Paleobotanical Locality 1991-17A

*Description* – *Growth rings* absent. *Wood* diffuse porous (Fig. 3.25A). *Vessels* solitary (94%) and in radial or oblique multiples of 2, diffuse, 11–33/mm<sup>2</sup> in areas between wide rays, solitary vessels round to oval in outline, tangential diameter average 82 (SD 14, range 51–102)  $\mu\text{m}$ ; vessel element length 395–873  $\mu\text{m}$  (Fig. 3.25B); perforation plates scalariform, average 10 (SD 4, range 6–23) bars per plate (Fig. 3.25C), bars of perforation plate sometimes forked; intervessel pits opposite to sometimes sub-alternate (Fig. 3.25D), minute to small, 3–5  $\mu\text{m}$  in diameter. *Vessel-*

*ray pits* with distinct borders, similar to intervessel pits, throughout the ray cell, crowded (Fig. 3.25E). *Vessel-axial parenchyma pitting* similar to vessel-ray pitting (Fig. 3.25F). *Tyloses* not observed. *Fibers* angular in cross section, medium to thick-walled, generally one row of distinctly bordered pits present in both radial and tangential walls (Fig. 3.25G), vasicentric tracheids with 2–3 rows of pits (Fig. 3.26A), non-septate, *Axial parenchyma* common, diffuse, diffuse-in-aggregates and scanty paratracheal (Fig. 3.26B), 3–4 cells per parenchyma strand. *Rays* heterocellular, rays of two sizes, wide multi-seriate 16–30 cells wide, ray height 3–10.8 mm (Fig. 3.26C), composed of procumbent cells in the central portion (Fig. 3.26D) with 1–4 or more marginal rows of square or upright cells (Fig. 3.26E–F) or multiseriate regions occasionally vertically fused by uniseriate regions, some rays composed of procumbent cells with square or upright rows intermixed; narrow rays 1–3 (mostly 1–2) cells wide (23% uniseriate), made up of procumbent and upright cells mixed together, ray height 4–31 cells or 160–870 µm; narrow rays 10–25 per mm in regions between the wider rays.

*Description in IAWA Hardwood List codes (IAWA Committee 1989) –*

2 5 9 14 15 16 21 22v 30 41 47 48 53 60 62 63 69 76 77 78 92 99 102 103 106 107  
108 109 115 116

*Remarks* – Features of this wood (Table 3.2) including exclusively scalariform perforation plates, opposite intervessel pits, fibers with distinctly bordered pits, diffuse axial parenchyma and heterocellular rays of two distinct sizes (the larger rays 15 to >20 cells wide) are consistent with the diagnosis for *Icacinoxylon* Shilkina (1956). This wood differs from the diagnosis in that perforation plates in the

present fossil have fewer bars (mean 10, up to 23) and smaller rays are commonly uniseriate (23%) whereas the diagnosis specifies small rays as 2-3 cells wide. The original diagnosis does not specify the presence of vasicentric tracheids, but it does describe pitting in two rows (opposite) between vessels and fibers that may represent the same anatomical structure. The McRae wood is designated as cf. *Icacinoxylon* because of the differences between it and the Shilkina diagnosis.

An exact match for the McRae wood was not found. Woods with similar features (e.g., perforation plates with fewer than 10 bars and abundant uniseriate rays) are recorded as species of *Icacinoxylon* in the InsideWood database (InsideWood, 2004-onwards). The McRae wood is similar to *I. kokubunii* Takahashi and Suzuki (2003) reported from the Yezo Group, Rumoi County, Hokkaido, Japan (Turonian) and *I. nishidae* Takahashi & Suzuki (2003), also from Rumoi County, Hokkaido, Japan (probably Coniancian to Santonian). Revision of the genus *Icacinoxylon* is needed to clarify the systematic relationships of woods with anatomical features that differ from the *Icacinoxylon* diagnosis.

A second specimen, TXSTATE 1266, collected from a site approximately 150 m from this specimen may represent the same xylotype. That specimen will be examined in more detail later. A more exhaustive search of the appropriate literature is required for final determination of species status.

### **McRae Group III: Exclusively simple perforation plates**

Eleven wood xylotypes with exclusively simple perforation plates are described in Group III. Group III xylotypes are further characterized by diffuse porous wood, without growth boundaries and alternate intervessel pits.

### **Group IIIA: Vessels exclusively solitary**

Group IIIA specimens (Table 3.5) have predominantly (> 80%) or exclusively (> 90%) solitary vessels. Xylotypes with rare axial parenchyma also have in common the presence of vasicentric tracheids and rays 1-2 seriate. This includes two McRae woods described previously as *Fulleroxylon armendarisense* (Estrada-Ruiz, Upchurch, Wheeler and Mack 2012b) and *Mcraeoxylon waddellii* (Estrada-Ruiz, Wheeler, Upchurch and Mack 2018). Xylotypes with common axial parenchyma are divided between types with wide rays (>10 seriate) and types with rays <10 seriate.

### **Group IIIA: Vessels exclusively solitary**

#### **a. Axial parenchyma rare, vasicentric tracheids, rays 1–2 seriate**

##### **i. Vessel diameter >100 µm, septate fibers**

*Clade* – Eudicots, Pentapetales, Rosids

*Order* – Oxalidales?

*Family* – Connaraceae? (contrary to Estrada-Ruiz et al. 2012b)

*Genus* – *Fulleroxylon* Estrada-Ruiz, Upchurch, Wheeler and Mack (2012a)

*Species* – *Fulleroxylon* sp. 1

*Holoxylotype* – TXSTATE 1275 (Fig. 3.27–3.29).

*Stratigraphic horizon* – McRae Formation, Jose Creek Member

*Age* – Late Campanian

*Material* – Estimated minimum stem diameter of 7 cm, collected as float

*Locality* – Texas State University Paleobotanical Locality 2013-32

*Paraxylotype* – TXSTATE 1276.

*Stratigraphic horizon* – McRae Formation, Jose Creek Member

*Age* – Late Campanian

*Material* – Estimated minimum stem diameter of 4.6 cm, collected as float

*Locality* – Texas State University Paleobotanical Locality 2013-32

*Paraxylotype* – TXSTATE 1277.

*Stratigraphic horizon* – McRae Formation, Jose Creek Member

*Age* – Late Campanian

*Material* – Estimated minimum stem diameter of 4.5 cm, collected as float

*Locality* – Texas State University Paleobotanical Locality 1992-3

*Description* – *Growth rings* absent. *Wood* diffuse porous (Fig. 3.27A). *Vessels* solitary (97-100%), mean of means 26 (4), range 23 (5)–31 (6)/mm<sup>2</sup>, round to slightly oval in outline, mean tangential diameter mean of means 145 (10), range 136 (41)–156 (22) μm. Vessel element length mean of means 356 (7), range 350 (90)–363 (69) μm (Fig. 3.27B); perforation plates simple (Fig. 3.27C), intervessel pits not observed; vessel-ray pits rounded (Fig. 3.27F), oval or irregular in shape with much reduced borders, some small pits with slit openings (Fig. 3.27G). Tyloses common, bubble-like (Fig. 3.27D, H). *Vasicentric tracheids* with several crowded rows of small, simple, reduced bordered or bordered pits (Fig. 3.28A). *Fibers* in the immediate vicinity of vessels non-septate, generally with one row of small, bordered pits (Fig. 3.28B) visible in both radial and tangential walls (Fig. 3.28C). Fibers farther removed from vessels with few or no pits, some septate (Fig. 3.28C–D); dark

content present in fibers (Fig. 3.28E–F), especially in areas where vessels have tyloses (Fig. 3.28E). Fibers thin-walled. *Axial parenchyma* not observed. *Rays* predominantly uniseriate, some partially 2–3 seriate (Fig. 3.28F) composed of procumbent cells with enlarged cells in the marginal row, or procumbent with 1 marginal row square or upright cells (Fig. 3.28G); ray height mean of means 10 (2), range 8 (5)–11 (5) cells or mean of means 159 (33), range 135 (77)–182 (87)  $\mu\text{m}$ , mean of means 21 (4), range 18 (5)–23 (8)/ mm. Remnants of incompletely preserved bark present, secondary phloem consisting of discontinuous bands of fibers alternating with areas (dark bands) of presumably crushed cells that may represent sieve elements (Fig. 3.49A); cortex composed of thick-walled, isodiametric parenchyma partitioned by tangential bands of longitudinal elements that may represent fibers (Fig. 3.49B) or possibly bands of developing phellem. Structures interpreted as isolated vessels (Fig. 3.49A) present in the secondary phloem represent a cambial variant. Large bubbly idioblasts forming vertically elongate cavities (Fig. 3.49C) present among the cortex parenchyma. Cavities interpreted as penetrating roots from another plant, vertically oriented, approximately 300–500  $\mu\text{m}$  diameter, irregularly occurring in secondary xylem and phloem. Crystals not observed.

*Description in IAWA Hardwood List codes (IAWA Committee 1989) –*

2 5 9 13 31 42 48 53 56 60 61 62 63 65 66 69 75 96 97v 104 106 116 135

*Remarks* – The combination of exclusively solitary vessels (9p) with simple perforation plates (13p), vessel-ray parenchyma pitting with only reduced borders (30a 31p), vasicentric tracheids (60p), rare axial parenchyma (75p) and

predominantly uniseriate rays (96p) without included phloem (134a) is consistent with the family Connaraceae (Metcalf & Chalk 1950, Dickison 1972, den Outer and van Veenendaal 1989, InsideWood 2004-onwards). Species selected in an expanded InsideWood search allowing 1 mismatch, include species in Calophyllaceae, Chrysobalanaceae and Myrtaceae. While the diversity of wood anatomical features in these families is not fully documented, they are tentatively excluded by having some combination of vessels in multiples, bordered vessel-ray parenchyma pitting, more common axial parenchyma or included phloem (Metcalf and Chalk 1950, InsideWood, 2004-onwards).

Based on an InsideWood database search, the fossil is most similar to Connaraceae, a family of primarily woody shrubs, climbers and lianas (Metcalf and Chalk 1950, Stevens 2001 onwards), particularly the genus *Rourea*. It differs in that rays in the fossil are less heterocellular and shorter than described by den Outer and van Veenendaal (1989), though within the range for *Rourea* as reported by Dickison (1972). The most striking difference is the high density of vessels observed in the fossil wood.

Affinity to the Connaraceae is supported by a combination of features, some not specifically recorded in the InsideWood database. Dickison (1972) describes the vessel-ray parenchyma pits as “distinctive in all genera--large, simple pits that are irregularly shaped and orientated.” However, images of Connaraceae show pitting which might be called very reduced bordered, with the borders somewhat irregular. There are also some small pits with slit openings. Whatever terminology is used, vessel-ray parenchyma pitting in the fossil, while not well preserved, is similar to

that observed in extant Connaraceae (Fig. 3.27F–H). Metcalfe and Chalk (1950) and den Outer and van Veenendall (1989) describe the fibers of Connaraceae as having content, and in the fossil, clusters of fibers are observed to contain dark content (Fig. 3.28E), particularly where vessels have abundant tyloses. Secondary phloem and bark are partially preserved in the fossil, and within the secondary phloem, areas of crushed cells presumed to be sieve elements are dissected by discontinuous, tangentially arranged bands of fibers, a characteristic of many species of extant Connaraceae (Metcalfe and Chalk 1950, Dickison 1973). This is a feature also observed by Jud (2017) for the fossil *Rourea blatta* which he described as having crescent-shaped fiber bands. The wood is further characterized by a form of anomalous secondary growth remarkably similar to that reported by Dickison (1973) for the genus *Agelaea* in which xylem tissue (xylem “arcs”) form within the secondary phloem. In the fossil, cavities interpreted as isolated solitary vessels, somewhat smaller than those of the xylem, are visible in transverse view. However, the presence of vessels among phloem fibers could not be confirmed conclusively in radial view. The features occur only sporadically and may not have been captured in the radial sections or the quality of phloem preservation may obscure the vessels. Dickison’s illustration shows that in extant *Agelaea*, fibers surrounding isolated vessels in the “arcs” are not as thick-walled as fibers in the secondary phloem fiber bands, a detail that cannot be confirmed in the fossil due to the quality of preservation. The occurrence of variant secondary growth of xylem is reported for liana stems, including *Rourea* (Fischer and Ewers 1992), which supports the possibility that the fossil is a liana type wood. Another feature consistent with

Connaraceae woods is observed in the fossil cortex, which consists of isodiametric thick-walled cells (Fig. 3.28G); Dickison (1973) described species of Connaraceae as having a persistent cortex with cells that become more sclerotic with age. Finally, large voids in the cortex (approximately 100  $\mu\text{m}$  in diameter, transverse view) appear in longitudinal view to be vertically elongate channels (Fig. 3.28G). Heimsch (1942) described “vertically elongated, scattered secretory cavities” in Connaraceae and Dickison (1973) reported finding “frothy mucilaginous idioblasts” in parenchymatous regions of extant species. The fossil “channels” may represent similar structures.

Neither Heimsch nor Dickison describe the presence of “root penetrations” in an extant Connaraceae wood, but both the phloem vessels and the cortex “frothy channels” are easily distinguished from the McRae wood “root penetrations.” The root penetrations are approximately 300–500  $\mu\text{m}$  in diameter compared to the mean vessel diameter of 156  $\mu\text{m}$ . In contrast, phloem vessels are generally distorted and crushed, but appear to be somewhat narrower than xylem vessels and the frothy vertical cavities in the cortex are approximately 100  $\mu\text{m}$  in diameter. Root penetrations are lined with a single or double layer of cells and have a central structure that consists of a small ring of cells with an innermost structure that appears spiral-like in longitudinal view. In longitudinal view, root penetrations have straight, smooth sides, whereas the frothy vertical structures have irregular margins.

To date, only two fossil woods have been reliably assigned to the Connaraceae.

Baas et al. (2017) described *Connaroxylon dimorphum* from the Deccan Intertrappean Beds of India, dated to  $67.5 \pm 1$  to 63 Ma with close affinity to the extant genus *Connarus*. *Connaroxylon dimorphum* differs from this wood by having some vessels in radial multiples, rays composed of square and upright cells, radial tubules in some rays and dimorphic fibers arranged in alternating bands of variable width, some wide. A second fossil wood from the Cucaracha Formation (~19 mya) described by Jud et al. (2017) as *Rourea blatta* is more similar to this wood. However, the vessels of *R. blatta* are narrower, the rays are composed primarily of square or upright cells, and crystals are present in some axial cells.

Specimens TXSTATE 1275, 1276 and 1277 are similar to *Fulleroxylon armendarisense* as described by Estrada-Ruiz et al. (2012a) (Table 3.6). The Estrada-Ruiz wood differs from this wood primarily in having indistinct growth rings marked by radially narrowed fibers, narrower, less crowded vessels and taller rays. The *F. armendarisense* bark tissue was not sufficiently preserved for comparison. The strong similarity between these woods supports assignment of this wood to the genus *Fulleroxylon*; differences observed in multiple axes (two of equal diameter to that from which *F. armendarisense* was described) and from multiple sites, warrant proposing a new species.

Estrada-Ruiz et al. (2012a) assigned *Fulleroxylon armendarisense* to Myrtaceae based on the combination of anatomical features (e.g., diffuse porous wood, exclusively simple perforation plates, alternate intervessel pits, vessel-ray parenchyma pits with reduced borders, vasicentric tracheids and predominantly uniseriate rays) that are consistent with the family. However, unlike the McRae

*Fulleroxylon* woods, species of the family Myrtaceae are characterized by patterns of more common axial parenchyma. Furthermore, I could not verify statistically the tendency for vessels to be of two distinct diameter classes as proposed by Estrada-Ruiz et al. for *F. armendarisense*. Both small and large vessels are present in *Fulleroxylon*, with a more or less continuous distribution of vessel sizes observed in *Fulleroxylon* sp. 1, and with only a modest decrease in the middle range of vessel diameters in *F. armendarisense*. Reassignment of the genus to the family Connaraceae is supported by a close match with the InsideWood search and the presence of several highly unusual features also present in some genera of Connaraceae. These include vessel arcs in the phloem, fibers with dark content, a persistent cortex with sclerotic parenchyma and vertically oriented frothy mucilaginous cavities among the cortex parenchyma.

**McRae Group IIIA: Vessels exclusively solitary**

**a. Axial parenchyma rare, vasicentric tracheids, rays 1–2 seriate**

**ii. Vessel diameter <100 µm, non-septate fibers**

*Family* – unknown

*Species* – McRae Group IIIA sp. 1

*Holoxylotype* – TXSTATE 1278 (Fig. 3.30–3.31).

*Stratigraphic horizon* – McRae Formation, Jose Creek Member

*Age* – Late Campanian

*Material* – Estimated minimum stem diameter of 24 cm, collected as float

*Locality* – Texas State University Paleobotanical Locality 2013-35

*Description* – *Growth rings* absent. *Wood* diffuse porous (Fig. 3.30A). *Vessels* solitary (97%) and in radial multiples of 2, average 42 (SD 10, range 27–55)/mm<sup>2</sup>, with a tendency for vessels to be arranged in radial or oblique rows, solitary vessels round in outline (Fig. 3.30B), tangential diameter mean 50 (SD 14, range 28–85)µm; vessel element length average 224 (SD 65, range 127–348) µm (Fig. 3.30C); perforation plates simple (Fig. 3.45D); intervessel pits alternate to sub-alternate (Fig. 3.30E), oval in outline, not crowded, minute, < 4 µm in diameter. *Vessel-ray pits* with distinct borders, similar to intervessel pits in size and shape throughout the cross field (Fig. 3.30F). *Tyloses* common, bubble-like (Fig. 3.30G). *Fibers* angular in cross section, thin-walled to thick-walled, vasicentric tracheids with several rows of small bordered pits twisting around vessels (Fig. 3.31A), fibers in the immediate vicinity of vasicentric tracheids with one row of bordered pits visible in radial and tangential walls (Fig. 3.31B–C), fibers not associated with vessels generally without pits (Fig. 3.31D), fibers non-septate. *Axial parenchyma* not observed. *Rays* 1–2 (mostly 1) seriate (Fig. 3.31E), biseriate rays often composed of just a few pairs of cells along an otherwise uniseriate ray; multiseriate rays homocellular composed of all procumbent cells, the marginal row often with large and barely procumbent cells (Fig. 3.31F), occasional rows of large, barely procumbent cells within rays; ray height average 141 (SD 69, range 39–334) µm, uniseriate rays as tall as biseriate rays, range for all rays 23–36 per mm.

*Description in IAWA Hardwood List codes (IAWA Committee 1989)* –

2 5 7v 9 13 22v 24 30 40 41 48 49 52 56 60 62 63 66 69 75 96 97v 104 106 116

*Remarks* – This Group IIIA wood (axial parenchyma rare) differs from *Fulleroxylon* sp. 1 (TXSTATE 1275) by having solitary vessels arranged in a radial or diagonal pattern, smaller diameter vessels and more vessels per square millimeter, smaller bordered vessel-ray parenchyma pits and only non-septate fibers.

**McRae Group IIIA: Vessels exclusively solitary**

**b. Axial parenchyma common**

**i. Rays >10 cells wide**

*Family* – unknown

*Species* – McRae Group IIIA sp. 2

*Holoxylotype* – TXSTATE 1279 (Fig. 3.32–3.33).

*Stratigraphic horizon* – McRae Formation, Jose Creek Member

*Age* – Late Campanian

*Material* – Estimated minimum stem diameter of 34 cm, collected as float

*Locality* – Texas State University Paleobotanical Locality 1992-3

*Description* – *Growth rings* absent. *Wood* diffuse porous (Fig. 3.32A). *Vessels* solitary (92%) and in radial multiples of 2, average 21 (SD 8, range 12–37)/mm<sup>2</sup> in the region between rays, average 9 (SD 2, range 7–11)/mm<sup>2</sup> including rays, solitary vessels oval in outline, vessel radial diameters wider than tangential diameter (Fig. 3.32B), mean tangential diameter 113 (SD 32, range 52–172) μm; vessel element length average 451 (SD 107, range 234–659) μm (Fig. 3.32C); perforation plates simple (Fig. 3.32C); intervessel pits not observed. *Vessel-ray pits* with distinct borders, small, throughout the cross field, not crowded (Fig. 3.32D). *Vessel-axial*

*parenchyma pitting* similar to vessel-ray pitting (Fig. 3.32E). *Tyloses* not observed. *Fibers* angular in cross section, thin-walled (Fig. 3.32F), non-septate with small simple pits. *Axial parenchyma* scanty paratracheal to vasicentric (Fig. 3.32C, 3.33A), diffuse or diffuse-in-aggregates forming short tangential or radial lines (Fig. 3.33B,C), 2–4 cells per parenchyma strand (Fig. 3.33D). *Rays* average 11 (SD 4, range 4–18) seriate (Fig. 3.33E), not strongly heterocellular, the body composed of fairly uniform procumbent cells, the marginal rows (1 to several) barely procumbent to square or upright (Fig. 3.33F–G); square or upright row(s) occasionally within rays; ray height average 979 (SD 398, range 278–1932)  $\mu\text{m}$ ; uniseriate rays not observed; range for all rays 2–4 per mm.

*Description in IAWA Hardwood List codes (IAWA Committee 1989) –*

2 5 9 13 22? 30 42 47 48 53 61 66 69 77 78 79 91 92 99 102v 104 106 107v 114

*Remarks* – This xylotype is distinguished from other Group IIIA (axial parenchyma common) by having exclusively simple perforation plates and rays >10 cells wide.

### **McRae Group IIIA: Vessels exclusively solitary**

#### **b. Axial parenchyma common**

##### **ii. Rays <10 cells wide**

*Family* – unknown

*Species* – McRae Group IIIA sp. 3

*Holoxylotype* – TXSTATE 1280 (Fig. 3.34–3.35).

*Stratigraphic horizon* – McRae Formation, Jose Creek Member

*Age* – Late Campanian

*Material* – Estimated minimum stem diameter of 40 cm, collected as float

*Locality* – Texas State University Paleobotanical Locality 1992-3

*Description* – *Growth rings* absent. *Wood* diffuse porous. *Vessels* solitary (91%) (Fig. 3.34A) and rarely in radial multiples of 2 (up to 3), average 5 (SD 1, range 4–8)/mm<sup>2</sup>, solitary vessels round to oval in outline, tangential diameter 72–168 (average 109, SD 22) µm; vessel element length average 259 (SD 38, range 156–299) µm (Fig. 3.34B); perforation plates simple (Fig. 3.34C), very rarely scalariform (Fig. 3.34D); intervessel pits alternate (Fig. 3.34E), polygonal in outline, medium to large, 8–12 µm in diameter. *Vessel-ray parenchyma pits* simple, pits elongated horizontally, crowded (Fig. 3.34F). *Vessel axial parenchyma pitting* like vessel-ray pitting. *Tyloses* occasionally present, bubble-like. *Fibers* angular in cross section, very thin-walled, short, generally non-septate, rarely septate with wispy septae, with simple or reduced border pits in radial view (Fig. 3.34G), pits 4–8 µm in diameter, or fibers somewhat longer, narrower and without obvious pits (Fig. 3.35A). *Axial parenchyma* common (Fig. 3.35A–D), vasicentric sheath of 1 to several cells, generally wider radially than tangentially, and diffuse-in-aggregates in lines 1–3 cells wide, spanning between rays (Fig. 3.35C) and sometimes across several rays, 2–4 cells per strand (Fig. 3.35D), with a tendency to be irregularly storied. *Rays* 3–7 (mostly 4–5) seriate (Fig. 3.35E), homocellular, composed of all procumbent cells, the marginal rows sometimes barely procumbent, or heterocellular and procumbent with 1 (up to 2) square or upright cells (Fig. 3.35F); ray height average 17 (SD 7,

range 6–35) cells or average 508 (SD 206, range 43–129)  $\mu\text{m}$ ; uniseriate or biseriate rays not observed; range for all rays 3–8 per mm.

*Description in IAWA Hardwood List codes (IAWA Committee 1989) –*

2 5 9 13v 22 23 26 27 32 42 47 52 61 65v 66 68 69 77 79 86v 91 92 98 104 106v  
114 115 122v

*Remarks* – This specimen shares some characteristics with McRae Group IIIA sp. 4 (TXSTATE 1281, see below). It differs by the round to oval shape of the vessels and larger vessel-ray pitting. Both xyloxytypes have longer, narrower, non-septate fibers that transition to shorter, wider, septate fibers with simple pits. However, the fibers of McRae Group IIIA sp. 3 are predominantly intermediate (i.e., shorter, wider, without pits or septae), with few fibers at the extremes of the continuum than McRae Group IIIA sp. 4. The rays of this specimen are wider and uniseriate rays are not observed. Specimen McRae Group IIIA sp. 3 represents a larger diameter stem (estimated diameter of 40 cm vs. 8 cm for TXSTATE 1281), which might account for differences in ray anatomy. If additional specimens are found that show anatomy transitional between these two xyloxytypes, the decision to “split” them into two xyloxytypes will be revisited.

*Family* – unknown

*Species* – McRae Group IIIA sp. 4

*Holoxylotype* – TXSTATE 1281 (Fig. 3.36–3.38).

*Stratigraphic horizon* – McRae Formation, Jose Creek Member

*Age* – Late Campanian

*Material* – Estimated minimum stem diameter of 8 cm, collected as float

*Locality* – Texas State University Paleobotanical Locality 1991-15

*Paraxylotype* – TXSTATE 1282.

*Stratigraphic horizon* – McRae Formation, Jose Creek Member

*Age* – Late Campanian

*Material* – Estimated minimum stem diameter of 4 cm, collected as float

*Locality* – Texas State University Paleobotanical Locality 1991-15

*Description* – *Growth rings* indistinct or absent. *Wood* diffuse porous (Fig. 3.36A); *vessels* solitary (82–85%) and in radial multiples of 2 (up to 3), mean of means 8 (3), range 7 (2)–8 (3) /mm<sup>2</sup>, solitary vessels angular in outline, tangential diameter mean of means 88 (3), range 86 (16)–90(16) μm; vessel element length average 270 (44), range 239 (38)–301 (48) μm; perforation plates exclusively simple (Fig. 3.36B), intervessel pits crowded alternate (Fig. 3.36C), polygonal in outline, sometime horizontally elongate and with wide apertures, medium to large, 7–12 μm in diameter. *Vessel-ray parenchyma pits* with reduced borders to simple, sometimes with many small ovals covering the cross field (Fig. 3.36D), or larger ovals, some horizontally to diagonally elongate with few per cross field (Fig. 3.36E). *Vessel-axial parenchyma pits* simple, horizontally elongate (Fig. 3.36F). *Tyloses* very thin-walled when present (Fig. 3.37A). *Fibers* transitional between two types; long, thin-walled, non-septate fibers, rarely with reduced bordered or simple pits, angular in shape as seen in transverse section, often radially narrowed for several rows forming discontinuous bands (Fig. 3.37B, D), transitioning to an intermediate form

of short, larger diameter, non-septate fibers without pitting (Fig. 3.37E–F), transitioning to short, large diameter, very thin-walled, septate fibers (Fig. 3.38A), often with reduced bordered or simple pits, angular to undulating in shape as seen in transverse section, pits minute to large diameter, predominantly on radial walls (Fig. 3.38A). Tangential bands of long fibers alternate with tangential regions of short fibers (Fig. 3.36A, 3.37C,D), with width of the alternating bands variable. *Axial parenchyma* common, vasicentric, narrow sheath and diffuse-in-aggregates forming discontinuous tangential lines 1 – several cells wide interspersed among both narrow and large diameter fibers (Fig. 3.38B), 2–4 cells per strand. *Rays*, 1–4 (to 5) (mostly 2–4) seriate (Fig. 3.38C), not strongly heterocellular, composed of procumbent cells with 1 marginal row of barely procumbent, upright or square cells (Fig. 3.38D), ray parenchyma variable in size (Fig. 3.38E); ray height mean of means 427 (81), range 369 (162)–484 (233)  $\mu\text{m}$ ; range for all rays 8–11 per mm.

*Description in IAWA Hardwood List codes (IAWA Committee 1989) –*

2 5 12 13 22v 23 26 27 31 32 41 47 52 61v 65 66 67 68 69 77 79 86v 91 92 97 98v  
104 106 115

*Remarks* – The two specimens (TXSTATE 1281 and 1282) were collected at the same site, and it is not possible to rule out they originate from the same individual plant. Both represent small-diameter axes, and the ranges of their anatomical features overlap.

The woods are similar to McRae Group IIIA sp. 3, which has similar vessel diameters and density, though rays of this xylotype are narrower. This xylotype differs from TXSTATE McRae Group IIIA sp. 3 in having vessels with angular outline,

smaller vessel-ray pits with reduced borders and marked differences in fiber anatomy, represented by two extreme distinct types of fibers (large diameter, short, thin-walled, septate fibers and narrow diameter, long, medium thick-walled, non-septate fibers). McRae Group IIIA sp. 4 is quite similar to McRae Group IIIA sp. 3 and eventually could be assigned to the same genus as a different species.

**McRae Group IIIB: Vessels both solitary and in radial multiples**

Group IIIB specimens (Table 3.7) have a combination of vessels solitary and in radial multiples. There are six types in this group; three types with rare to scanty axial parenchyma and three with common axial parenchyma either in lines one to several cells wide or vasicentric to lozenge-aliform.

**McRae Group IIIB: Vessels both solitary and in radial multiples**

**a. Axial parenchyma rare to scanty paratracheal**

*Family* – unknown

*Species* – McRae Group IIIB sp. 1

*Holoxylotype* – TXSTATE 1283 (Fig. 3.39–3.40).

*Stratigraphic horizon* – McRae Formation, Jose Creek Member

*Age* – Late Campanian

*Material* – Estimated minimum stem diameter of 18 cm, collected as float

*Locality* – Texas State University Paleobotanical Locality 2012-50

*Description* – *Growth rings* absent. (Fig. 3.39B). *Wood* diffuse porous. *Vessels* solitary (26%) and in radial or oblique multiples of 2–3 (up to 6) (Fig. 3.39A), average 55 (SD 34, range 33–82)/mm<sup>2</sup>, solitary vessels oval in outline, mean

tangential diameter 69 (SD 16, range 40–98)  $\mu\text{m}$ ; vessel element length average 442 (SD 145, range 171–717)  $\mu\text{m}$ ; perforation plates simple (Fig. 3.39C); intervessel pits alternate (Fig. 3.39D), polygonal in outline, small to medium, 6–10  $\mu\text{m}$  in diameter. *Vessel-ray pits* with reduced borders or simple, round to horizontally or diagonally oval, or irregular in shape, small to large in size, not crowded (Fig. 3.39E). *Tyloses* common, bubble-like and segmenting vessels (Fig. 3.39F). *Fibers* not strongly angular in cross section, thin-walled (Fig. 3.40A), mostly non-septate, occasionally septate (Fig. 3.40B), pitting not observed. *Axial parenchyma* not common, scanty paratracheal (Fig. 3.40C), strand length not observed. *Rays* 1–3 seriate (Fig. 3.40D), multiseriate rays homocellular, composed of more-or-less uniform procumbent cells, the marginal rows sometimes larger (Fig. 3.40E), multiseriate ray height average 311 (SD 260, range 72–871 (mostly < 500, rarely > 1mm)  $\mu\text{m}$ ; uniseriate rays (27%), <20 cells tall, up to 300  $\mu\text{m}$  tall; range for all rays 15–37 per mm. *Prismatic crystals* present in ray cells (Fig. 3.40F).

*Description in IAWA Hardwood List codes (IAWA Committee 1989) –*

2 5 10v 13 22 23 25 26 31 32v 41 48 49 53 56 65v 66 69 75v 78 97 104 116 136  
138

*Remarks* – The description of this xylotype indicates the absence of growth boundaries. There is one area of radially narrowed fibers (Fig. 3.39A) in transverse view, but because the area was discontinuous (did not extend tangentially across the slide), it is not interpreted as a growth boundary.

McRae Group IIIB sp. 1 differs from McRae Group IIIA sp. 2 by having a higher percentage of solitary vessels, only reduced bordered vessel-ray parenchyma

pits, a higher percentage of uniseriate rays, rays with all procumbent cells and crystals in the ray parenchyma.

*Family* – unknown

*Species* – McRae Group IIIB sp. 2

*Holoxylotype* – TXSTATE 1284 (Fig. 3.41–3.42).

*Stratigraphic horizon* – McRae Formation, Jose Creek Member

*Age* – Late Campanian

*Material* – Estimated minimum stem diameter of 26 cm, collected as float

*Locality* – Texas State University Paleobotanical Locality 1991-17A

*Paraxylotype* – TXSTATE 1285 (Fig. 3.43)

*Stratigraphic horizon* – McRae Formation, Jose Creek Member

*Age* – Late Campanian

*Material* – Estimated minimum stem diameter of 24 cm, collected as float

*Locality* – Texas State University Paleobotanical Locality 2014-15

*Description* – *Growth rings* absent. *Wood* diffuse porous. *Vessels* solitary (11-38%) and in radial or oblique multiples of 2–4 (-6) (Fig. 3.41A), mean of means 50 (SD 37, range 24–76)/mm<sup>2</sup>, solitary vessels round to oval in outline, tangential diameter mean of means 67 (SD 14, range 57–77) μm; vessel element length mean of means 249 (SD 49, range 214–283) μm (Fig. 3.41B); perforation plates simple (Fig. 3.41C); intervessel pits alternate (Fig. 3.41D), polygonal in outline, small to large, 6–12 μm in diameter. *Vessel-ray pits* with reduced borders to simple or with

slightly reduced borders to bordered, oval to elongate or irregular in shape or, round to horizontally, diagonally or vertically oval, sometimes elongate, sometimes irregular in shape, small to large in size (Fig. 3.41E). *Vessel-axial parenchyma pitting* with reduced borders, horizontally elongate ovals (Fig. 3.41F). *Tyloses* common, segmenting vessels and bubble-like (Fig. 3.41G). *Fibers* thin-walled (Fig. 3.42A), septate (Fig. 3.42B) and non-septate (Fig. 3.42C). *Axial parenchyma* not common, scanty paratracheal to very scanty paratracheal, strand length not observed. *Rays* 2–4 (rarely 1, mostly 3) seriate (Fig. 3.42D), multiseriate rays homocellular and composed of all more-or-less uniformly-sized procumbent cells, the marginal row sometimes large procumbent (Fig. 3.42E), or heterocellular composed of procumbent cells with one marginal row upright or square cells (Fig. 3.42F), multiseriate ray height mean of means 187 (SD 43, range 156–217)  $\mu\text{m}$ ; uniseriate rays uncommon, < 100  $\mu\text{m}$  tall; range of means for all rays 14–21 per mm.

*Description in IAWA Hardwood List codes (IAWA Committee 1989) –*

2 5 10v 13 22 23 25 26 27 31 32 41 48 49 52 56 65 66 69 78v 97 98 104 106 116

*Remarks* – Data from specimens TXSTATE 1284 and TXSTATE 1285 were combined for this xylotype. Specimen TXSTATE 1285 differs from TXSTATE 1284 in having a higher percentage of solitary vessels, shorter vessel multiples (radial multiples of four vessels present) (Fig. 3.43A), larger vessels at lower density (24/mm<sup>2</sup> vs. 76/mm<sup>2</sup>), larger intervessel pits (Fig. 3.43B), rays spaced farther apart (Fig. 3.43D) and more obvious areas with non-septate fibers (Fig. 3.43F). The specimens are approximately equal in estimated diameter, so it is unlikely that differences are due to position within the stem. Qualitative features (e.g., vessel-ray

pitting (Fig. 3.43C), septate fibers (Fig. 3.43F) and ray cellular composition (Fig. 3.43G, I) were very similar. The specimens are clearly related and would be assigned to the same genus. Differences might warrant splitting into separate species if such anatomical features prove to have been useful for differentiating species in the extant affinity, once identified.

McRae Group IIIB sp. 2 differs from McRae Group IIIA sp. 1 by having a lower percentage of solitary vessels, both bordered and reduced bordered vessel-ray parenchyma pits, a lower percentage of uniseriate rays, some rays with one marginal row of square or upright cells and crystals not observed in the ray parenchyma.

### **McRae Group IIIB: Vessels solitary and in radial multiples**

#### **b. Axial parenchyma common (vasicentric-lozenge aliform)**

*Family* – unknown

*Species* – McRae Group IIIB sp. 3

*Holoxylotype* – TXSTATE 1286 (Fig. 3.44–3.45).

*Stratigraphic horizon* – McRae Formation, Jose Creek Member

*Age* – Late Campanian

*Material* – Estimated minimum stem diameter of 8 cm, collected as float

*Locality* – Texas State University Paleobotanical Locality 1991-15

*Description* – Wood diffuse porous. *Growth rings* absent. *Vessels* solitary (45%) and in radial multiples of 2–3 (up to 4) (Fig. 3.44A), diffuse, average 26 (SD 5, range 17–31)/mm<sup>2</sup>, solitary vessels oval in outline, mean tangential diameter 64

(SD 12, range, 43–92)  $\mu\text{m}$ ; vessel element length average 175 (SD 47, range 72–267)  $\mu\text{m}$  (Fig. 3.44B); perforation plates simple (Fig. 3.44C); intervessel pits alternate (Fig. 3.44D), polygonal in outline, small to medium, 6–10  $\mu\text{m}$  in diameter. *Vessel-ray parenchyma pits* with reduced borders to simple, round to horizontal elongate, some large simple, horizontally elongate oval (Fig. 3.44E–F). *Tyloses* not common. *Fibers* angular in transverse view, thin-walled (Fig. 3.44G), pits not observed, fibers non-septate (Fig. 3.45A). *Axial parenchyma* common, vasicentric (broad sheath) to lozenge-aliform (Fig. 3.45B), 2–4 (rarely up to 8) cells per strand (Fig. 3.45C). *Rays* 1–2 (3) seriate (Fig. 3.45D), nearly homocellular, composed of procumbent cells (Fig. 3.45E), rarely with a few square or upright cells on the marginal row; ray height average 8 (SD 4, range 2–15) cells or average 131 (SD 66, range 40–288)  $\mu\text{m}$ ; range for all rays 7–23 per mm.

*Description in IAWA Hardwood List codes (IAWA Committee 1989) –*

2 5 12v 13 22 23 25 26 31 32 41 48 52 66 69 79 80 81 91 92 93v 97 104 106v 116

*Remarks* – This xylotype differs from other woods in Group IIIB (axial parenchyma common) by the small vessel diameters, higher vessel density, reduced bordered vessel-ray pits (bordered pits not observed), vasicentric to lozenge-aliform axial parenchyma, narrow and short rays, and the nearly homocellular rays.

The wood was host to a well-preserved fungus with reproductive structures (Harper et al. 2018) (Fig. 3.45F–G).

#### **McRae Group IV: Simple and scalariform perforation plates (absent oil cells)**

The vast majority of woods found at the McRae have exclusively scalariform or exclusively simple perforation plates. To date, only two xylotypes with both

simple and scalariform plates have been recognized (Table 3.8). One has oil cells and is included in Group I, the other is assigned to Group IV (below). Save for the presence of some scalariform perforation plates, this wood would fall within Group IIIB.

*Family* – unknown

*Species* – McRae Group IVB sp. 1

*Holoxylotype* – TXSTATE 1289 (Fig. 3.46–3.47).

*Stratigraphic horizon* – McRae Formation, Jose Creek Member

*Age* – Late Campanian

*Material* – Estimated minimum stem diameter of 25 cm, collected as float

*Locality* – Texas State University Paleobotanical Locality 2013-33

*Description* – *Growth rings* absent. *Wood* diffuse porous. *Vessels* solitary (40%) and in radial multiples of 2–3 (4) (Fig. 3.46A), average 120 (SD 14, range 105–135)/mm<sup>2</sup>, solitary vessels round to oval in outline (Fig. 3.46B), mean tangential diameter 36 (SD 9, range 19–51) µm; vessel element length average 350 (SD 93, range 148–514) µm (Fig. 3.46); perforation plates (Fig. 3.46D, F) mostly simple, less commonly scalariform with 1 or 2 bars, occasionally multiperforate plates with 2 or 3 adjacent large, circular, simple openings; intervessel pits alternate (Fig. 3.46G), 5–7 µm in diameter. *Vessel-ray pits* with reduced borders to simple, round (Fig. 3.46H) to horizontal or diagonal ovals (Fig. 3.46A), large, often spanning the full height of the cell. *Tyloses* common, bubble-like (Fig. 3.47B). *Fibers* thin-walled, pits not observed, septate (Fig. 3.47C). *Axial parenchyma* absent, strand

length not observed. Rays 1–3 (mostly 1–2) seriate (Fig. 3.47D), multiseriate rays homocellular composed of procumbent cells (Fig. 3.47E), the marginal rows sometimes large procumbent or heterocellular with 1–2 marginal rows of upright or square cells (Fig. 3.47F), occasionally with 1–2 rows square or upright cells within the ray body, multiseriate rays 2–3 cells wide along their entire length, not just a few cell pairs; ray height average 208 (SD 113, range 43–433)  $\mu\text{m}$ ; uniseriate rays composed of procumbent and square or upright cells, 43–306  $\mu\text{m}$  tall; range for all rays 13–30 per mm.

*Description in IAWA Hardwood List codes (IAWA Committee 1989) –*

2 5 13 14 15 22 25 31 40 49 50 52 53 56 65 69 75 97 104 106 107v 116

*Remarks* – Key anatomical features of this fossil wood include vessels solitary and in radial multiples up to four, a combination of simple perforation plates and scalariform plates having only one or two bars, occasionally multiperforate plates with 2 or 3 adjacent large, circular, simple openings, alternate intervessel pitting, vessel-ray pits simple or with reduced borders, narrow rays (mostly 1–2 cells wide) composed predominantly of procumbent cells and few square or upright marginal rows, septate fibers and axial parenchyma absent.

## DISCUSSION

This report is a continuation of the exploration of woods from the Jose Creek Member of the McRae Formation. The initial work has focused on canvassing Jose Creek wood-bearing localities to collect different wood types and to accumulate data for comparison with other Cretaceous and Paleogene fossil wood floras. The significance of this flora is heightened by the fact that few Cretaceous wood floras

share this level of diversity or quality of preservation, nor are they composed primarily of mature specimens.

The species richness of the Jose Creek Member angiosperm flora rivals that described by Page (1967, 1968, 1970, 1979, 1980, 1981) for the Upper Cretaceous (Maastrichtian) Panoche of Central California, USA. The Panoche flora, with 47 described basic wood types, is significant, though many types could not be assigned to a modern family. Limited preservation of the specimens meant that critical anatomical features were often missing from the descriptions, and approximately 70% of the specimens comprise small diameter axes that represent branches or roots, the anatomical features of which can be significantly different from those of mature specimens (Barghoorn 1941, Bailey 1944). Because comparison to mature woods was incomplete, Page placed the woods in an artificial classification system. In contrast, approximately 71% of the Jose Creek angiosperm xyloids are described from mature wood (estimated stem diameter >10 cm) with good preservation. Critical features are observed for most woods, and many are described in sufficient detail to distinguish among unrelated families with similar anatomical features.

The significance of the Jose Creek Member flora is becoming apparent. In terms of numbers, the 35 Jose Creek non-monocot angiosperm xyloids approaches the Panoche total. Since exploration of known localities of the Jose Creek is ongoing, it is anticipated that additional xyloids will be discovered. Among the Jose Creek descriptions, first reports of woods in some genera and families (e.g.,

Sapotaceae and Connaraceae) distinguish this flora from that of the Panoche Formation.

The Panoche flora is characterized by the absence of some specialized anatomical features (Page 1980). Page noted the absence of axial parenchyma in multiseriate bands or aliform sheaths in the Panoche xyloids. The Panoche woods also have a high percentage of scalariform perforation plates, an anatomical feature considered ancestral in terms of the Baileyan transformation series (Bailey 1953, cf. Olson 2012) and which has a much higher incidence in the Cretaceous than the present day (Wheeler and Baas 1991). The late Campanian McRae Formation, though from an earlier time period than the Maastrichtian Panoche Formation, has multiple xyloids with these features. Of the 35 described Jose Creek non-monocot angiosperm xyloids, 60% have exclusively simple perforation plates and 20% have common axial parenchyma in the form of diffuse-in-aggregate lines, "patches," aliform or confluent distributions. Intervessel pitting is alternate in 57% of xyloids, also a feature considered to be derived. Page considered specimen CASG 60432 to be the most specialized of the Panoche woods, in part, because axial parenchyma was absent and uniseriate rays infrequent. Of the Jose Creek xyloids, 17% have rare or absent axial parenchyma, and 46% have few uniseriate rays. Our understanding of the level of evolutionary advancement of a flora is based on the type and frequency of such anatomical features, independent of the affinities of the wood (Wheeler and Baas 1991). The relatively derived features present in the Jose Creek flora distinguish it from the better known flora of Central California described by Page (1967, 1968, 1970, 1979, 1980, 1981).

## **Climatic evidence**

The following paleoenvironmental proxies present at the Jose Creek Member sites can be used to independently reconstruct the climate. Previous studies demonstrate that the combination of taxa represented by the leaf macrofossils present in the Jose Creek Member (palms and cycads, Zingiberaceae, Magnoliidae, and conifers) is consistent with evergreen vegetation that today occurs only where temperatures are consistently above freezing (Upchurch and Mack 1998, Estrada-Ruiz 2012b). Today, palms are restricted to climates where the Mean Annual Temperature (MAT) is at least 13°C and the Cold Month Mean Temperature (CMMT) is at least 5°C (Greenwood and Wing 1995, Markwick 2007). This boundary for the minimum temperature is consistent with leaf physiognomy studies that estimate MAT for the the southern Western Interior climate as megathermal (20 – 25°C), with year-round precipitation and little seasonality (Wolfe and Upchurch 1987, Upchurch and Wolf 1987, Upchurch et al. 2015). The absence of annual rings in most Jose Creek angiosperm and conifer woods is consistent with those findings, as is the presence of palms and cycads that are susceptible to freezing and require consistent moisture availability (Upchurch and Mack 1998, Estrada-Ruiz et al 2012b, this report). Paleosols in the Jose Creek Member support the conclusions regarding precipitation, given that modern udalf soils, like those present in the Jose Creek Member, are typically found in areas with annual precipitation greater than 75-100 cm (Buck and Mack 1995).

## Search for family affinity

Over 100 specimens have been sectioned and sorted into 35 non-monocot angiosperm xylotypes, 19 of which are described in this chapter. The remaining woods were described by Estrada-Ruiz et al. (2012a, 2012b, 2018) or are contained in chapters of this dissertation. Some woods represent common elements in the fossil record. For example, six of the 35 woods (17%) have anatomical features consistent with the family Lauraceae, in particular idioblasts thought to represent oil cells. *Pygmaeoxyton* (Estrada-Ruiz et al. 2012a) also has idioblasts thought to represent oil cells, and appears to belong to the magnoliid clade, though wide rays exclude it from Lauraceae. The percentage of magnoliid clade xylotypes in the Jose Creek wood flora (Fig. 1.3, 1.4, Fig. 3.2–3.11) is only slightly lower than the 25% Magnoliidae species present in the early Eocene London Clay fruit and seed flora that Wolfe et al. (1975) thought revealed the importance of magnoliids in Eocene megathermal vegetation relative to that of the modern day. It is also consistent with the common occurrence of floral remains belonging to Lauraceae in Early and Late Cretaceous floras (e.g., Friis et al. 2011).

*Paraphyllanthoxylon*-like wood, the dominant taxon at the Forest of Giants locality, is common in Cretaceous floras. Jud et al. (2017) provide a comparison of Cretaceous *Paraphyllanthoxylon* species and a map of their global distribution. The details of the McRae *Paraphyllanthoxylon*-like wood are discussed at length in Chapter 1 of this dissertation. The phylogenetic position of *Paraphyllanthoxylon* remains unresolved. A search of the InsideWood database supports affinity with families currently recognized as the monophyletic clade [Kirkiaceae +

[Anacardiaceae +Burseraceae]] in Sapindales, with the greatest similarity to Kirkiaceae. This is consistent with observations by Spackman (1948) who also reported similarities between *Paraphyllanthoxylon* and woods of Anacardiaceae, Burseraceae and *Kirka*, a genus then attributed to Simaroubaceae, as well as Euphorbiaceae. The resemblance of *Paraphyllanthoxylon* woods to multiple families, as noted in the earliest reports, contributed to the long-held belief that woods of *Paraphyllanthoxylon* should remain a form genus without designated family affinity (Bailey 1924, Spackman 1948, Thayne and Tidwell 1984, Wheeler et al. 1987). If *Paraphyllanthoxylon* affinity with Sapindales is confirmed, it emphasizes the importance of eudicots as large trees in Cretaceous landscapes.

A second hypothesis for *Paraphyllanthoxylon* affinity is based on the description of reproductive axes (*Mauldinia mirabilis* Drinnan, Crane, Friis et Pedersen) that Herendeen (1991a) reported to link the wood of *Paraphyllanthoxylon marylandense* to Lauraceae. The *Mauldinia* floral axis was reevaluated by Doyle and Endress (2010) and the affinity proposed as sister to Lauraceae and Hernandiaceae or, perhaps, closer to Monimiaceae. If *P. marylandense* is correctly assigned to the genus *Paraphyllanthoxylon*, this would increase the proportion of magnoliids (though not specifically Lauraceae) in fossil wood floras and demonstrate dominance of magnoliids in sites like the Forest of Giants, which is predominately *Paraphyllanthoxylon*. Without a *Paraphyllanthoxylon* Lauraceae relationship, the two Forest of Giants species with oil cells (*Paraphyllanthoxylon* and a second species from the logjam area related to the

Forest of Giants) would still suggest that Laurales were an important floral component of the forest association.

Specimen TXSTATE 1265 is similar to the type species of *Icacinoxylon* and differs primarily in the width of the narrow rays. Page (1979) described woods from the upper portions of the Great Valley Sequence that share some features with Icacinaceae, but the samples could not be identified with certainty. Woods assigned to *Icacinoxylon* have been reported from the Lower Cretaceous Cedar Mountain Formation of Utah (Thayn et al. 1985) and the Potomac Group of eastern North America (Herendeen 1991b). This genus is also reported from Asia and Europe: the Turonian of Hokkaido, Japan (Takahashi et al. 2003), Cenomanian of the Czech Republic (Oakley et al. 2009) and Sweden and Portugal (Herendeen 1991b). The extent to which these woods conform to the original diagnosis of *Icacinoxylon*, and their relationships with extant taxa, must be the subject of future studies.

Four xylotypes with exceptionally wide (>10 cells) and nearly homocellular rays appear related to the family Platanaceae (see Chapter 2). While these wood types differ from extant *Platanus* in having exclusively scalariform perforation plates and exclusively solitary vessels, there is a continuum of character states between these Cretaceous woods and the extant genus. The woods will be assigned to a fossil genus within the Platanaceae in formal publication. Woods similar to the McRae *Platanus*-like woods are a common element in fossil assemblages of Cretaceous and early Cenozoic age. Wheeler (1991) reported *Platanus*-like woods from the Paleocene Black Peaks in Big Bend, TX, USA. Species assigned to *Platanoxylon* are known from the lower Maastrichtian Kirtland Formation, San Juan

Basin of New Mexico (Wheeler et al. 1995) and Upper Cretaceous sites in Hokkaido, Japan (Takahashi and Suzuki 2003). While these woods share some of the anatomical features found in the McRae xylo types, they differ in others (Table 2.2, 2.3). *Platanus*-like woods more similar to the McRae xylo types were described by Page (1968) from the Panoche Formation of California, USA and by Crawley (1989) from the upper Paleocene Reading Beds, UK. Further study of the fossil *Platanus*-like species is warranted to distinguish between woods that fall within the generic diagnosis of *Platanoxylon* and those falling within the new genus.

Two Jose Creek Member genera with exclusively scalariform perforation plates are known from other Late Cretaceous wood assemblages: *Agujoxylon*, first reported from the Aguja Formation of Big Bend National Park, Texas (Wheeler and Lehman 2000) and *Metcalfexylon*, first described from the lower Kirtland Formation of San Juan Basin (Wheeler et al. 1995). *Metcalfexylon* was also found in the Aguja Formation of Big Bend (Wheeler and Lehman 2000) and was later discovered in the Olmos Formation of Coahuila, Mexico, and the Crevasse Canyon Formation of New Mexico, which underlies the McRae Formation (Estrada-Ruiz et al. 2010, 2012a, 2012b). Both *Agujoxylon* and *Metcalfexylon* are known from large-diameter specimens (Table 3.3). The largest Big Bend *Agujoxylon* and *Metcalfexylon* specimens exceed 100 cm stem diameter; the largest Crevasse Canyon *in situ* *Metcalfexylon* stump is 75 cm diameter.

A search for affinities for the majority of McRae xylo types with exclusively simple perforation plates (or a combination of simple and scalariform plates) has not been conducted, with the exception of specimen TXSTATE 1275, described in

this chapter as a probable Connaraceae and the Forest of Giants woods. The Forest of Giants xylotypes are discussed at length in Chapter 1.

### **Future study**

As the study of family affinities of the McRae woods progresses, continued comparison to fossil and modern floras in terms of species composition will be possible. Additional McRae species may represent first records of families. Species that are unequivocally assigned to a family, where possible, will be placed in phylogenetic context. The woods will then be available to evaluate biogeographic analyses, or possibly, to serve as calibration fossils in molecular clock analyses.

Anatomical data from the McRae xylotypes (prior to assignment of family affinity) can be used to infer paleoclimate and to determine the functional / ecological attributes of the wood flora. Once available, results of the analyses will be compared to fossil wood floras from different latitudes and various environments. For example, the diameter of fossil stumps and logs and estimated diameter of samples collected as “float” can be used to estimate tree height (Rich et al. 1986) and to compare the role of conifers and angiosperms in the forest canopy. Potential conductivity and  $P_{50}$  address resistance to drought and the potential for movement of water through the xylem. Calculation of vulnerability indices (Carlquist 1975) for the woods may provide insight into the occurrence of freezing temperatures or drought. The specific gravity profile of an assemblage can be used for understanding the growth strategy of the woods (fast growth / low carbon investment vs. slow growth / high carbon investment) (Wiemann and Williamson 2002, Wheeler et al. 2007). Specific gravity also relates to temperature and moisture availability in the

environment (Chudnoff 1976, Barajas-Moraes 1987, Wiemann and Williamson 2002). The percentage of axial parenchyma cross-sectional area relates to moisture availability in tropical habitats (Fichtler and Worbes 2012).

Exploration of the Jose Creek Member is ongoing. Wood specimens from past field seasons remain to be processed, known localities warrant revisiting and new sites should be evaluated in upcoming field seasons.

Table 3.1. Groups IA, IB, IC – McRae Formation woods with oil cells.

Taxon	ESD (cm)	VA	V/mm <sup>2</sup>	VMTD	IVP (µm)	V-RP	F	AP	RW (cells)	RCC	RH (µm)	R/mm	Oil cells
<i>Laurinoxylon</i> sp. 1 Group IA sp. 1 TXSTATE 1250 Forest of Giants	60	25% sol, 2-3 (4-5)	12	127	alt, 6-10	rb, r/o/he	s, n-s	scp	2-6	1	557	9	large, m (s)
<i>Laurinoxylon</i> sp. 2 Group IA sp. 2 TXSTATE 1251	20	47% sol, 2-3 (4)	18	65	alt, 3-5	rb, r/o/he/de/c	s, n-s	scp	2-6, mostly 4-6	1-2	336	13	(large), m, s, w
<i>Pygmaeoxyton</i> <i>paucipora</i> <sup>1</sup> TXSTATE 1204	2.5	sol, 2 (4)	5.5	55	alt	rb, he	n-s	scp	3-10	sq, pro	>2mm	NA	in rays
<i>Laurinoxylon</i> sp. 3 Group IA sp. 3 TXSTATE 1252-1253	15, 35	24-33% sol, 2-3 (4-5+)	22-2 5	85-93	alt, 5-12	two types: rb, r/ o/he/de/c; large s	s	scp	3-7	1-2, w	477- 612	9-18	small, m, s, w
<i>Laurinoxylon</i> sp. 4 TXSTATE 1254 Group IA sp. 4	15	15% sol, 2-3 (4-5)	58	83	alt, 3-5	two types: rb, r/ o/he/de/c; large s	N Ob	scp	2-5	1, lg pro	319	10	small, m, (s)
Group IB sp. 1 TXSTATE 1255-1256	17	47-56% sol, 2-3 (4)	12-1 4	53-65	alt, 6-8	b, o	n-s	d, dia, alif-con	2-7, mostly 3-4	1, lg pro	259- 347	12	exp, m, s, w
<i>Laurinoxylon</i> <i>rennerae</i> <sup>2</sup> TXSTATE 1222	50	36% sol, 2-3 (4)	19	84	alt (opp) 8-10	rb, r/he	s (rare), n-s,	d, scp, v	(1) 2-4	1-2 (4)	396	9	m

<sup>1</sup> Estrada-Ruiz et al. 2012b.

<sup>2</sup> Estrada-Ruiz et al. 2018.

Table 3.1. Groups IA, IB, IC – McRae Formation woods with oil cells

*Legend:* ESD = estimated stem diameter in cm; VA = vessel arrangement, (sol) = solitary, range represents common radial vessel multiples, range in parentheses represents rare radial multiples; V/mm<sup>2</sup> = average vessel density, range equals range of mean values for multiple samples; VMTD = vessel mean tangential diameter, range represents range of means for multiple samples; IVP = intervessel pits, (alt) = alternate, range of pit diameters (μm); V-RP = vessel-ray parenchyma pits, (b) = bordered, (rb) = reduced borders, (s) = simple, (r) = round, (o) = oval, (he) = horizontally, (de) = diagonal elongate, (c) = curved; F = fiber, (s) = septate fibers, (n-s) = non-septate fibers; AP = axial parenchyma, (d) = diffuse, (dia) = diffuse-in-aggregates, (scp) = scanty paratracheal, (alif) = aliform, (con) = confluent, (v) = vasicentric; RW = range of ray widths; RCC = ray cellular composition, number range = number of uniseriate margin rows of square or upright cells, (w) = square or upright cells within ray, (lg pro) = margin row(s) composed of large procumbent cells; RH = mean ray height, range represents range of means for multiple samples; R/mm = average number of rays per millimeter or range for multiple samples; Oil cells = idioblasts with dark content, (m) = at the ray margin, (s) = at the side of the ray as seen in tangential view, (w) = within the ray as seen in tangential view, (axp) = in axial parenchyma. N Ob = Not observed due to quality of sample preservation.

Table 3.2. Groups IIA, IIB – McRae Formation woods with exclusively scalariform perforation plates.

Taxon	ESD (cm)	V/ mm <sup>2</sup>	VMTD	PP-#B	IVP	V-RP	FP	VT, #rows	AP	RW Multi (cells)	RCC	RW Uni	R/mm	Cr
<b>Group IIA: Rays &lt;10 cells wide</b>														
<i>Agujoxylon olacaceoides</i> TXSTATE 1257	m <sup>1</sup>	36	71	20-55	0	2 types: small s or rb, r/o/e & large s or rb o	1, con	-	com: d, scp	2-7	1-many, w, alt	-	12	-
Group IIA sp. 1 TXSTATE 1259	3	52	39	34-72	o-sc	b, iv, cr, very small	1, con	-	com: d, dia, scp	1-5 mostly 1-2	1-13, w, (alt)	33%	34	-
Group IIA sp. 2 TXSTATE 1260	7	48	47	20-28	0	rb, r/o, not cr, small	1, con	+, 2-3, sm	com: d	1-6	1-many, sh, not alt	23%	11	-
<i>Metcalfeoxylon kirtlandense</i> TXSTATE 1261	20	1-6	133	11-28	sub-o	b, not cr, very small	1, con	+	com: dia, sl, scp	1-5	1-26, w, alt	17%	14	-
Group IIA sp. 3 TXSTATE 1262-1264	7-60	16-39	56-66	15-45	0	b or rb, r/o/e	1, dis	+, 1, lg	Rare, d, scp	1-6	1-many, sh, alt	6-25%	18-27	- or r
<i>Baasia aremendarisense</i> 2 TXSTATE 1200	14	25	37, 43	38	o-alt	iv	-	-	d, scp	1, 4-7	1-10, alt	+	12-18	-
<i>Turneroxylon newmexicoensis</i> <sup>3</sup> TXSTATE 1213	12-24	8-22	80	13-31	o, sc	b or rb or s, r/o/e, cr or not cr	+	+, 1	d, dia	1, 3-6 (8)	1-2 (7)	+	6-15	-
<b>Group IIB: Rays &gt;10 cells wide, uniseriate rays common</b>														
cf. <i>lacinioxylon</i> sp. 1 TXSTATE 1265	9	18 between rays	82	6-23	0	b, r/o, cr	1, con	+, 2-3, sm	com: d, dia, scp	1-3, 16-30	1-4+	23%	18 (no rays)	-

Table 3.2. Groups IIA, IIB – McRae Formation woods with exclusively scalariform perforation plates.

*Legend:* Fossil woods are in bold type. ESD = estimated stem diameter in cm;  $V/mm^2$  = average vessel density, range equals range of mean values for multiple samples; VMTD = vessel mean tangential diameter; PP-#B = range of bars per perforation plate; IVP = intervessel pits, (o) = opposite, (sc) = scalariform, (v-t) = vessel tail; V-RP = vessel-ray parenchyma pits, (iv) = like intervessel pitting, (b) = bordered, (rb) = reduced borders, (s) = simple, (r) = round, (o) = oval, (e) = horizontally elongate, (cr) = crowded; FP = number of rows of pits on fibers, (con) = pits continuous over the length of the fiber, (dis) = short rows of pits alternating with areas without pits; VT, #rows = number of rows of pits on vasicentric tracheids, (+) = vasicentric tracheids present, (-) = vasicentric tracheids absent, (sm) = small pits, (lg) = large pits; AP = axial parenchyma, (d) = diffuse, (dia) = diffuse-in-aggregates, (scp) = scanty paratracheal, (v) vasicentric, (sl) = short lines, (com) = common; RW = range of ray widths; RCC = ray cellular composition, number range = number of uniseriate margin rows of square or upright cells, (w) = square or upright cells within ray, (sh) = sheath cells, (alt) = multiseriate ray portions joined by uniseriate ray portions; RW Uni = percentage of uniseriate rays, (+) = present, (-) = absent; R/mm = range of rays per millimeter; Cr = prismatic crystals, (-) = not observed, (r) = present in ray parenchyma, (ax p) = present in axial parenchyma.  
Blank spaces indicate unavailable information.

<sup>1</sup> Parallel rays indicate mature wood, but preclude estimation of stem diameter

<sup>2</sup> Estrada-Ruiz et al. 2012a

<sup>3</sup> Estrada-Ruiz et al. 2018

Table 3.3. Group IIA – Comparison of McRae Formation *Agujoxylon* and *Metcalfeoxylon* specimens to type species and previously reported occurrences from North America.

Taxon	ESD (cm)	V/mm <sup>2</sup>	VMT D	PP-#B	IVP	V-RP	FP	VT, #rows	AP	RW Multi (cells)	RCC	RW Uni	R/mm	Cr
<i>Agujoxylon. olacaceoides</i> TXSTATE 1257	m <sup>1</sup>	36	71	20-55	o	2 types: small, s or rb, r/o/e & large s or rb o	1, con	-	com: d, scp	2-7	1-many, w, alt	-	12	-
<i>Agujoxylon</i> sp. Crevasse Canyon TXSTATE 1258	24	30	58	30-68	o-sc	2 types: small, s or rb, r/o/e & large s or rb/o	1, dis	-	com: d, dia, sl, scp	1-6 mostly 4	1-30, alt	10%	16	r
<i>Agujoxylon olacaceoides</i> Big Bend <sup>2</sup>	> 40 -111	14-35	68	>20	o-sc	2 types: small, s or rb, r/o/e & large s or rb o	+	-	com: dia	4-6	alt	+	5-14	ax p
<i>Metcalfeoxylon kirtlandense</i> TXSTATE 1261	20	48	133	11-28	sub-o	b, not cr, very small	1, con	+	com: dia, sl, scp	1-5	1-26, w, alt	17%	11	-
<i>M. kirtlandense</i> San Juan Basin <sup>3</sup>	7	4	121	10-19	o	iv	+	+, 2+	com: d	1-4	15-20	+	6-9	-
<i>M. kirtlandense</i> Big Bend <sup>2</sup>	40-100	2-15	115	8-16	o-a	iv	+	+, >1	com: d	1-3	2-31	+	6-18	-
<i>M. kirtlandense</i> Olmos Formation <sup>4</sup>	6.2	4	121	10-26	o, a	iv	1-2	+, >2	d, dia, sl, scp, v	3-5	1-59	+	NA	-
<i>M. kirtlandense</i> TXSTATE 1206-1211 Crevasse Canyon <sup>5</sup>	400-750	5	144	< 20	o-a	iv	1	+, 2-3	com: d, dia	mostly 3	1-many	+	7-13	-

<sup>1</sup> Parallel rays indicate mature wood, but preclude estimation of stem diameter  
<sup>2</sup> Wheeler & Lehman (2000)

<sup>3</sup> Wheeler, McClammer and LaPasha (1995)

<sup>4</sup> Estrada-Ruiz, Martinez-Cabrera, and Cevallos-Ferriz, (2010)

<sup>5</sup> Estrada-Ruiz et al. 2012a, 2012b)

Table 3.3. Group IIA – Comparison of McRae Formation *Agujoxylon* and *Metcalfeoxylon* specimens to type species and previously reported occurrences from North America.

*Legend:* Fossil woods are in bold type. ESD = estimated stem diameter in cm; V/mm<sup>2</sup> = average vessel density, range equals range of mean values for multiple samples; VMTD = vessel mean tangential diameter; PP-#B = range of bars per perforation plate; IVP = intervessel pits, (o) = opposite, (sc) = scalariform, (v-t) = vessel tail; V-RP = vessel-ray parenchyma pits, (iv) = like intervessel pitting, (b) = bordered, (rb) = reduced borders, (s) = simple, (r) = round, (o) = oval, (e) = horizontally elongate, (cr) = crowded; FP = number of rows of pits on fibers, (con) = pits continuous over the length of the fiber, (dis) = short rows of pits alternating with areas without pits; VT, #rows = number of rows of pits on vasicentric tracheids, (+) = vasicentric tracheids present, (-) = vasicentric tracheids absent, (sm) = small pits, (lg) = large pits; AP = axial parenchyma, (d) = diffuse, (dia) = diffuse-in-aggregates, (scp) = scanty paratracheal, (v) vasicentric, (sl) = short lines, (com) = common; RW = range of ray widths; RCC = ray cellular composition, number range = number of uniseriate margin rows of square or upright cells, (w) = square or upright cells within ray, (sh) = sheath cells, (alt) = multiseriate ray portions joined by uniseriate ray portions; RW Uni = percentage of uniseriate rays, (+) = present, (-) = absent; R/mm = range of rays per millimeter; Cr = prismatic crystals, (-) = not observed, (r) = present in ray parenchyma, (ax p) = present in axial parenchyma.  
Blank spaces indicate unavailable information.

Table 3.4. Group IIA – Comparison of the McRae Formation Group IIA specimens “lumped” into Group IIA sp. 3.

Taxon	ESD (cm)	V/mm <sup>2</sup>	VMTD	PP-#B	IVP	V-RP	FP	VT, #rows	AP	RW (cells)	RCC	RH (µm)	RW Uni	R/mm	Cr
TXSTATE 1262	17	16	64	15-35	o-sc	b or rb, r/o, not cr, small	1, dis	-	rare: d, scp	1-5	1-30, w, sh, alt	293	25%	18	-
TXSTATE 1263	≈60	23	66	20-40	o-sc (v-t)	b or rb, o	1, dis	+, 1, lg	Rare: d	1-6	0-1 (to <10), sh, alt	453	6%	20	-
TXSTATE 1264	7	39	56	24-45	o-sc	b or rb, o/e, small	1, dis	+, 1, lg	N Ob	1-4	1-many, w, alt	248	20%	27	r
Group IIA sp 3. TXSTATE 1262-1264	7-60	16-39	56-66	15-45	o	b or rb, r/o/e	1, dis	+, 1, lg	Rare: d, scp	1-6	1-many, sh, alt	331	6-25%	18-27	- or r
Turneroxylon newmexicoensis <sup>1</sup> TXSTATE 1213	12-24	8-22	80	13-31	o, sc	b or rb or s, r/o/e, cr or not cr	+	Y, 1	d, dia	1, 3-6	1-2 (7)	545	+	6-15	-

<sup>1</sup> Estrada-Ruiz et al. 2018

Table 3.4. Group IIA – Comparison of the McRae Formation Group IIA specimens “lumped” into Group IIA sp. 3.

*Legend:* Fossil woods are in bold type. ESD = estimated stem diameter in cm;  $V/mm^2$  = average vessel density, range equals range of mean values for multiple samples; VMTD = vessel mean tangential diameter; PP-#B = range of bars per perforation plate; IVP = intervessel pits, (o) = opposite, (sc) = scalariform, (v-t) = vessel tail; V-RP = vessel-ray parenchyma pits, (iv) = like intervessel pitting, (b) = bordered, (rb) = reduced borders, (s) = simple, (r) = round, (o) = oval, (e) = horizontally elongate, (cr) = crowded; FP = number of rows of pits on fibers, (con) = pits continuous over the length of the fiber, (dis) = short rows of pits alternating with areas without pits; VT, #rows = number of rows of pits on vasicentric tracheids, (+) = vasicentric tracheids present, (-) = vasicentric tracheids absent, (sm) = small pits, (lg) = large pits; AP = axial parenchyma, (d) = diffuse, (dia) = diffuse-in-aggregates, (scp) = scanty paratracheal, (v) vasicentric, (sl) = short lines, (com) = common; RW = range of ray widths; RCC = ray cellular composition, number range = number of uniseriate margin rows of square or upright cells, (w) = square or upright cells within ray, (sh) = sheath cells, (alt) = multiseriate ray portions joined by uniseriate ray portions; RW Uni = percentage of uniseriate rays, (+) = present, (-) = absent; R/mm = range of rays per millimeter; Cr = prismatic crystals, (-) = not observed, (r) = present in ray parenchyma, (ax p) = present in axial parenchyma.  
N Ob = Not observed due to quality of sample preservation. Blank spaces indicate unavailable information.

Table 3.5. Group IIIA – McRae Formation woods with simple perforation plates, vessels exclusively solitary.

Taxon	ESD (cm)	VA	V/ mm <sup>2</sup>	VMTD	IVP (µm)	V-RP	VT, #rows	FP	F
<b>Axial parenchyma rare</b>									
<i>Fulleroxylon aremendarisense</i> <sup>1</sup> TXSTATE 1201	4.5	98% sol, 2	16	overall 95; wide 109, narrow 56	alt	rb, r	1-2, rad & tan	s	s
<i>Fulleroxylon</i> sp.1 TXSTATE 1275-1277	7	97-100% sol, 2	23-31	136- 156	alt 3-6	rb, r/o/he/ ve	1-3, rad & tan	-	s
Group IIIA sp.1 TXSTATE 1278	24	97% sol, 2, diag	42	50	alt	b, iv, small	1-2, rad & tan	-	N Ob
<i>Mcraeoxyton waddellii</i> <sup>2</sup> TXSTATE 1202	3.4	28% sol, 2-4	144	51	alt	rb, r/o	-	-	s, n-s
<b>Axial parenchyma common</b>									
Group IIIA sp.2 TXSTATE 1279	34	96% sol, 2	9 overall; 21 between rays	113	N Ob	b, small	N Ob	-	s
Group IIIA sp.3 TXSTATE 1280	40	91% sol, 2	5	109	alt, 8-12	rb-s, he	-	rb-s, rad	(s)
Group IIIA sp.4 TXSTATE 1281	8	82-85% sol, 2	5-8	86-90	alt (sc), 7-10	rb-s, o/he	-	rb-s, rad	s, n-s

<sup>1</sup> Estrada-Ruiz et al. (2012b)

<sup>2</sup> Estrada-Ruiz et al. (2018)

Table 3.5. Continued. Group IIIA – McRae Formation woods with simple perforation plates, vessels exclusively solitary.

Taxon	AP	RW Uni	RW (cells)	RCC	RH ( $\mu$ m)	R/mm
<b>Axial parenchyma rare</b>						
<i>Fulleroxylon aremendarisense</i> <sup>1</sup> TXSTATE 1201	rare: d?	+	1 (2)	mostly procumbent	13, 5-41 cells	7-16
<i>Fulleroxylon</i> sp.1 TXSTATE 1275-1277	rare or absent	93%	1 (2)	all pro (large), or 1	135-182	18-23
Group IIIA sp.1 TXSTATE 1278	absent	67%	1-2	all pro (often large), or 1	141	23-36
<i>Mcraeoxylon waddellii</i> <sup>2</sup> TXSTATE 1202	rare	NA	1-2	all pro, or 1, or w	547	18-27
<b>Axial parenchyma common</b>						
Group IIIA sp.2 TXSTATE 1279	d, dia, scp, v	0%	4-18	all pro (vari size), or 1-3, or w	979	2-4
Group IIIA sp.3 TXSTATE 1280	dia: lines of 1-4 cells wide; v: sh of 1-several cells	0%	3-7, mostly 4-5	all pro, or 1 sq	508	6
Group IIIA sp.4 TXSTATE 1281	dia: lines of 1-4 cells wide, v: sh narrow	3-10%	1-4 (5), mostly 2-4	all pro, or 1 sq	369-484	8-11

<sup>1</sup> Estrada-Ruiz et al. (2012b)

<sup>2</sup> Estrada-Ruiz et al. (2018)

Table 3.5. Group IIIA – McRae Formation woods with simple perforation plates, vessels exclusively solitary.

*Legend:* Fossil woods are in bold type. ESD = estimated stem diameter in cm; VA = vessel arrangement, (sol) = solitary, range represents common radial vessel multiples, range in parentheses represents rare radial multiples; V/mm<sup>2</sup> = average vessel density, range equals range of mean values for multiple samples; VMTD = vessel mean tangential diameter; IVP = intervessel pits, (o) = opposite, (sc) = scalariform, (v-t) = vessel tail; V-RP = vessel-ray parenchyma pits, (iv) = like intervessel pitting, (b) = bordered, (rb) = reduced borders, (s) = simple, (r) = round, (o) = oval, (he) = horizontally elongate, (ve) = vertically elongate, (cr) = crowded; VT, #rows = number of rows of pits on vasicentric tracheids, (+) = vasicentric tracheids present, (-) = vasicentric tracheids absent, (sm) = small pits, (lg) = large pits; FP = number of rows of pits on fibers, (con) = pits continuous over the length of the fiber, (dis) = short rows of pits alternating with areas without pits; F = fiber, (s) = septate fibers, (n-s) = non-septate fibers; AP = axial parenchyma, (d) = diffuse, (dia) = diffuse-in-aggregates, (scp) = scanty paratracheal, (v) vasicentric, (sl) = short lines, (com) = common; RW Uni = percentage of uniseriate rays, (+) = present, (-) = absent; RW = range of ray widths; RCC = ray cellular composition, number range = number of uniseriate margin rows of square or upright cells, (w) = square or upright cells within ray, (sh) = sheath cells, (alt) = multiseriate ray portions joined by uniseriate ray portions; RH = ray height, mean, largest number observed in parentheses, range of means for multiple samples; R/mm = range of rays per millimeter.

N Ob = Not observed due to quality of sample preservation. Blank spaces indicate unavailable information.

Table 3.6. Group IIIA – Comparison of specimens representing *Fulleroxylon* sp. nov. and *Fulleroxylon aremendarisense*.

Taxon	ESD (cm)	GB	VA	V/ mm <sup>2</sup>	VMTD	IVP (µm)	V-RP
TXSTATE 1275	7.0	Absent	97% sol, 2	25	156	alt, 3-6	b-rb, r/o/he
TXSTATE 1276	4.6	Absent	100% sol	31	136	N Ob	N Ob
TXSTATE 1277	4.5	Absent	97-100% sol, 2	23	144	N Ob	N Ob
<i>Fulleroxylon aremendarisense</i> <sup>1</sup>	4.5	Indistinct	98% sol, 2	16	overall 95; wide 109, narrow 56	alt	rb, r

Taxon	VT, #rows	FP	F	AP	RW Uni	RW (cells)	RCC	RH (cells)	RH (µm)	R/mm
TXSTATE 1275	1-3, rad & tan	s	s	rare or absent	93%	1 (2)	all pro (large), or 1	8 (5), 2-20	135	23
TXSTATE 1276	N Ob	N Ob	N Ob	N Ob	77%	1-2 (3)	N Ob	11 (5), 4-26	182	18
TXSTATE 1277	N Ob	N Ob	N Ob	N Ob	N Ob	N Ob	N Ob	N Ob	N Ob	N Ob
<i>Fulleroxylon aremendarisense</i> <sup>1</sup>	1-2, rad & tan	s	s	rare: d?	NA	1 (2)	mostly procumbent	13, 5-41	??	7-16

<sup>1</sup> Estrada-Ruiz et al. (2012b)

Table 3.6. Group IIIA – Comparison of specimens representing *Fulleroxylon* sp. nov. and *Fulleroxylon armendarisense*.

**Legend:** Fossil woods are in bold type. ESD = estimated stem diameter in cm; GB = growth boundaries, (-) = absent, (l) = indistinct, (+) = distinct; VA = vessel arrangement, (sol) = solitary, range represents common radial vessel multiples, range in parentheses represents rare radial multiples;  $V/mm^2$  = average vessel density, range equals range of mean values for multiple samples; VMTD = vessel mean tangential diameter; IVP = intervessel pits, (o) = opposite, (sc) = scalariform, (v-t) = vessel tail; V-RP = vessel-ray parenchyma pits, (iv) = like intervessel pitting, (b) = bordered, (rb) = reduced borders, (s) = simple, (r) = round, (o) = oval, (he) = horizontally elongate, (cr) = crowded; VT, #rows = number of rows of pits on vasicentric tracheids, (+) = vasicentric tracheids present, (-) = vasicentric tracheids absent, (sm) = small pits, (lg) = large pits; FP = number of rows of pits on fibers, (con) = pits continuous over the length of the fiber, (dis) = short rows of pits alternating with areas without pits; F = fiber, (s) = septate fibers, (n-s) = non-septate fibers; AP = axial parenchyma, (d) = diffuse, (dia) = diffuse-in-aggregates, (scp) = scanty paratracheal, (v) vasicentric, (sl) = short lines, (com) = common; RW Uni = percentage of uniseriate rays, (+) = present, (-) = absent; RW = range of ray widths; RCC = ray cellular composition, number range = number of uniseriate margin rows of square or upright cells, (w) = square or upright cells within ray, (sh) = sheath cells, (alt) = multiseriate ray portions joined by uniseriate ray portions; RH = ray height, mean, largest number observed in parentheses, range of means for multiple samples; R/mm = range of rays per millimeter.  
 N Ob = Not observed due to quality of sample preservation. Blank spaces indicate unavailable information.

Table 3.7. Group IIIB – McRae Formation woods with simple perforation plates, vessels solitary and in radial multiples.

Taxon	ESD (cm)	VA	VP	IVP (µm)	VMTD	V-RP	V/mm <sup>2</sup>	F
<b>Axial parenchyma rare to scanty paratracheal</b>								
Group IIIB sp. 1 TXSTATE 1283	18	26% sol, 2-3 (4)	diffuse porous	alt, 6-10	69	rb-s, r/o, large	55	(s), n-s
Group IIIB sp. 2 TXSTATE 1284	26	11% sol, 2-4 (5-6)	diffuse porous	alt, 6-9	57	b, o/e, or irr, med; rb-s, o/he/ve, (irr), med	76	s, n-s
McRae <i>Paraphyllanthoxylon</i> cf. <i>Kirkiaceae</i> <i>Burseraceae</i> <i>Anacardiaceae</i>	70 - 200	47% sol, 2-3 (5)	diffuse porous	alt, 12-18	195- 234	s, r, med-large	4-7	s, n-s
<b>Axial parenchyma common - vasicentric to lozenge-aliform</b>								
Group IIIB sp. 3 TXSTATE 1286	8	45% sol, 2-3 (4)	diffuse porous	alt, 6-10	64	rb-s, r/he	26	N Ob
Group IIIB sp. 4 TXSTATE 1287 cf. <i>Cannabaceae</i> ? <i>Moraceae</i> ? <i>Urticaceae</i> ?	69	64% sol, 2-3	diffuse porous	alt, 7-10	127	b-rb, o/he	3	N Ob
Group IIIB sp. 5 TXSTATE 1288 cf. <i>Sapotaceae</i>	80	63% sol, 2-3 (4)	Tending to diagonal or radial	alt, 7-12	156	b-rb, o/he	6	N Ob

Table 3.7. Continued. Group IIIB – McRae Formation woods with simple perforation plates, vessels solitary and in radial multiples.

Taxon	AP	RW Uni	RW (cells)	RH (µm)	RCC	R/mm	Cr
<b>Axial parenchyma rare to scanty paratracheal</b>							
Group IIIB sp. 1 TXSTATE 1283	scp	27%	1-3	311	all pro (large)	27	r
Group IIIB sp. 2 TXSTATE 1284	scp	3%	(1) 2-4	217	all pro, or 1 sq	21	-
McRae <i>Paraphyllanthoxylon</i> cf. <i>Kirkiaceae</i> <i>Burseraceae</i> <i>Anacardiaceae</i>	scp, (nearly v)	< 2%	(1) 2-4 (6), mostly 3-4	536- 1184	all pro, or 1 (-5)	7-10	-
<b>Axial parenchyma common - vasicentric to lozenge-aliform</b>							
Group IIIB sp. 3 TXSTATE 1286	d; v: sh broad to ali	37% 68 µm tall	1-2 (3)	131	all pro	15	-
Group IIIB sp. 4 TXSTATE 1287 cf. <i>Cannabaceae?</i> <i>Moraceae?</i> <i>Urticaceae?</i>	v to aliform; apotracheal clusters	23% 257 µm tall	1-6	505	1-6	9	-
Group IIIB sp. 5 TXSTATE 1288 cf. <i>Sapotaceae</i>	dia: lines 1-3 cells wide; scp	33%, 345 µm tall	1-4	338	1-8	10	-

Table 3.7. Group IIIB – McRae Formation woods with simple perforation plates, vessels solitary and in radial multiples.

*Legend:* Fossil woods are in bold type. ESD = estimated stem diameter in cmd; VA = vessel arrangement, (sol) = solitary, range represents common radial vessel multiples, range in parentheses represents rare radial multiples; VP = vessel porosity; IVP = intervessel pits, (o) = opposite, (sc) = scalariform, (v-t) = vessel tail; VMTD = vessel mean tangential diameter; V-RP = vessel-ray parenchyma pits, (iv) = like intervessel pitting, (b) = bordered, (rb) = reduced borders, (s) = simple, (r) = round, (o) = oval, (he) = horizontally elongate, (ve) = vertically elongate, (cr) = crowded; V/mm<sup>2</sup> = average vessel density, range equals range of mean values for multiple samples; F = fiber, (s) = septate fibers, (n-s) = non-septate fibers; AP = axial parenchyma, (d) = diffuse, (dia) = diffuse-in-aggregates, (scp) = scanty paratracheal, (v) vasicentric, (sl) = short lines, (com) = common; RW Uni = percentage of uniseriate rays, (+) = present, (-) = absent; RW = range of ray widths; RH = ray height, mean, largest number observed in parentheses, range of means for multiple samples; RCC = ray cellular composition, number range = number of uniseriate margin rows of square or upright cells, (w) = square or upright cells within ray, (sh) = sheath cells, (alt) = multiseriate ray portions joined by uniseriate ray portions; R/mm = range of rays per millimeter. Cr = prismatic crystals, (-) = not observed, (r) = present in ray parenchyma. N Ob = Not observed due to quality of sample preservation. Blank spaces indicate unavailable information.

Table 3.8. Group IV – McRae Formation wood with both simple and scalariform perforation plates (oil cells absent).

Taxon	ESD (cm)	VA	V/mm <sup>2</sup>	VMTD	IVP (µm)	V-RP	F	AP	RW (cells)	RCC	RH (µm)	RW Uni	R/mm
Group IV sp. 1 TXSTATE 1289	25	40% sol, 2-3 (4)	135	36	alt, 5-7	rb-s, r/o, large	s	rare or absent	1-3, mostly 1-2	all pro (variable size)	208	40%	21

*Legend:* ESD = estimated stem diameter in cm; VA = vessel arrangement, (sol) = solitary, range represents common radial vessel multiples, range in parentheses represents rare radial multiples; V/mm<sup>2</sup> = average vessel density, range equals range of mean values for multiple samples; VMTD = vessel mean tangential diameter, range represents range of means for multiple samples; IVP = intervessel pits, (alt) = alternate, range of pit diameters (µm); V-RP = vessel-ray parenchyma pits, (iv) = like intervessel pitting, (b) = bordered, (rb) = reduced borders, (s) = simple, (r) = round, (o) = oval, (e) = horizontally elongate; F = fiber, (s) = septate fibers, (n-s) = non-septate fibers; AP = axial parenchyma, (dia) = diffuse-in-aggregates, (scp) = scanty paratracheal, (v) = vascentric; RW = range of ray widths; RCC = ray cellular composition, (all pro) = ray parenchyma all procumbent, number range = number of uniseriate margin rows of square or upright cells; RH = mean ray height, range represents range of means for multiple samples; RW Uni = % uniseriate rays; R/mm = average number of rays per millimeter or range for multiple samples.

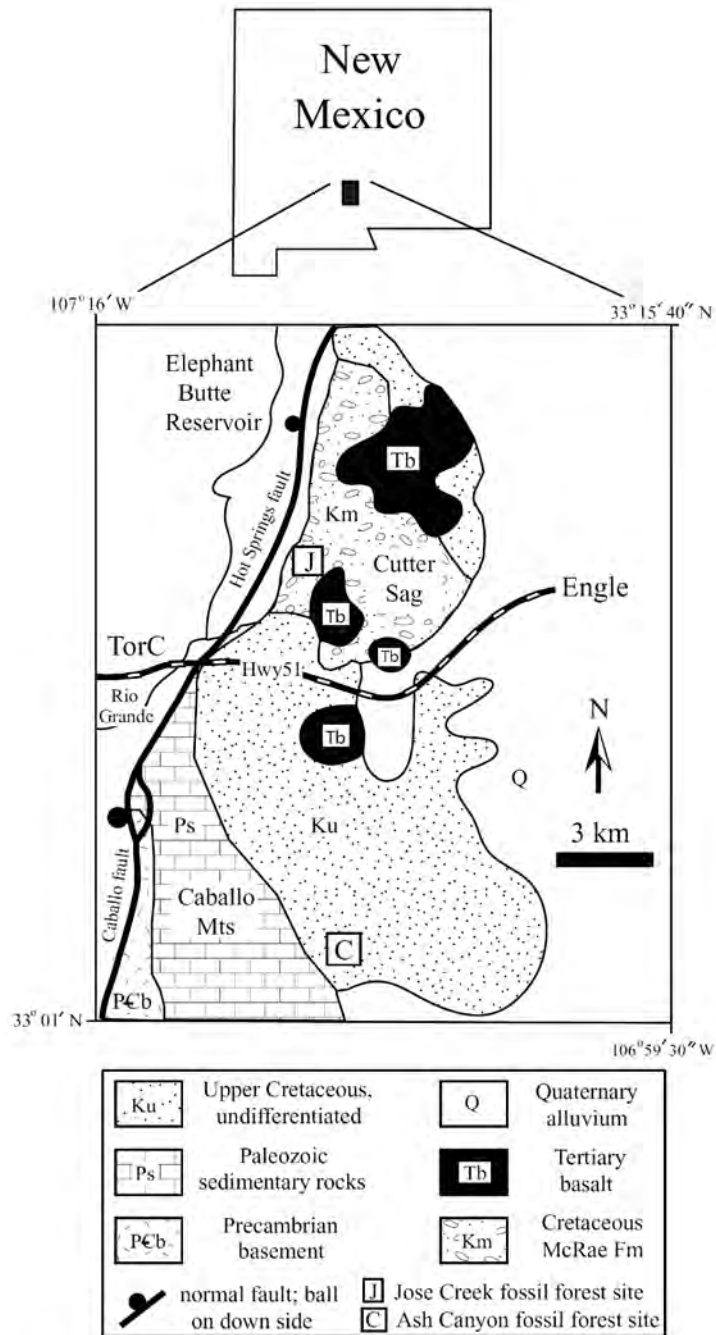


Figure 3.1. Map showing the location and geology of the McRae Formation, south-central New Mexico (Estrada-Ruiz et al. 2018).

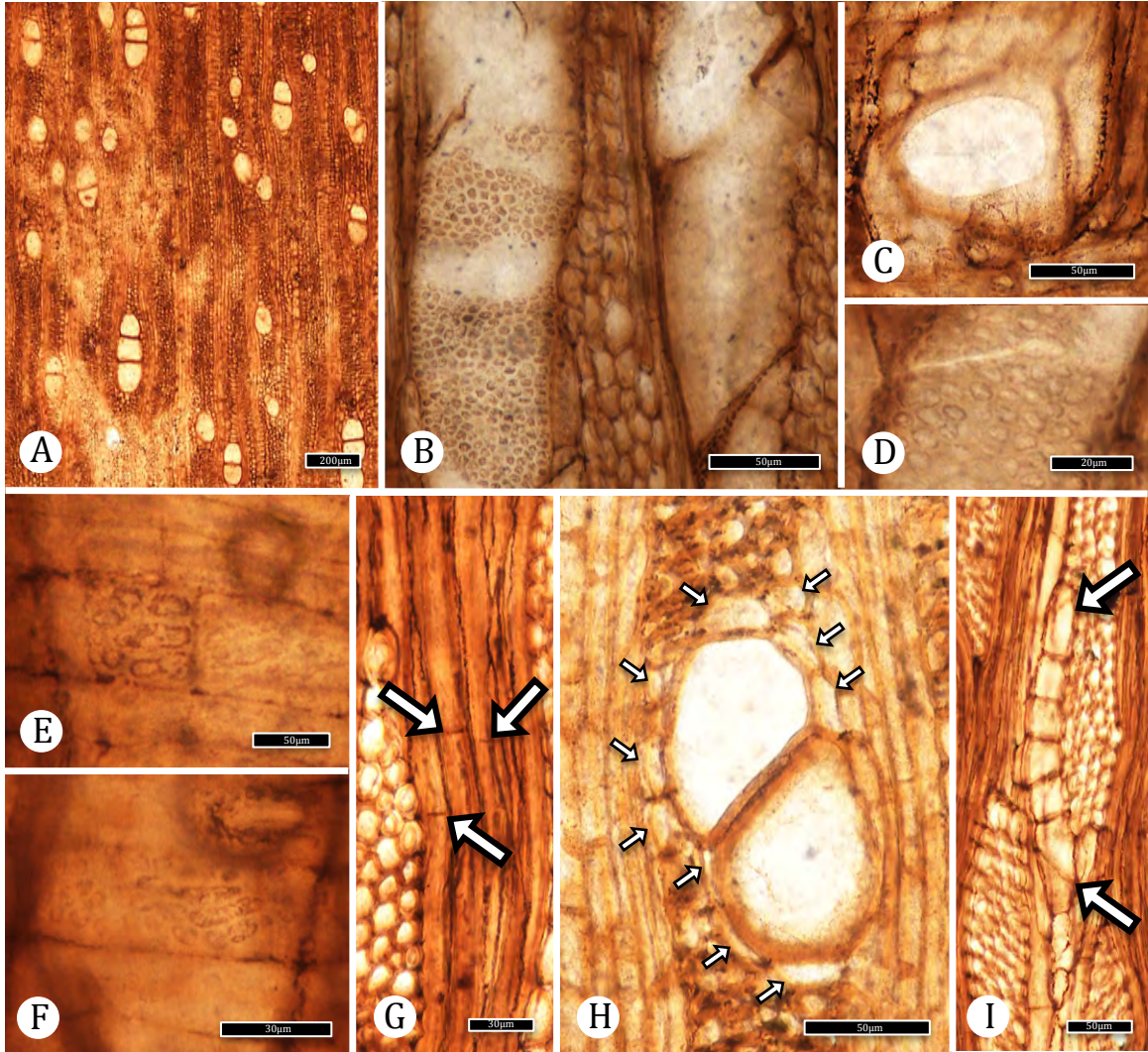


Figure 3.2. McRae wood holoxylotype Group IA sp. 2 (TXSTATE 1251) Lauraceae.  
 – A: TS. Vessels diffuse-porous, solitary or in radial multiples of 2–3. TXSTATE 1251, X-3. Scale bar = 200  $\mu$ m. – B: TLS. Alternate intervessel pits, simple perforation plates. TXSTATE 1251, T-3. Scale bar = 50  $\mu$ m. – C: RLS. Simple perforation plate. TXSTATE 1251, R-3. Scale bar = 50  $\mu$ m. – D: TLS. Alternate intervessel pits. TXSTATE 1251, T-3. Scale bar = 20  $\mu$ m. – E: RLS. Vessel-ray pits with reduced borders. TXSTATE 1251, R-2. Scale bar = 50  $\mu$ m. – F RLS. Vessel-ray pits with reduced borders. TXSTATE 1251, R-2. Scale bar = 30  $\mu$ m. . – G: TLS. Septate fibers (arrows). TXSTATE 140#-S#. Scale bar = 30  $\mu$ m. – H: TS. Axial parenchyma (P) scanty paratracheal, to nearly narrow vasicentric. TXSTATE 1251, X-1. Scale bar = 50  $\mu$ m. – I: TLS. Axial parenchyma 6 cells per strand (arrows). TXSTATE 1251, T-3. Scale bar = 50  $\mu$ m.

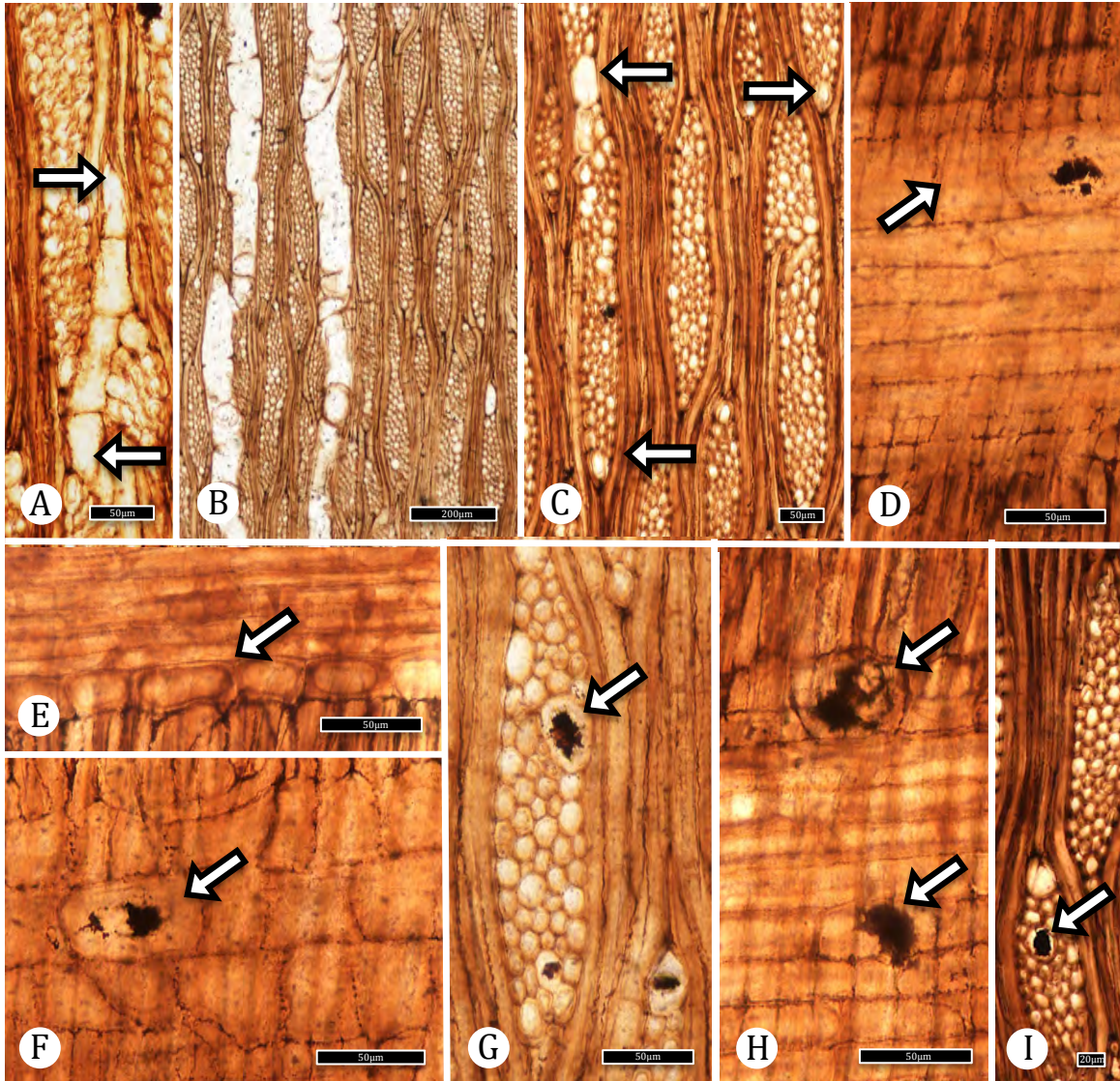


Figure 3.3. McRae wood holoxylotype Group IA sp. 2 (TXSTATE 1251) Lauraceae.  
 – A: TLS. Axial parenchyma strand of 4 cells (arrows). TXSTATE 1251, T-3. Scale bar = 50  $\mu\text{m}$  – B: TLS. Rays mostly 5 seriate; uniseriate rays uncommon. TXSTATE 1251, T-1. Scale bar = 200  $\mu\text{m}$ . – C: TLS. Large cells at ray margins may be large procumbent cells, square or upright cells, or idioblasts (arrows). TXSTATE 1251, T-3. Scale bar = 50  $\mu\text{m}$ – D: RLS. Rays composed of procumbent cells with one row of square cells (arrow) and an idioblast. TXSTATE 1251, R-3. Scale bar = 50  $\mu\text{m}$ . – E: RLS. Ray composed of all procumbent cells. (arrow). TXSTATE 1251, R-3. Scale bar = 50  $\mu\text{m}$ . – F: RLS. Short ray consisting of square and upright cells, oil cell within ray (arrow). TXSTATE R-3. Scale bar = 50  $\mu\text{m}$ . – G: TLS. Oil cell at the ray edge (arrow). TXSTATE 1251, T-3. Scale bar = 50  $\mu\text{m}$ . – H: RLS. Oil cells at the margin or within ray (arrows). TXSTATE 1251, R-3. Scale bar = 50  $\mu\text{m}$ . – I: TLS. Oil cell within ray (arrow). TXSTATE 1251, T-3. Scale bar = 20  $\mu\text{m}$ .

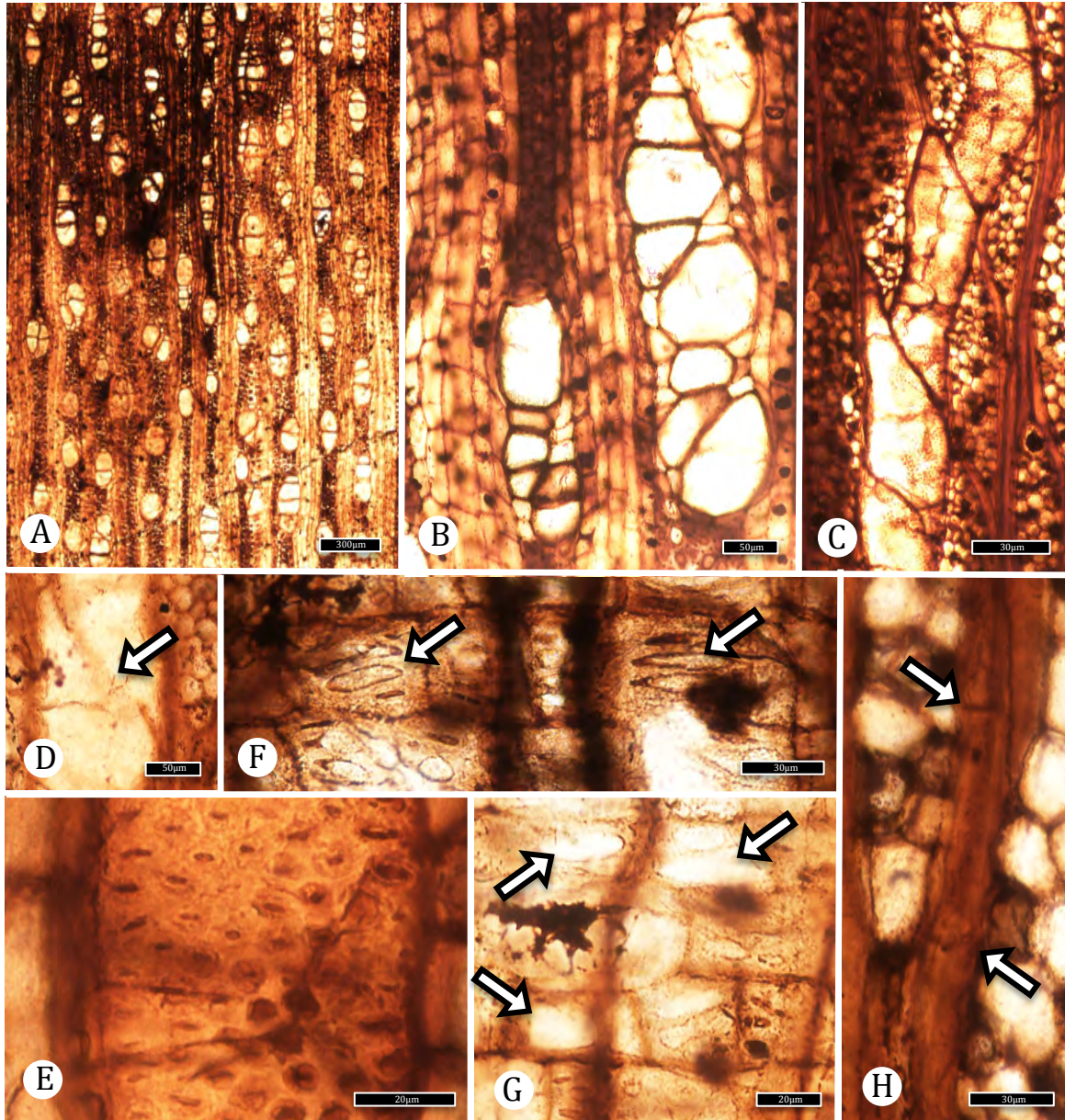


Figure 3.4. McRae wood holoxylotype Group IA sp. 3 (TXSTATE 1252) Lauraceae.  
 – A: TS. Diffuse-porous wood with solitary vessels, radial multiples and small clusters. TXSTATE 1252, X-4. Scale bar = 300  $\mu\text{m}$ . – B: TS. Radial and oblique vessel multiples. TXSTATE 1252, X-4. Scale bar = 50  $\mu\text{m}$ . – C: TLS. Vessel elements with oblique end walls, simple perforation plates. TXSTATE 1252, T-3. Scale bar = 30  $\mu\text{m}$ . – D: Simple perforation plate. (arrow). TXSTATE 1252, T-2. Scale bar = 50  $\mu\text{m}$ . – E: TLS. Alternate intervessel pits, polygonal in outline. TXSTATE 1252, T-3. Scale bar = 30  $\mu\text{m}$ . – F: RLS. Vessel-ray pits with reduced borders, gash-like (arrows). TXSTATE 1252, R-2. Scale bar = 20  $\mu\text{m}$ . – G: RLS. Vessel-ray pits simple and window-like. (arrows). TXSTATE 1252, R-2. Scale bar = 20  $\mu\text{m}$ . – H: TLS. Fibers septate (arrows). TXSTATE T-1. Scale bar = 30  $\mu\text{m}$ .

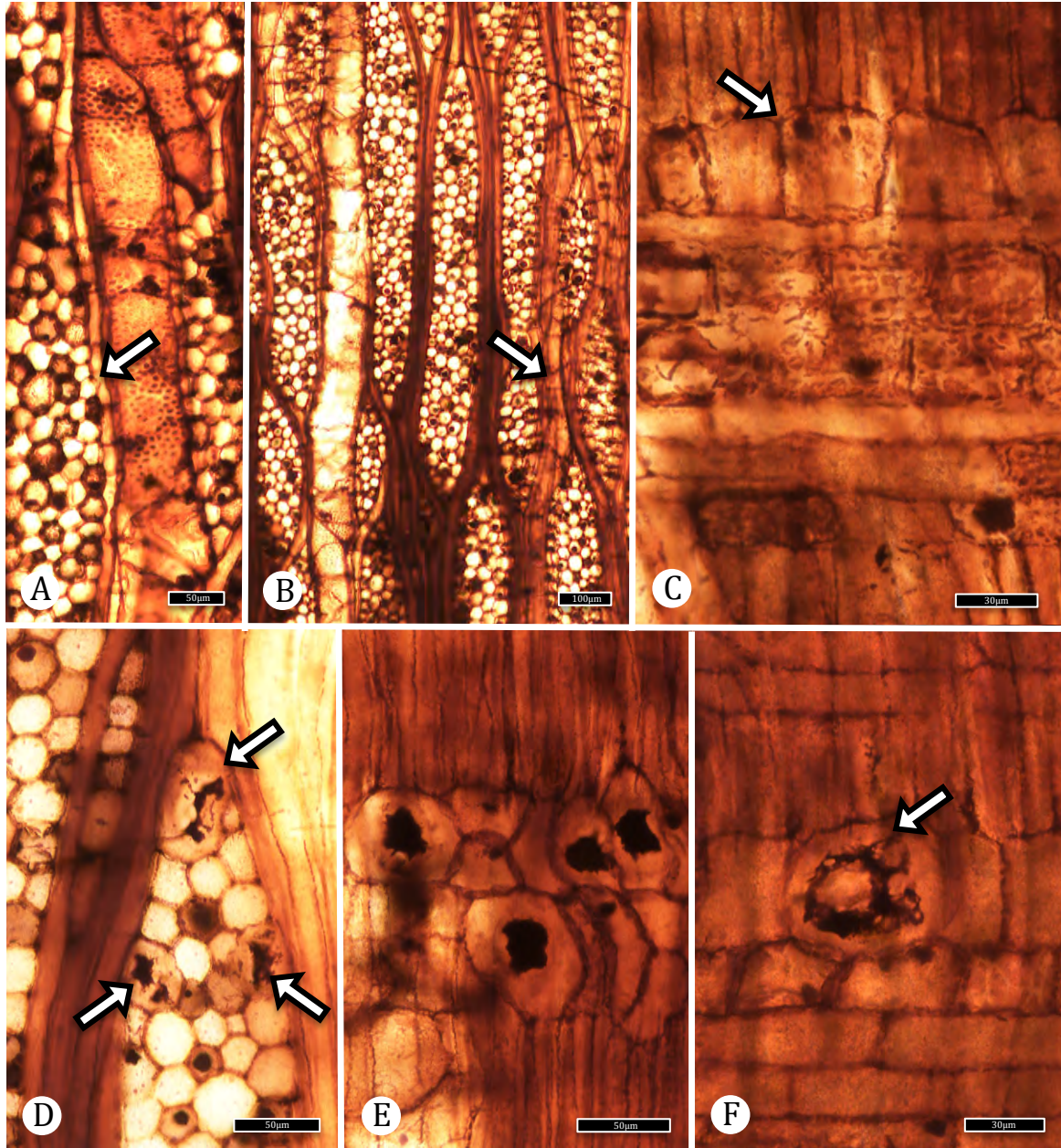


Figure 3.5. McRae wood holoxylotype Group IA sp. 3 (continued) (TXSTATE 1252) Lauraceae. – A: TLS. Axial parenchyma scanty paratracheal, 4-8 cells per strand. (arrow). TXSTATE 1252, T-3. Scale bar = 50  $\mu\text{m}$ . – B: TLS. Rays 3–7 seriate. Axial parenchyma diffuse (arrow) TXSTATE 1252, T-3. Scale bar = 100  $\mu\text{m}$ . – C: RLS. Ray parenchyma procumbent and with one row square or upright cells (arrow). TXSTATE 1252, R-2. Scale bar = 30  $\mu\text{m}$ . – D: TLS. Idioblasts at the ray margin or along side of ray (arrows). TXSTATE 1252, T-2. Scale bar = 50  $\mu\text{m}$ . – E: RLS. Idioblasts in cluster. TXSTATE 1252, R-2. Scale bar = 50  $\mu\text{m}$ . – F: RLS. Idioblast at margin of ray (arrow). TXSTATE 1252, R-2. Scale bar = 30  $\mu\text{m}$ .

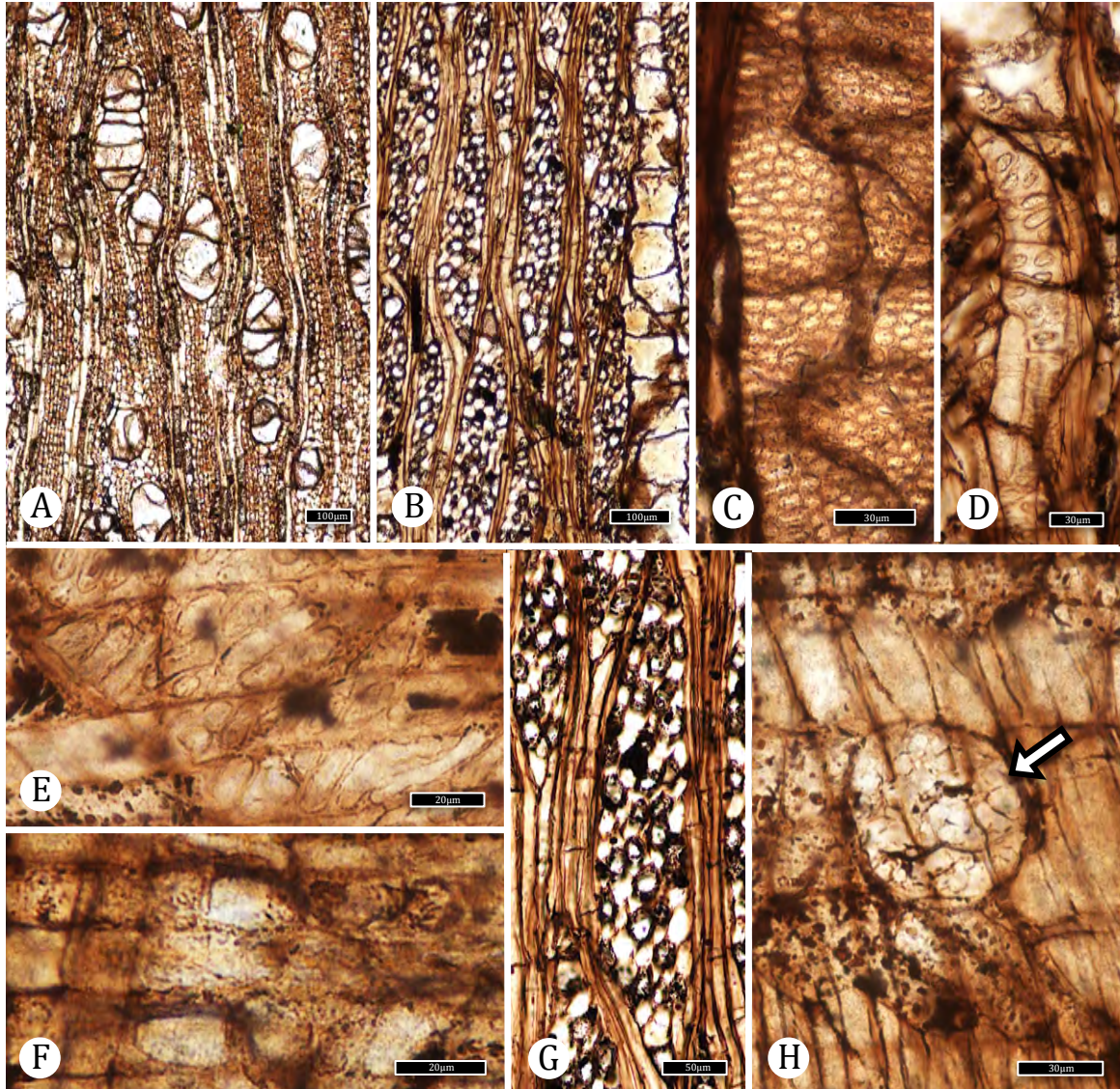


Figure 3.6. McRae wood paraxylotype Group IA sp. 3 (TXSTATE 1253) Lauraceae.  
 – A: TS. Wood diffuse porous. Vessels solitary and in radial multiples of 2–3 (up to 5). TXSTATE 1253, X-1 . Scale bar = 100  $\mu\text{m}$ – B: TLS. Rays mostly 5 seriate. TXSTATE 1253, T-2. Scale bar = 100  $\mu\text{m}$ . – C: TLS. Alternate intervessel pits. TXSTATE 1253, T-1. Scale bar = 30  $\mu\text{m}$ . – D: TLS. Scanty paratracheal axial parenchyma have oval pits with reduced borders. TXSTATE 1253, T-4. Scale bar = 30 $\mu\text{m}$ . – E–F Vessel-ray pits of two types. – E: RLS. Vessel-ray pits with reduced borders, round to horizontally elongate, sometimes irregular in shape. TXSTATE 1253, R-1. Scale bar = 20  $\mu\text{m}$ . – F: RLS. Large, simple, window-like vessel-ray pits. TXSTATE 1253, R-1. Scale bar = 20  $\mu\text{m}$ – G: TLS. Septate fibers. TXSTATE 1253, T-2. Scale bar = 50  $\mu\text{m}$ . – H: RLS. Large idioblast at the ray margin (arrow). TXSTATE 1253, R-1. Scale bar = 30 $\mu\text{m}$ .

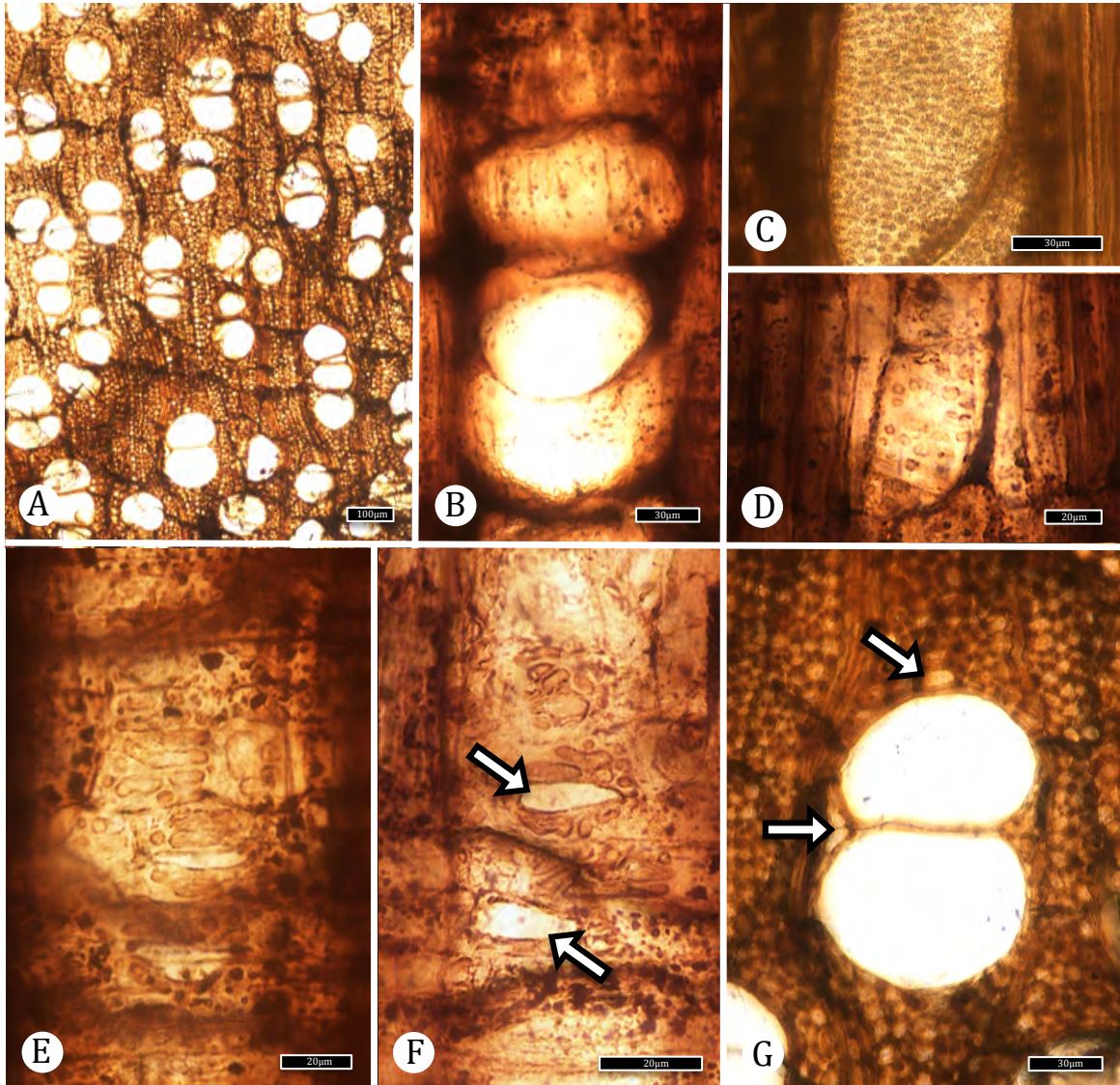


Figure 3.7. McRae wood holoxylotype Group IA sp. 4 (TXSTATE 1254) Lauraceae.  
 – A: TS. Wood diffuse-porous. Vessels solitary and in radial multiples. TXSTATE 1254, X-1. Scale bar = 100  $\mu\text{m}$ . – B: RLS. Simple perforation plate. TXSTATE 1254, R-2. Scale bar = 30  $\mu\text{m}$ . – C: TLS. Alternate intervessel pitting, minute to small. TXSTATE 1254, T-4. Scale bar = 30  $\mu\text{m}$ . – D: RLS. Vessel-axial parenchyma pits with slightly reduced borders, generally smaller than vessel-ray pitting. TXSTATE 1254, R-2. Scale bar = 20  $\mu\text{m}$ . – E: RLS. Vessel-ray pits round to elongate ovals, or irregular. TXSTATE 1254, R-2. Scale bar = 20  $\mu\text{m}$ . – F: RLS. Vessel-ray pit size variable, small with reduced borders to large and simple (arrows). TXSTATE 1254, R-2. Scale bar = 20  $\mu\text{m}$ . – G: LS. Axial parenchyma scanty paratracheal (arrows). TXSTATE 1254, X-1. Scale bar = 30  $\mu\text{m}$ .

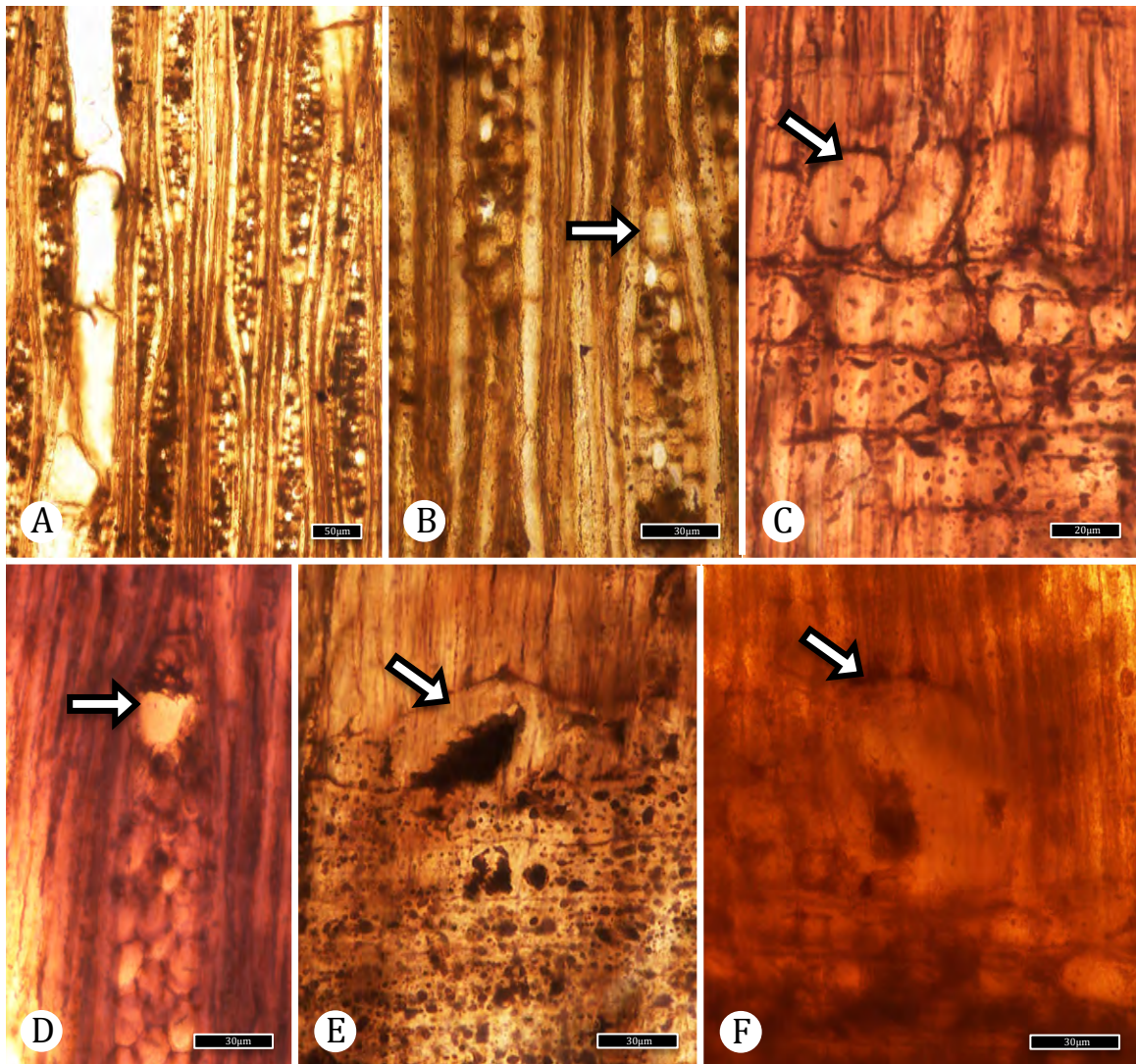


Figure 3.8. McRae wood holoxylotype Group IA sp. 4 (TXSTATE 1254) Lauraceae.  
 – A: TLS. Rays heterocellular; 3–5 seriate. Uniseriate rays rare. TXSTATE 1254, T-4. Scale bar = 50  $\mu\text{m}$ . – B: TLS. Rays composed of uniformly-sized procumbent body cells with a marginal row of large procumbent or square or upright cells (arrow). TXSTATE 1254, T-4. Scale bar = 30  $\mu\text{m}$ . – C: RLS. Marginal row composed of square and upright cells (arrow). TXSTATE 1254, R-3. Scale bar = 20  $\mu\text{m}$ . – D: TLS. Large idioblast at the ray margin (arrow). TXSTATE 1254, T-5. Scale bar = 30  $\mu\text{m}$ . – E: RLS. Large idioblast with dark content at the ray margin (arrow). TXSTATE 1254, R-2. Scale bar = 30  $\mu\text{m}$ . – F: RLS. . Large idioblast at the ray margin (arrow). TXSTATE 1254, R-1. Scale bar = 30  $\mu\text{m}$ .

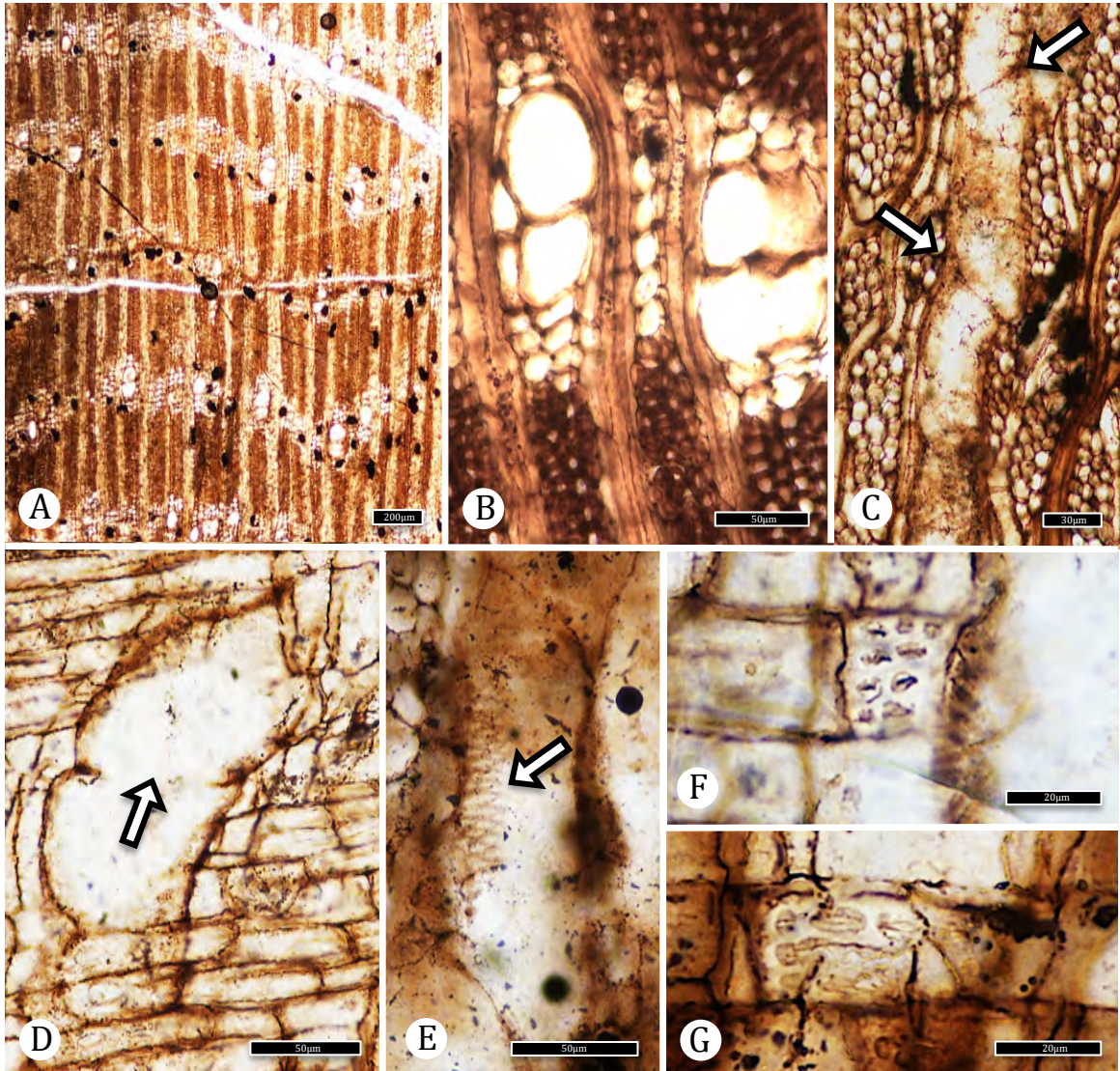


Figure 3.9. McRae wood holoxylotype Group IB sp. 1 (TXSTATE 1255) Lauraceae.  
 – A: TS. Tendency for vessels to occur in tangential bands. Axial parenchyma confluent. TXSTATE 1255, X-1. Scale bar = 200 µm. – B: TS. Axial parenchyma confluent. TXSTATE 1255, X-3. Scale bar = 50 µm. – C: TLS. Vessel element. TXSTATE 1255, T-1. Scale bar = 30 µm. – D: RLS. Simple perforation plate (arrow). TXSTATE 1255, R-9. Scale bar = 50 µm. – E: Alternate intervessel pits, elongate. (arrow). TXSTATE 1255, T-7. Scale bar = 50 µm. – F: RLS. Vessel-ray pits with borders. TXSTATE 1255, R-9. Scale bar = 20 µm. – G: RLS. Vessel-ray pits with slightly reduced borders, oval, some horizontally elongate. TXSTATE R-9. Scale bar = 20 µm.

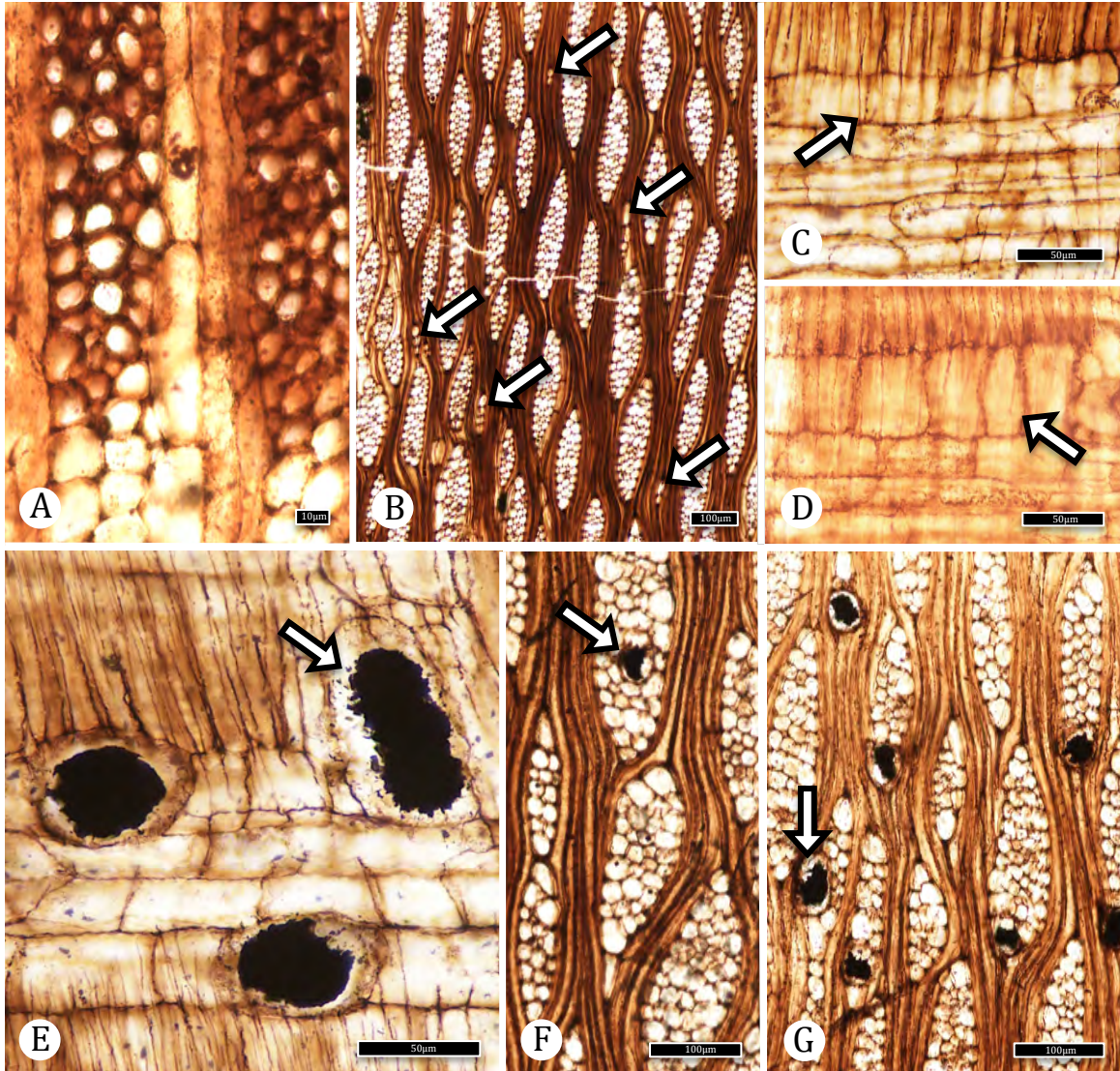


Figure 3.10. McRae wood holoxylotype Group IB sp. 1 (TXSTATE 1255) Lauraceae. – A: . TS. Fibers thin-walled, angular in outline. TXSTATE 1255, X-3. Scale bar = 10  $\mu\text{m}$ . – B: TLS. Rays heterocellular, 1-5 seriate, uniseriate rays common (arrows). TXSTATE 1255, T-6. Scale bar = 100  $\mu\text{m}$ . – C: RLS. Ray cells all procumbent, the marginal row larger (arrow). TXSTATE 1255, R-9. Scale bar = 50  $\mu\text{m}$ . – D: RLS. Ray cells procumbent, with one row upright cells (arrow). TXSTATE 1255, R-9. Scale bar = 50  $\mu\text{m}$ . – E: Oil cells located in ray margin rows or axial parenchyma (arrow). TXSTATE 1255, R-9. Scale bar = 50  $\mu\text{m}$ . – F: TLS. Oil cell nestled within ray (arrow). TXSTATE 1255, T-7. Scale bar = 100  $\mu\text{m}$ . – G: TLS. Oil cells at ray margins or along the ray edge (arrow). TXSTATE 1255, T-7. Scale bar = 100  $\mu\text{m}$ .

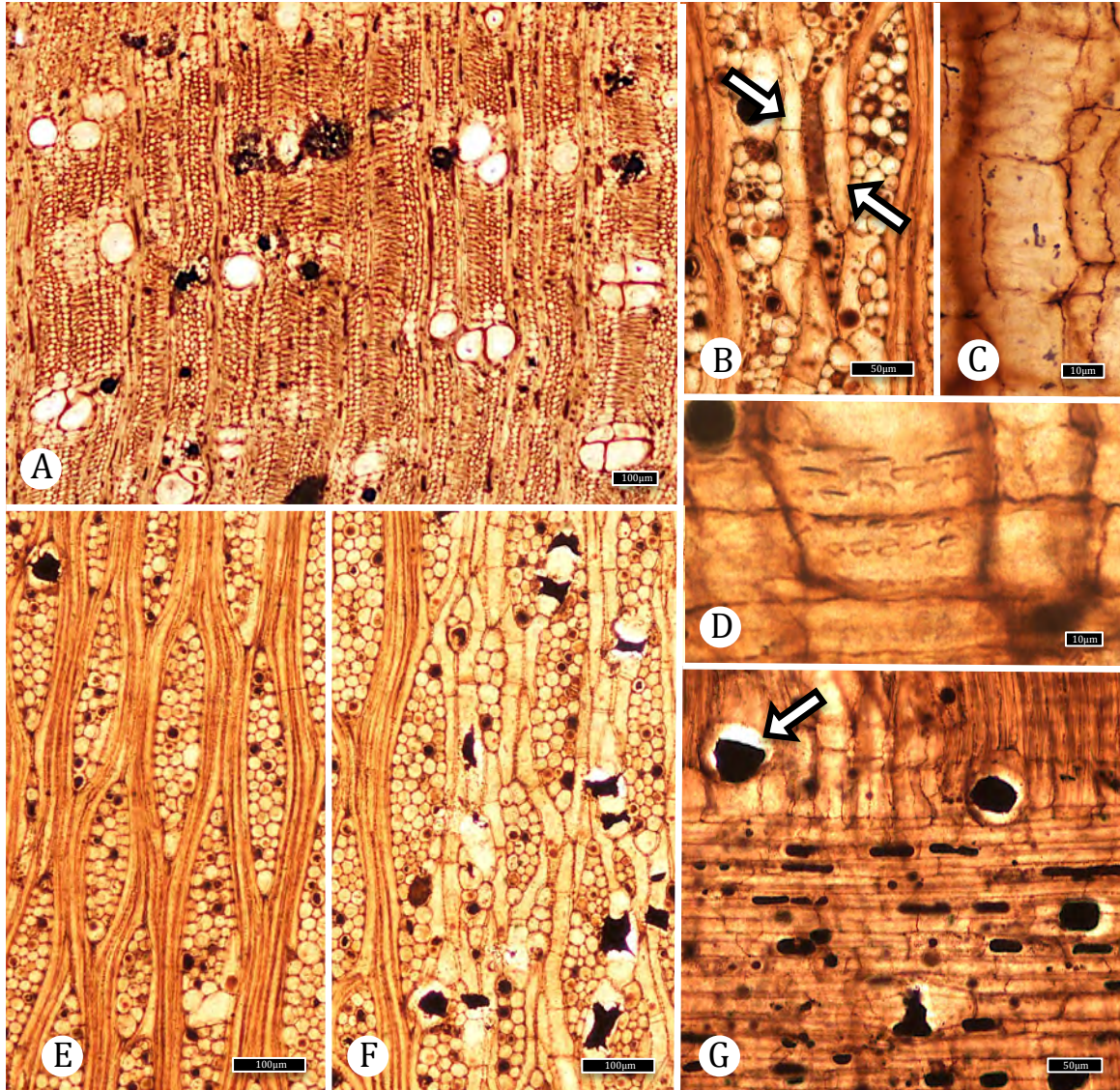


Figure 3.11. McRae wood paraxylotype Group IB sp. 1 (TXSTATE 1256) Lauraceae. – A: TS. Vessels solitary or in radial, oblique or tangential multiples. Axial parenchyma lozenge-aliform to confluent. TXSTATE 1256, X-2. Scale bar = 100  $\mu$ m. – B: TLS. Axial parenchyma 2–4 cells per parenchyma strand (arrows). TXSTATE 1256, T-1. Scale bar = 50  $\mu$ m. – C: TLS. Axial parenchyma with reduced bordered to simple pits, horizontally elongate ovals. TXSTATE 1256, R-1. Scale bar = 10  $\mu$ m. – D: RLS. Vesel-ray pits bordered, oval, some elongate. TXSTATE 1256, R-3. Scale bar = 10  $\mu$ m. – E: TLS. Rays 1–5 seriate. Oil cells less common in rays passing through areas of fibers not associated with axial parenchyma. Fibers non-septate. TXSTATE 1256, T-1. Scale bar = 100  $\mu$ m. – F: TLS. Oil cells concentrated in the axial parenchyma and rays near axial parenchyma. TXSTATE 1256, T-1. Scale bar = 100  $\mu$ m. – G: RLS. Oil cells in the ray margin, within ray and in the axial parenchyma (arrow). TXSTATE 1256, R-1. Scale bar = 50  $\mu$ m.

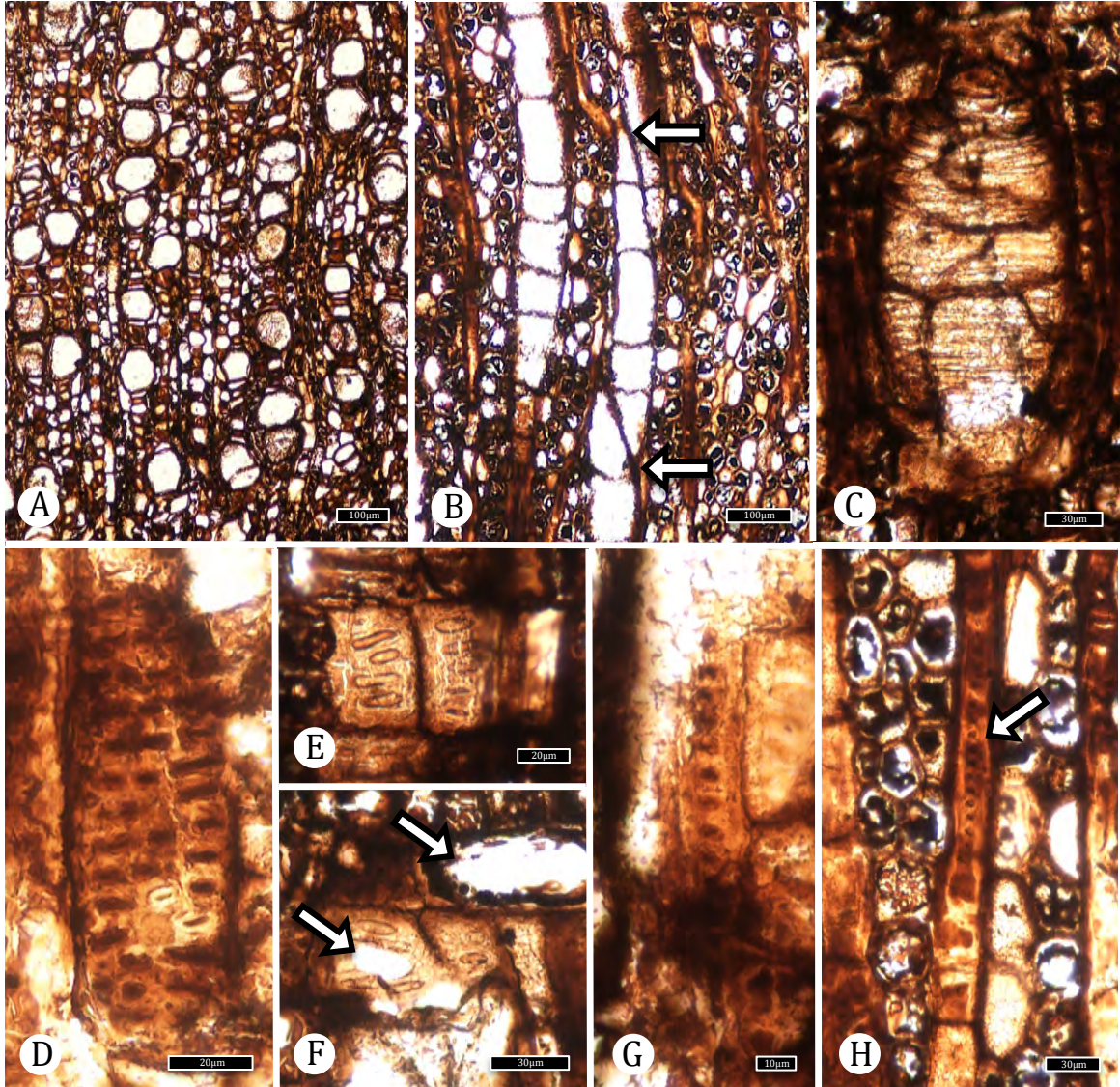


Figure 3.12. *Agujoxylon olacaceoides* Wheeler and Lehman (TXSTATE 1257) cf. Olacaceae. – A: TS. Vessels solitary (87%) and in short radial multiples. TXSTATE 1257, X-2. Scale bar = 100  $\mu\text{m}$ . – B: TLS. Vessel element with steeply inclined end walls (arrows), tyloses segmenting the vessels. TXSTATE 1257, T-3. Scale bar = 100  $\mu\text{m}$ . – C: RLS. Scalariform perforation plate. TXSTATE 1257, R-5. Scale bar = 30  $\mu\text{m}$ . – D: TLS. Opposite to scalariform intervessel pitting. TXSTATE 1257, T-1. Scale bar = 20  $\mu\text{m}$ . – E – F: Vessel-ray pits of two types. E: RLS. Vessel ray pits with reduced borders or simple, horizontally elongate. TXSTATE 1257, R-5. Scale bar = 20  $\mu\text{m}$ . – F: RLS. Large, simple vessel-ray pits, some occupying nearly the entire cross field area (arrows). TXSTATE 1257, R-3. Scale bar = 30  $\mu\text{m}$ . – G: RLS. Vessel-axial parenchyma pitting similar to intervessel pitting. TXSTATE 1257, T-2#. Scale bar = 10  $\mu\text{m}$ . – H: RLS. Fibers with bordered pits (arrow). TXSTATE 1257, T-3. Scale bar = 30  $\mu\text{m}$ .

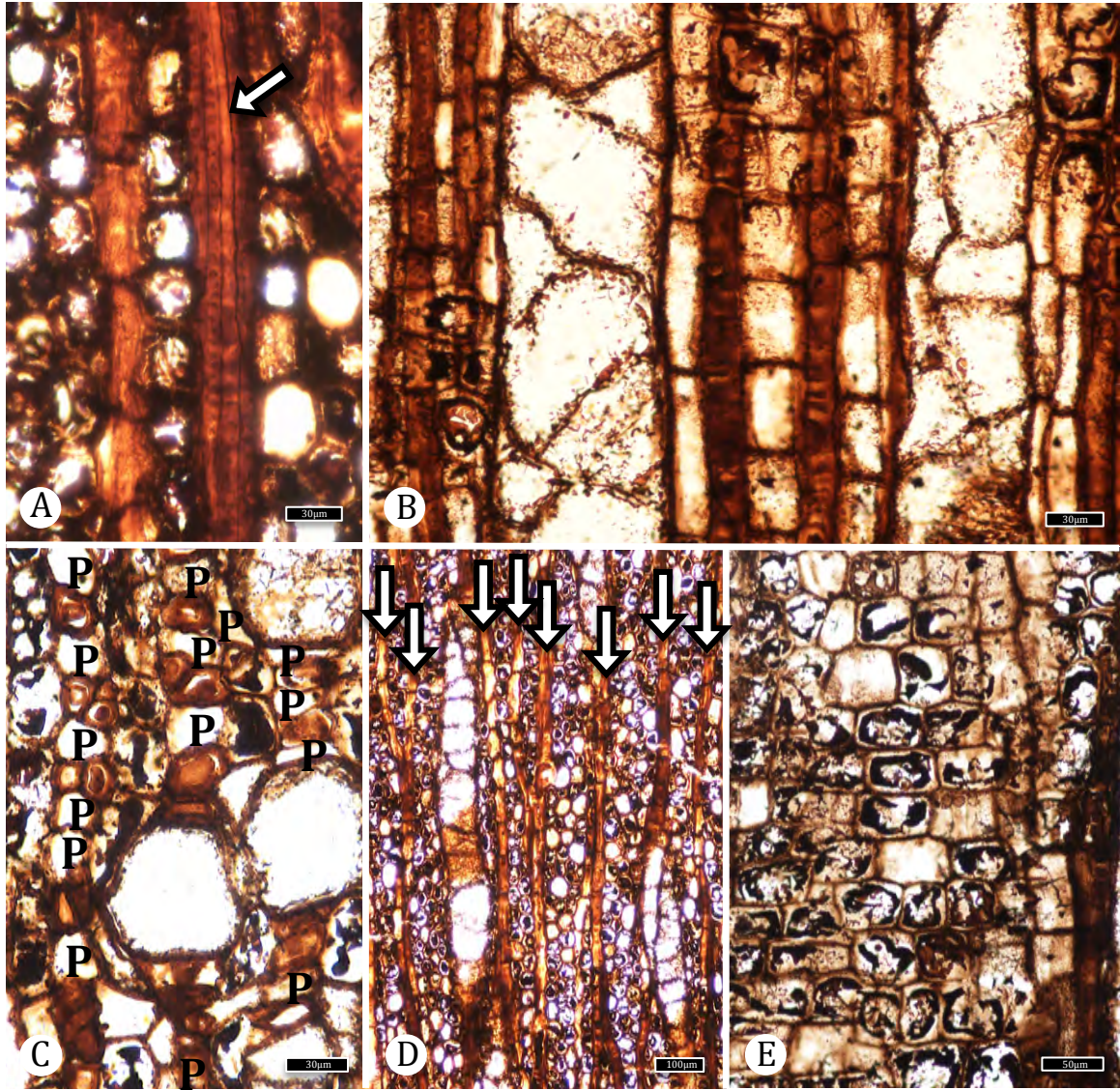


Figure 3.13. *Agujoxylon olacaceoides* Wheeler and Lehman (TXSTATE 1257) cf. Olacaceae. – A: Fibers non-septate. TXSTATE 1257, T-3. Scale bar = XX 30. – B: TLS. Axial parenchyma strands with cells of variable size, more-or-less alternating with fibers radially; tyloses in vessels. TXSTATE 1257, R-3. Scale bar = 30  $\mu\text{m}$ . – C: TS. Axial parenchyma predominantly diffuse apotracheal, more-or-less alternating with fibers, and scanty paratracheal. TXSTATE 1257, X-2. Scale bar = 30  $\mu\text{m}$ . – D: TLS. Rays 2–7 seriate, composed of procumbent cells with many rows of square and upright cells at the margins and throughout the ray. Axial parenchyma strands more than eight cells long (arrows). TXSTATE 1257, T-3. Scale bar = 100  $\mu\text{m}$  – E: RLS. Square and upright cells throughout the ray. TXSTATE 1257, R-4. Scale bar = 50  $\mu\text{m}$ .

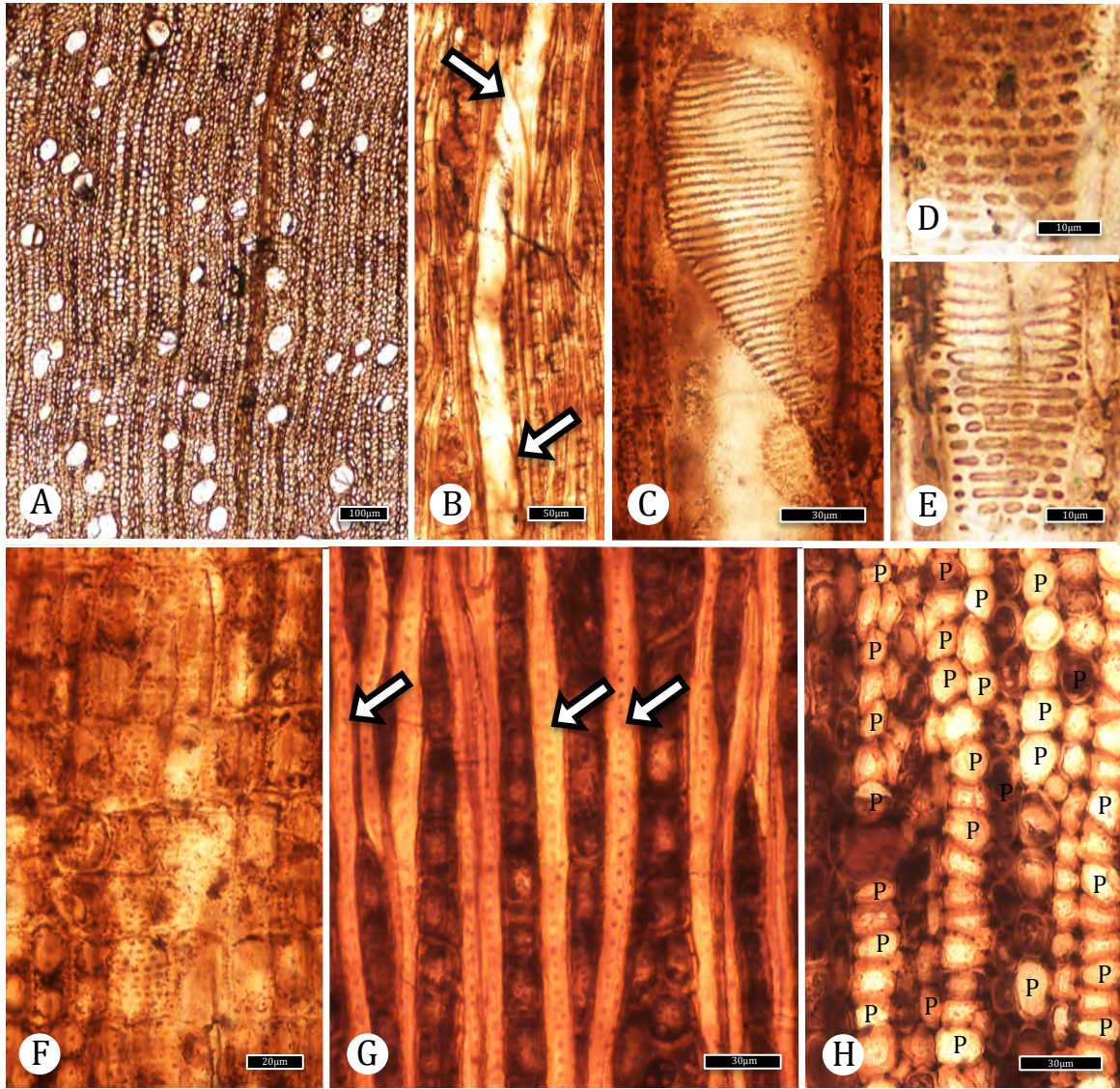


Figure 3.14. McRae wood holoxylotype Group IIA sp. 1 (TXSTATE 1259). – A: TS. Vessels solitary and oblique multiples of 2. TXSTATE 1259, X-4. Scale bar = 100  $\mu\text{m}$ . – B: TLS. Incline ends of vessel elements (arrows). TXSTATE 1259, T-7. Scale bar = 50  $\mu\text{m}$ . – C: RLS. Scalariform perforation plates with > 40 bars. TXSTATE 1259, R-4. Scale bar = 30  $\mu\text{m}$ . – D: RLS. Opposite intervessel pitting. TXSTATE 1259, R-4. Scale bar = 10  $\mu\text{m}$ . – E: RLS. Pitting on vessel element tails often horizontally elongate to scalariform. TXSTATE 1259-R-6. Scale bar = 10  $\mu\text{m}$ . – F: RLS. Vessel-ray pits with distinct borders. TXSTATE 1259, R-4#. Scale bar = 20  $\mu\text{m}$ . – G: TLS. Fibers with bordered pits, non-septate (arrows). TXSTATE T-5. Scale bar = 30  $\mu\text{m}$ . – H: TS. Axial parenchyma (P) diffuse and diffuse-in-aggregates. TXSTATE X-1. Scale bar = 30  $\mu\text{m}$ .

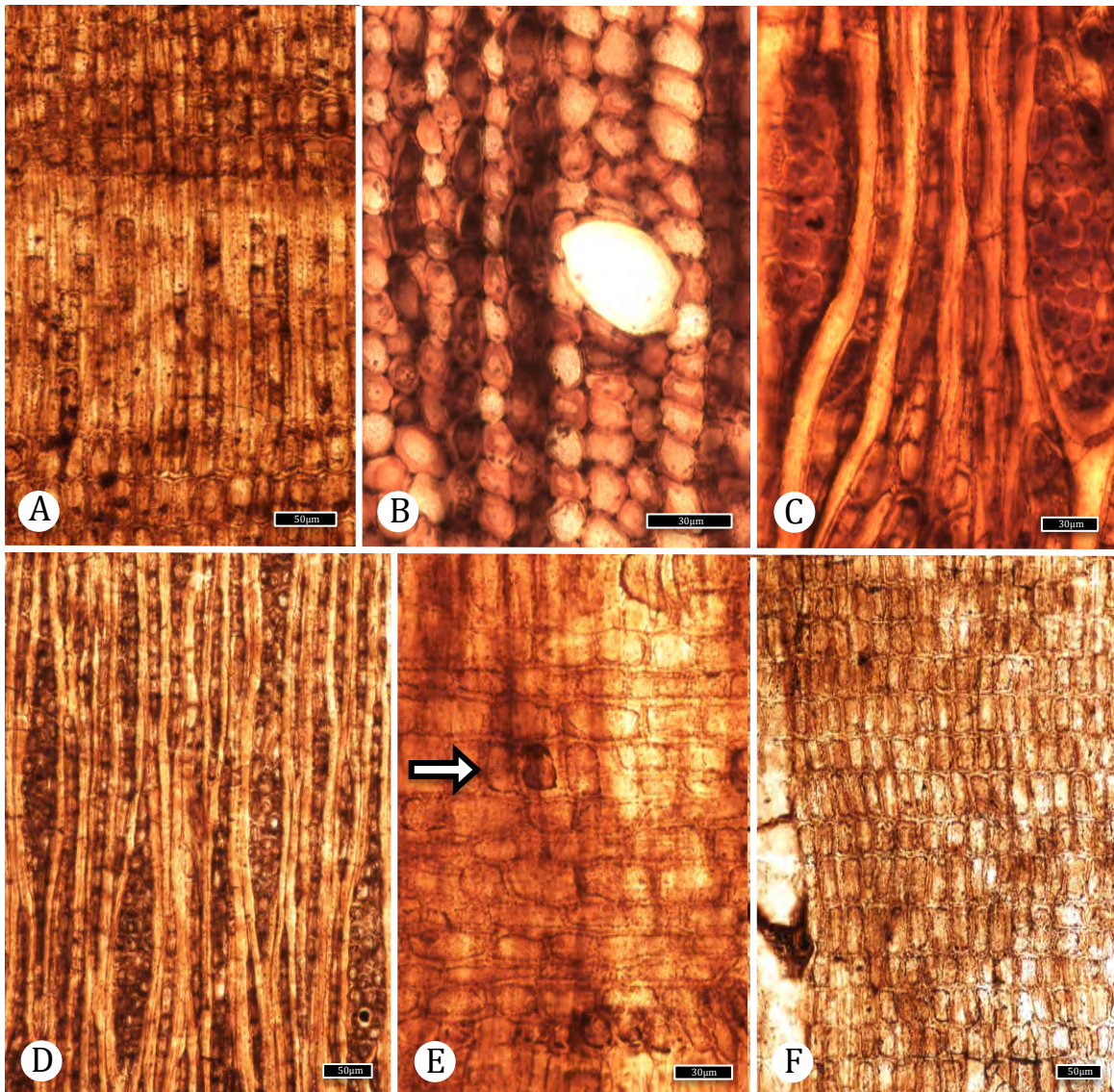


Figure 3.15. McRae wood holoxylotype Group IIA sp. 1 (TXSTATE 1259).  
 – A: RLS. Radial section showing axial parenchyma strands. TXSTATE 1259, R-4. Scale bar = 50  $\mu\text{m}$ . – B: TS. Axial parenchyma scanty paratracheal. TXSTATE 1259, X-1#. Scale bar = 30  $\mu\text{m}$ . – C: TLS. Axial parenchyma strands. TXSTATE 1259, T-4. Scale bar = 30  $\mu\text{m}$ . – D: TLS. Multiseriate rays heterocellular with one to many square or upright marginal rows. Uniseriate and biseriate rays common. TXSTATE 1259, T-3. Scale bar = 100  $\mu\text{m}$ . – E: RLS. Row of upright cells among procumbent cells (arrow). TXSTATE 1259, R-5#. Scale bar = 30  $\mu\text{m}$ . – F: RLS. Uniseriate rays composed of all square or upright cells. TXSTATE 1259, R-5. Scale bar = 50  $\mu\text{m}$ .

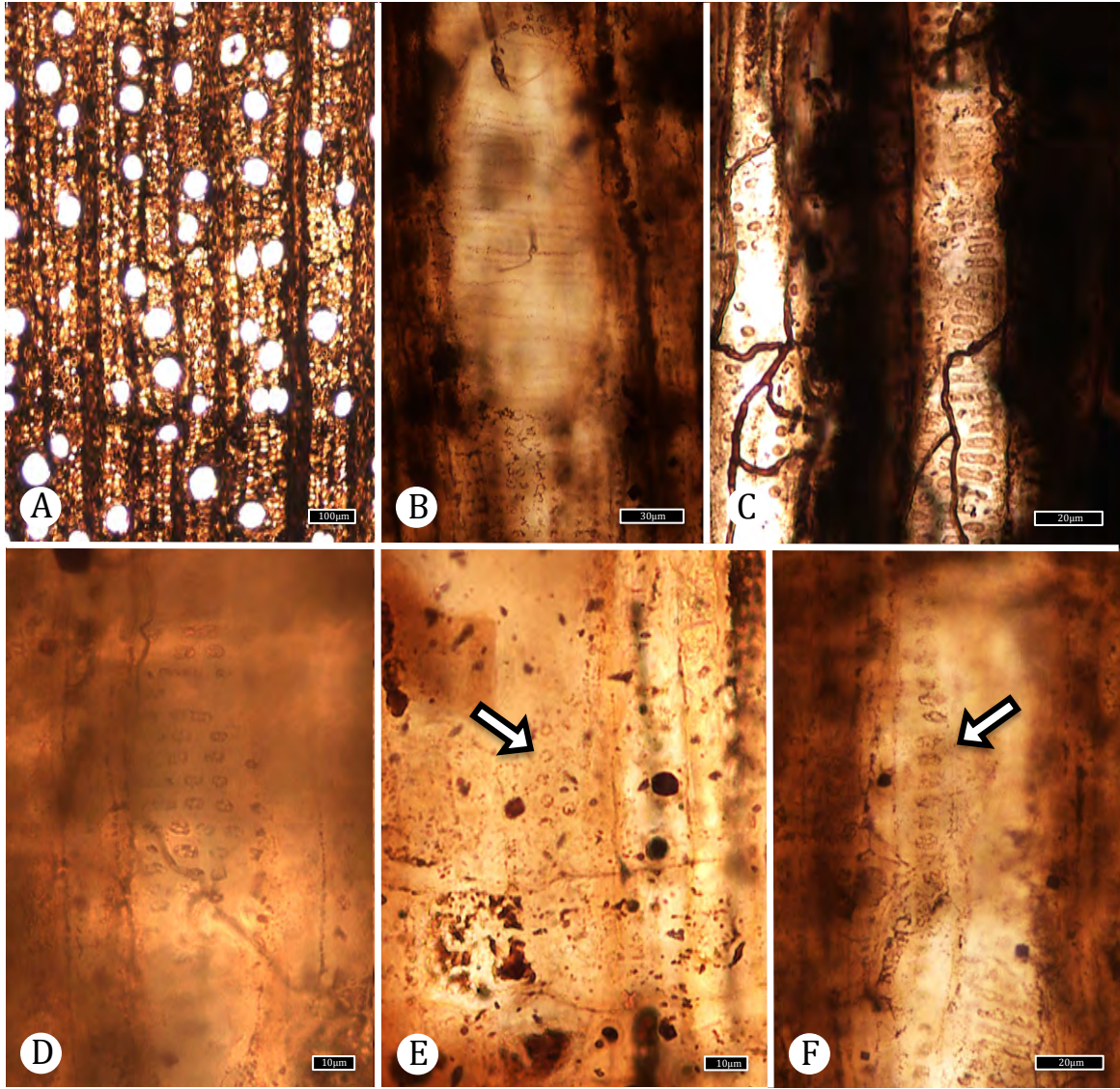


Figure 3.16. McRae wood holoxylotype Group IIA sp. 2 (TXSTATE 1260). – A: TS. Wood diffuse porous, vessels exclusively solitary. TXSTATE 1260, X-1. Scale bar = 100  $\mu\text{m}$ . – B: RLS. Scalariform perforation plate with >20 bars. TXSTATE 1260, R-1. Scale bar = 30  $\mu\text{m}$ . – C: TLS. Intervessel pitting round to oval to scalariform. Fungal hyphae present. TXSTATE 1260, T-1. Scale bar = 20  $\mu\text{m}$ . – D: RLS. Intervessel pitting oval to horizontally elongate. TXSTATE 1260, R-2. Scale bar = 10  $\mu\text{m}$ . – E: RLS: Vessel-ray pitting with reduced borders, small, round to oval and not crowded (arrow). TXSTATE 1260, R-2. Scale bar = 10  $\mu\text{m}$ . – F: RLS. Vessel-axial parenchyma pitting similar to intervessel pitting (arrow). TXSTATE 1260, R-1. Scale bar = 20  $\mu\text{m}$ .

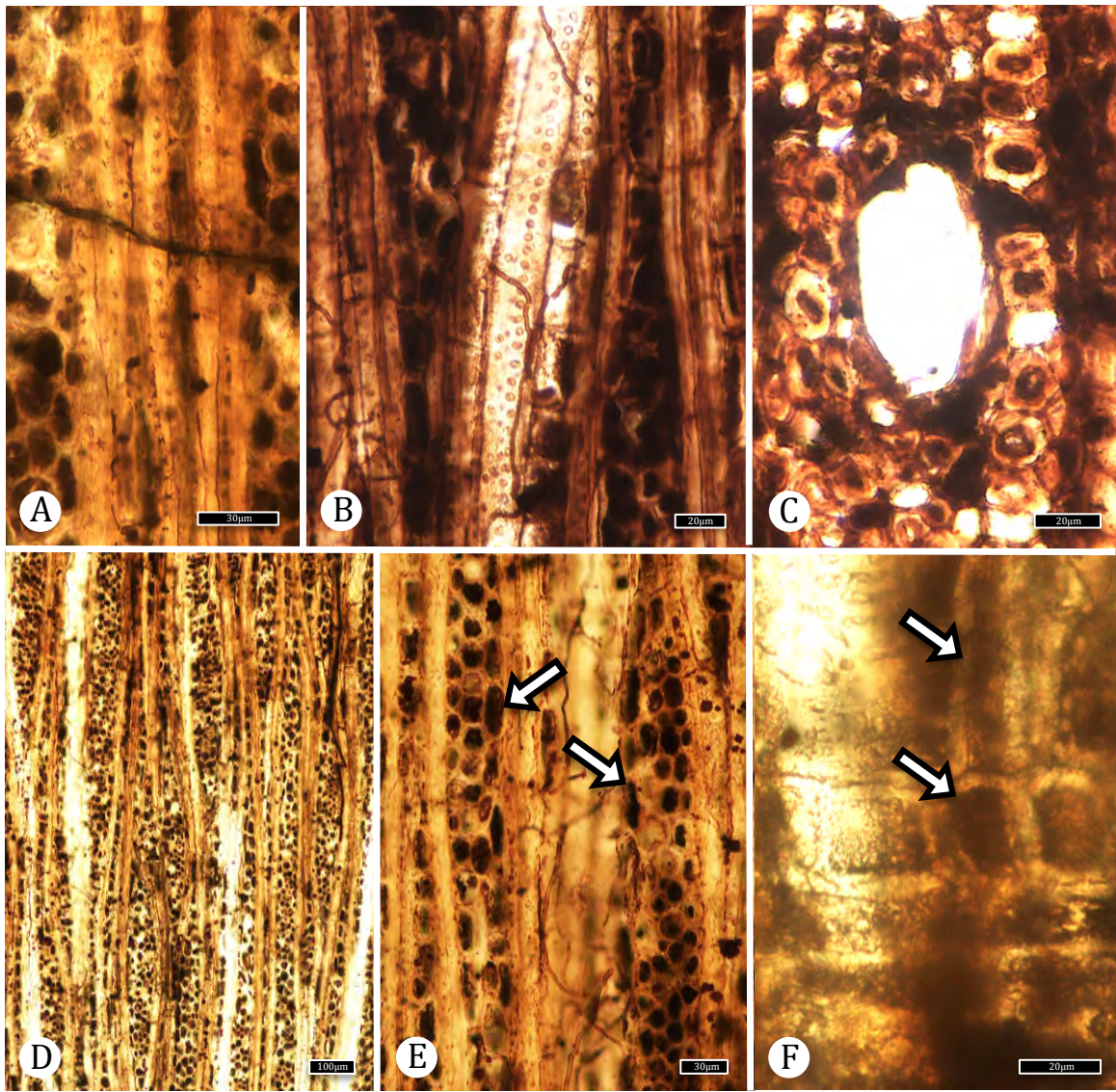


Figure 3.17. McRae wood holoxylotype Group IIA sp. 2 (TXSTATE 1260).  
 – A: TLS. Fibers with a single row of bordered pits. TXSTATE 1260, T-2. Scale bar = 30  $\mu\text{m}$ . – B: TLS. Vasicentric tracheids with 2–3 rows of pits. TXSTATE 1260, T-1. Scale bar = 20  $\mu\text{m}$ . – C: TS. Axial parenchyma not uncommon, diffuse. TXSTATE 1260, X-1. Scale bar = 20  $\mu\text{m}$ . – D: TLS. Rays composed of procumbent cells with 1 to usually less than 5 upright marginal rows. TXSTATE 1260, T-2. Scale bar = 100  $\mu\text{m}$ . – E: Sheath cells present (arrows). TXSTATE 1260, T-2. Scale bar = 30  $\mu\text{m}$ . – F: RLS. Ray with square and upright cells (arrows). TXSTATE 1260, R-1. Scale bar = 20  $\mu\text{m}$ .

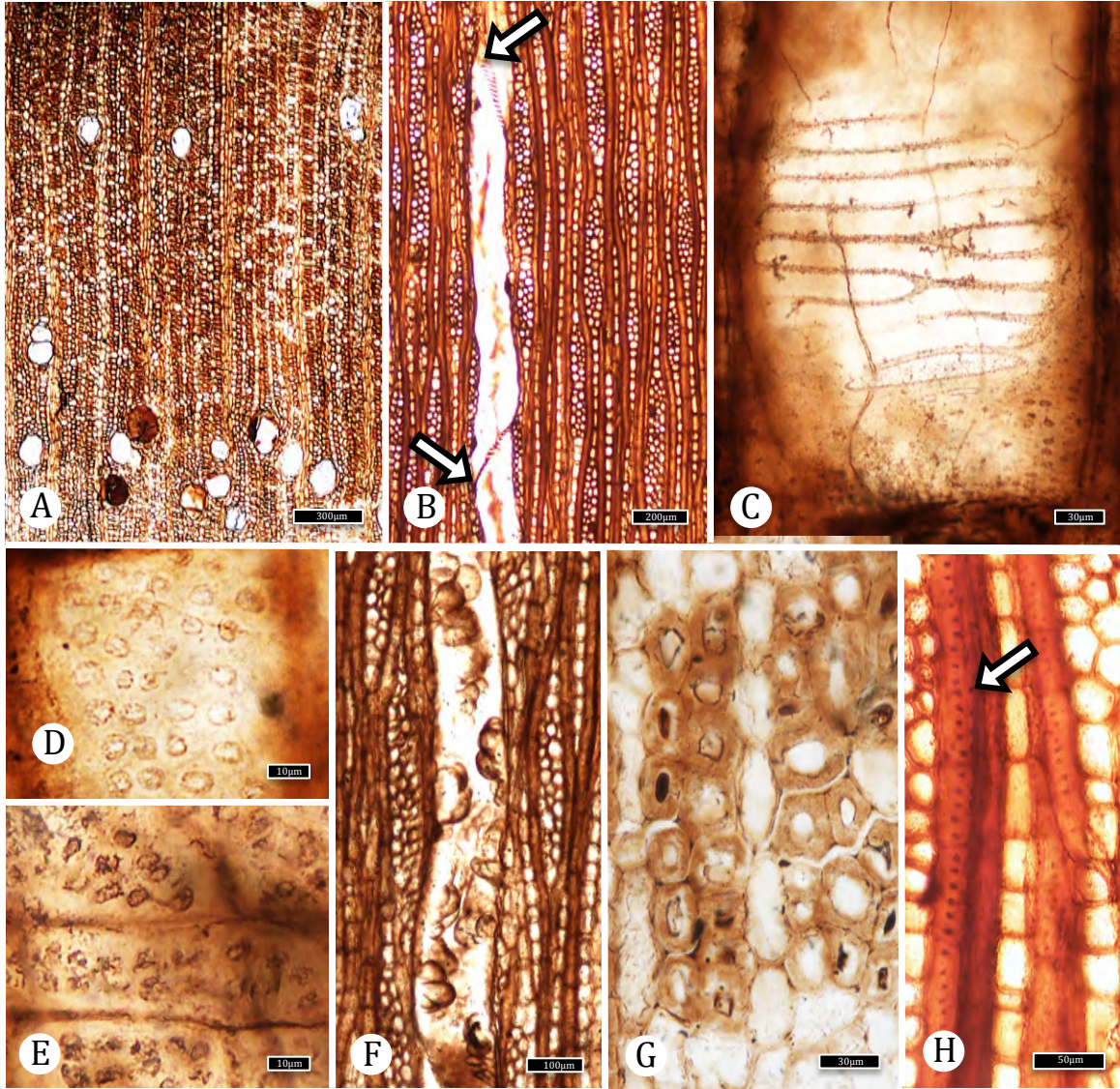


Figure 3.18. *Metcalfeoxylon kirtlandense* Wheeler, McClammer and LaPasha (TXSTATE 1261). – A: TS. Vessels solitary (93%). Some areas without vessels; axial parenchyma diffuse to diffuse-in-aggregates, sometimes forming short lines. TXSTATE 1261, X-2. Scale bar = 300  $\mu\text{m}$ . – B: TLS. Vessel element (between arrows). TXSTATE 1261, T-4. Scale bar = 200  $\mu\text{m}$ . – C: RLS. Scalariform perforation plate with forked bars. TXSTATE 1261, r-4. Scale bar = 30  $\mu\text{m}$ . – D: RLS. Intervessel pitting opposite to alternate. TXSTATE 1261, R-4. Scale bar = 10  $\mu\text{m}$ . – E: RLS: Vessel-ray pits with distinct borders. TXSTATE 1261, R-3. Scale bar = 10  $\mu\text{m}$ . – F: TLS: Tyloses bubble-like. TXSTATE 1261, T-3. Scale bar = 100  $\mu\text{m}$ . – G: TS. Fibers medium to thick-walled. TXSTATE 1261, X-2. Scale bar = 30  $\mu\text{m}$ . – H: Fibers with distinctly bordered pits (arrow). TXSTATE 1261, T-2. Scale bar = 30  $\mu\text{m}$ .

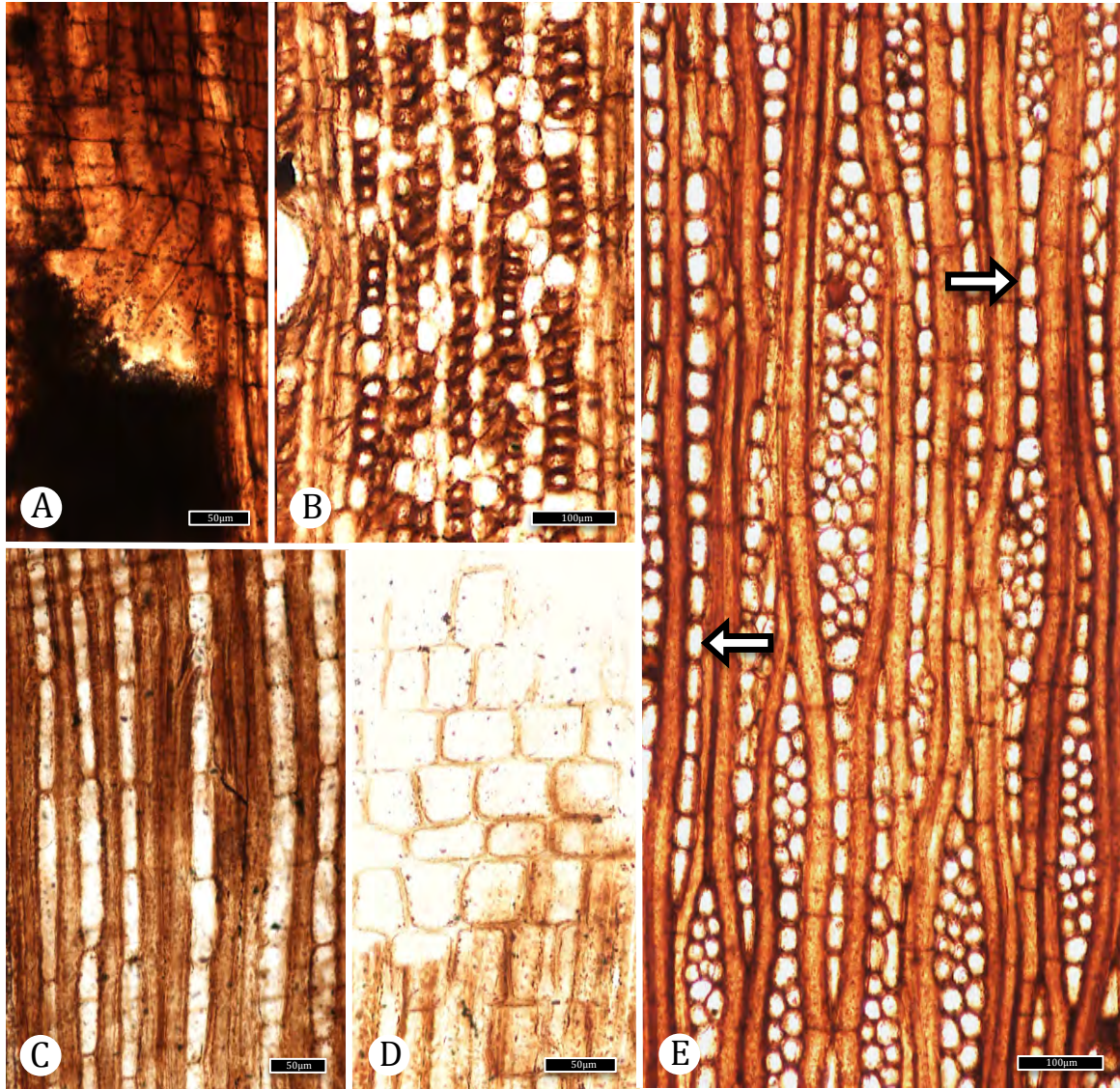


Figure 3.19. *Metcalfeoxylon kirtlandense* Wheeler, McClammer and LaPasha (TXSTATE 1261). – A: RLS. Vasicentric tracheids with several rows of pits. TXSTATE 1261, R-3. Scale bar = 50  $\mu\text{m}$ . – B: TS. Axial parenchyma diffuse, diffuse-in-aggregates, forming short lines TXSTATE 1261, X-1. Scale bar = 100  $\mu\text{m}$ . – C: RLS. Axial parenchyma alternating with fibers in radial view. TXSTATE 1261, R-5. Scale bar = 50  $\mu\text{m}$ . – D: RLS. Square and upright cells intermixed with barely procumbent ray cells. TXSTATE 1261, R-5. Scale bar = 50  $\mu\text{m}$ . – E: Multiseriate rays with many uniseriate margin rows of square or upright cells. Multiseriate portions of rays joined by long, uniseriate sections of square or upright cells (right arrow). Uniseriate rays predominately composed of square or upright cells, generally < 20 cells (left arrow). TXSTATE 1261, T-4. Scale bar = 100  $\mu\text{m}$ .

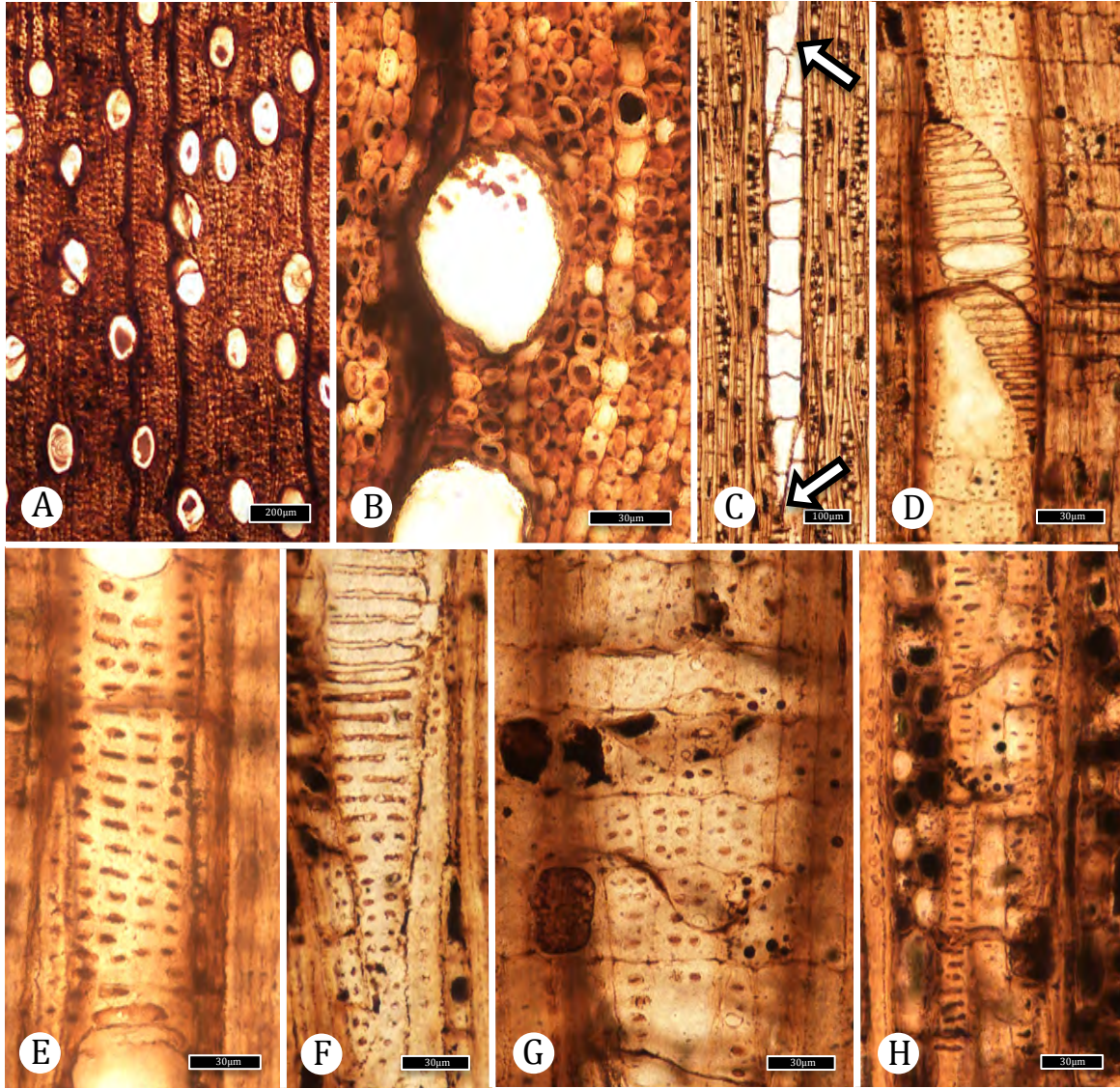


Figure 3.20. McRae wood holoxylotype Group IIA sp. 3 (TXSTATE 1262). – A: TS. Wood diffuse-porous. Vessels solitary. TXSTATE 1262, X-1. Scale bar = 200  $\mu\text{m}$ . – B: TS. Vessels oval in outline. TXSTATE 1262, X-2. Scale bar = 30  $\mu\text{m}$ . – C: TLS. Vessel element with oblique end walls (arrows). TXSTATE 1262, T-2. Scale bar = 100  $\mu\text{m}$ . – D: RLS. Scalariform perforation plate. TXSTATE 1262, R-2. Scale bar = 30  $\mu\text{m}$ . – E: RLS. Opposite intervessel pits. TXSTATE 1262, R-2. Scale bar = 30  $\mu\text{m}$ . – F: TLS. Vessel tail with opposite to scalariform pitting. TXSTATE 1262, T-2. Scale bar = 30  $\mu\text{m}$ . – G: RLS. Vessel-ray pits similar to intervessel pits. TXSTATE 1262, R-2. Scale bar = 30  $\mu\text{m}$ . – H: TLS. Vessel-axial parenchyma pits similar to intervessel pits. TXSTATE 1262, T-2. Scale bar = 30  $\mu\text{m}$ .

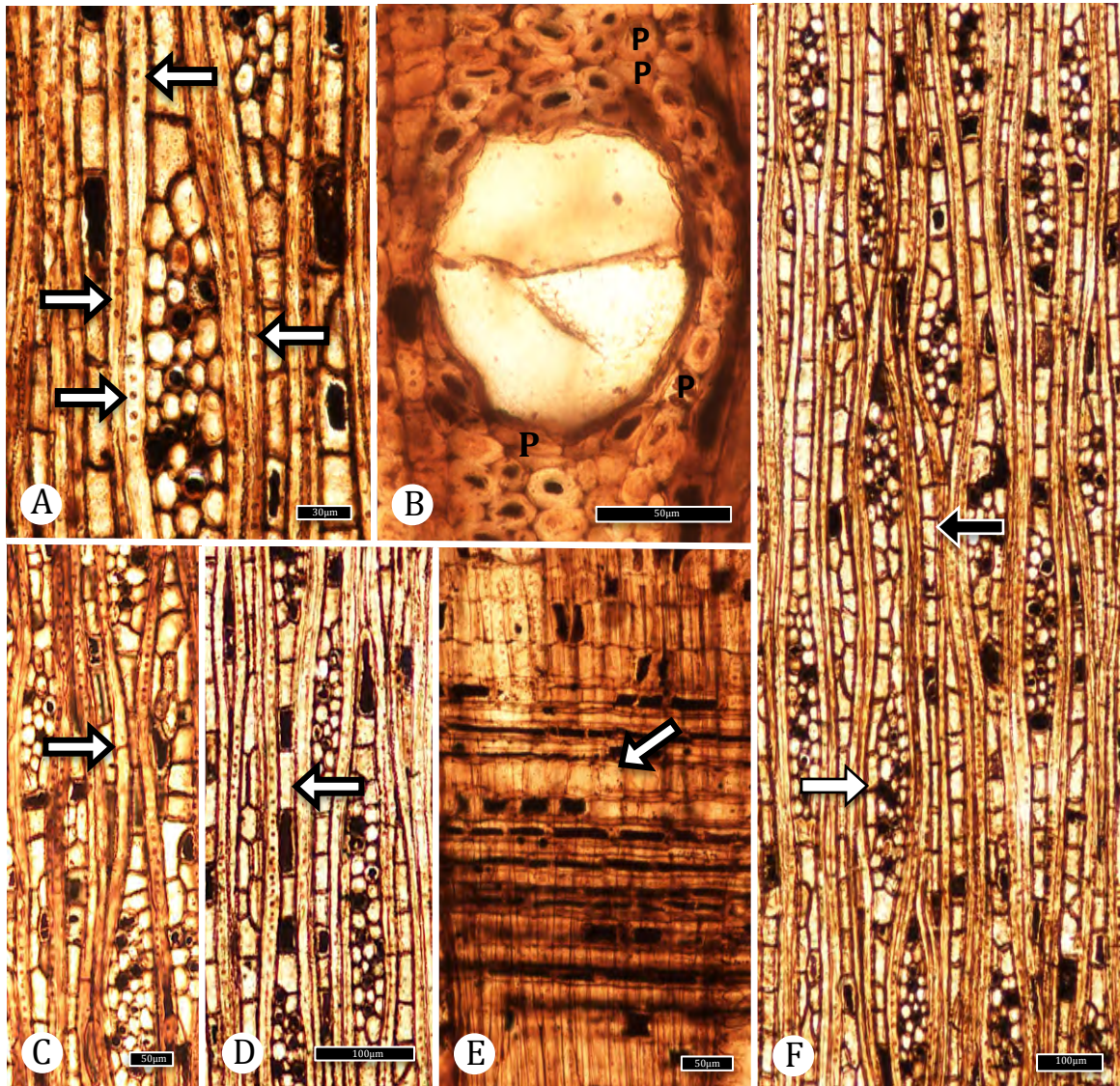


Figure 3.21. McRae wood holoxylotype Group IIA sp. 3 (TXSTATE 1262).  
 - A: TLS. Fibers with bordered pits in discontinuous rows (arrows). TXSTATE 1262, T-1. Scale bar = 30  $\mu\text{m}$ . - B: TS. Axial parenchyma (P) uncommon, diffuse and scanty paratracheal. TXSTATE 1262, X-2. Scale bar = 50  $\mu\text{m}$ . - C: TLS. Axial parenchyma 2 (arrow) to 4 cells per strand. TXSTATE 1262, T-1. Scale bar = 50  $\mu\text{m}$ . - D: TLS. Multiseriate ray portions connected by a few to many uniseriate square or upright cells (arrows). TXSTATE 1262, T-1. Scale bar = 100  $\mu\text{m}$ . - E: RLS. Multiseriate rays composed of procumbent cells with one to many square or upright margin rows; square or upright row within ray (arrow). TXSTATE 1262, R-2. Scale bar = 50  $\mu\text{m}$ . - F: TLS. Multiseriate rays mostly 2-4 seriate, composed of procumbent cells with one to many square or upright margin rows. Uniseriate rays mostly square and upright cells (black arrow). Sheath cells occasionally present (white arrow). TXSTATE 1262, T-1. Scale bar = 100  $\mu\text{m}$ .

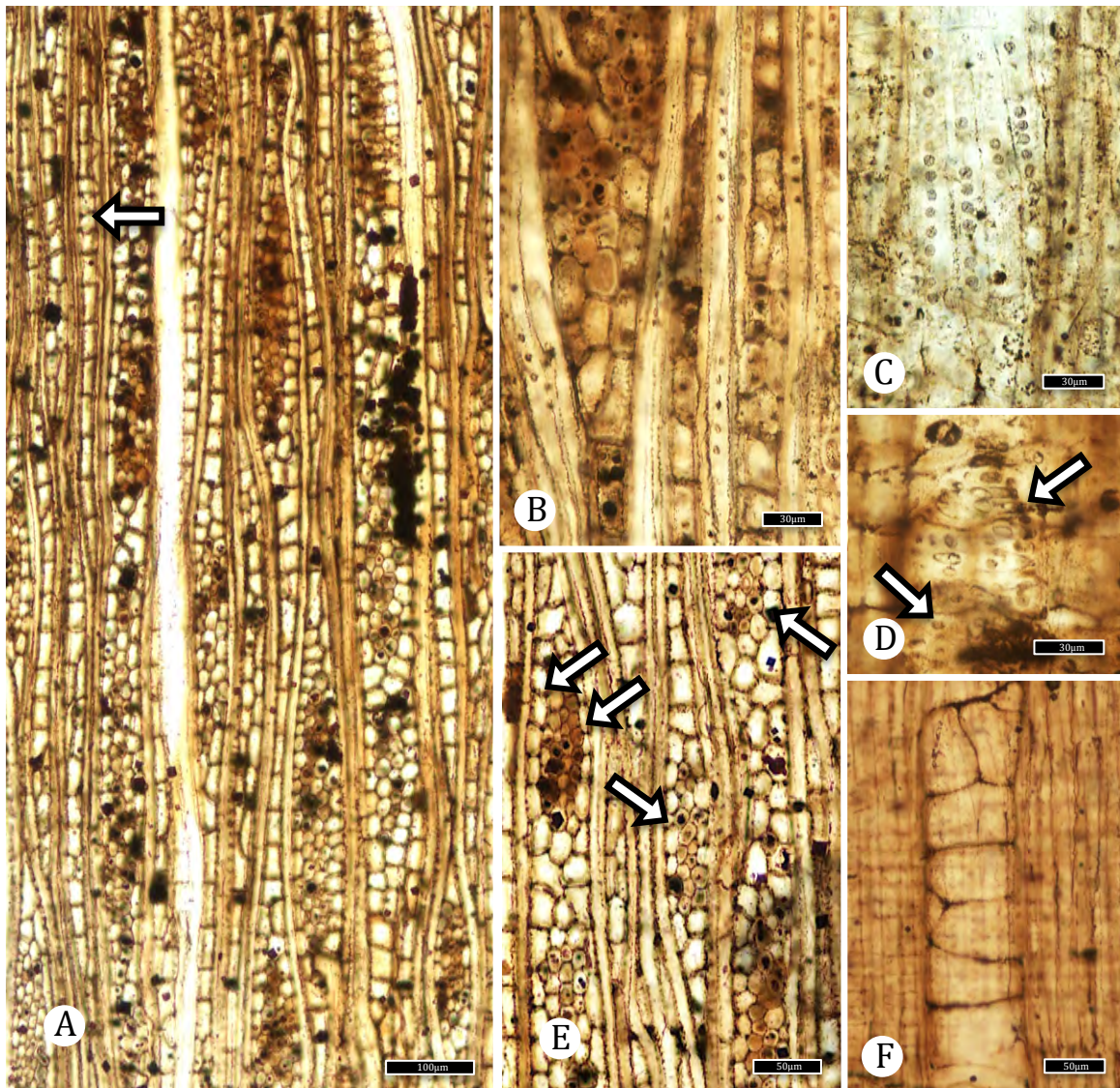


Figure 3.22. McRae wood paraxylotype Group IIA sp. 3 (TXSTATE 1263). – A: TLS. Multiseriate rays 2-6 cells wide; uniseriate rays not common (6%), composed of upright and possibly procumbent cells (arrow). TXSTATE 1263, T-1. Scale bar = 100  $\mu\text{m}$ . – B: TLS. Bordered fiber pits “discontinuous” along the length of the fiber. TXSTATE 1262, T-4. Scale bar = 30  $\mu\text{m}$ . – C: RLS. Vasicentric tracheids with one row of bordered pits. TXSTATE 1262, R-4. Scale bar = 30  $\mu\text{m}$ . – D: TLS. Vessel-ray pits either bordered (round or oval) (bottom arrow) or with reduced borders (oval to horizontally elongate) (top arrow). TXSTATE 1262, R-4. Scale bar = 30  $\mu\text{m}$ . – E: TLS. Sheath cells common (arrows). TXSTATE 1262, T-1. Scale bar = 50  $\mu\text{m}$ . – F: Tyloses sometimes segmenting. TXSTATE 1262, R-1. Scale bar = 50  $\mu\text{m}$ .

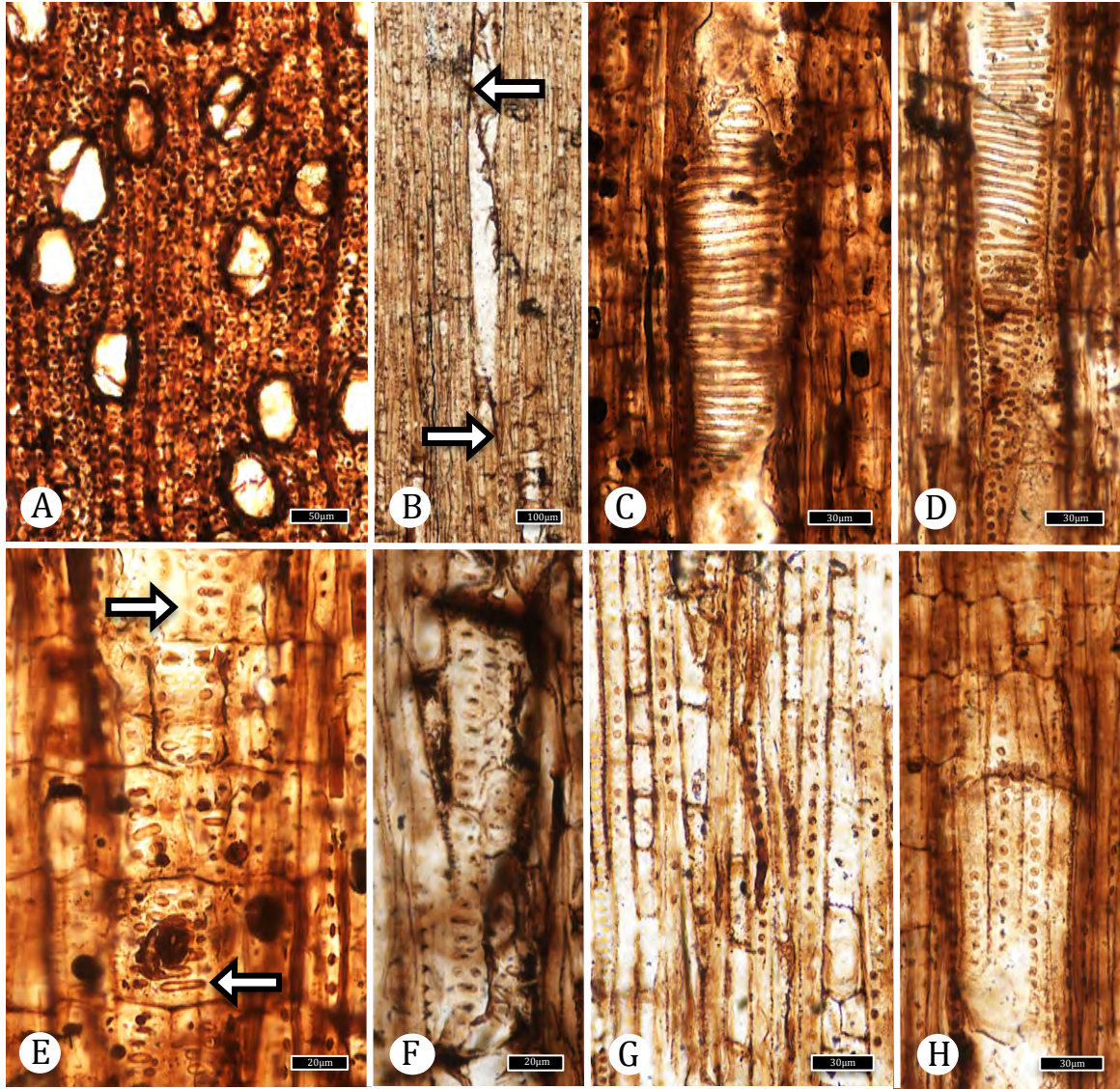


Figure 3.23. McRae wood paraxylotype Group IIA sp. 3 (TXSTATE 1264). – A: TS. Vessels solitary, diffuse porous. TXSTATE 1264, X-2. Scale bar = 50  $\mu\text{m}$ . – B: TLS. Vessel element (arrows). TXSTATE 1264, T-2. Scale bar = 100  $\mu\text{m}$ . – C: RLS. Scalariform perforation plate. TXSTATE 1264, R-2. Scale bar = 30  $\mu\text{m}$ . – D: RLS. Vessel with scalariform intervessel pitting. TXSTATE 1264, R-2. Scale bar = 30  $\mu\text{m}$ . – E: RLS. Vessel-ray pitting bordered, round to oval (top arrow) or with reduced borders and oval to horizontally elongate (bottom arrow). TXSTATE 1264, R-2. Scale bar = 20  $\mu\text{m}$ . – F: TLS. Vessel-axial parenchyma pitting with distinct borders, horizontally oval. TXSTATE 1264, T-2. Scale bar = 20  $\mu\text{m}$ . – G: TLS. Fiber pits with distinctly bordered pits arranged in groups and alternating with areas without pits. TXSTATE 1264, T-1. Scale bar = 30  $\mu\text{m}$ . – H: RLS. Vasicentric tracheids with one continuous row of distinctly bordered pits. TXSTATE 1264, R-2. Scale bar = 30  $\mu\text{m}$ .

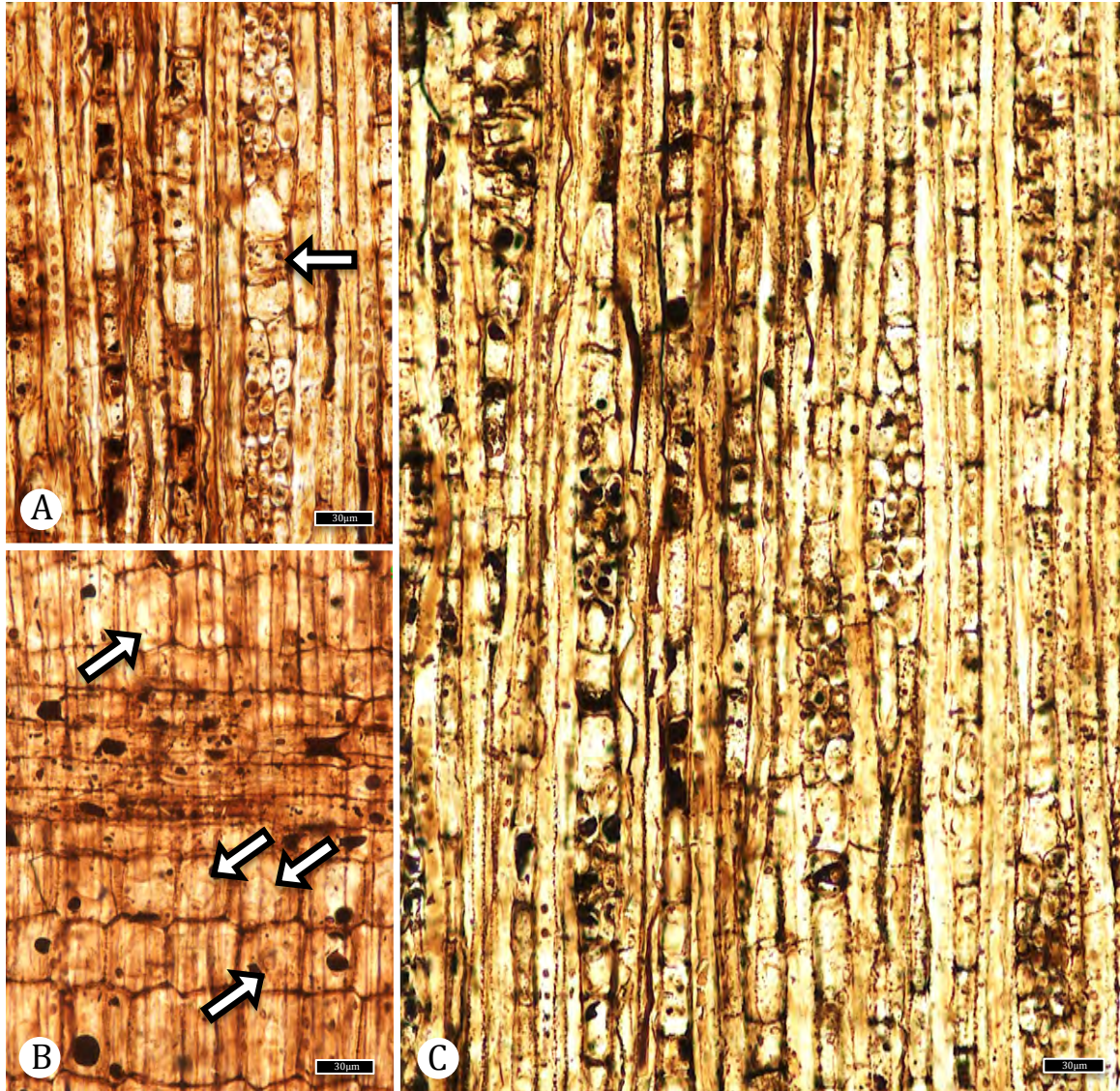


Figure 3.24. McRae wood paraxylotype Group IIA sp. 3 (TXSTATE 1264).  
 - A: TLS. Multiseriate portion of ray as wide as uniseriate portion (arrow). TXSTATE 1264, T-2. Scale bar = 30 µm. - B: RLS. Prismatic crystals in ray parenchyma (arrows). TXSTATE 1264, R-1#. Scale bar = 30 µm. - C: TLS. Rays mostly 3 cells wide. TXSTATE 1264, T-2. Scale bar = 30 µm.

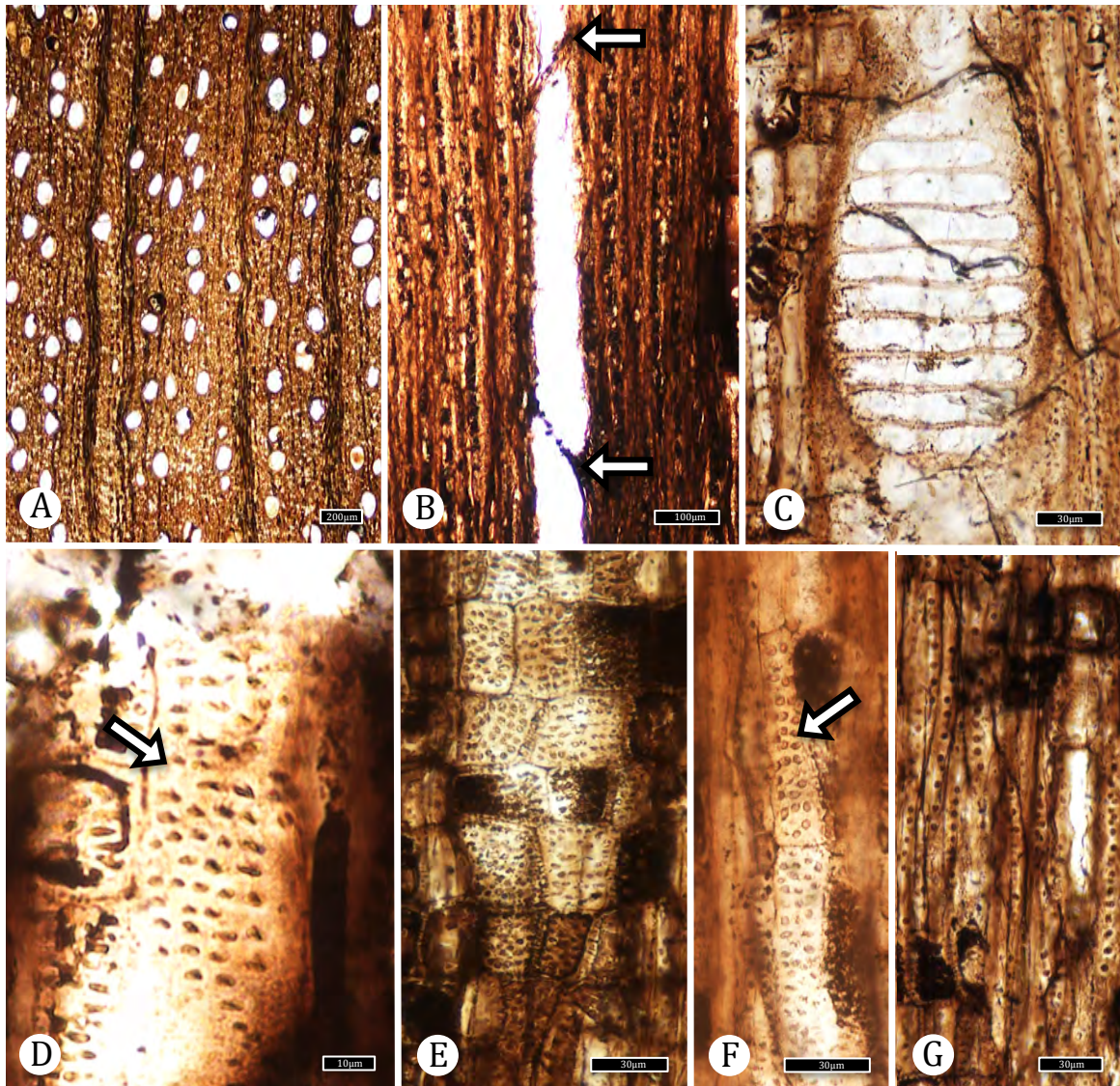


Figure 3.25. Cf. *Icacinnoxylon* sp. 1 (holoxylotype) (TXSTATE 1265) cf. Icacinaceae.  
 - A: TS. Solitary vessels. Rays of two sizes. TXSTATE 1265, X-1. Scale bar = 200  $\mu\text{m}$ .  
 - B: TLS. Vessel element with inclined end walls (arrows). TXSTATE 1265, T-7 Scale bar = 100  $\mu\text{m}$ .  
 - C: RLS. Scalariform perforation plate. TXSTATE 1265, R-1. Scale bar = 30  $\mu\text{m}$ .  
 - D: TLS. Intervessel pitting opposite to sub-alternate (arrow). TXSTATE 1265, T-5. Scale bar = 10  $\mu\text{m}$ .  
 - E: RLS. Vessel-ray pits with distinct borders, crowded, covering the entire ray cell. TXSTATE 1265, R-1. Scale bar = 30  $\mu\text{m}$ .  
 - F: TLS. Vessel-axial parenchyma (arrow) pitting similar to vessel-ray pitting. TXSTATE 1265, T-2. Scale bar = 30  $\mu\text{m}$ .  
 - G: Fibers with distinctly bordered pits. TXSTATE 1265, R-1. Scale bar = 30  $\mu\text{m}$ .

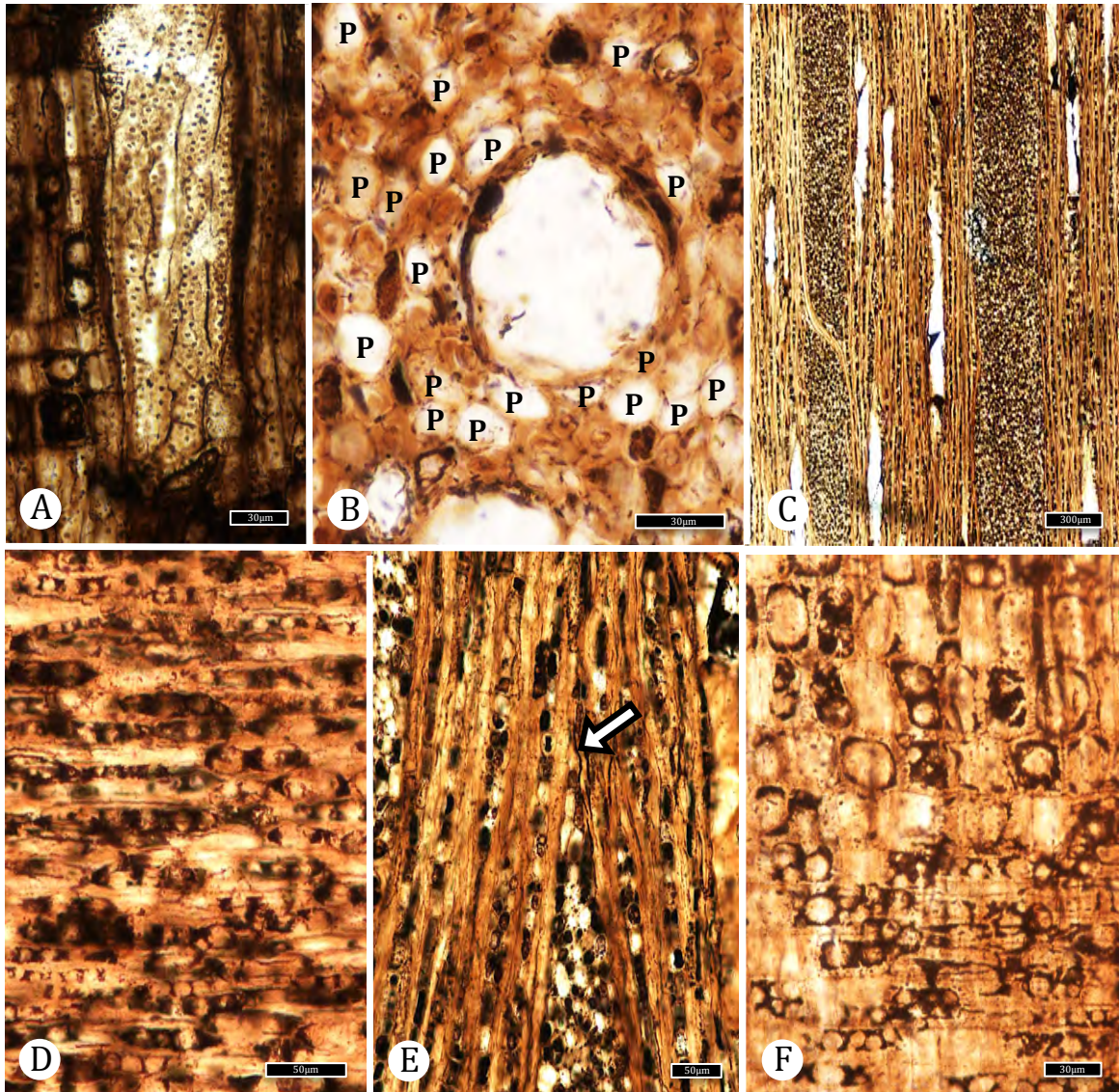


Figure 3.26. Cf. *Icacinoxylon* sp1 (holoxylotype)(TXSTATE 1265) cf. Icacinaceae. – A: RLS. Vasicentric tracheids with 2-3 rows of pits. TXSTATE 1265, R-1. Scale bar = 30  $\mu$ m. – B: TS. Axial parenchyma (P) diffuse, diffuse-in-aggregates and scanty paratracheal. TXSTATE 1265, X-4. Scale bar = 30  $\mu$ m. – C: TLS. Larger rays >10 cells wide and >1 mm tall. TXSTATE 1265, T-1. Scale bar = 300  $\mu$ m. – D: RLS. Body of the ray composed of procumbent cells. TXSTATE 1265, R-4. Scale bar = 50  $\mu$ m. – E: TLS. Body of ray composed of procumbent cells with a few to over 4 rows of upright or square marginal rows (arrow). TXSTATE 1265, T-1. Scale bar = 50  $\mu$ m.– F: RLS. Ray with many square or upright marginal rows. TXSTATE 1265, R-2. Scale bar = 30  $\mu$ m.

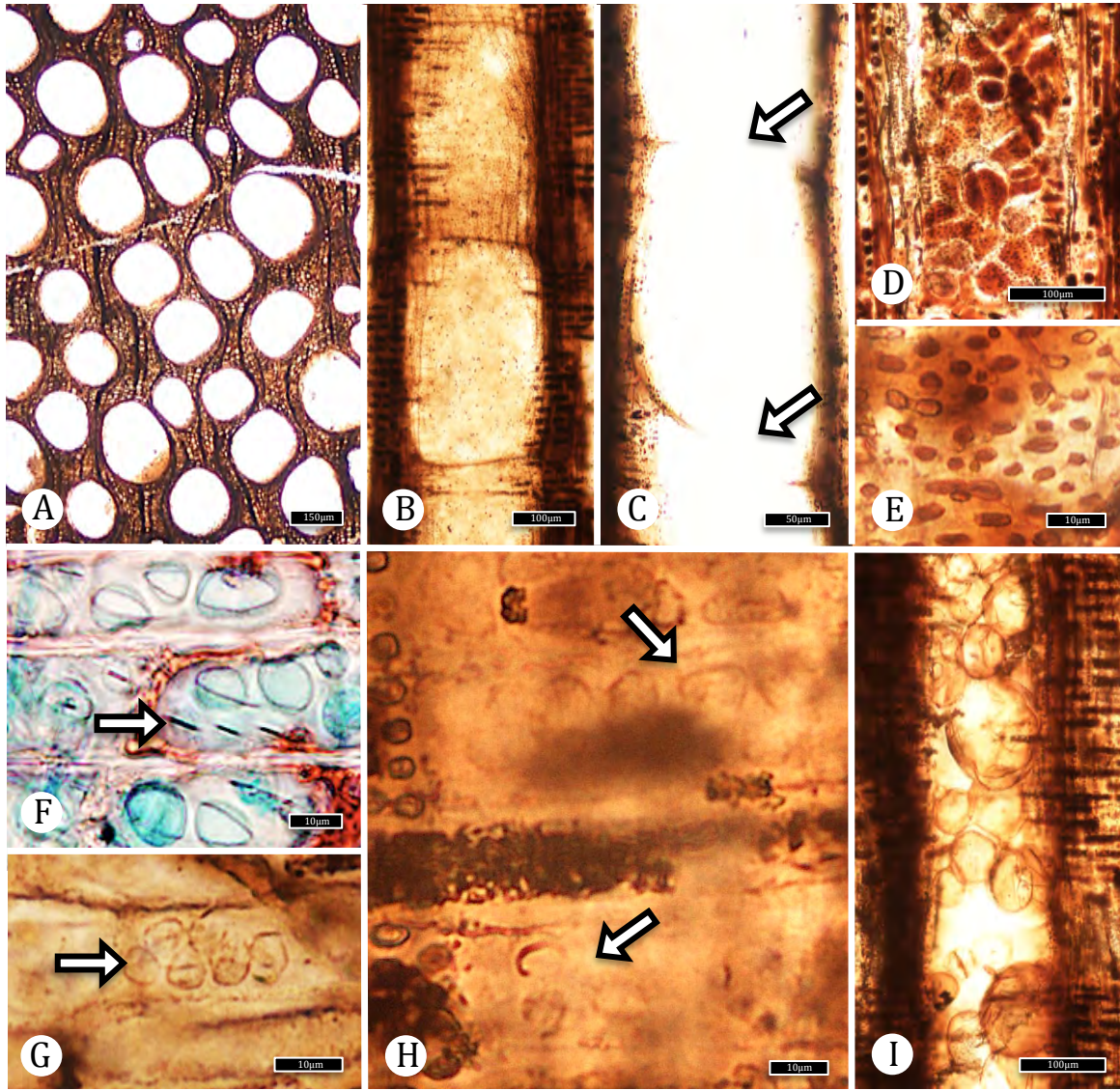


Figure 3.27. *Fulleroxylon* sp 1 (holoxylotype) (TXSTATE 1275) cf. Connaraceae. – A: TS. Vessels diffuse-porous, vessels densely arranged. TXSTATE 1275, X-2. Scale bar = 150  $\mu\text{m}$ . – B: RLS. Vessel elements with near horizontal end walls. TXSTATE 1275, R-2. Scale bar = 100  $\mu\text{m}$ . – C: TLS. Simple perforation plates (arrows). TXSTATE 1275, T-1. Scale bar = 50  $\mu\text{m}$ . – D: TLS. Pitting superimposed on tyloses may represent vessel-vasicentric tracheid pits. TXSTATE 1275, R-2. Scale bar = 100  $\mu\text{m}$ . – E: TLS. Detail of image Fig. 43D. TXSTATE 1275, R-2. Scale bar = 10  $\mu\text{m}$ . – F: RLS. Vessel-ray parenchyma pitting with reduced borders in extant Connaraceae mostly comparable to pits in Fig. 3.27H. Arrow indicates pits similar to fossil pits in Fig. 3.27G. (photo courtesy E. Wheeler). Scale bar = 10  $\mu\text{m}$ . – G: RLS. Vessel-ray pits, rounded. (arrow). TXSTATE 1275, R-2. Scale bar = 10  $\mu\text{m}$ . – H: RLS. Vessel-ray pits irregularly shaped (top arrow), with reduced borders, round to oval (bottom arrow). TXSTATE 1275, R-1. Scale bar = 10  $\mu\text{m}$ . – I: RLS. Tyloses abundant, bubble-like. TXSTATE 1275, R-1. Scale bar = 100  $\mu\text{m}$ .

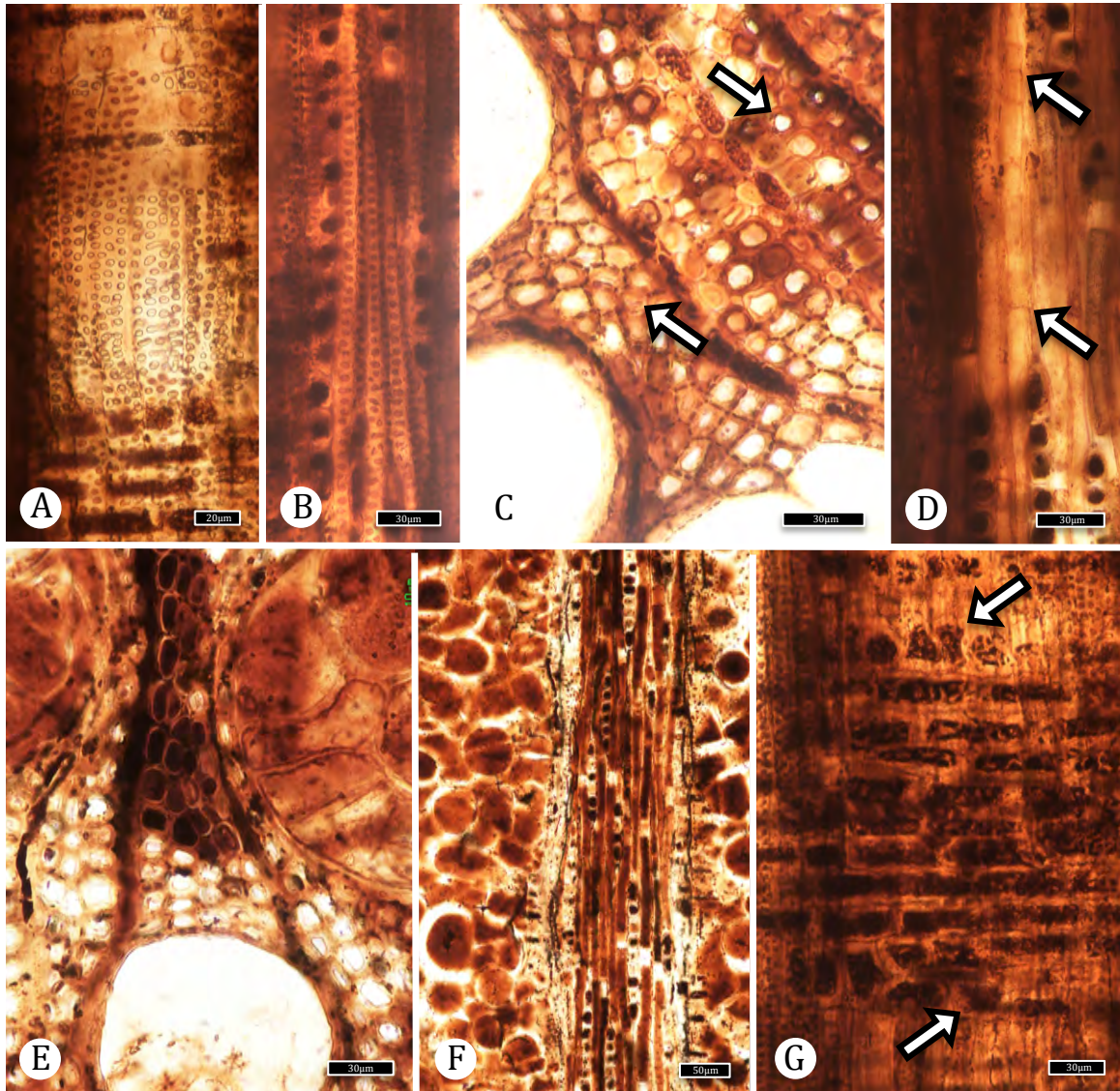


Figure 3.28. *Fulleroxylon* sp 1 (holoxylotype) (TXSTATE 1275) cf. Connaraceae.  
 – A: RLS. Vasicentric tracheids with multiple rows of pits. TXSTATE 1275, R-1. Scale bar = 20  $\mu\text{m}$ . – B: TLS. Fibers with one row of bordered pits. TXSTATE 1275, T-1. Scale bar = 30  $\mu\text{m}$ . – C: TS. Fiber pits in radial and tangential walls. (bottom arrow). Fibers farther removed from vessels without pits (top arrow). TXSTATE 1275, X-2. Scale bar = 30  $\mu\text{m}$ . – D: TLS. Septate fibers (arrow). TXSTATE 1275, T-1. Scale bar = 30  $\mu\text{m}$ . – E: TS. Fibers with dark content near vessels with tyloses. TXSTATE 1275, T-1. Scale bar = 30  $\mu\text{m}$ . – F: TLS. Rays mostly uniseriate. Fibers with dark contents. TXSTATE 1275, T-1. Scale bar = 30  $\mu\text{m}$ . – G: RLS. Rays composed of procumbent cells, with marginal rows of large cells (bottom arrow) or with one row of square or upright cells (top arrow). TXSTATE 1275, R-2. Scale bar = 30  $\mu\text{m}$ .

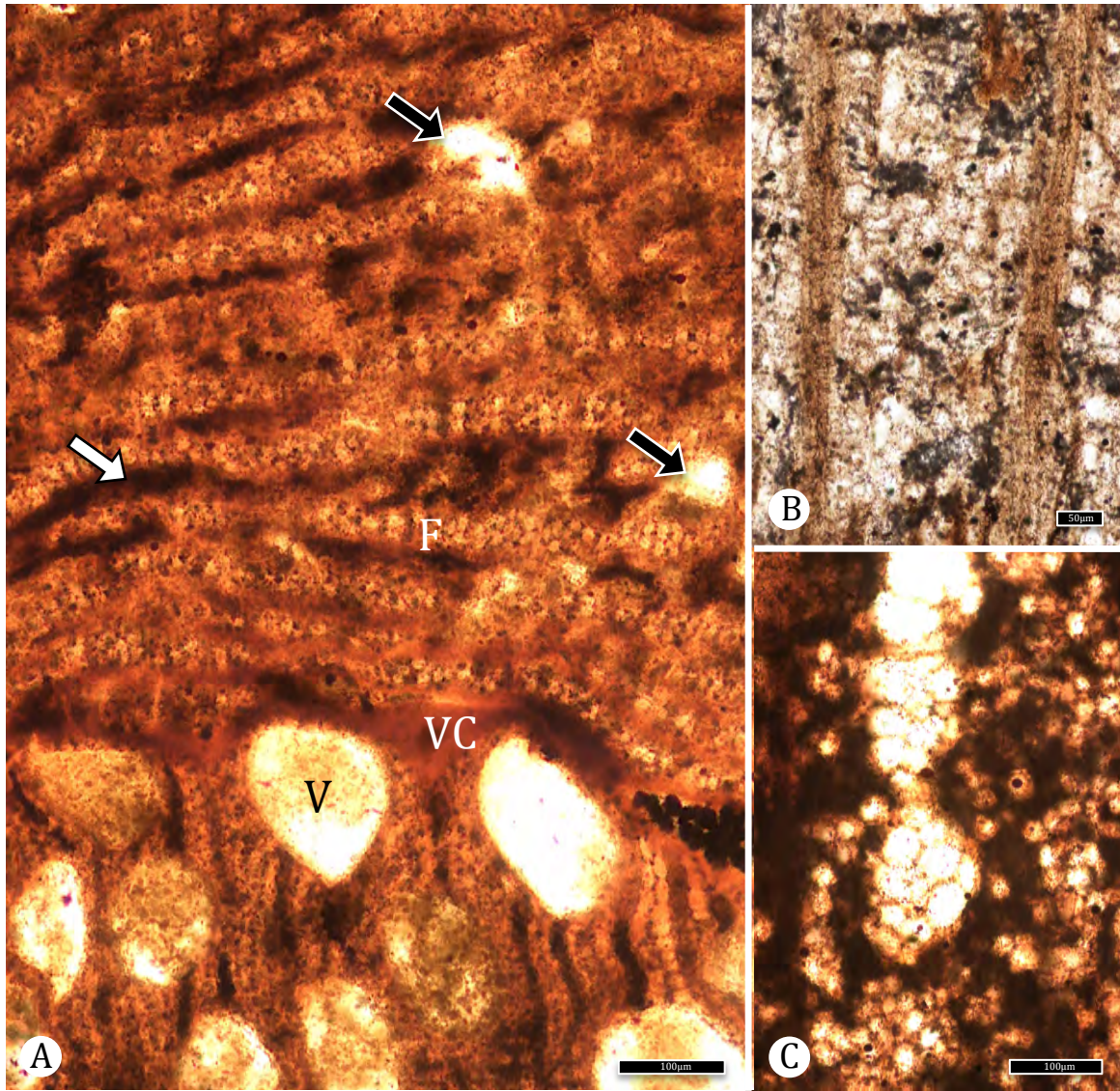


Figure 3.29. *Fulleroxylon* sp 1 (holoxylotype) (TXSTATE 1275) cf. Connaraceae.  
 – A: TS. Secondary xylem vessel (V) and approximate location of vascular cambium (VC). Secondary phloem with areas interpreted as discontinuous bands of fibers (F), crushed phloem sieve elements (white arrow) and cavities interpreted as anomalous secondary xylem arc vessels (black arrows). TXSTATE 1277, X-3. Scale bar = 100  $\mu\text{m}$ . – B: TLS. Thick-walled, isodiametric cortex parenchyma dissected by possible fiber bands. TXSTATE 1276, T-1. Scale bar = 50  $\mu\text{m}$ . – C: RLS. Vertically elongate cavity in cortex. TXSTATE 1276, R-1. Scale bar = 100  $\mu\text{m}$ .

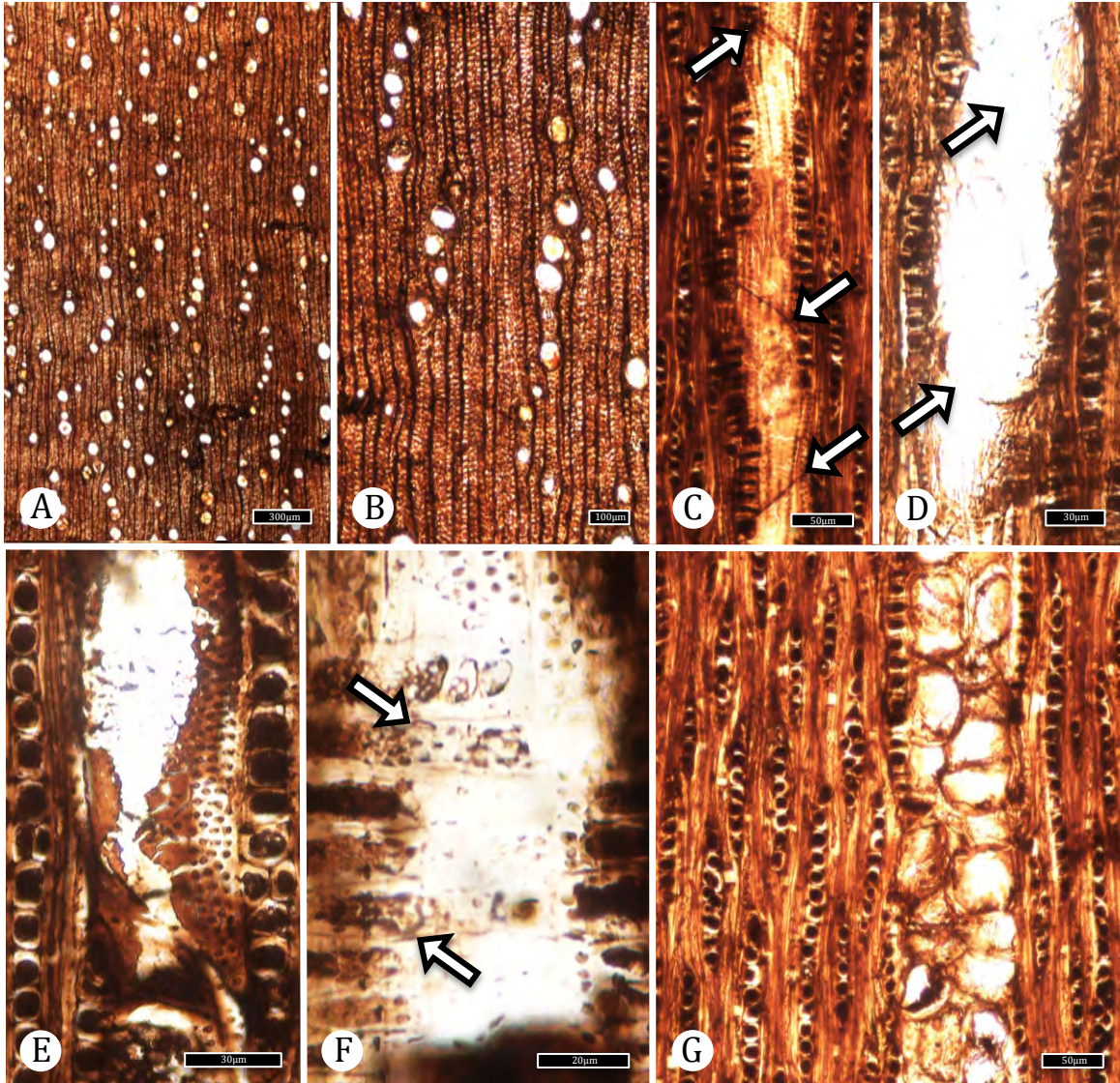


Figure 3.30. McRae wood holoxylotype Group IIIA sp. 1 (TXSTATE 1278). – A: TS. Growth rings absent, wood diffuse porous with vessels tending to be in a radial or diagonal pattern. TXSTATE 1278, X-8. Scale bar = 300  $\mu\text{m}$ . – B: TS. Tendency for vessels to be arranged in radial or diagonal pattern. Vessels solitary and rounded. Vessels solitary and rounded. TXSTATE 1278, X-8. Scale bar = 100  $\mu\text{m}$ . – C: TLS. Vessel element end walls (arrows). TXSTATE 1278, T-3. Scale bar = 50  $\mu\text{m}$ . – D: TLS. Simple perforation plates (arrows). TXSTATE 1278, T-4. Scale bar = 30  $\mu\text{m}$ . – E: TLS. Intervessel pits minute and alternate to sub-alternate. TXSTATE 1278, T-2. Scale bar = 30  $\mu\text{m}$ . – F: Vessel-ray pits similar to intervessel pitting (arrows). TXSTATE 1278, R-1. Scale bar = 20  $\mu\text{m}$ . – G: TLS. Vessel with bubble-like tyloses. TXSTATE 1278, T-3. Scale bar = 50  $\mu\text{m}$ .

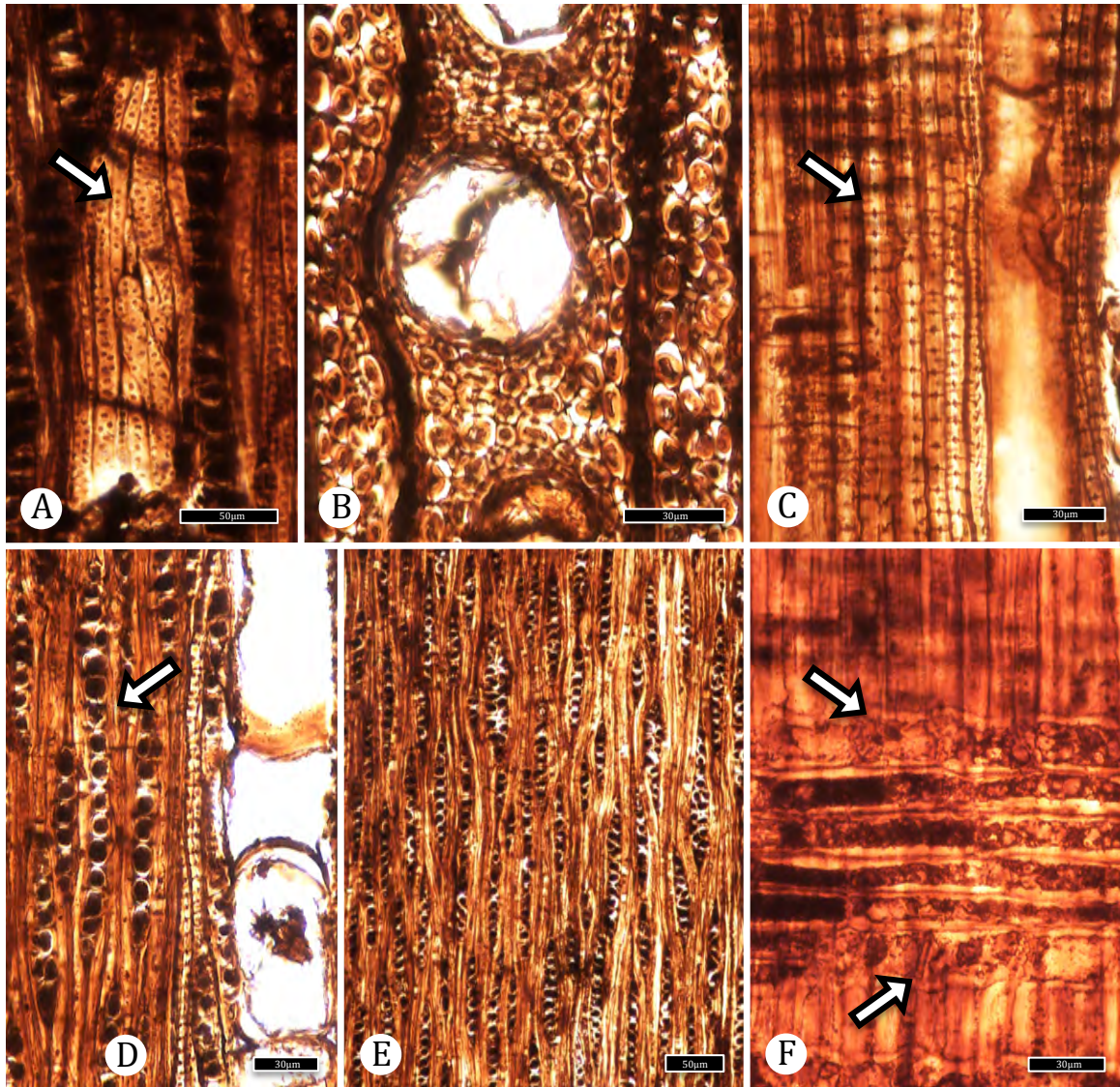


Figure 3.31. McRae wood holoxylotype Group IIIA sp. 1 (TXSTATE 1278). – A: TLS. Vascentric tracheids with multiple rows of small bordered pits (arrow). TXSTATE 1278, T-3. Scale bar = 30  $\mu\text{m}$ . – B: TS. Fibers angular in outline. Areas interpreted as pits between fibers surrounding vessels. TXSTATE 1278, X-2. Scale bar = 30  $\mu\text{m}$ . – C: RLS. Fibers adjacent to vessels with bordered pits. (arrow). TXSTATE 1278, R-1. Scale bar = 30  $\mu\text{m}$ . – D: TLS. Fibers a short distance from vessels with few or no pits (arrow). TXSTATE 1278, T-4. Scale bar = 30  $\mu\text{m}$ . – E: TLS. Rays mostly uniseriate with some biseriate rays. TXSTATE 1278, T-3. Scale bar = 50  $\mu\text{m}$ . – F: RLS. Rays not strongly heterocellular, often composed of all procumbent cells, but with marginal rows of enlarged cells (arrows). TXSTATE 1278, R-1. Scale bar = 30  $\mu\text{m}$ .

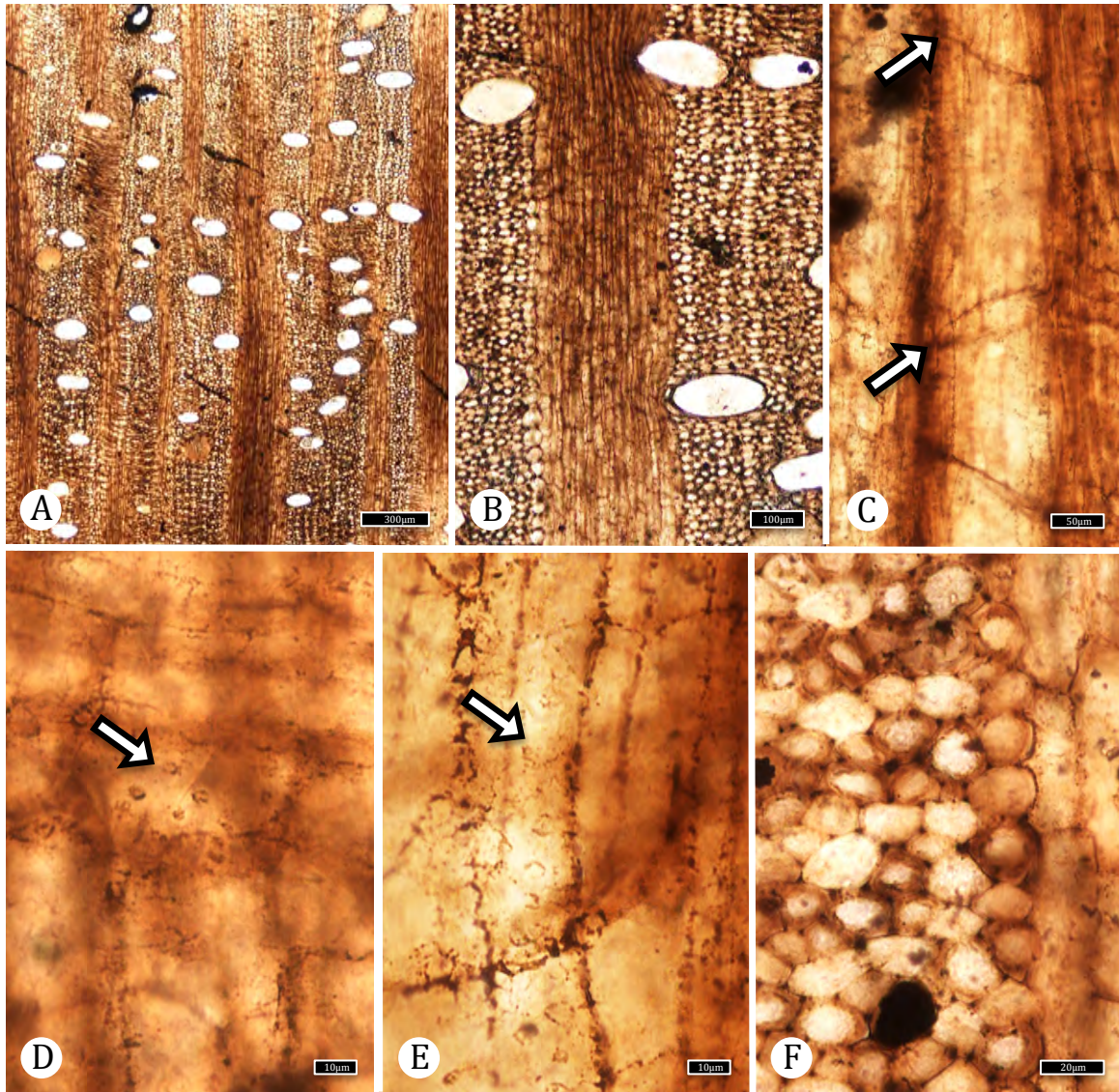


Figure 3.32. McRae wood holoxylotype Group IIIA sp. 2 (TXSTATE 1279). – A: TS. Wood diffuse-porous, predominantly solitary vessels. TXSTATE 1279, X-6. Scale bar = 300 µm – B: TS. Solitary vessels are round to oval. Rays greater than ten cells wide. TXSTATE 1279, X-6. Scale bar = 100 µm. – C: RLS. Vessel element length (between arrows). Simple perforation plates. TXSTATE 1279, R-4. Scale bar = 50 µm. – D: RLS. Vessel-ray parenchyma pits (arrow) with distinct borders, small and not crowded. TXSTATE 1279, R-3. Scale bar = 10 µm. – E: RLS. Vessel-axial parenchyma pitting (arrow) similar to vessel-ray pitting. TXSTATE 1279, R-3. Scale bar = 10 µm. – F: TS. Fibers thin-walled and angular in outline. Axial parenchyma diffuse and diffuse-in-aggregates. TXSTATE 1279, X-6. Scale bar = 20 µm.

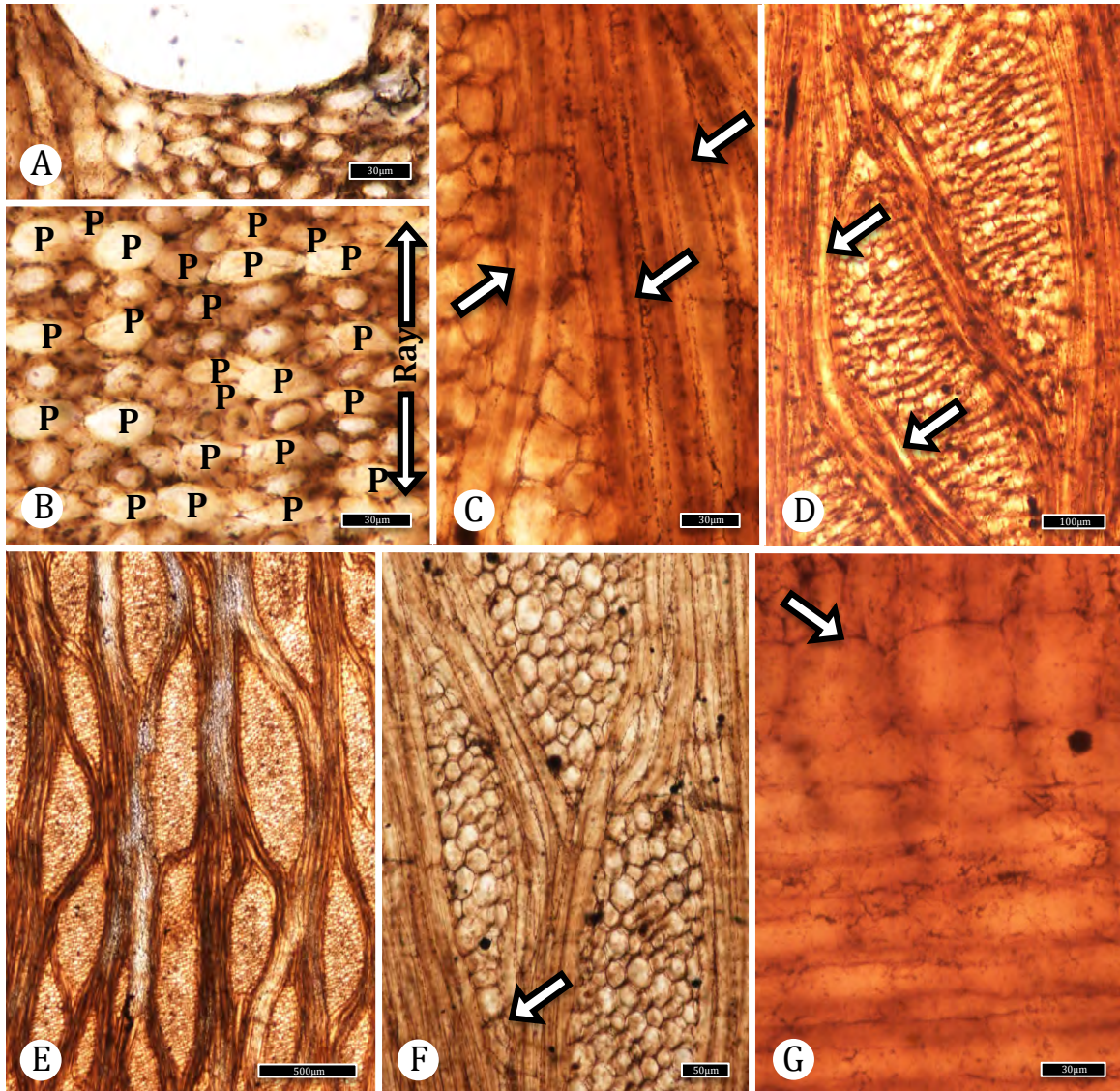


Figure 3.33. McRae wood holoxylotype Group IIIA sp. 2 (TXSTATE 1279). – A: TS. Axial parenchyma scanty paratracheal. TXSTATE 1279, X-6. Scale bar = 30. – B: TS. Axial parenchyma diffuse and diffuse-in-aggregates forming short lines. TXSTATE 1279, X-6. Scale bar = 30  $\mu\text{m}$ . – C: TLS. Axial parenchyma strands (arrows) common among fibers. TXSTATE 1279, T-5. Scale bar = 30  $\mu\text{m}$ . – D: TLS. Axial parenchyma three cells per strand (right arrow) to eight cells per strand (left arrow). TXSTATE 1279, T-5. Scale bar = 100  $\mu\text{m}$ . – E: TLS. Rays not strongly heterocellular, mostly greater than ten cells in width. TXSTATE 1279, T-4. Scale bar = 500  $\mu\text{m}$ . – F: TLS. Rays cells generally procumbent with one to several (arrow) marginal rows of square or upright cells. TXSTATE 1279, T-5. Scale bar = 50  $\mu\text{m}$ . – G: RLS. Rays composed of procumbent cells with one (arrow) to several marginal row of square or upright cells. TXSTATE 1279, R-2. Scale bar = 30  $\mu\text{m}$ .

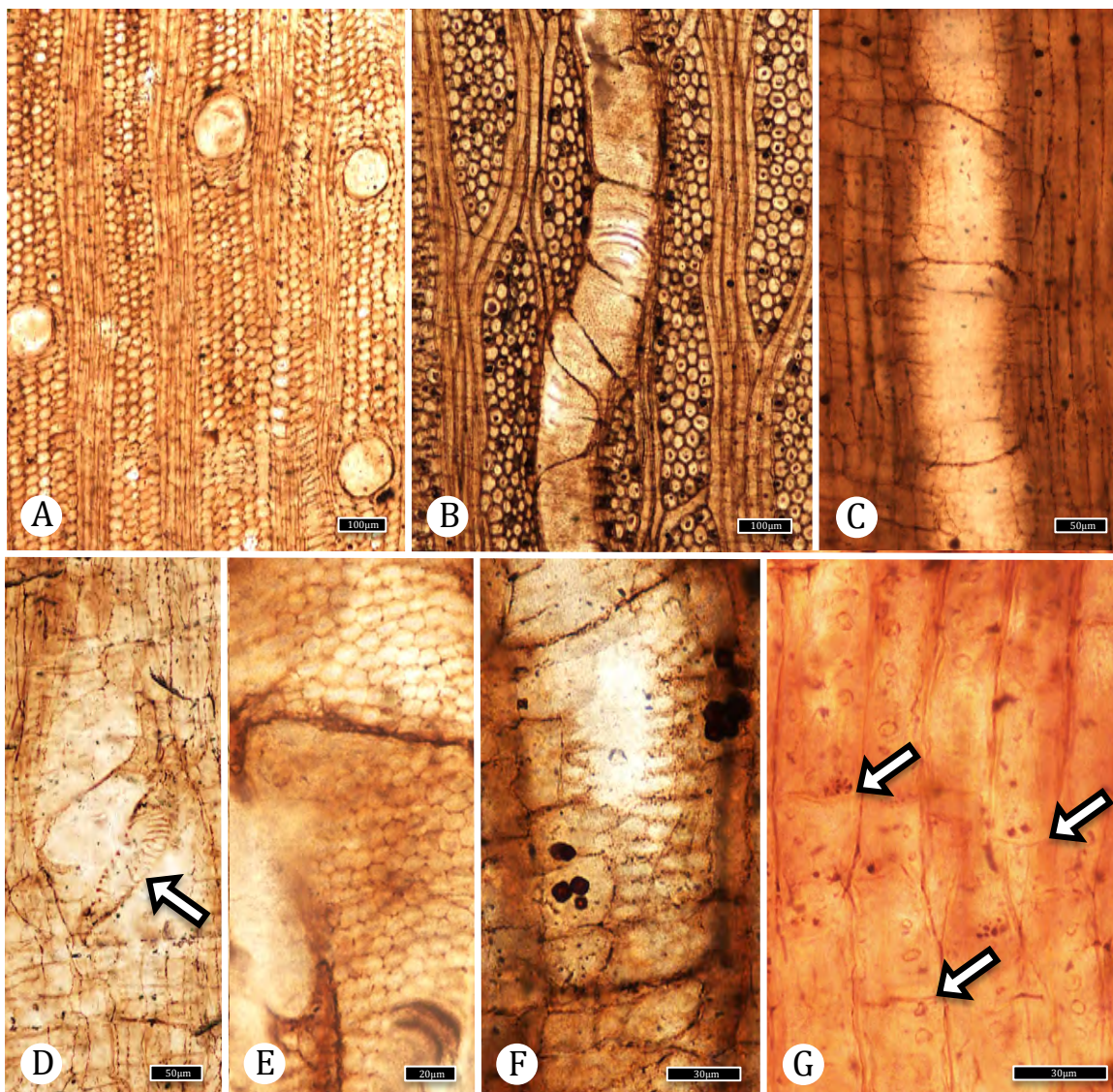


Figure 3.34. McRae wood holoxylotype Group IIIA sp. 3 (TXSTATE 1280). – A: TS. Vessels solitary. TXSTATE 1280, X-4. Scale bar = 100  $\mu\text{m}$ . – B: TLS. Series of vessel elements and exclusively multiseriate rays. TXSTATE 1280, T-1. Scale bar = 100  $\mu\text{m}$ . – C: RLS. Simple perforation plates. TXSTATE 1280, R-10. Scale bar = 50  $\mu\text{m}$ . . – D: RLS. Perforation plates rarely scalariform (arrow). TXSTATE 1280, R-8. Scale bar = 50  $\mu\text{m}$ . – E: TLS. Alternate intervessel pits, polygonal in outline. TXSTATE 1280, R-6. Scale bar = 20  $\mu\text{m}$ . – F: RLS. Vessel ray pits simple, oval to horizontally elongate. TXSTATE 1280, R-5. Scale bar = 30  $\mu\text{m}$ . – G: RLS. Thin-walled, septate fibers with reduced bordered pits. Arrows indicate thin septa. TXSTATE 1280, R-11. Scale bar = 30  $\mu\text{m}$ .

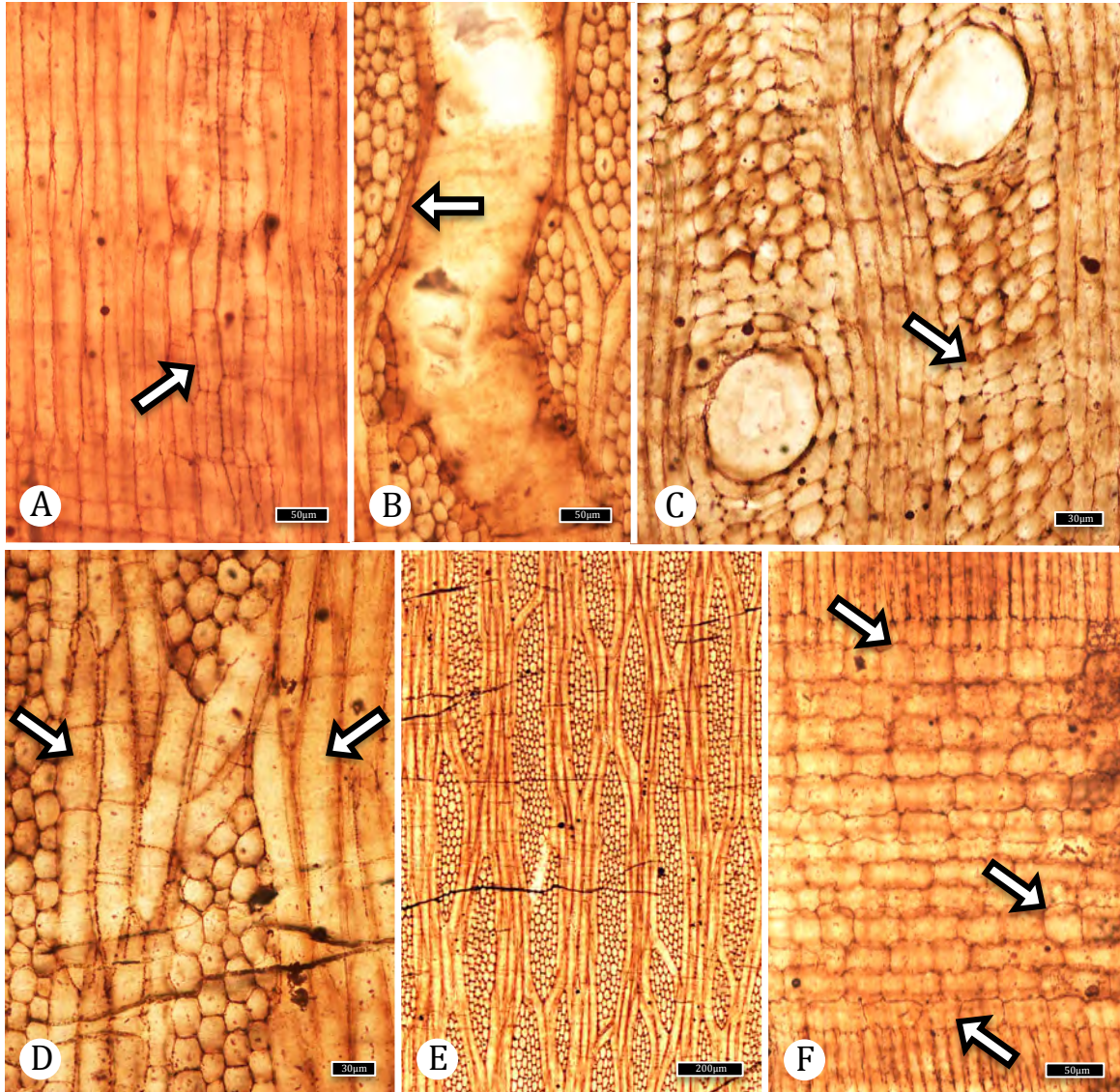


Figure 3.35. McRae wood holoxylotype Group IIIA sp. 3 (1280). – A: RLS. Axial parenchyma strands (arrow) among longer, narrow fibers that do not have pitting. TXSTATE 1280, R-10. Scale bar = 50  $\mu\text{m}$ . – B: TLS. Axial parenchyma adjacent to vessel (arrow). TXSTATE 1280, T-4#. Scale bar = 50  $\mu\text{m}$ . – C: TS. Axial parenchyma vasicentric and between rays in narrow bands (arrows). TXSTATE 1280, X-5. Scale bar = 30  $\mu\text{m}$ . – D: TLS. Axial parenchyma 2-4 cells per strand (left arrow) extending between rays. Thin-walled, non-septate fibers (right arrow). TXSTATE 1280, T-4. Scale bar = 30  $\mu\text{m}$ . – E: TLS. Rays 3-7 (mostly 4-5) seriate. TXSTATE 1280, T-2. Scale bar = 200  $\mu\text{m}$ . – F: RLS. Ray cells procumbent, or 1 (up to 2) rows barely procumbent, with some square or upright cells (arrows). TXSTATE 1280, R-6. Scale bar = 50  $\mu\text{m}$ .

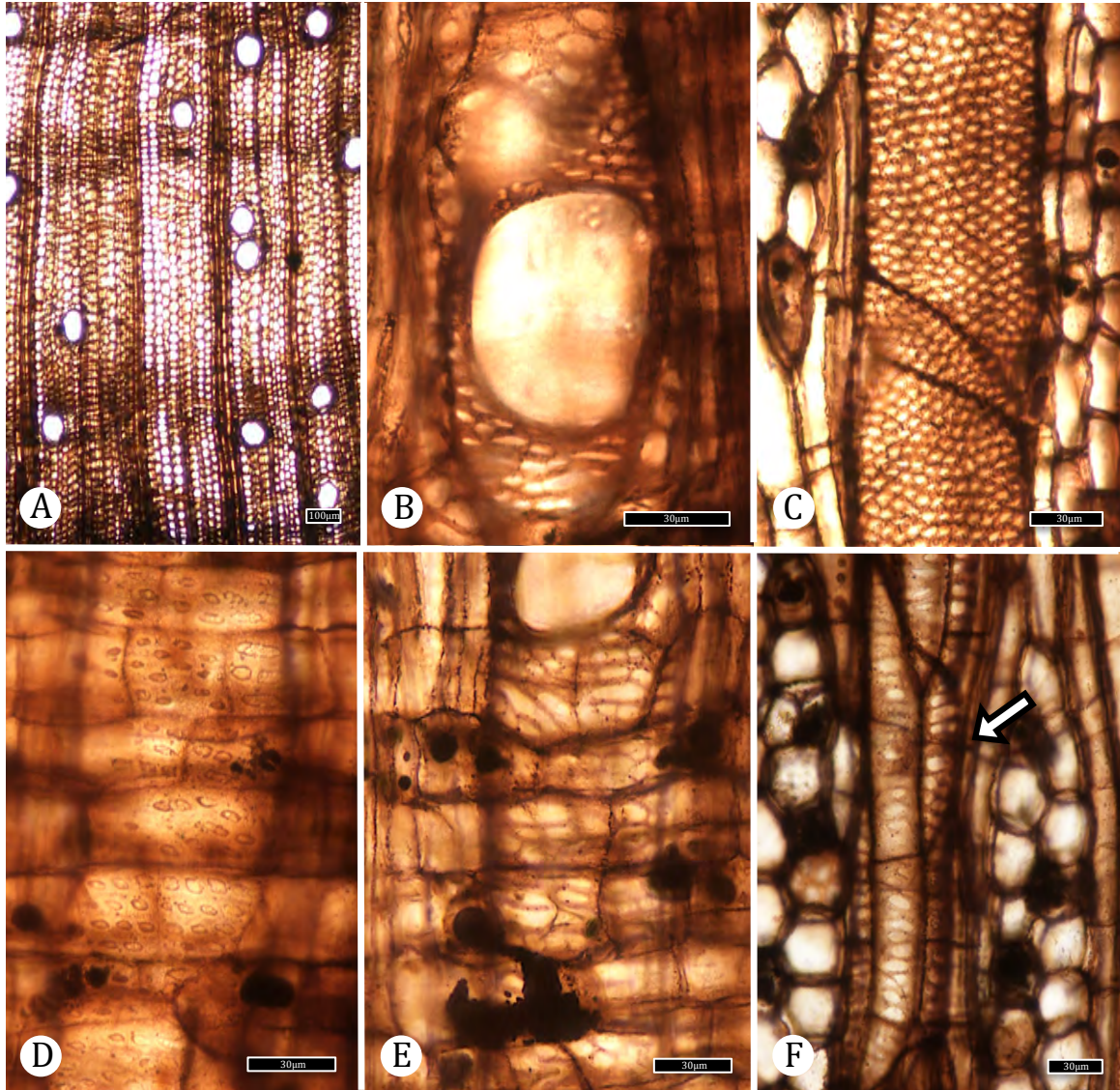


Figure 3.36. McRae wood holoxylotype Group IIIA sp. 4 (TXSTATE 1281). – A: TS. Diffuse-porous wood with predominantly solitary vessels. TXSTATE 1281, X-2. Scale bar = 100  $\mu\text{m}$ . – B: RLS. Simple perforation plate. TXSTATE 1281, R-2. Scale bar = 30  $\mu\text{m}$ . – C: TLS. Alternate intervessel pitting. TXSTATE 1281, T-3. Scale bar = 30  $\mu\text{m}$ . – D: RLS. Vessel-ray parenchyma pits with reduced borders, oval. TXSTATE 1281, R-2. Scale bar = 30  $\mu\text{m}$ . – E: RLS. Vessel-ray pits simple, oval to diagonally or horizontally elongate. TXSTATE 1281, R-2. Scale bar = 30  $\mu\text{m}$ . – F: TLS. Axial parenchyma with simple, elongate pitting (arrow). TXSTATE 1281, T-3. Scale bar = 30  $\mu\text{m}$ .

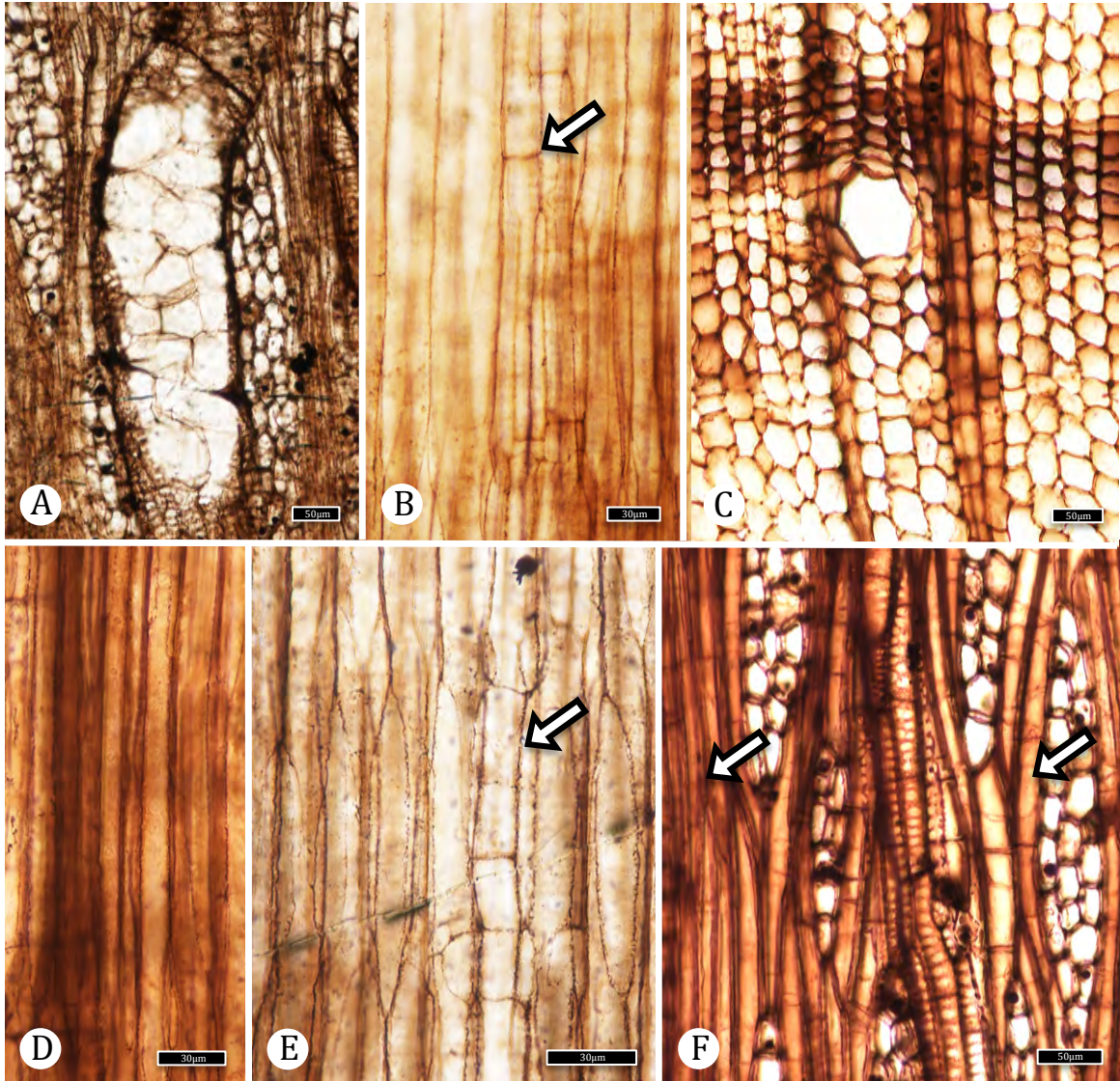


Figure 3.37. McRae wood holoxylotype Group IIIA sp. 4 (TXSTATE 1281).  
 – A: TLS. Tyloses bubble-like. TXSTATE 1281, T-3. Scale bar = 50  $\mu\text{m}$ . – B: RLS. Axial parenchyma strands (arrow) among thin-walled fibers. TXSTATE 1281, R-2. Scale bar = 30  $\mu\text{m}$ . – C: TS. Tangential bands of radially narrowed fibers. TXSTATE 1281, X-2. Scale bar = 50  $\mu\text{m}$ . – D: RLS. Long, narrow, non-septate fibers without pitting. TXSTATE 1281, R-2. Scale bar = 30  $\mu\text{m}$ . – E: RLS. Short, non-septate fibers without pitting. Axial parenchyma strand among the fibers (arrow). TXSTATE 1281, R-2. Scale bar = 30  $\mu\text{m}$ . – F: TLS. Vessel-axial parenchyma pitting simple (center). Non-septate fibers (left arrow) and thin-walled septate fibers (right arrow). TXSTATE 1281, T-3. Scale bar = 30  $\mu\text{m}$ .

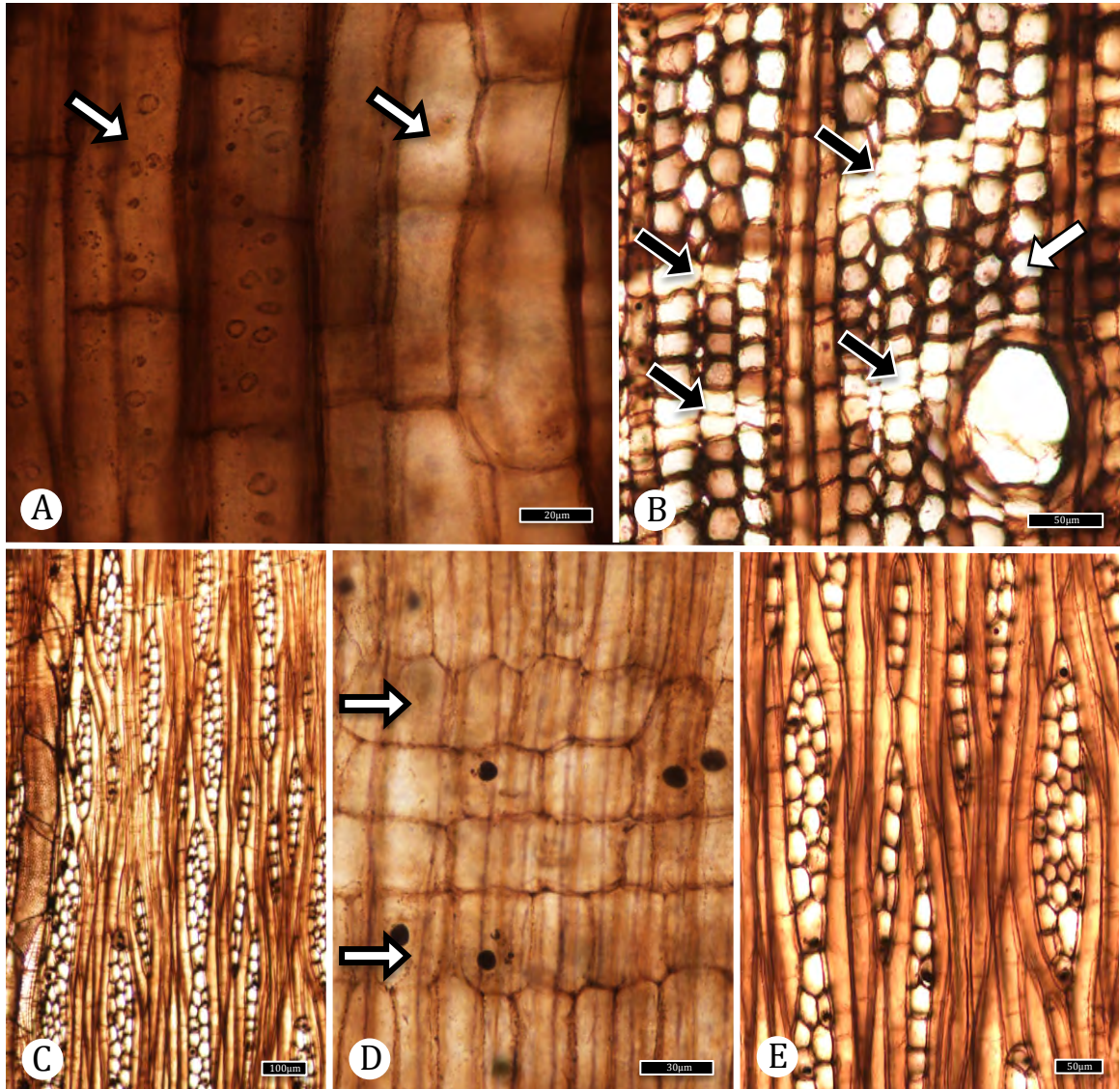


Figure 3.38. McRae wood holoxylotype Group IIIA sp. 4 (TXSTATE 1281). – A: RLS. Short septate fibers with simple pitting on radial walls (left arrow) adjacent to axial parenchyma (right arrow). TXSTATE 1281, R-2. Scale bar = 20  $\mu\text{m}$ . – B: TS. Bands of axial parenchyma (black arrows) extend between rays. Large diameter fibers at top of photo. Smaller diameter fibers (white arrow). TXSTATE 1281, X-2. Scale bar = 50  $\mu\text{m}$ . – C: TLS. Rays 1–4 seriate. TXSTATE 1281, T-3. Scale bar = 100  $\mu\text{m}$ . – D: RLS. Rays composed of procumbent cells with one row of square or upright marginal cells (arrows). TXSTATE 1281, R-2. Scale bar = 30  $\mu\text{m}$ . – E: TLS. Uniseriate rays not uncommon. TXSTATE 1281, T-3. Scale bar = 50  $\mu\text{m}$ .

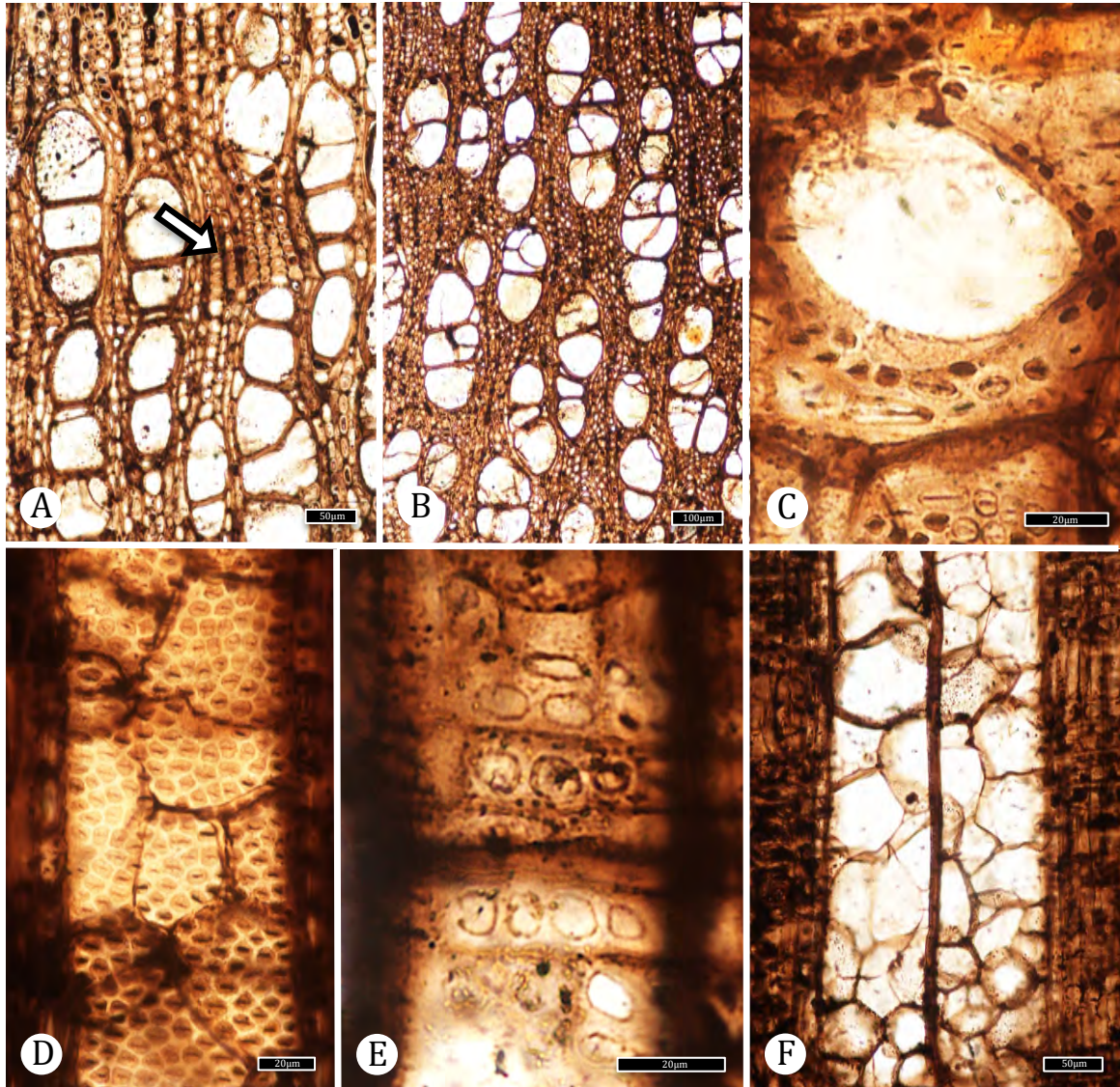


Figure 3.39. McRae wood holoxylotype Group IIIB sp. 1 (TXSTATE 1283). – A: TS. Fibers radially narrowed in a discontinuous band (arrow). TXSTATE 1283, X-2. Scale bar = 50  $\mu\text{m}$ . – B: TS. Wood diffuse porous. Vessels solitary and in radial or oblique multiples of four or more common. TXSTATE 1283, X-2. Scale bar = 100  $\mu\text{m}$ . – C: RLS. Simple perforation plate. TXSTATE 1283, R-2. Scale bar = 20  $\mu\text{m}$ . – D: TLS. Alternate intervessel pits. TXSTATE 1283, T-3. Scale bar = 20  $\mu\text{m}$ . – E: RLS. Vessel-ray pits with reduced borders or simple, often large. TXSTATE 1283, R-3. Scale bar = 20  $\mu\text{m}$ . – F: RLS. Tyloses bubble-like. TXSTATE 1283, R-1. Scale bar = 50  $\mu\text{m}$ .

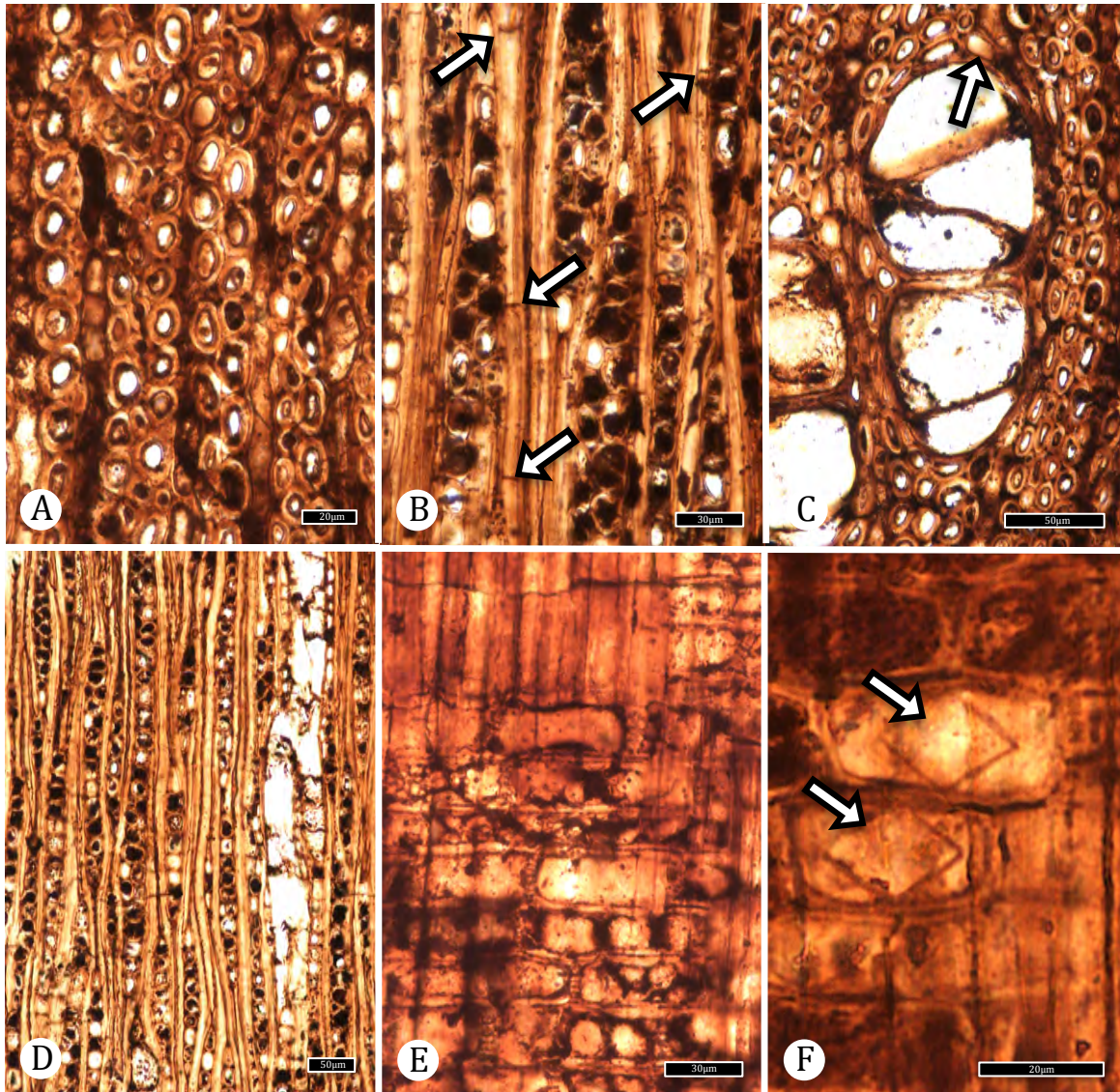


Figure 3.40. McRae wood holoxylotype Group IIIB sp. 1 (TXSTATE 1283).  
 - A: TS. Fibers thin-walled, not strongly angular in outline. TXSTATE 1283, X-2. Scale bar = 50  $\mu\text{m}$ . - B: TLS. Fibers septate (arrow) and non-septate. TXSTATE 1283, T-2. Scale bar = 30  $\mu\text{m}$ . - C: TS. Axial parenchyma scanty paratracheal and rare (arrow). TXSTATE 1283, X-2. Scale bar = 50  $\mu\text{m}$ . - D: TLS. Rays 1 - 3 seriate, mostly < 500  $\mu\text{m}$  tall. TXSTATE 1283, T-2. Scale bar = 50  $\mu\text{m}$ . - E: RLS. Rays made up of more-or-less uniform procumbent cells. TXSTATE 1283, R-2. Scale bar = 30  $\mu\text{m}$ . - F: RLS. Prismatic crystals in ray parenchyma (arrows). TXSTATE 1283, R-2. Scale bar = 50  $\mu\text{m}$ .

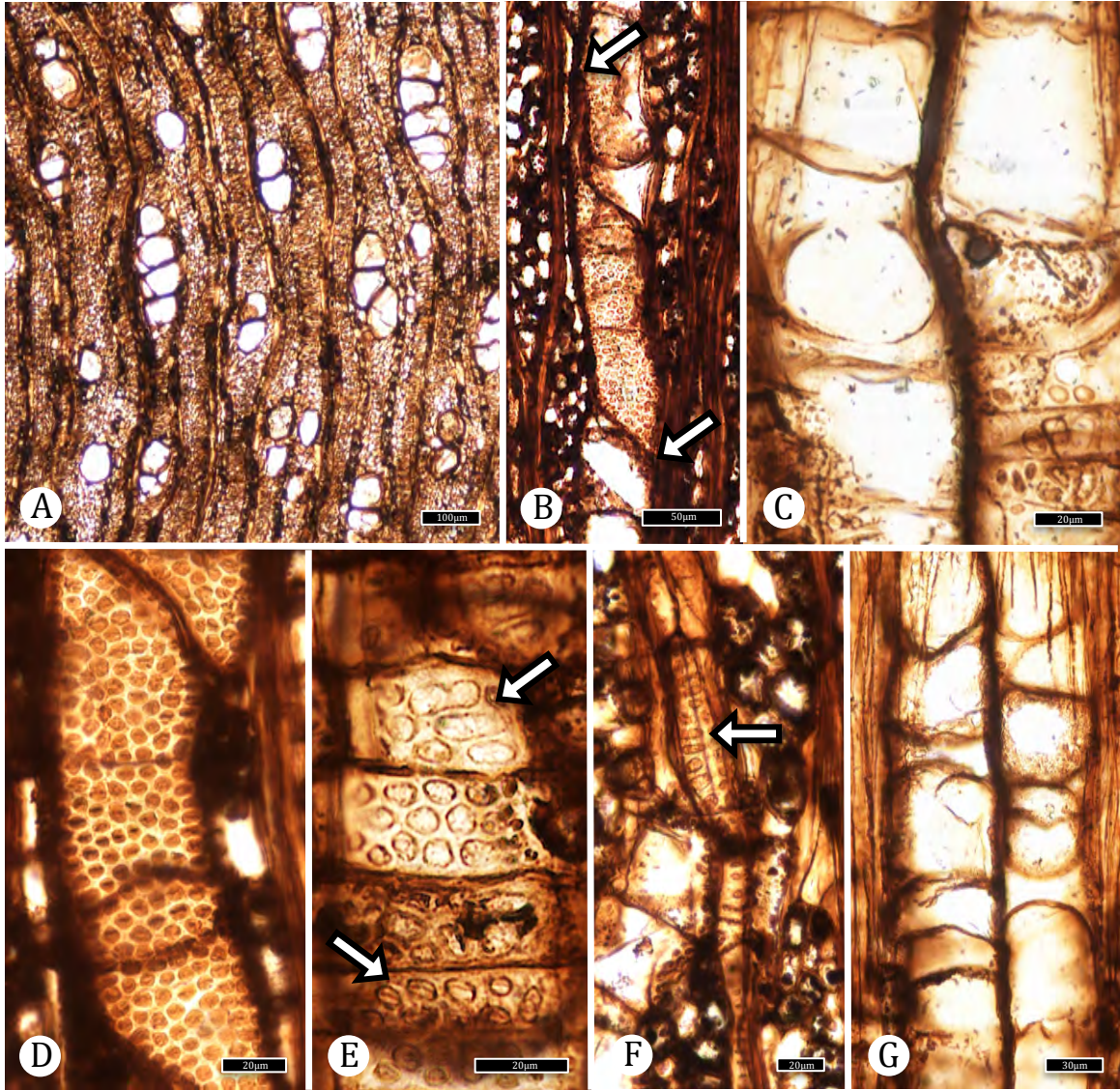


Figure 3.41. McRae wood holoxylotype Group IIIB sp. 2 (TXSTATE 1284). – A: TS. Diffuse-porous wood with solitary vessels and radial multiples of 2 and 4 (up to 6). TXSTATE 1284, X-2. Scale bar = 100  $\mu\text{m}$ . – B: TLS. Vessel element (arrows). TXSTATE 1284, T-2. Scale bar = 50  $\mu\text{m}$ . – C: RLS. Simple perforation plate. TXSTATE 1283, R-1. Scale bar = 20  $\mu\text{m}$ . – D: TLS. Alternate intervessel pitting. TXSTATE 1284, T-2. Scale bar = 20  $\mu\text{m}$ . – E: Vessel-ray parenchyma pits simple or with reduced borders (top arrow) or with slightly reduced borders to bordered (bottom arrow). TXSTATE 1284, R-2. Scale bar = 20  $\mu\text{m}$ . – F: TLS. Vessel-axial parenchyma pits bordered, elongate ovals (arrow). TXSTATE 1284, T-2. Scale bar = 20  $\mu\text{m}$ . – G: RLS. Tyloses bubble-like. TXSTATE 1284, R-2. Scale bar = 30  $\mu\text{m}$ .

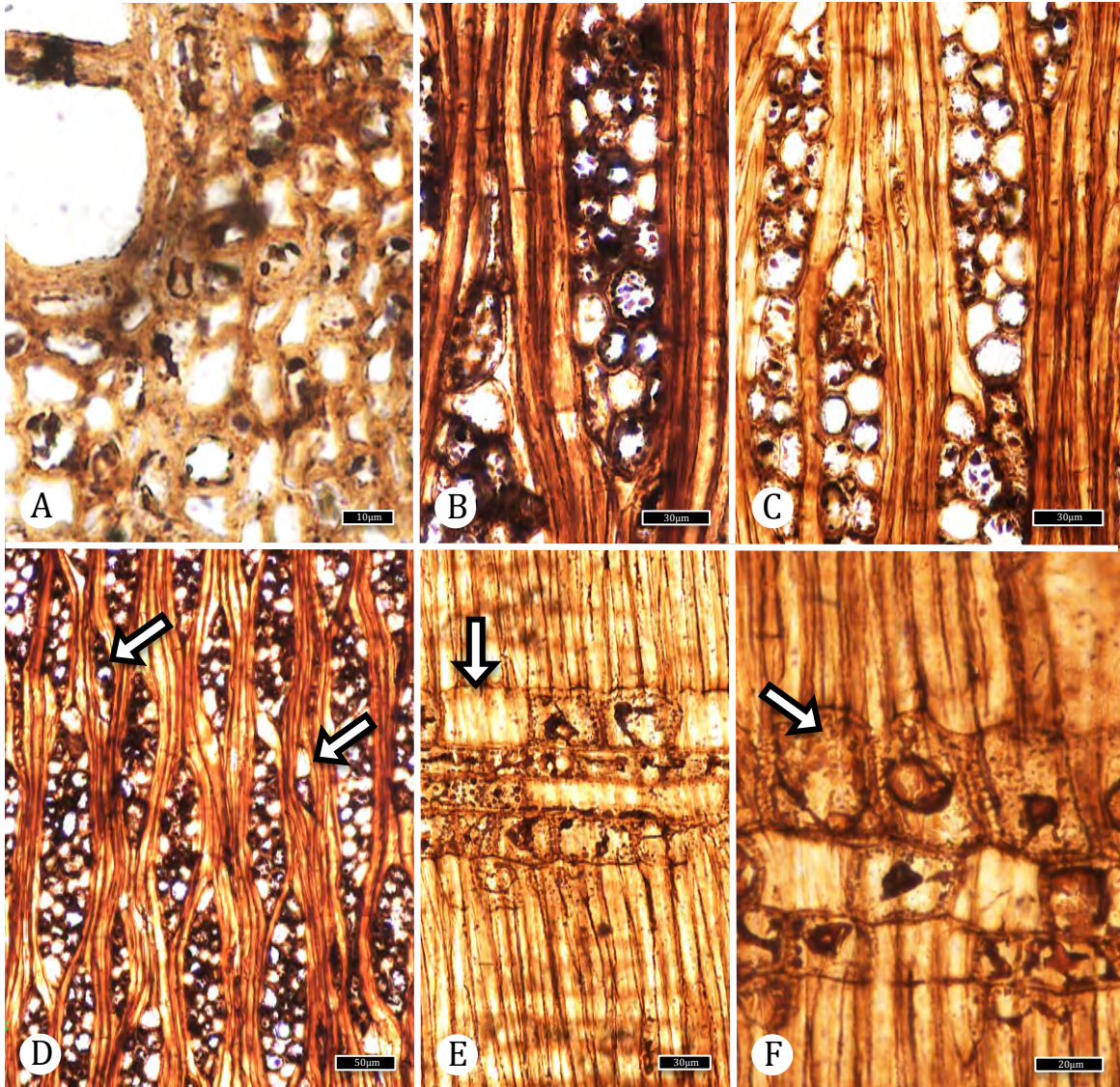


Figure 3.42. McRae wood holoxylotype Group IIIB sp. 2 (TXSTATE 1284).  
 – A: TS. Fibers thin-walled. TXSTATE 1284, X-2. Scale bar = 10  $\mu\text{m}$ . – B: TLS. Wider fibers septate. TXSTATE 1284, T-2. Scale bar = 30  $\mu\text{m}$ . – C: TLS. Narrow fibers non-septate. TXSTATE 1284, T-2. Scale bar = 30  $\mu\text{m}$ . – D: TLS. . Rays mostly 2–4 cells wide. Uniseriate rays uncommon (arrows). TXSTATE 1284, T-2. Scale bar = 50  $\mu\text{m}$ . – E: Rays composed of procumbent body cells with enlarged marginal row cells (arrow). TXSTATE 1284, R-2. Scale bar = 30  $\mu\text{m}$ . – F: RLS. Rays composed of procumbent cells with one row of square or upright margin cells (arrow). TXSTATE 1284, R-2. Scale bar = 20  $\mu\text{m}$ .

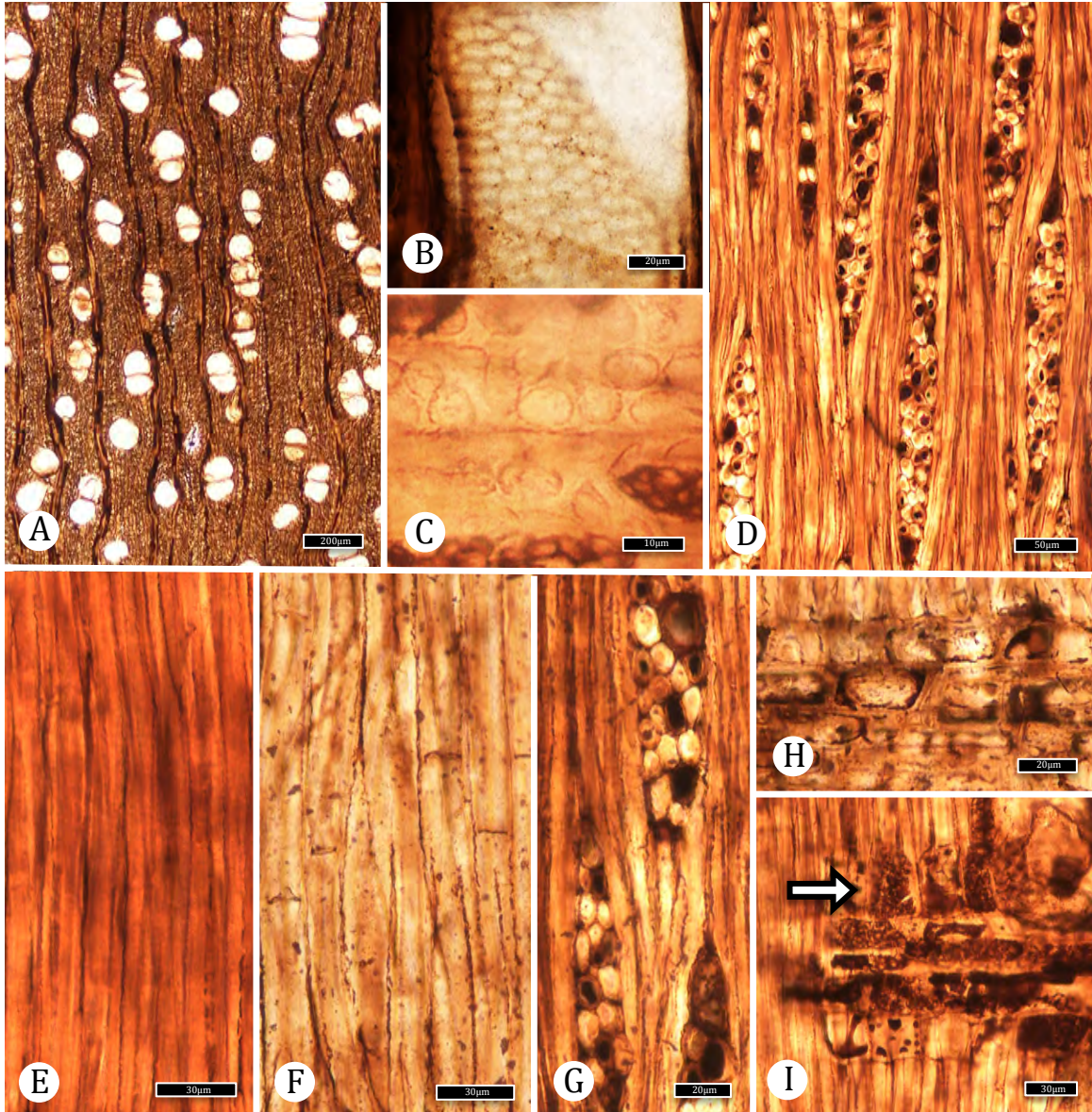


Figure 3.43. McRae wood paraxylotype Group IIIB sp. 2 (TXSTATE 1285). – A: TS. Diffuse-porous wood with vessels solitary and in radial multiples of 2–3. TXSTATE 1285, X-3. Scale bar = 200  $\mu\text{m}$ . – B: TLS. Alternate intervessel pitting, polygonal. TXSTATE 1285, T-1. Scale bar = 20  $\mu\text{m}$ . – C: RLS. Vessel-ray parenchyma pits simple or with reduced borders. TXSTATE 1285, R-2. Scale bar = 10  $\mu\text{m}$ . – D: TLS. Rays mostly 3–4 cells wide, uniseriate rays rare fibers appearing non-septate. TXSTATE 1285, T-1. Scale bar = 50  $\mu\text{m}$ . – E: Fibers with few or no septa. TXSTATE 1285, R-2. Scale bar = 30  $\mu\text{m}$ . – F: RLS. Septate fibers. TXSTATE 1285, R-1. Scale bar = 30  $\mu\text{m}$ . – G: TLS. Marginal rows composed of large cells or upright cells. TXSTATE 1285, T-1. Scale bar = 20  $\mu\text{m}$ . – H: RLS. Enlarged procumbent marginal cells in ray composed of all procumbent cells. TXSTATE 1285, R-1. Scale bar = 20  $\mu\text{m}$ . – I: RLS. Ray composed of procumbent cells with one row of square or upright margin cells (arrow). TXSTATE 1285, R-2. Scale bar = 30  $\mu\text{m}$ .

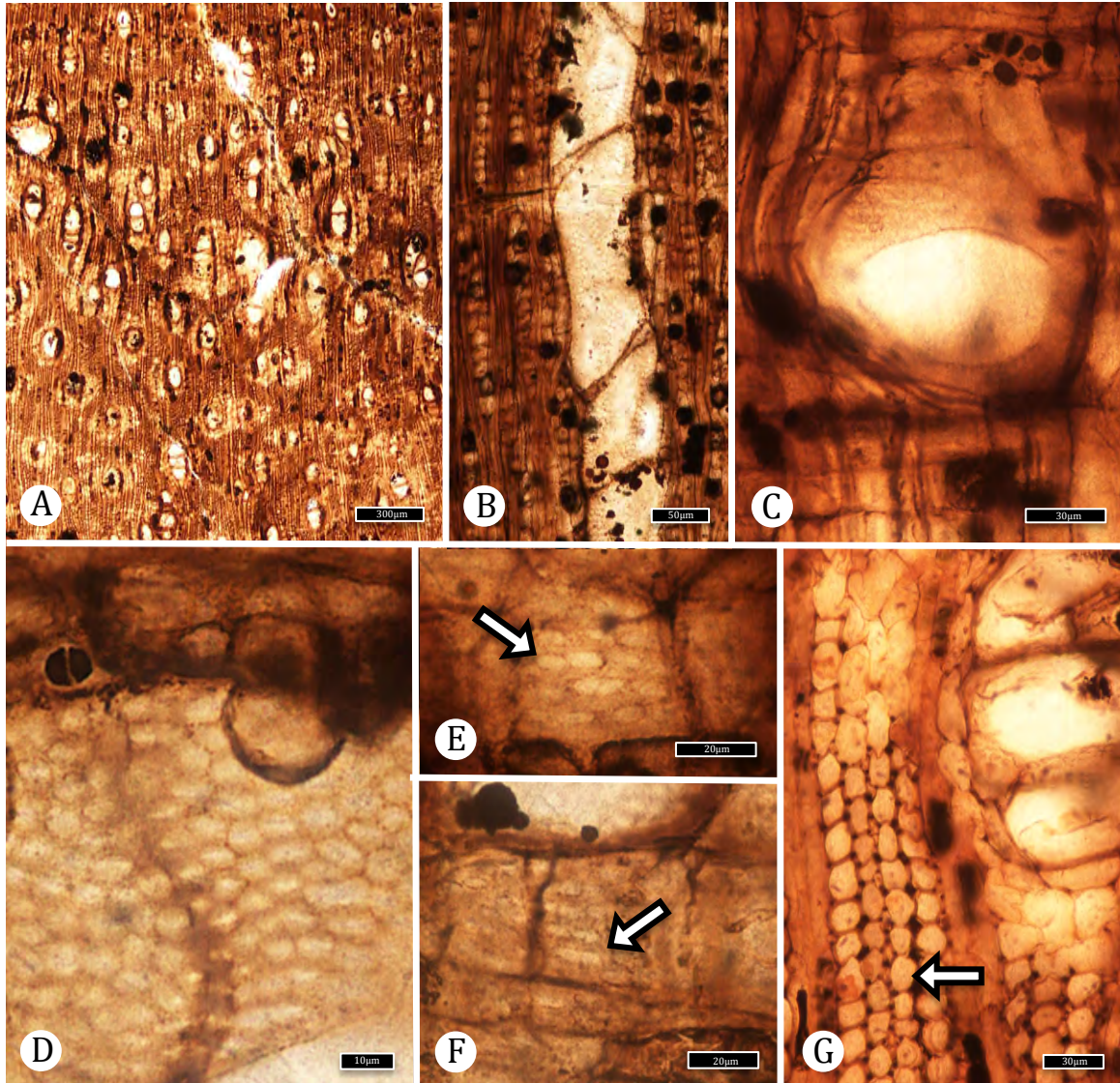


Figure 3.44. McRae wood holoxylotype Group IIIB sp. 3 (TXSTATE 1286). – A: TS. Vessels solitary and in radial multiples of 2–3, vasicentric and lozenge aliform axial parenchyma. TXSTATE 1286, X-1. Scale bar = 300  $\mu\text{m}$ . TXSTATE 1286, T-1. Scale bar = 100  $\mu\text{m}$ . – B: TLS. Vessel element with simple perforation plates. TXSTATE 140#-S#. Scale bar = 50  $\mu\text{m}$ . – C: RLS. Simple perforation plate. TXSTATE 1286, R-3. Scale bar = 30  $\mu\text{m}$ . – D: RLS. Alternate intervessel pits, polygonal in outline. TXSTATE 1286, R-3. Scale bar = 10  $\mu\text{m}$ . – E: RLS. Vessel-ray pits with reduced borders to simple, round to horizontal elongate (arrow). TXSTATE 1286, R-3. Scale bar = 20  $\mu\text{m}$ . – F: RLS. Vessel-ray pits with reduced borders to simple, round to horizontal elongate (arrow). TXSTATE 1286, R-3. Scale bar = 20  $\mu\text{m}$ . – G: TS. Fiber walls incompletely preserved. (arrow). TXSTATE 1286, X-2. Scale bar = 30  $\mu\text{m}$ .

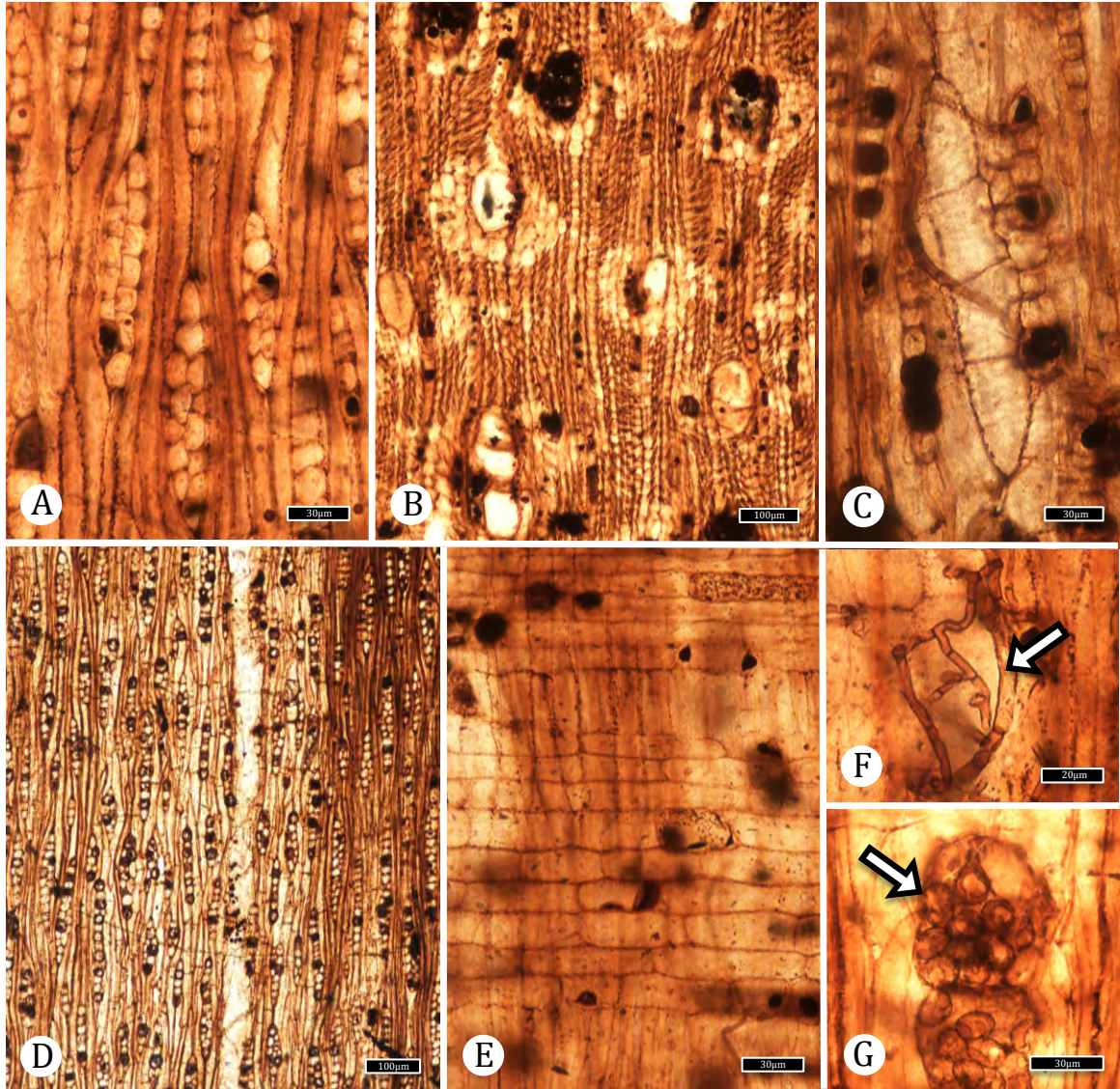


Figure 3.45. McRae wood holoxylotype Group IIIB sp. 3 (TXSTATE 1286).  
 – A: TLS. Fibers non-septate. TXSTATE 1286, T-1. Scale bar = 30 µm. – B: TS. Axial parenchyma vasicentric (sheath broad) to lozenge-aliform. TXSTATE 1286, X-1. Scale bar = 30 µm. – C: TLS. Axial parenchyma strand with 4 cells. TXSTATE 1286, T-1. Scale bar = 30 µm. – D: TLS. Rays 1–2 seriate. TXSTATE 1286, T-1. Scale bar = 100 µm. – E: RLS. Rays composed of procumbent cells. TXSTATE 1286, R-1. Scale bar = 30 µm. – F: RLS. Fungal hyphae (arrow). TXSTATE 1286, R-1. Scale bar = 20 µm. – G: RLS. Fungal reproductive structures (arrow). TXSTATE 1286, R-3. Scale bar = 30 µm.

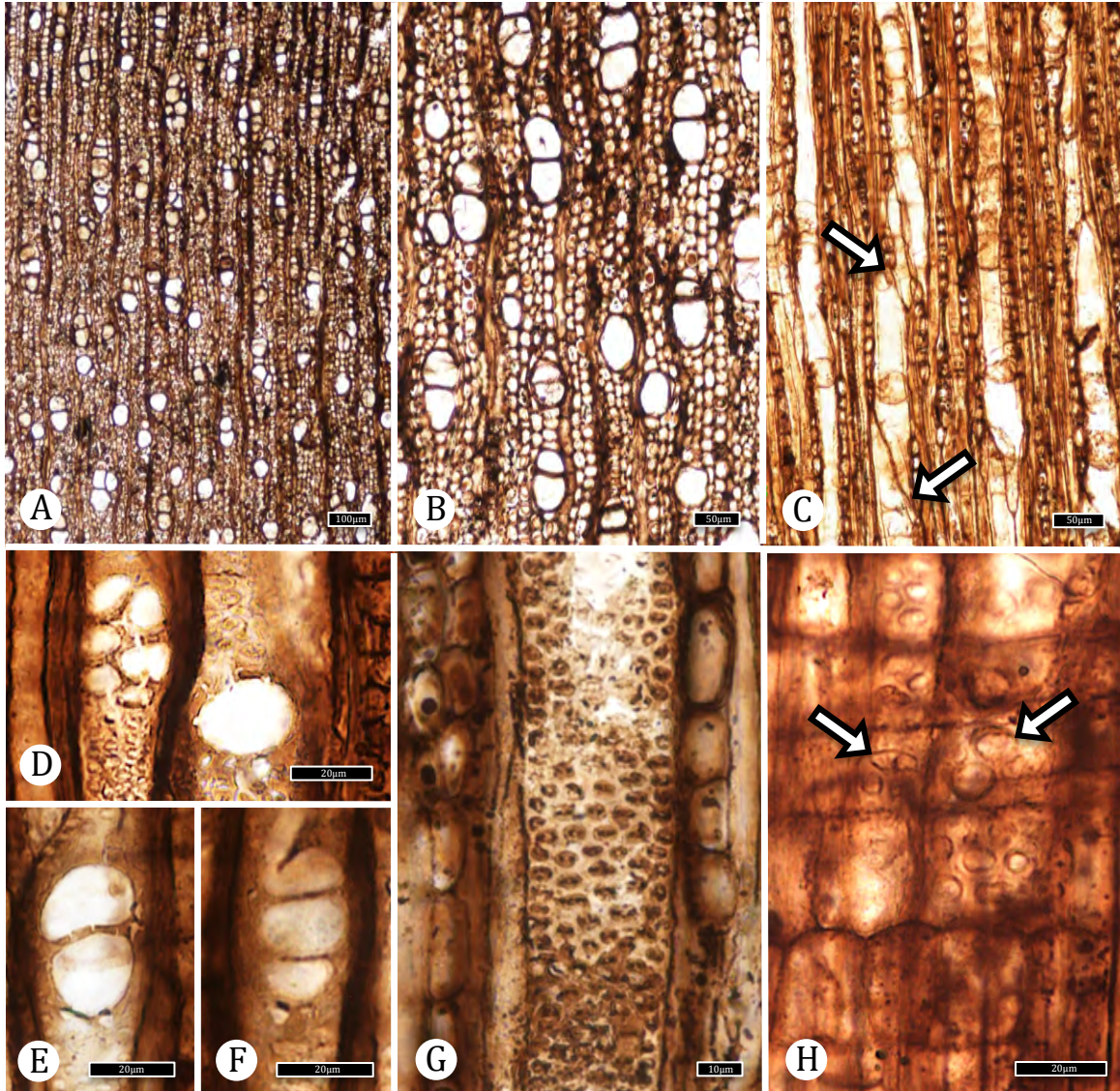


Figure 3.46. McRae wood holoxylotype Group IV sp. 1 (TXSTATE 1289). – A: TS. Diffuse porous wood with solitary vessels and in radial or oblique multiples. TXSTATE 1289, X-4. Scale bar = 100  $\mu\text{m}$ . – B: TS. Solitary vessels oval in outline. TXSTATE 1289, X-4. Scale bar = 50  $\mu\text{m}$ . – C: TLS. Vessel element with steeply inclined end walls (arrows). TXSTATE 1289, T-2. Scale bar = 50  $\mu\text{m}$ . – D – F: Simple and scalariform perforation plates. – D: RLS. Multiperforate perforation plate (left) and simple perforation plate (right). TXSTATE 1289, R-2. Scale bar = 20  $\mu\text{m}$ . – E: RLS. Scalariform perforation plate with one bar. TXSTATE 1289, R-2. Scale bar = 20  $\mu\text{m}$ . – F: RLS. Scalariform perforation plate with two bars. TXSTATE 1289, R-2. Scale bar = 20  $\mu\text{m}$ . – G: TLS. Alternate intervessel pits. TXSTATE 1289, T-2. Scale bar = 10  $\mu\text{m}$ . – H: RLS. Vessel-ray pits with reduced borders to simple, horizontal (left arrow) or round and large, often spanning the full height of the cell (right arrow). TXSTATE 1289, R-2. Scale bar = 20  $\mu\text{m}$ .

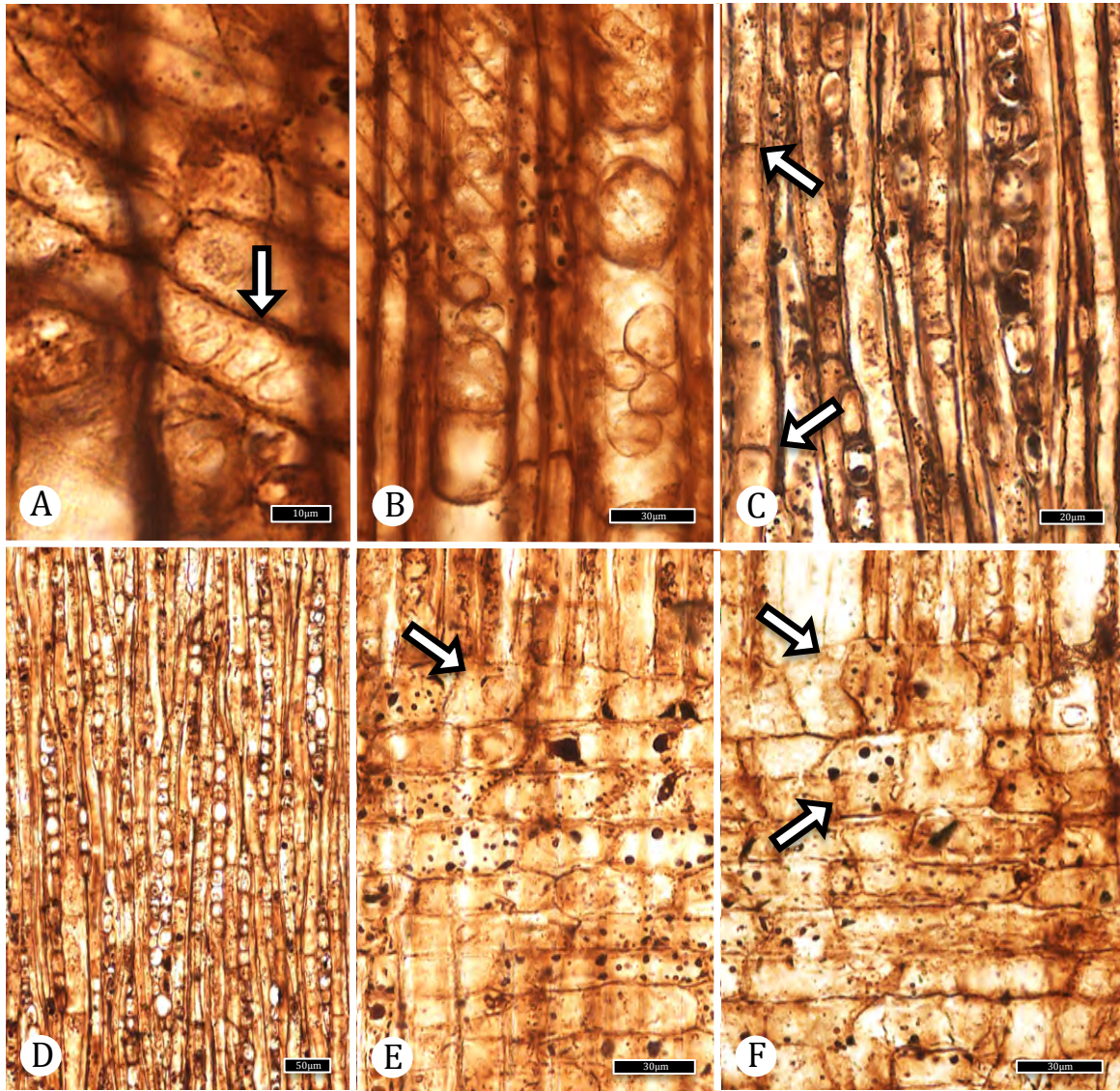


Figure 3.47. McRae wood holoxylotype Group IV sp. 1 (1289. – A: RLS. Vessel-ray pits diagonal ovals (arrows). TXSTATE 1289, R-2. Scale bar = 10  $\mu\text{m}$ . . – B: RLS. Bubble-like tyloses. TXSTATE 1289, R-2. Scale bar = 30  $\mu\text{m}$ . – C: TLS. Septate fibers. TXSTATE 1289, T-2. Scale bar = 20  $\mu\text{m}$ . – D: TLS. Rays mostly 1–2 seriate. TXSTATE 1289, T-2. Scale bar = 50  $\mu\text{m}$ . – E: RLS. Ray with all procumbent cells, the marginal row with barely procumbent cells. TXSTATE 1289, R-2. Scale bar = 30  $\mu\text{m}$ . – F: RLS. Ray composed of procumbent cells with one or two margin row of square and upright cells (arrows). TXSTATE 1289, R-2. Scale bar = 30  $\mu\text{m}$ .

## REFERENCES

- Amato JM, Mack GH, Jonell TN, Seager WR, Upchurch GR. 2017. Onset of the Laramide orogeny and associated magmatism in southern New Mexico based on U-Pb geochronology. *GSA Bull.* 129: 1209–1226.
- Baas P, Manchester SR, Wheeler EA, Srivastava R. 2017. Fossil wood with dimorphic fibers from the Deccan Intertrappean Beds of India – the oldest fossil Connaraceae? *IAWA J.* 38: 124–133.
- Bailey IW. 1924. Problem of identifying the wood of Cretaceous and later dicotyledons- *Paraphyllanthoxylon arizonense*, *Ann. Bot.* 38: 439–451.
- Bailey IW. 1944. The development of vessels in angiosperms and its significance in morphological research. *Am. J. Bot.* 31: 421–428.
- Barajas-Morales J. 1987. Wood specific gravity in species from two tropical forests in Mexico. *IAWA Bull.* 8: 143–148.
- Buck BJ, Mack GH. 1995. Latest Cretaceous (Maastrichtian) aridity indicated by paleosols in the McRae Formation, south-central New Mexico. *Cretaceous Research.* 16: 559–572.
- Cantino PD, Doyle JA, Graham SW, Judd WS, Olmstead RG, Soltis DE, Soltis PS, Donoghue MJ. 2007. Towards a phylogenetic nomenclature of *Tracheophyta*. *Taxon.* 56: 1E–44E.
- Carlquist SJ. 1975. Ecological strategies of xylem evolution. University of California Press.

- Chase MW, Christenhusz MJM, Fay MF, Byng JW, Judd WS, Soltis DE, Soltis PS, Stevens PF, Stevens PF. 2016. An update of the Angiosperm Phylogeny Group classification for the orders and families of flowering plants: APG IV. Bot. J. Linn. Soc. 181: 1–20.
- Chudnoff M. 1976. Density of tropical timbers as influenced by climatic life zones. The Commonwealth Forestry Review, 203–217.
- Crawley M. 1989. Dicotyledonous wood from the lower Tertiary of Britain, Palaeontology, 32: 597–622.
- den Outer RW, van Veenendaal WLH, In Breteler FJ 1989. The Connaraceae. A taxonomic study with emphasis on Africa. Agric. Univ. Wageningen Pap. 89: 403.
- Dickison WC. 1972. Anatomical studies in the Connaraceae. II. Wood anatomy. Journal of the Elisha Mitchell Scientific Society, 120–136.
- Dickison WC. 1973. Anatomical studies in the Connaraceae. III. Leaf anatomy. Journal of the Elisha Mitchell Scientific Society, 121–138.
- Dupéron-Laudoueneix M, Dupéron J. 2005. Bois fossiles de Lauraceae: nouvelle découverte au Cameroun, inventaire et discussion. In Annales de Paléontologie, 91: 127–151.
- Dupéron J, Dupéron -Laudoueneix M, Sakala J, De Franceschi D. 2008. *Ulminium diluviale* Unger: historical data on the discovery and new study. Ann. Paléontol. 94 (2008) 1–12.

- Estrada-Ruiz E, Martínez-Cabrera HI, Cevallos-Ferriz SRS. 2010. Fossil woods from the Olmos Formation (late Campanian-early Maastrichtian), Coahuila, Mexico. *Am. J. Bot.* 97: 1179–1194.
- Estrada-Ruiz E, Upchurch GR, Wolfe JA, Cevallos-Ferriz SRS. 2011. Comparative morphology of fossil and extant leaves of Nelumbonaceae, including a new genus from the Late Cretaceous of Western North America. *Syst. Bot.* 32: 337–351.
- Estrada-Ruiz E, Upchurch GR, Wheeler EA, Mack GH. 2012a. Late Cretaceous angiosperm woods from the Crevasse Canyon and McRae formations, south-central New Mexico, USA: part 1. *Intern. J. Plant Sci.* 173: 412–428.
- Estrada-Ruiz E, Parrott JM, Upchurch GR, Wheeler EA, Thompson DL, Mack G, Mindy MM. 2012b. The Wood Flora from the Upper Cretaceous Crevasse Canyon and McRae Formations, South-central New Mexico, USA: A progress report. In *New Mexico Geological Society Guidebook, 63rd Field Conference, Warm Springs Region*. 503–518.
- Estrada-Ruiz E, Wheeler EA, Upchurch GR, Mack GH. 2018. Late Cretaceous angiosperm woods from the McRae Formation, South-central New Mexico, USA-part 2. *Int. J. Plant Sci.* 179: 136–150.
- Fichtler E, Worbes M. 2012. Wood anatomical variables in tropical trees and their relation to site conditions and individual tree morphology. *IAWA J.* 33: 119–140.
- Fisher JB, Ewers FW. 1992. Xylem pathways in liana stems with variant secondary growth. *Bot. J. Linn. Soc.* 108: 181–202.

- Gillette DD, Wolbert DB, Hunt AP. 1986. Tyrannosaurus Rex from the McRae Formation (Lancian, Upper Cretaceous), Elephant Butte Reservoir, Sierra County, New Mexico. New Mexico Geological Society Guidebook, 37th Field Conference, Truth or Consequences. 235–238.
- Greenwood DR, Wing SL. 1995. Eocene continental climates and latitudinal temperature gradients. *Geology*. 23: 1044-1048.
- Gregory M, Poole I, Wheeler EA. 2009. Fossil dicot wood names - an annotated list with full bibliography. *IAWA J. Suppl.* 6: 1–220.
- Harper C, Parrott JM, Upchurch GR, Krings M. 2018. Angiosperm wood-colonizing fungi (Ascomycota) from the Upper Cretaceous of New Mexico, USA. *Bot. Soc. Am. Meeting. Abstract*: 423.
- Heimsch C. 1942. Comparative anatomy of the secondary xylem in the 'Gruinales' and 'Terebinthales' of Wettstein with reference to taxonomic grouping. *Lilloa*. 8: 83–198.
- Herendeen PS. 1991a. Lauraceous wood from the mid-Cretaceous Potomac group of eastern North America: *Paraphyllanthoxylon marylandense* sp. nov. *Rev. Palaeobot. Palynol.* 69:277–290.
- Herendeen PS. 1991b. Charcoalified angiosperm wood from the Cretaceous of eastern North America and Europe. *Rev. Palaeobot. Palynol.* 69: 225–239.
- IAWA Committee. 1989. IAWA list of microscopic features for hardwood identification. *IAWA Bull. n.s.* 10: 219–332.
- InsideWood. 2004-onwards. Published on the Internet:  
<http://insidewood.lib.ncsu.edu/search> [accessed August 7, 2018].

- Jud NA, Nelson CW. 2017. A liana from the lower Miocene of Panama and the fossil record of Connaraceae. *Am. J. Bot.* 104: 685–693.
- Lee WT. 1906. The Engle coal field, New Mexico. *US Geol. Survey, B.* 240.
- Lozinsky RP, Hunt AP, Wolberg DL, Lucas SG. 1984. Late Cretaceous (Lancian) dinosaurs from the McRae Formation, Sierra County, New Mexico. *N. M. Geol.* 6: 72–77.
- Lucas SG, Mack GH, Estep JW. 1998. The ceratopsian dinosaur *Torosaurus* from the Upper Cretaceous McRae Formation, Sierra County, New Mexico. In *Las Cruces Country II, New Mexico Geological Society, 49th Annual Field Conference Guidebook*, 223–227.
- Mack GH, Kottlowski FE, Seager WR. 1998. The stratigraphy of South-Central New Mexico, *New Mexico Geological Society Guidebook, 49<sup>th</sup> Field Conference, Las Cruces Country II*.
- Markwick PJ. 2007. The palaeogeographic and palaeoclimatic significance of climate proxies for data-model comparisons. *Deep-time perspectives on climate change: marrying the signal from computer models and biological proxies*, 251-312.
- Metcalf CR, Chalk L. 1950. *Anatomy of the Dicotyledons. Vols. 1 & 2.* Clarendon Press, Oxford.
- Oakley D, Falcon-Lang HD. 2009. Morphometric analysis of Cretaceous (Cenomanian) angiosperm woods from the Czech Republic, *Rev. Palaeobot. Palynol.* 153: 375–385.

- Olson ME. 2012. Linear trends in botanical systematics and the major trends of xylem evolution. *Bot. Rev.* 78: 154–183.
- Page VM. 1967. Angiosperm wood from the Upper Cretaceous of Central California Part I -Virginia M. Page -*American Journal of Botany*, Vol. 54, No. 4. (Apr., 1967), pp. 510-514.
- Page VM. 1968. Angiosperm wood from the Upper Cretaceous of central California: part II. *Am. J. Bot.* 55: 168–172.
- Page VM. 1970. Angiosperm wood from the Upper Cretaceous of central California. III. *Am. J. Bot.* 57: 1139–1144.
- Page VM. 1979. Dicotyledonous wood from the Upper Cretaceous of central California. I. *J. Arnold Arbor.* 60: 323–349.
- Page VM. 1980. Dicotyledonous wood from the Upper Cretaceous of central California II. *J. Arnold Arbor.* 61: 723–748.
- Page VM. 1981. Dicotyledonous wood from the Upper Cretaceous of central California III Conclusions. *J. Arnold Arbor.* 62: 437–455.
- Rich PM, Helenurm K, Kearns D, Morse SR, Palmer MW, Short L. 1986. Height and stem diameter relationships for dicotyledonous trees and arborescent palms of Costa Rican tropical wet forest. *Bull. Torrey Bot. Club* 113: 241–246.
- Richter HG. 1981. Anatomie des sekundären xylems und der rinde der Lauraceae. *Sonderbände Naturwiss. Vereins Hamburg* 5: 1–148.
- Richter HG. 1987. Lauraceae. Mature secondary xylem. In: Metcalfe CR (ed.), *Anatomy of the Dicotyledons*. Ed. 2. Vol. III: 167–171. Oxford Science Publications.

- Roberts LNR, Kirschbaum MA. 1995. Paleogeography of the Late Cretaceous of the Western Interior of Middle North America—coal distribution and sediment accumulation: U. S. Geological Survey, Professional Paper, 1561: 116.
- Seager WR, Mack GH, Raimonde MS, Ryan RG. 1986. Laramide basement-cored uplift and basins in south-central New Mexico. Truth or Consequences Region New Mexico. NM Geol. Soc. Guide. 37: 123–130.
- Seager WR, Mack GH, Lawton TF. 1997. Structural kinematics and depositional history of a Laramide uplift-basin pair in southern New Mexico: implications for development of intraforeland basins. Geol. Soc. Am. Bull. 109: 1389–1401.
- Shilkina AI. 1956. Icacinnoxylon. In New families and genera, records of palaeontology. Ministerstvo Geologii i Ochrany Nedr, SSSR, Vses. Nauchno-Issled. Geol. Inst.(VSEGEI), Palaeontologiya, ns 12: 260.
- Spackman W. 1948. A dicotyledonous wood found associated with the Idaho tempskyas. Ann. Miss. Bot. Gard. 35: 107–115.
- Stevens PF. 2001 onwards. Angiosperm phylogeny website. Version 14, July 2017 [and more or less continuously updated since].
- Süss H, Mädler E. 1958. Über Lorbeerhölzer aus miozänen Schichten von Randeck (Schwäbische Alb) und Ipolytarnóc (Ungarn). Geologie 7: 80–99.
- Takahashi KI, Suzuki M. 2003. Dicotyledonous fossil wood flora and early evolution of wood characters in the Cretaceous of Hokkaido, Japan. IAWA J. 24: 269–309.

- Thayn GF, Tidwell WD, Stokes WL. 1985 Flora of the lower Cretaceous Cedar Mountain Formation of Utah and Colorado. Part III- *Icacinoxylon pittense* n. sp. Bot. 72: 175–180.
- Turland NJ, Wiersema JH, Barrie FR, Greuter W, Hawksworth DL, Herendeen PS, Knapp S, Kusber W-H, Li D-Z, Marhold K, May TW, McNeill J, Monro AM, Prado J, Price MJ, Smith GF (eds.) 2018: International Code of Nomenclature for algae, fungi, and plants (Shenzhen Code) adopted by the Nineteenth International Botanical Congress Shenzhen, China, July 2017. Regnum Vegetabile 159. Glashütten: Koeltz Botanical Books. DOI <https://doi.org/10.12705/Code.2018>.
- Upchurch GR, Wolfe JA. 1987. Mid-Cretaceous to Early Tertiary vegetation and climate: evidence from fossil leaves and woods. Origins of angiosperms and their biological consequences/edited by EM Friis, WG Chaloner, and PR Crane.
- Upchurch GR, Mack GH. 1998. Latest Cretaceous leaf megafloras from the Jose Creek Member, McRae Formation of New Mexico. N. M. Geol. Soc. Guide. 49: 209–222.
- Upchurch GR, Kiehl J, Shields C, Scherer J, Scotese C. 2015. Latitudinal temperature gradients and high-latitude temperatures during the latest Cretaceous: congruence of geologic data and climate models. Geology 43: 683–686. Supplementary material: GSA Data Repository item 2015238.

- Wheeler EA. 1991. Paleocene dicotyledonous trees from Big Bend National Park, Texas: variability in wood types common in the Late Cretaceous and Early Tertiary, and ecological inferences. *Am. J. Bot.* 78: 658–671.
- Wheeler EA, Lee M, Matten LC. 1987. Dicotyledonous woods from the Upper Cretaceous of southern Illinois. *Bot. J. Linn. Soc.* 95: 77–100.
- Wheeler EA, Baas P. 1991. A survey of the fossil record for dicotyledonous wood and its significance for the evolutionary and ecological wood anatomy. *IAWA Bull.* n.s. 12: 275–332.
- Wheeler EA, McClammer J, LaPasha CA. 1995. Similarities and differences in dicotyledonous woods of the Cretaceous and Paleocene. San Juan Basin, New Mexico, USA. *IAWA J.* 16: 223–254.
- Wheeler EA, Lehman TM. 2000. Late Cretaceous woody dicots from the Aguja and Javelina Formations, Big Bend National Park, Texas, USA. *IAWA J.* 21: 83–120.
- Wheeler EA, Wiemann MC, Fleagle JG. 2007. Woods from the Miocene Bakate Formation, Ethiopia: anatomical characteristics, estimates of original specific gravity and ecological inferences. *Rev. Palaeobot. Palynol.* 146: 193–207.
- Wiemann MC, Williamson GB. 2002. Geographic variation in wood specific gravity: effects of latitude, temperature, and precipitation. *Wood and Fiber Science.* 34: 96–107.
- Wolfe JA, Doyle JA, Page VM. 1975. The bases of angiosperm phylogeny. *Ann. Missouri Bot. Gard.* 62: 801–824.
- Wolfe JA, Upchurch GR. 1987. North American nonmarine climates and vegetation during the Late Cretaceous. *Palaeogeogr., Palaeoclim., Palaeoecol.* 61: 33–77.